ALMA MATER STUDIORUM
UNIVERSITÀ DI BOLOGNA

DOTTORATO DI RICERCA IN

SCIENZE E TECNOLOGIE AGRARIE, AMBIENTALI E ALIMENTARI

Ciclo XXXVII

Settore Concorsuale: 07/E1

Settore Scientifico Disciplinare: AGR/14 - PEDOLOGIA

ARTIFICIAL CANALS RESTORATION THROUGH NATURE-BASED SOLUTIONS: EXPERIENCE IN PO PLAIN WITH A VEGETATION AND WATER QUALITY VIEW POINT

Presentata da: **Andrea Morsolin**

Coordinatore Dottorato

Prof.ssa Diana Di Gioia

Supervisore

Prof.ssa Livia Vittori Antisari

Co-supervisore

Prof.ssa Gloria Falsone

Esame finale anno 2025

Abstract

Floodplains carry significant value for social and ecological outcomes within a region. Their proximity to water and flat, fertile land make them ideal for human settlements, while simultaneously serving to deliver ecosystem benefits for the catchment as a whole. However, structural measures such as levees (dikes), dams, and engineered canals encouraged by urban and agricultural development in the floodplain threaten the ecosystem services of these environments. The Po Plain is one of Europe's largest alluvial plains, formed by sediments from the Alps and Apennines carried by the Po River and its tributaries. Its fertile land has long supported human settlement and agriculture. In the last century, land reclamation, intensive farming, and urbanization disrupted natural fluvial processes. Artificial canals were built to ensure hydraulic safety, manage drainage, and supply irrigation water. However, these changes reduced riparian vegetation diversity and increased nutrient buildup in water and bed sediments. In this context, the present dissertation aimed to apply pond construction and canal bank reshaping as nature- based solution to improve the quality of canal from vegetation, water and sediment viewpoint. To reach this general goal, a 5-years study was conducted in a floodplain area located in Emilia-Romagna Region (Italy) through the monitoring of water, sediment and vegetation. The present study showed that both water and sediments did not have any risk for both agriculture and wild habitats. However, it was observed a negligible short-term effect of the applied nature-based solutions on water and sediment quality likely due the small area affected by the interventions.

It is important to mention that the negligible effects can be also attributed to the floods in 2023 which negatively affect the quality of both water and sediment. The vegetation biodiversity, instead, seemed to be positively affected by the interventions even if the floods and the interventions themselves reduced their coverage. Overall, this study showed the potential of the acted nature-based solutions to improve the quality of agricultural floodplains, but it needs longer monitoring time to observe tangible changes.

INDEX

1 Introduction

Riverine floodplains (hereinafter called floodplains) are among the most species-rich and dynamic ecosystems providing a broad range of ecosystem functions and services (Tockner and Stanford, 2002). Floodplains are specific parts of the natural landscape, whose formation and existence are due to their association with a watercourse, allowing the exchange of water, sediment, nutrients, and organisms (Amoros and Bornette, 2002; Benjankar *et al*., 2011). Floodplain ecosystems result from the long-lasting interaction of geomorphic, hydrological, and biological processes (Tockner and Stanford, 2002). In Europe, floodplains cover 7% of the total area and host 12% of the European population (Kaniansk *et al*., 2022). While, in China, floodplain covers 12.1% of the country and 33 % of Chinese population lives in such area (Han *et al*., 2020). Because of the overtime flood pulses, floodplains are characterized by a marked variability of aquatic, semi-aquatic and terrestrial habitats (De Stevan et al., 2015), with different degrees of connectivity among themselves and with the main river (Knox et al., 2022; Benjankar et al., 2011).

1.1 The impact of human activities on floodplain ecosystems: historical transformations and current degradation.

Floodplain ecosystems all over the world are strongly threatened by anthropogenic activities (Dotterweich, 2008;) and their extension reduced approximately by 600,000 km^2 from 1992 to 2019 (Rajib *et al*., 2023). In Europe, roughly 70–90% of the current floodplain area is estimated to be ecologically degraded due to human activities over the centuries, especially since the early 1950s (EEA, 2018). In addition, Europe is the continent most affected by disconnecting floodplains from rivers (Steinfeld and Kingsford, 2013). The construction of dams and levees, the straightening and dredging of channels, and the expansion of agricultural and urban land use are compromising their existence and functions (Knox et al., 2022a, b; Wohl *et al*., 2017; Rajib *et al*., 2021).

Although human presence in floodplains has substantially arisen in many parts of the world over the past decades (Früh-Müller *et al*., 2015; Han et al., 2020),

many human settlements have been in floodplains since ancient times (Gibling, 2018). Therefore, because of the fertile soils, the availability of water and other natural resources, a marked transition from a strongly nature-dominated to an increasingly human-dominated environment occurred in floodplains. The proximity of these communities to watercourses facilitated irrigation, water supply, and fishing activities (Amorosi *et al*., 1999b). The growth of the ancient civilizations occurring between 3000 B.C. and 500 A.D. forced a more structured management of floodplains to promote favourable conditions for cultural organization, agricultural development, trade, and economic growth. Hydraulic infrastructures such as irrigation canals, levees, and retention basins were constructed to control flooding and optimize water use for agriculture. However, these activities altered the water flow regime of rivers, sometimes leading to issues such as soil salinization and ecological degradation (Amorosi *et al*., 2004; Cremaschi, 1978).

During the Middle Ages (500–1500 A.D.), floodplains in Europe and other parts of the world were further transformed by agricultural expansion. Drainage systems were introduced to reclaim wetlands and to make land arable. These modifications, however, exacerbated soil degradation, as the land was often intensively exploited without proper management practices (Cremaschi, 1978).

A marked transformation of floodplains occurred during the Industrial Revolution (18th–19th century). Rapid urbanization led to the construction of cities along rivers, while the expansion of infrastructure such as railways and roads further fragmented ecosystems. Simultaneously, agricultural intensification and the uncontrolled use of fertilizers and pesticides caused significant water pollution. The construction of dams and barriers drastically altered river flows, disrupting natural sedimentation cycles and hydraulic connectivity (Amorosi, *et al*., 2000; Cremaschi, 1978).

In the 20th and 21st centuries, the impact of human activities on floodplains has become increasingly evident. The growing demand for urban expansion, resource extraction, and climate change has boosted the degradation of these ecosystems (Blum and Törnqvist, 2000; Cremaschi, 1978). Global issues such as biodiversity loss, coastal erosion, and water eutrophication have emerged as

critical challenges. In fact, it is recognized that the transformations affecting floodplains have not only altered hydraulic dynamics but also significantly impacted ecological balances (Cremaschi, 1978).

Hence, human activities negatively affect the dynamic links between various water bodies of the floodplain and the main river (Amoros and Bornette, 2002), leading to permanent alterations in freshwater biodiversity (Tockner and Stanford, 2002) and ecosystem functioning (Funk *et al.,* 2019).

In recent decades, to cope with the increasing degradation processes of floodplains, renaturalization projects and restoration program initiatives have been launched (Paillex *et al.,* 2009). For example, the LIFE Danube Floodplain Project (2018-2024) aimed to reconnect the floodplain habitats through the removal of embankments and barriers, the restoration of wetlands, and the creation of ecological corridors to facilitate species migration. These actions might help to improve flood management, enhance biodiversity, and increase carbon storage in sediments (European Commission, 2020). The Nidda restoration project (Germany, started in 1993 and continued through subsequent phases, with recent actions documented in Stoltefaut et al., 2024) made efforts to enhance flood protection, to improve water quality, to restore habitats and biodiversity within the floodplain of the Nidda river. In USA, the Mississippi River Alluvial Valley underwent restoration beginning in the early 1990s under the U.S. Department of Agriculture's Wetlands Reserve Program (De Steven et al., 2015). In such floodplain, forest habitat was restored by the methods of tree planting (afforestation) and local hydrologic enhancement on reclaimed croplands. One of the largest restoration initiatives in the USA concerned the Kissimmee River floodplain (Florida), where works began in the 1990s and were completed in 2019. The restoration activities included the reshaping of river levees and the conversion of arable lands into natural ecosystems to improve biodiversity and water quality (Koebel & Kenner, 1999).

The restoration activities could have ecological benefits for waterways and societal advantages, such as reduced flood risk and improved water quality. However, the high reclamation and restoration costs, which are much greater

than those in other landscape types, make these interventions hard to be carried out (Vitousek *et al.,* 1997; Revenga *et al*., 2000).

1.2 Degradation factors of floodplains

Floodplains are dynamic and complex ecosystems, characterized by constant interaction with their surrounding environment (Tomscha *et al.,* 2017). However, these areas are currently exposed to various disturbances (mostly human-like disturbances), which have the potential to deteriorate their biophysical status and ecosystem services in the long run.

The main disturbances that could promote the degradation of the floodplains are (Tockner *et al.,* 2002):

- **Dam construction**: dams limit the natural flow of rivers, impeding sediment transport and modifying hydrological cycles. This reduces the regeneration of riverine habitats and the availability of water resources downstream. The resulting loss of river connectivity negatively affects biodiversity by limiting the mobility of both aquatic and terrestrial species.
- **Channelization and levees**: levee construction and river isolation reduce ecological connectivity, confining rivers to artificial canals (Hein et al., 2016). Historically, these interventions and infrastructures have been implemented to protect agricultural areas, infrastructure, and cities from floods. While they are effective tools for flood control, they have numerous negative environmental impacts. Specifically, they alter natural habitats, reduce biodiversity due to the isolation that hinders natural species distribution, and disrupt natural ecological cycles.
- **Urbanization**: urban expansion encroaches on floodplain areas and contributes to soil impermeability, increasing flood risks and reducing water absorption capacity. Urban infrastructure often interferes with ecological corridors, further fragmenting habitats and limiting ecosystem functionality. Roads, railways, and buildings fragment natural landscapes into isolated sections, thereby limiting the movement of organisms and reducing gene flow among populations.

- **Intensive agriculture**: the conversion of floodplains into intensively cultivated farmlands has led to the loss of natural habitats, pollution from fertilizers and pesticides, and soil compaction. These practices degrade soil quality, compromising the floodplains' ability to sustain rich and functional biodiversity.
- **Invasive species**: the simplification of landscapes resulting from the transformation of natural habitats into agricultural, urban, or industrial areas reduces ecological diversity, creating conditions that facilitate the expansion of invasive species. Invasive species pose significant threats: over the past four centuries, they have been the leading cause of global extinctions, contributing to the loss of 54% of species (ISPRA, 2010). Plants as the tree-of-heaven (*Ailanthus altissima*) and black locust (*Robinia pseudoacacia*) compete with native flora, reducing local biodiversity and altering habitat structure. For example, *Ailanthus altissima* grows rapidly and forms dense stands that hinder native vegetation growth.
- **Resource extraction**: the removal of gravel, sand, and groundwater contributes to subsidence[1], a phenomenon that increases flood risks and reduces ecosystem stability. Furthermore, resource extraction alters river morphology, reducing habitat complexity for aquatic species.
- **Climate change**: frequent droughts and severe wet events are increasing the vulnerability (for example to flooding and soil erosion) of floodplains, further preventing their ability to provide ecosystem services. Drought periods lead to a reduction in river discharge. Consequently, in coastal areas or those near saline aquifers, the decrease in freshwater flow could

[1] The phenomenon of subsidence refers to the sinking of the soil, which can occur due to various natural and anthropogenic factors. In floodplains, subsidence is often associated with the extraction of underground resources such as water, sand, and gravel, or with the compaction of sediments during drainage. Changes in natural hydrology, such as the disruption of flood and dry cycles, can also contribute to subsidence.
This phenomenon has significant effects on land stability, as it lowers the surface elevation relative to sea level, increasing the risk of flooding. Moreover, subsidence reduces the soil's ability to support natural ecosystems and agricultural crops, compromising the ecosystem services these areas provide. The loss of drainage and water retention capacity in an area affected by subsidence can also accelerate erosion and alter water quality, further worsening the ecological and economic situation.
Sektiawan, A., *et al.,* (2016); ISPRA (recuperato il 20/12/2024, da https://www.isprambiente.gov.it/it/attivita/suolo-e-territorio/rischio-ad-evoluzione-lenta/subsidenza).

promote saltwater intrusion into floodplains subject to periods of prolonged aridity and not far from the coast, increasing soil salinity and reducing fertility. While intense rainfall increases water flow, eroding riverbanks and carrying away sediments and nutrients. Floodplains are naturally capable of absorbing floods, but extreme events can disrupt these systems, damaging ecosystems.

Climate change and the combination of drought periods followed by intense rainfall can affect river hydrology, altering the seasonal variation in water flow rate, with significant impacts on riparian ecosystems.

The combination of these factors undermines both the ecological functionality of floodplains and the essential ecosystem services that they provide, such as flood regulation, water purification, and biodiversity support (Gumiero *et al.,* 2015).

1.3 Floodplain water quality

Water is the primary element of floodplains, forming part of a system comprised of canals, rivers, ponds, and groundwater. Water supports life and plays a crucial role in maintaining the ecological and functional balance of floodplain ecosystems. Through water, there is an exchange of materials, organisms, and nutrients between the various areas that make up these ecosystems. Therefore, monitoring water quality is essential to ensure ecosystem health, protect biodiversity, support human activities, and mitigate environmental risks (Phys.org, 2022).

Its quality can be assessed through indices and indicators that can be classified into chemical, physical, and biological categories. They can include:

- **Nutrients (nitrogen and phosphorus)**: the assessment of their concentration is essential for monitoring eutrophication, safeguarding aquatic ecosystems, and evaluating anthropogenic impacts. Excessive concentrations promote algal blooms and a decrease in dissolved oxygen levels. Conversely, reduced concentrations can lead to a potential decline

in productivity by organism's dependent on these nutrients (e.g., algae, bacteria, aquatic plants) (Schindler, 2006; Howarth and Marino, 2006).

- **Eutrophication index:** eutrophication is widely recognized as one of the most impacting threats for the ecological status and integrity of water bodies. The eutrophication index is used to assess the risk of harmful algal blooms and is based on nutrient concentrations (nitrogen and phosphorus) and the associated biological productivity (algal biomass, oxygen levels, and water transparency). Low values generally indicate a balanced ecosystem, high transparency, and dissolved oxygen, while high values indicate an extremely nutrient-rich condition and algal proliferation (Smith, 2003).
- **Dissolved oxygen (DO):** low oxygen concentrations can prevent the survival of fish and macroinvertebrates. Conversely, nutrient enrichment can promote algal blooms that cause oxygen supersaturation during the day and oxygen depletion (anoxia) at night, leading to harmful conditions for aquatic fauna. Values above 5-6 mg/L are considered good for most organisms, while values approaching 0 indicate anoxia, making the environment lethal for aerobic organisms (Chapman, 1996).
- **Sodium adsorption ratio (SAR):** this index is used to assess water quality, particularly for irrigation purposes, in relation to the risk of soil sodicity. High values indicate water rich in sodium compared to calcium and magnesium, which can lead to soil compaction, reducing fertility and permeability. Low values indicate a good balance between ions (Rhoades, 1982). The SAR is often combined with other parameters, such as electrical conductivity (EC), to assess overall salinity and water quality.
- **Water quality index (WQI):** this index is a single dimensionless number expressing the water quality in a simple form by aggregating the measurements of selected parameters (Uddin et al., 2021). High values represent good water quality, suitable for most uses, while low values indicate degraded conditions with potential negative impacts on human health and ecosystems (Hassan and Taseer, 2018).

An assessment of these indicators and their threshold values is essential for understanding the health status of a floodplain and implementing sustainable management strategies. Each indicator provides valuable information on specific aspects of water quality, and their combination in an integrated analysis allows for the identification of environmental pressures, risks, and intervention opportunities.

1.3.1 Natural and anthropogenic factors influencing water quality

Floodplain water bodies are important providers of water for drinking, irrigation, and industrial use (Kummu et al., 2014; Kingsford, 2000). The deterioration of water quality has become a primary environmental concern since high quality of the fresh water is a key resource for ecosystem conservation and social development (Shi *et al.*, 2017; Pérez-Gutiérrez *et al.,* 2017).

The water quality is controlled by the combination of anthropogenic activities and natural factors (Akhtar *et al*., 2021):

- **Water flow rate**: floods carry nutrient-rich sediments that can enrich both the nutrient and suspended material load of water. An excess of sediment can reduce water transparency, hindering photosynthesis and altering habitats.
- **Soil interaction**: the characteristics of the soil in floodplains influence the filtration capacity of the waters. Sandy soils favor greater percolation than finer textured soils, while clayey soils tend to retain water, regulating its release.
- **Intensive agriculture**: excessive fertilizer use on agricultural land is one of the greatest contributors of nitrogen and phosphorus in water (Pérez-Gutiérrez *et al*., 2017). Nutrient enrichment within surface waters due to the oversupply of phosphorus and nitrogen in agriculture increases the risk of eutrophication.
- **Industrial discharges**: cities and industries often discharge wastewater and stormwater runoff into nearby water bodies. This can introduce heavy metals, toxic chemicals, and excess nutrients, all of which can degrade

water quality. These substances can bioaccumulate in organisms and cause toxic effects even at low concentrations. Wastewater treatment plant inefficiencies can further exacerbate this issue.

- **Wastewater treatment plants**: urban wastewater and livestock waste introduce pathogenic bacteria and viruses that can contaminate water resources.

1.3.2 Pollution mitigation techniques

Restoring the natural conditions of floodplains is essential for improving water quality and ecological functionality. Because of this, it is necessary to address their protection by implementing natural and engineering solutions (Hughes *et al.,* 2005).

The main interventions include (Akhtar *et al., 2021*):

- **River restoration**: removing artificial embankments and/or creating controlled floodplain areas to promote natural sedimentation and water filtration.
- **Wetland restoration**: wetlands act as natural filters, trapping sediments, nitrates, and phosphates. Their presence is particularly useful in agricultural areas where nutrient load results to be high due to the use of fertilizers.
- **Creation of buffer strips**: planting native vegetation along watercourses can help to reduce the surface runoff of soil particles containing nutrients and pesticide residues.
- **Retention zones**: these are areas designed to slow down water flow, allowing nutrients to settle before reaching main watercourses.
- **Phytoremediation**: uses aquatic plants to remove nutrients, heavy metals, and organic compounds from water bodies. The most common plant species used for such purposes are bulrush and reed (*Phragmites australis*).

1.3.3 Water quality monitoring

Floodplains are primarily fed by rivers and streams, which deposit sediments during flood events. The alternation between flood and dry periods promotes the formation of wetlands, marshes, and shallow aquifers, which function as natural reservoirs.

The water bodies in these environments are dynamic, with variations of water flow in response to rainfalls and seasonal cycles (Wendland *et al.,* 2008).

Floodplain water plays a crucial role in maintaining local ecosystems and the ecosystem services they provide. During flood events, water is temporarily stored in the flooded plain, helping to manage extreme events (Raymond *et al., 2020*). The infiltration capacity of these areas helps sustain them during drought periods, but the high presence of nutrients such as nitrogen (N) and phosphorus (P) is creating severe environmental problems (Raymond *et al., 2020*).

To monitor water quality, a range of physical-chemical and biological indicators can be used (Mandarino, 2019). Among the most common physical-chemical indicators are pH, temperature, dissolved oxygen concentration, turbidity, and nutrient levels such as nitrogen (N) and phosphorus (P) (APAT, 2004). These parameters provide insights into the health of the aquatic ecosystem and its ability to support life. For example, high concentrations of nutrients can indicate eutrophication, a process that leads to algal blooms and a reduction in available oxygen for aquatic species.

Biological indicators, on the other hand, are based on the presence and abundance of organisms sensitive to water quality, such as macroinvertebrates, fish, and diatoms. The composition of biological communities can reflect the long-term ecological state of the environment, offering a more complete picture than chemical parameters alone. For instance, a reduced diversity of macroinvertebrates is often associated with water quality degradation caused by pollution or physical habitat alterations (ARPAL, n.d.).

The need to control, manage, and regulate water flows in a complex context clash with the broad planning responsibilities, which involve not only the national level but also regional administrative levels and intermediary authorities, such as basin

authorities (Salvati, *et al.,* 2012). Continuous monitoring is essential to identify pollution sources and assess their impact.

Regional planning mainly operates through integrated tools, involving regional landscape plans, provincial coordination plans, basin plans, and more detailed intervention planning, enabling effective organization of both water regulation and emergency water resource management (Bajocco *et al.,* 2012).

The used techniques include:

- **Chemical analysis**: measuring nutrient levels, dissolved oxygen, pH, heavy metals, and pesticides.
- **Biomonitoring**: using bioindicator organisms, such as aquatic macroinvertebrates or algae, to assess the ecological state of water.
- **Remote sensing**: the use of satellites and drones allows large-scale monitoring of changes in water quality, identifying changes in turbidity or vegetation cover.

1.4 Ecosystem services of floodplains

Ecosystem services are broadly defined as the benefits people obtain from ecosystems (MEA, 2005). Floodplains provide a wide array of ecosystem services including the provisioning, supporting, regulating and cultural services (MEA, 2005). Specifically, floodplains act as natural buffers against flooding by absorbing excess water during heavy rainfalls, reducing flood severity downstream. The vegetation and soils filter pollutants, nutrients and suspended particles from both runoff water and leachates, preserving water quality in water bodies. Rich in habitats, floodplains support a huge biodiversity of plants and animals. They play a key role in nutrient cycling, especially nitrogen and phosphorus, which on the one hand supports plant growth and on the other hand prevents eutrophication. Additionally, floodplains store carbon in their soils, climate change mitigation. These ecosystems support commercial and recreational fisheries. Floodplains also have cultural and recreational significance, offering opportunities for activities like hiking, birdwatching, and fishing, boosting local tourism. They enhance aesthetic value, promoting eco-tourism and human well-being. By allowing water to seep into the ground,

floodplains recharge groundwater aquifers, ensuring freshwater supplies. Their fertile soils support food production, and they serve as important sites for environmental education, offering a practical understanding of hydrology, ecology, and human impacts on nature.

Because of the numerous ecosystem services provided by floodplains, it has been estimated a yearly economic value spanning from 25,021 to 27,021 $/ha (values in 2007 International dollars, Costanza et al., 1997, 2014; De Groot et al., 2012).

Despite the numerous benefits, floodplains are threatened by pollution, invasive species, river regulation, and land-use changes. Therefore, Jakubínský et al. (2021) highlighted the importance to protect the ecosystem services provided by floodplains, particularly through nature-based solutions, to counteract human impacts and support the conservation of these environments. Additionally, it emphasized that understanding ecosystem functions and services is crucial for formulating effective management and conservation policies.

1.5 Importance of floodplain conservation and restoration

Floodplains provide several physical and ecological functions and support critical habitat for a variety of terrestrial and aquatic species. At the same time, they are subject to intense use by humans. The water flow control structures through the construction of dams and levees, as well as agricultural, industrial, and urban development have simplified watercourse networks, disrupted lateral connectivity and reduced biodiversity in floodplains. The tremendous loss in floodplain area and changes in water exchange conditions due to water regulation call for scientifically sound restoration schemes. According to the EEA (2018), the conservation and restoration of floodplains are already promoted within environmental policies, and targeted interventions, such as river re-naturalization and sustainable land management, can help to restore the ecological functionality of these environments, ensuring benefits for both nature and humans (Dolejš *et al.,* 2022). An integrated approach is needed to balance economic needs with environmental protection, promoting innovative and nature-based solutions. Restoring river connectivity, reducing the pressure of invasive species, and

adopting sustainable agricultural practices are some of the key actions to safeguard these valuable ecosystems (ISPRA, 2005; Trentini et al., 2012).

The types of actions for the conservation and restoration of these environments are diverse and can be divided into hydraulic-naturalistic interventions; interventions for the control of riverbank erosion; interventions for water quality improvement; vegetation maintenance; urban canal rehabilitation; and management of canals in Natura 2000 sites. To achieve the conservation and restoration objectives, it is essential to identify the environmental and anthropic issues in the area of interest, to evaluate the specific characteristics of the territory, and to ensure active participation from stakeholders (Ball, 2008).

1.6 The role of biodiversity and vegetation in floodplain

While floodplains provide multiple ecological functions and support a variety of species, their long-term capacity to deliver these functions depends strongly on biodiversity and vegetation structure. Within this framework, biodiversity is a key component of ecosystem functioning, shaping productivity, stability, and resilience (Cardinale, B. J., et al., 2012; Mace, G. M., et al., 2012).

In floodplain landscapes, diverse and structurally complex vegetation increases the provision of regulating services (water purification, carbon sequestration, flood mitigation) and supporting services (habitat provision, genetic diversity conservation).

In highly anthropogenic lowland floodplains, where land reclamation and intensive agriculture have fragmented and simplified habitats, semi-natural elements such as riparian strips, hedgerows, and small wetlands act as biodiversity reservoirs and ecological stepping stones (Bennett, A. F., et al., 2006; Bianchi, F. J. J. A., et al., 2006). These habitats enhance landscape connectivity, host species that cannot persist in intensively managed fields, and support recolonization after disturbances (Tscharntke, T. et al., 2005). Their conservation and integration into canal networks are therefore crucial to maintain ecosystem functions and services in such altered environments.

Historically, large areas of floodplain forests have been removed from the Po Plain and other European lowlands to make space for agriculture and settlements

(Hughes, F. M & Rood, S. B., 2003). This deforestation interrupted the natural successional trajectory that would lead to a forested climax community (Decocq, G., et al., 2004). In their absence, vegetation tends to persist in early or mid-successional stages dominated by herbaceous or shrubby species adapted to frequent disturbances, high nutrient availability, and altered hydrology (Bornette, G., et al., 1998). The lack of forest cover reduces structural complexity, microhabitat diversity and long-term habitat stability, further decreasing the resilience of these systems to extreme events. Preserving and expanding semi-natural habitats within the canal network can partly compensate for the absence of climax forests, supporting biodiversity and restoring ecological functions. These considerations highlight the need for innovative approaches, such as nature-based solutions, to reconcile conservation objectives with the human pressures on floodplain landscapes.

2 Nature-Based Solutions for floodplain restoration

A sustainability transition that has entered the European policy domain over the past decade is the mainstreaming of nature-based solutions (NBS). European Commission defines the NBS as:

“Solutions that are inspired and supported by nature, which are cost-effective, simultaneously provide environmental, social and economic benefits and help build resilience. Such solutions bring more, and more diverse, nature and natural features and processes into cities, landscapes and seascapes, through locally adapted, resource-efficient and systemic interventions. Nature-based solutions must therefore benefit biodiversity and support the delivery of a range of ecosystem services.” (Directorate-General for Communication, 2022).

NBS utilize natural ecosystem processes to address multiple sustainability challenges (Maes, J., & Jacobs, S. 2017; Seddon, N., et al., 2022), including water management, food security, health, climate change adaptation, and biodiversity protection (Raymond, C. M., et al., 2017; Seddon, N., et al., 2022). In the specific context of floodplains, vegetation represents a key component of NBS, as plants regulate hydrological and biogeochemical cycles, stabilize sediments, and provide habitat and trophic resources.

Species with high phytoremediation capacity, such as *Phragmites australis*, *Typha latifolia* or *Carex* spp., are widely used in constructed wetlands to improve water quality (Mitsch, W. J., & Gosselink, J. G., 2015). Fast-growing woody species such as *Salix* and *Populus* are often planted in riparian buffer strips and reforestation projects to stabilize soils, filter nutrients, and support successional recovery (Hughes, F. M., & Rood, S. B., 2003). The selection of species is therefore not only ecological but also functional, aiming to increase resilience to hydrological disturbance, enhance nutrient and pollutant uptake, and promote habitat complexity.

By integrating ecological engineering and restoration principles, NBS offer a range of techniques and interventions that can provide numerous environmental, social and economic benefits to floodplain areas including:

- **Water quality improvement:** constructed wetlands are recognized to be efficient ecologically engineered artificial structures able to remove organic

and/or inorganic contaminants from surface waters and runoff through phytopurification by vegetation and adsorption by soil (Mitsch and Gosselink, 2015).

- **Flood protection:** retention basins and levee setback have been documented to reduce floods and flood-related disasters (Barbier et al., 2011; Serra-Llobet et al., 2022).
- **Protection and enhancement of biodiversity:** green-blue infrastructures are NBS used to reconnect floodplain habitats (Penning et al., 2023). The green-blue infrastructures consist of green ecosystems (e.g., shrublands, woodlands, riparian vegetation, permanent grasslands), as well as blue ecosystems (e.g. pools, ponds, wetlands, watercourses), that provide structural and functional connectivity across landscapes (European Environment Agency, 2011). They are promising tools for floodplain planning that encompass the objective of maintain and enhance biodiversity (Cohen-Shacham et al., 2016; Barbosa et al., 2019; Nguyen et al., 2021).
- **Climate adaptation:** the green-blue infrastructures vegetation reduces surface heat and flooding of stormwater (Almaaitah et al., 2021; Choi et al., 2021).
- **Societal well-being:** NBS can help to alleviate societal challenges such as air pollution and water shortage besides recreational benefits (Raymond et al., 2017).
- **Cost-efficiency:** NBS offer a plethora of benefits and co-benefits for the environment and society. In addition, NBS often require lower investment than traditional infrastructure making them cost-effective and long-term solutions for floodplain protection (Ruangpan et al., 2024).
- **Economic growth - green growth:** activities that include design, implementation and monitoring of NBS, stimulate employment in natural resource management and the ecotourism sector (Wolch et al., 2014).

Depending on the type of solution to be adopted and its objectives, NBS can be merged into three categories (Cohen-Shacham et al., 2016) (Figure 1):

1. **Minimal intervention in ecosystems:** this typology is based on the conservation or natural restoration of ecosystems with negligible alteration of their structure or functioning. Therefore, human intervention is minimized, allowing natural processes to prevail. An example is the protection and restoration of natural riverine wetlands, which can improve hydrological regulation and support biodiversity (Acreman and Holden, 2013). The intervention is limited to protection or passive restoration measures, such as abandoning intensive agricultural practices in critical areas and promoting the natural regeneration of vegetation typical of floodplain environments (Tockner and Stanford, 2002).
2. **Some interventions on ecosystems and landscapes:** they plan to implement solutions through new sustainable management procedures of restored ecosystems. The goal is to enhance the resilience of floodplains by improving soil and water quality, reducing the impact of intensive agricultural practices, and promoting the multifunctionality of ecosystems. An example is the adoption of agroforestry systems that combine agricultural crops with the planting of native floodplain vegetation, improving soil structure and resilience to floods or droughts (Jose, 2009).
3. **Extensive ecosystem changes**: they involve the creation of new ecosystems. This typology includes the creation of artificial wetlands, which are human-designed ecosystems that mimic the ecological functions of natural wetlands. These interventions are highly planned and designed to meet specific objectives, such as creating habitats to enhance biodiversity. Additionally, these systems act as storage basins, reducing water flow in urban or agricultural areas during flood events (Cohen-Shacham et al., 2016).

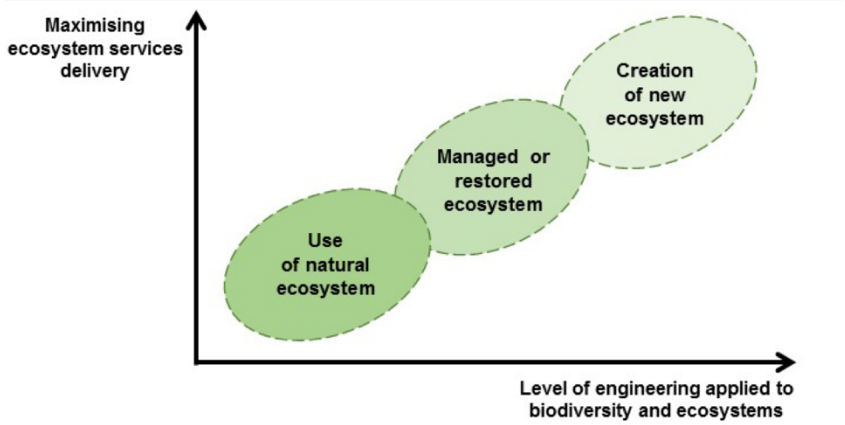

Figure 1 - Nature-based solutions typologies (Cohen-Shacham E., et al., 2016)

NBS propose systems that sometimes allow the application of management and/or recovery interventions, making the engineering interventions minimal and sometimes zero.

2.1 NBS as key action in water resource improvement

Water pollution is a pervasive pressure on freshwater of floodplains, putting physiological stress on aquatic organisms via reduction in oxygen levels, increased temperatures, excessive algal growth, and increased turbidity, and driving system-scale eutrophication of freshwater habitats (Dudgeon et al., 2006; Reid et al., 2019). The NBS have the capacity to improve water quality, especially in floodplains affected by urban and agricultural lands, while delivering other services such as the protection of freshwater biodiversity.

NBS such as constructed wetlands, green-blue infrastructures, detention ponds, levee reshaping, creation of buffer strips and barrier removals can improve freshwater quality through various mechanisms including sedimentation, denitrification, and anaerobic ammonium oxidation (Serra-Llobet et al., 2022; Tschikof et al., 2022). For instance, constructed wetlands remove pollutants and excess nutrients, such as nitrogen and phosphorus, from stormwater runoff by increasing residence time and providing conditions for the metabolism and settling (Chavan and Dennett, 2008; Guerrero, et al., 2020). These nutrients can be absorbed by the soil and taken up by plants and microorganisms (Biswal and Balasubramanian, 2022). Even small waterbodies as ponds are known for their

large role in supporting biodiversity and delivering ecosystem services, mostly by offering refuges for aquatic species that rely on processes and habitats no longer found in broader disturbed landscapes (Biggs et al., 2017). Ponds have been largely used for reducing nutrients loadings of wastewater (That and Hoang, 2024; Senzia et al., 2003) and stormwater (Janke et al., 2022; Yazdi et al., 2021). These NBS practices can reduce erosion and excess sediment influx on the river and improve downstream water quality by reducing flow velocity and increasing the residence time of water in the floodplain, where pollutants can settle out or be metabolized (Tschikof et al., 2022). The restoration of flooding dynamics by levee setbacks provides ideal conditions for denitrification (low oxygen and abundant organic carbon), by local bacterial assemblages, leading to the removal of bioavailable nitrogen from the water column and improvements in water quality (Messer et al., 2012). This is especially important in agricultural catchments where fertilizer runoff can trigger algal blooms and other disruptive pressures on aquatic life (Tilman, 1999).

Across the world, several are the NBS applied with the aim of enhancing the floodplain ecosystem quality. For example, the renaturalization project of the Iser River in Germany involved the removal of artificial embankments and the creation of new wetland areas. These actions resulted in improved water quality within the aquatic habitats, reduced flood risks, and enhanced ecological connectivity (UBA, 2010).

Molle et al. (2008) highlighted the role of constructed wetlands for the agricultural wastewater treatment as valuable nature-based solution for reducing nitrogen and phosphorus loads in waterbodies of the Camargue Nature Park in France. NBS as the planting of the native aquatic plants was adopted to improve water quality and restore habitats for migratory species in the Loire floodplain in France (Chavan et al., 2015).

In Nigeria, agroforestry systems were developed to improve water resource management in floodplains. The planting and introduction of trees alongside agricultural crops were strategies used to control soil erosion, improve water quality, and regulate runoff. Farmers integrated crops such as rice and maize with

fruit and timber trees, creating an agroforestry system that increased biodiversity, improved water retention, and reduced soil erosion (Nair, 2011).

Example of NBS applied in urban areas located in floodplain concerns the integration of green spaces, green roofs, rain gardens and swales in Melbourne, Australia. Such NBS allowed to increase urban biodiversity, to reduce the impacts of stormwater runoff, and to improve the local microclimate (McFarlane et al., 2015).

3 The Po Plain

The Po Plain is one of the largest plains in Europe, primarily formed by materials transported by rivers (Amorosi, et al, 2004).

This area is characterized as a vast tectonic depression located between the Alpine arc and the northern Apennines. It has historically acted as a sedimentation basin, accumulating significant quantities of materials carried mostly by Po River, Apennine rivers, and the Eastern Alps rivers, and to lesser extent by marine flooding (Greggio, N., et al., 2018).

Specifically, according to Zanderri, A. (2006), the western and central part of the Po Plain is dominated by recent alluvial sediments, deposited mostly by Po, Adige, Adda and Ticino rivers. Such sediments are featured mainly by gravel, sand and limes (Fookes and Higginbottom, 1975). In the eastern part of the Po plain, close to the Adriatic Sea, there are marine and deltaic deposits. During the Holocene post-glacial sea-level rise (after the Last Glacial Maximum, around 11,700 years ago), the Adriatic Sea has moved inland, favouring the deposition of clay and marine sand. (Correggiari, A., et al., 2006).

Stratigraphic studies carried out in Po plain (Centamore et al., 1986) documented the presence of deep marine clays and marl deposits that represent the first stages of sedimentation in the Po plain of Pre-Quaternary period. While, during the Quaternary period, gravel, sand, lime and clay deposited during the Pleistocene and Holocene epoch. These sediments are closely associated with the glacial and fluvial cycles that featured the Quaternary period. During the glaciation, rivers carried large quantities of debris from mountain areas, contributing to the formation of alluvial conoids (Centamore et al., 1986).

Because of its fertile soils, Po plain experienced a long process of land reclamation since Roman times (Bruno et al., 2013, Curtis and Campopiano, 2014). During the Roman age, the natural landscape was changed dividing the cultivated land into square fields by a regular grid of roads and ditches (Brandolini and Cremaschi, 2018). The channelization and reclamation work started in the 10th century AD and increased between the 12th and the 13th centuries, promoted both by monasteries (Brandolini and Cremaschi, 2018). The most extensive land reclamation works through the construction of artificial canals and

the reinforcement and raisement of the river the embankments occurred during 19th and 20th Centuries (Marchetti, 2002). The construction of artificial canals has altered the flood dynamics, significantly reducing terrestrial and aquatic biodiversity (Bastiani, 2011).

Land reclamation activities together with urbanization and intensive agriculture of Po plain led to degradation, including soil subsidence, erosion, water and land pollution and loss of biodiversity.

Severe land subsidence occurring in coastal and Po deltaic areas due to the excessive abstraction of groundwater for agricultural and industrial purposes has caused a considerable lowering of the soil (Bastiani, 2011). Soil and water pollution due to the intensive use of chemical fertilizers, pesticides and industrial activities negatively affected the health of river and marsh ecosystems (ISPRA, 2022). Land simplification by the conversion of natural ecosystems to agricultural areas caused the loss of habitats which, in turn, caused the decline of biodiversity (Peipoch, 2015). Further, the Po Plain experienced an intense human exploitation and soil sealing, which increased the vulnerability of the entire territory compromising both the quality of surface waters and the functionality of the local ecosystem (Ferronato et al., 2015).

Since the Po plain is characterized by a complex network of rivers and artificial canals, to prevent their degradation and/or the improvement of their quality could allow the ecosystem function restoration of the Po plain. The maintenance of watercourses network quality can establish a dynamic interaction with the surrounding territory, giving rise to micro-ecosystems that support the survival of numerous species and promote ecological connections between different areas (Kietzka et al., 2021). Therefore, the artificial canals like the natural watercourses can be considered as real artificial ecological corridors capable of strengthening the Natura 2000 network (Harvolk et al. 2014).

The natural vegetation of the Po Plain was historically dominated by extensive floodplain forests and wetlands, mainly composed of *Quercus robur*, *Ulmus minor*, *Fraxinus angustifolia*, *Populus alba*, *Salix alba* and *Alnus glutinosa* (Poldini, L., et al. 2020; Gennai, M., et al. 2021). However, centuries of

land reclamation, agriculture, and urban expansion have reduced these forests to small, fragmented remnants, often confined to riparian strips or protected areas.

Along rivers and canals, vegetation today is mostly represented by riparian strips and aquatic macrophytes. The banks are frequently colonized by *Salix* spp. and *Populus* spp., while herbaceous fringes are dominated by *Phragmites australis*, *Typha latifolia*, *Schoenoplectus lacustris*, and nitrophilous ruderal species (*Urtica dioica*, *Artemisia vulgaris*) (Latella, M., et al. 2020; Bolpagni, R., et al. 2018).

In canals and drainage ditches, submerged macrophytes such as *Ceratophyllum demersum*, *Myriophyllum spicatum*, and *Potamogeton* spp. play a role in water quality regulation but are often impacted by eutrophication and invasive alien species like *Elodea canadensis* and *Ludwigia grandiflora* (Nehring, S., & Kolthoff, J., 2011; Gori, B., et al. 2024). The management of vegetation along rivers and canals is mainly driven by hydraulic safety concerns. Regular cutting of riparian vegetation, dredging of canals, and removal of macrophytes are carried out to maintain water flow and reduce flood risk (Casanova, M. T., & Brock, M. A., 2020). However, such practices often conflict with ecological objectives, reducing habitat heterogeneity and disrupting ecological corridors. A shift toward integrated management, where hydraulic safety is combined with ecological functionality, is increasingly recommended (Clerici, N., & Vogt, P., 2013).

The Natura 2000 network plays a key role in preserving the remaining biodiversity of the Po Plain. Several habitat types listed in the EU Habitats Directive are present in this area, including:

91E0 alluvial forests with *Alnus glutinosa* and *Fraxinus excelsior*, 92A0 *Salix alba* and *Populus alba* galleries; 3150 natural eutrophic lakes with Magnopotamion or Hydrocharition vegetation (European Commission, 2013). These habitats are crucial for maintaining ecological connectivity across a highly fragmented landscape and represent priority targets for conservation and restoration projects.

4 Aim of the work

The purpose of this work was to evaluate the short-term ecological effects of restoration measures, specifically canal bank reshaping and pond creation, implemented as nature-based solutions (NBS) in artificial canals of an agricultural floodplain. To this end, water, sediments, and riparian vegetation were monitored before and after the interventions in order to assess whether these actions improved ecological quality and resilience in a heavily modified landscape.

The overall objective of this study was to monitor the effects of NBS on the environmental quality of artificial canals in an agricultural floodplain. Restoration measures included the creation of ponds and the remodelling of canal banks. By assessing water, sediment and riparian vegetation before and after interventions, the study aimed to assess the effectiveness of NBS in improving ecological quality and resilience in heavily modified landscapes.

This research followed a monitoring-based approach, in which the expected results of the restoration guided the design of the analyses and sampling. Specifically, it has been hypothesized that:

- Water quality could improve through reduced nutrient and metal concentrations, thanks to improved phytopurification and sedimentation processes promoted by ponds and riparian vegetation.
- Sediment quality could benefit from reduced nutrient and contaminant loads, as bank reorganization and vegetation settlement would limit erosion and filtered inputs from surrounding farmland.
- Vegetation could increase in species richness and structural complexity, as ponds served as nurseries for aquatic macrophytes, and bank remodeling provided suitable habitats for riparian plants and helophytes.

Consequently, the specific objectives of this study were to

1. obtain a detailed overview of water and sediment quality by analysing its physicochemical parameters;
2. analyse the floristic composition and structure of riparian vegetation;

3. assess whether restoration measures have led to measurable ecological improvements in all compartments;
4. contribute to the development of environmentally friendly management strategies for artificial canals in agricultural floodplains.

5 Study area

5.1 Environmental features of study area

The floodplain extending within the territories of the municipalities of Baricella, Minerbio, Budrio, Medicina and Molinella, in Emilia-Romagna Region (Italy) can be considered representative of the anthropogenic activities and degradation processes that the Po plain faced during the last half-century (Figure 2). Specifically, the floodplain selected as study area is bounded at North-East and South-East by Reno and Sillaro rivers, respectively, and at North-West and South-West by Navile and Emiliano Romagnolo canals, respectively. The area lies in a temperate climate zone with a mean annual air temperature of 14.5 °C and a mean cumulative annual rainfall of 575 mm, with fall season as the wettest one. It belongs to the temperate subcontinental bioclimatic region of the Po Plain, characterized by hot dry summers and cold wet winters.

This area is 40,790 ha wide and is crossed by roughly 620 km of artificial canals. The artificial canals are managed by Renana Remediation Consortium. The canals are used for hydraulic safety, floodrisk mitigation, irrigation supporting, and draining of urban and industrial settlements wastewater and agricultural area. Within the study area, the water flow is controlled by a detailed hydraulic scheme with pumps and gates.

The area includes six Sites of Community Importance (SCI) and Special Protection Areas (SPA), whose habitats are protected by the EU Habitat Directive 92/43 covering approximately 21% of the study area. Among the most representative are riparian forests dominated by *Populus alba* and *Salix alba* (92A0), mixed alluvial forests with *Quercus robur* and *Fraxinus excelsior* (91F0), and aquatic habitats such as standing or slow-flowing waters with *Hydrocharition*-type vegetation (3130) and natural eutrophic lakes with *Magnopotamion* communities (3150).

For the purpose to improve the suitability of artificial canals as ecological corridors, 9 study sites have been identified across artificial canals connecting habitats Natura 2000 (Figure 2).

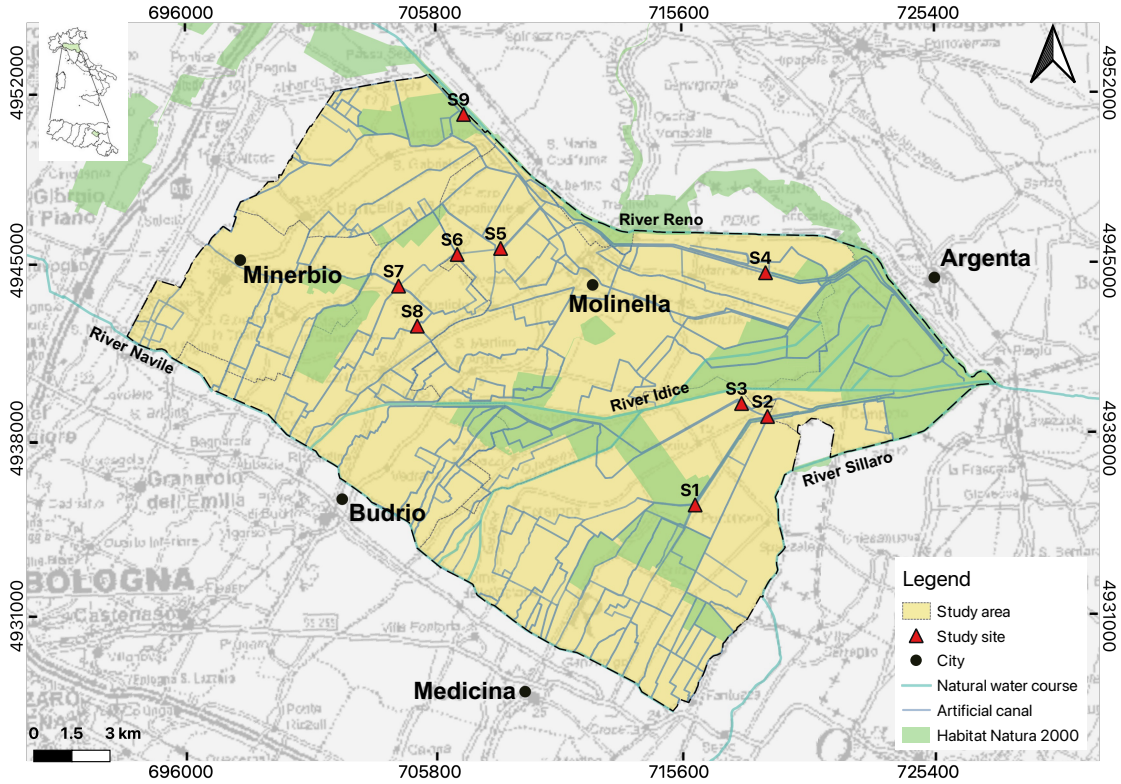

Figure 2 – Technical map of the study area. Coordinate reference system: ETRS89 UTM 32 N.

Agricultural land (croplands, orchards, and livestock settlements) is the predominant land use in the study area, covering about 85% of its surface (Figure 3). Roughly 5,000 ha are characterized by wetlands, artificial canals and water retention basins; about 2,000 ha of urban areas, industrial settlements and infrastructures as railways and roads; roughly 1,000 ha of green areas as parks and reforested areas (RER, 2023).

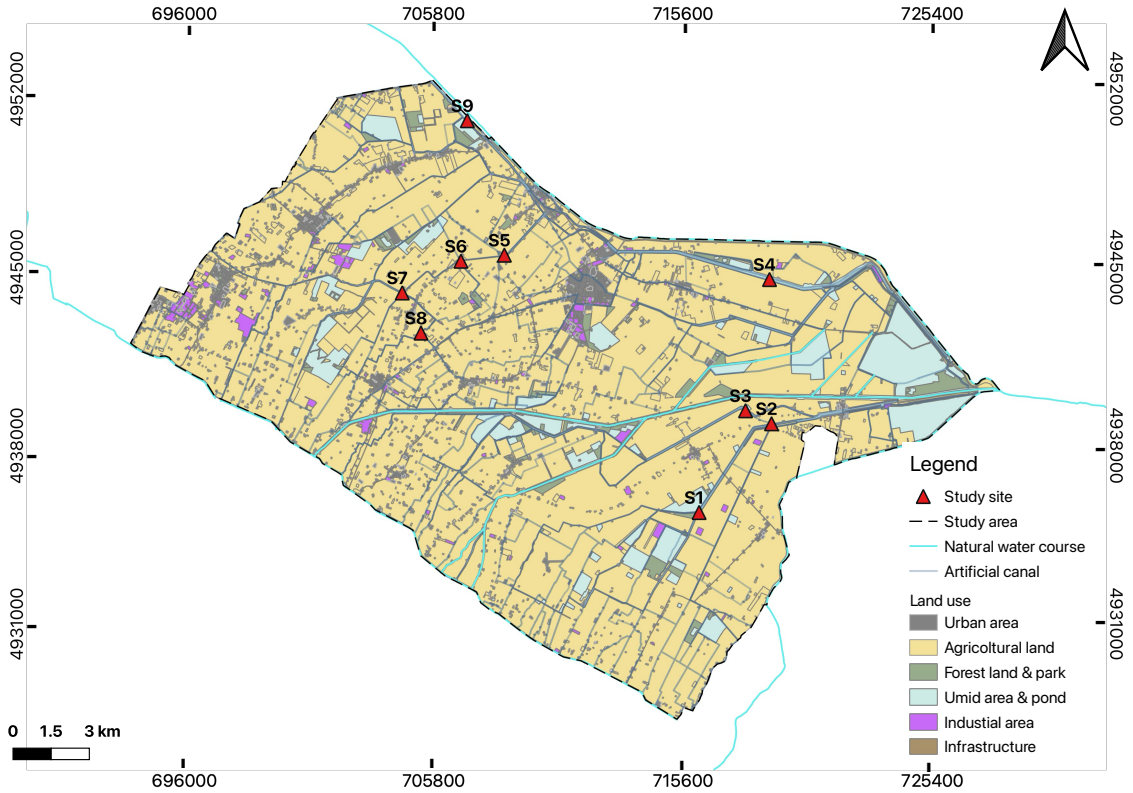

Figure 3 - Land use map of the study area. Coordinate reference system: ETRS89 UTM 32 N.

The study area is characterized by alluvial deposits with a medium and fine texture (RER, 2008). Specifically, the medium-textured deposits can be found close to the paleoriver of Reno, as well as close to the Savena, Idice, and Sillaro rivers. In contrast, the fine-textured deposits are located in morphologically lower areas that correspond to ancient marsh valleys (Figure 4).

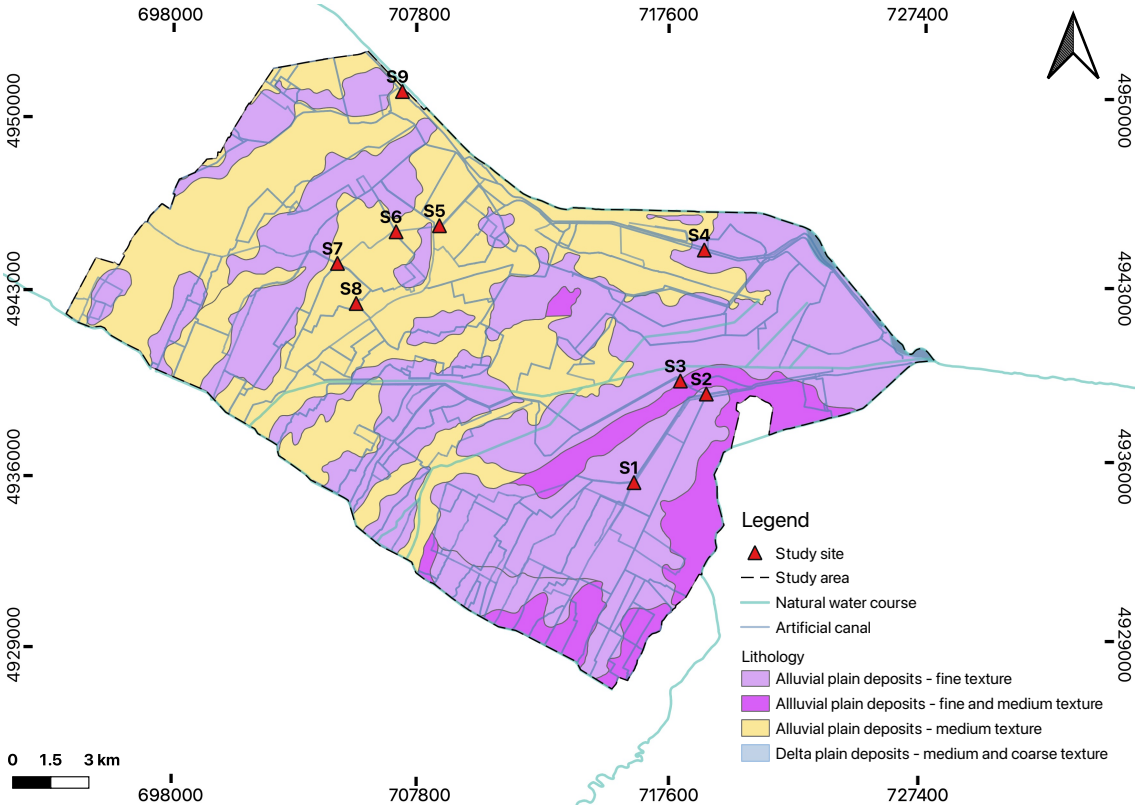

Figure 4 – Lithological map of the study area. Coordinate reference system: ETRS89 UTM 32 N.

The soils are mainly Cambisols (RER 2021 IUSS Working Group WRB, 2007), characterized by low soil formation processes due to the recent formation of the floodplain, and Vertisols (IUSS Working Group WRB, 2007), which contain a high clay content (Figure 5). Most of the Cambisols showed fluvic and calcaric features indicating the presence of visible stratification of the recent fluvial sediments and having calcaric material, respectively. While, because of the finer texture, Vertisols have reducing conditions.

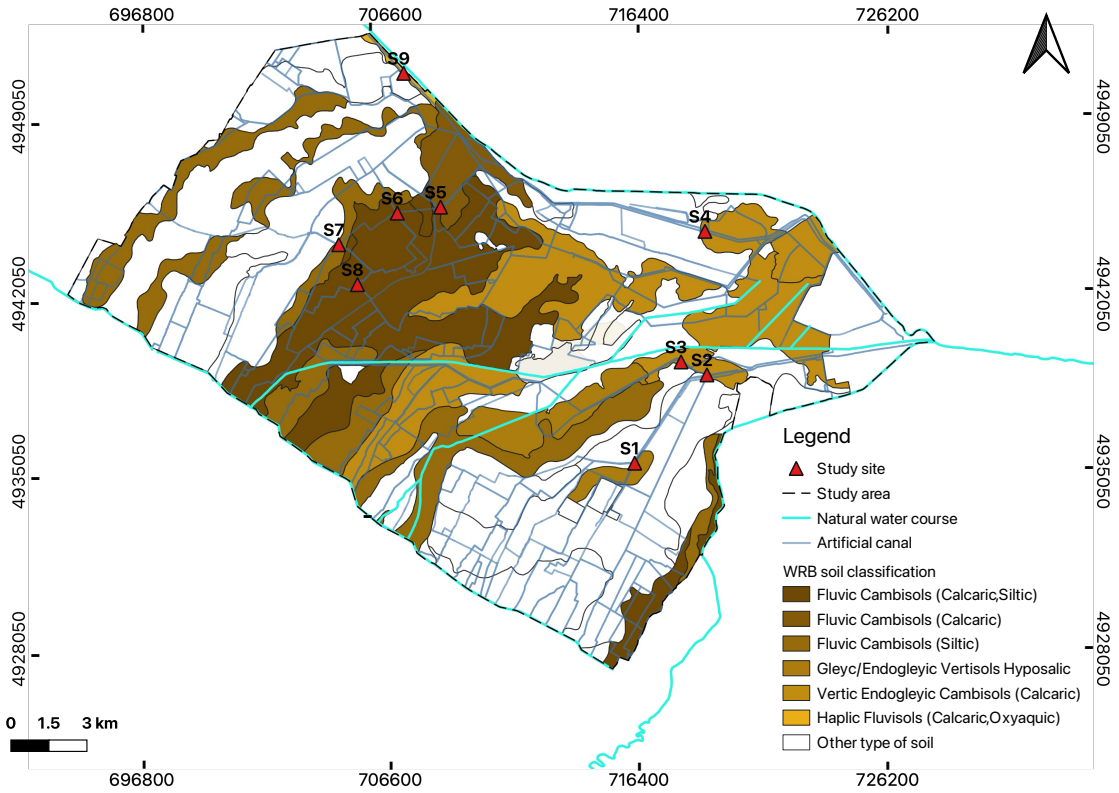

Figure 5 - Soil map of the study area. Coordinate reference system: ETRS89 UTM 32 N.

5.2 Study sites

The selected sites correspond to canals where restoration works were carried out between 2021 and 2023 by the Consorzio della Bonifica Renana. These interventions tested the application of Nature-Based Solutions (NBS) in an agricultural floodplain context. A summary of the main interventions is provided in Table 1, while details on soil characteristics, irrigation districts, Natura 2000 habitats in proximity to the sites, and full planting schemes are reported in Appendix 1.

Table 1 - Summary of restoration interventions carried out at the study sites.

Site	Year of intervention	Type of intervention	Additional actions
S1	2021-2022	Bank reshaping (left bank)	Planting of 147 pots of wetland plants (11 spp.); 84 woody plants (trees/shrubs)
S2	2022	Bank reshaping (both banks at canal confluence)	Planting of 93 pots of wetland plants (18 spp.); 40 woody plants
S4	2021-2022	Bank reshaping + creation of pond (220 m²)	Planting of 116 pots of wetland plants (16 spp.)
S5	2022-2023	Bank reshaping (left bank + adjacent strip)	Planting of 789 pots of wetland plants (21 spp.)
S6	2022-2023	Bank reshaping (right bank) + creation of pond (270 m²)	Planting of 241 pots of wetland plants (19 spp.)
S7	2022-2023	Creation of pond (80 m²)	Planting of 107 pots of wetland plants (15 spp.)
S8	2022-2023	Bank reshaping (confluence of canals)	Planting of 128 pots of wetland plants (15 spp.)
S9	2021-2022	Bank reshaping (left bank) + creation of pond (650 m²)	Planting of 825 pots of wetland plants (29 spp.)

Site selection was guided by the ecological potential of each area, particularly in terms of their proximity to Natura 2000 Network sites and existing wetland systems, which are supplied with water through drainage canals. Additional

selection criteria included the available surface area and the type and morphology of the adjacent canal.

Based on these parameters, six main canals were identified as suitable for intervention. These are characterized by medium to large cross-sections, and in the sections concerned, often lack embankments, allowing for greater morphological adaptability. The selected canals are also used to supply irrigation water to agricultural fields during the summer months. As such, they are seasonally filled with water, primarily diverted from the Canale Emiliano Romagnolo - a major artificial water infrastructure that sources water from the Po River and conveys it as far as the city of Rimini, serving both irrigation and drinking water purposes.

The irrigation function of these canals - common to much of the artificial hydraulic network managed by the Renana Reclamation Consortium - is not limited to supporting agricultural production. These canals also play a crucial role in supplying water to various scattered wetland areas, many of which are included within Natura 2000 sites.

A brief description of the selected study sites is reported below, while more detailed information on them and interventions can be found in the Appendix.

Site S1

Total area: 3,000 m²

Coordinates: 44°32'20"N 11°43'17"E

Elevation: 4-7 m a.s.l.

Location: left bank of the Garda Basso canal (Municipality of Medicina) (Figure 6).

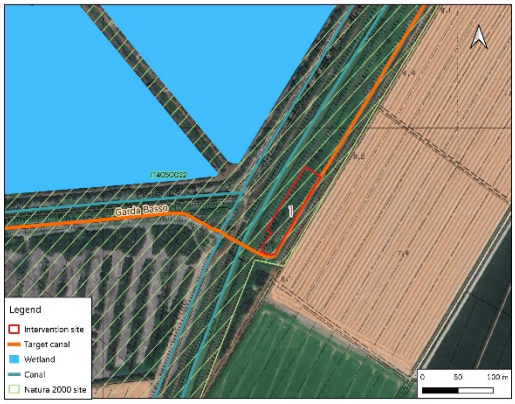

Figure 6 - Cartographic framing of S1.

Figure 7 - S1 after intervention.

S1 is situated 4.7 km upstream from the Garda Basso canal outfall (Figure 7), close to the eastern boundary of the Natura 2000 site IT4050022 - SAC SPA - “Biotopes and Environmental Restorations of Medicina and Molinella”, and adjacent to the wetlands of “Tenuta Vallona”. It is also 1 km from the “Oasi del Quadrone”, an historic wetland complex representative of Po Plain habitats. Access is along a 1.7 km track following the left bank of the Garda Basso canal from the Via Bassa bridge southwards, running along the embankment of the Garda Alto canal. The intervention stretches 140 m along the left bank beginning at the point where the Garda Basso canal passes beneath the Garda Alto canal. Morphologically the site consists of two zones: a long, gently sloping bank rising from the canal to the crown of the levee, and a service track bordered by a linear strip of mixed native trees and shrubs.

In March 2021, the embankment at this site was modified by raising it to soften the slope.

On completion of the work, in March 2022, 147 pots of native wetland plants belonging to 11 species were planted.

Site S2

Total area: 1,300 m²

Coordinates: 44°34'11"N 11°45'32"E

Elevation: 5 m a.s.l.

Location: Confluence of the Sesto Basso and Sant'Antonio canals (Municipality of Medicina) (Figure 8).

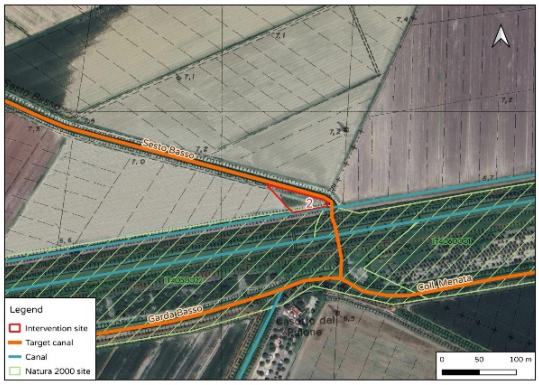

Figure 8 - Cartographic framing of S2.

Figure 9 - S2 after intervention.

S2 is located at the end of the Sesto Basso canal (Figure 9), close to the upstream boundary of two Natura 2000 site: IT4050022 "Biotopes and environmental restorations of Medicina and Molinella" and IT4060001 - SCI-SPA "Valli di Argenta", within the Po Delta Regional Park. It occupies the flat tongue of land at the confluence where the Sant'Antonio canal enters the Sesto Basso canal, spanning both the right and left banks of the two canals (Figure 12). Access is 700 m along the right bank of the Sesto Basso canal from the Via M. Cappelletti bridge, heading southeast towards the Garda Alto canal embankment. Until 2021 the land was cultivated as arable by an adjacent farm.

In January 2022, the banks of the two canals at this site were modified by raising them to soften the slope.

On completion of the work, in March 2022, 93 pots of plants native to wetland environments, belonging to 18 species, were planted.

Site S4

Total area: 3,000 m²

Coordinates: 44°37'16"N 11°45'29"E

Elevation: 5-7 m a.s.l.

Location: Embankment between the left bank of the Lorgana canal and the right embankment of the Botte canal (Municipality of Molinella) (Figure 10).

Figure 10 – Cartographic framing of S4.

Figure 11 – S4 after intervention.

S4 is situated 400 m upstream of the point where the Lorgana canal enters the Natura 2000 site IT4050022 “Biotopes and environmental restorations of Medicina and Molinella” (Figure 11). It is reachable by proceeding 300 m westwards along the left bank of the Lorgana canal from the parking area near the Via Zanolini bridge.

From the site 5 km upstream lies the protected area IT4060017 - SPA “Po di Primaro e Bacini di Traghetto”, whereas 2.7 km downstream begins IT4060001 - SCI-SPA “Valli di Argenta.” The intervention area corresponds to a 120 m long, 25 m wide embankment between the left bank of the Lorgana canal and the right embankment of the Botte canal. The two canals run parallel for most of their courses resulting in a continuous belt chiefly composed of shrubs, mature trees and patches of reedbed.

In August 2021, the bank of the canal was modified at this site by raising it to soften the slope, and a pond of 220 m^2 was created.

On completion of the work, in March 2022,116 pots of native wetland plants, belonging to 16 species, were planted.

Site S5

Total area: 7,000 m²

Coordinates: 44°37'56"N 11°37'49"E

Elevation: 5-7 m a.s.l.

Location: Left embankment and riparian strip of the Allacciante IV Circondario canal (Municipality of Molinella) (Figure 12).

Figure 12 - Cartographic framing of S5.

Figure 13 – S5 after intervention.

S5 lies on Allacciante IV Circondario canal (Figure 13), 150 m downstream of the Via Idice Abbandonato bridge. It occupies a position almost equidistant between two Natura 2000 sites, within a predominantly agricultural landscape that lacks natural or semi-natural areas. It is 2.5 km from Natura 2000 site IT4050023 - SCI-SPA “Biotopes and environmental restorations of Budrio and Minerbio” and 3 km from Natura 2000 site IT4060017 - SPA “Po di Primaro e Bacini di Traghetto”.

The site can be reached by proceeding 1,000 m along the unpaved Via Vescovo on the right bank of the canal to the farm bridge that provides access.

The intervention area corresponds to the left embankment of the canal downstream of the bridge, extending for 300 m. In addition, it includes the adjoining plot situated between the canal and the small Bonello di San Pietro drain, of equal linear extent and an average width of 20 m. The land owned by the Renana Remediation Consortium was used as arable fields by the neighbouring farmer until mid-2022. In November 2022, the bank of the canal was modified at this site by moving the bank and widening the riverbed, to soften the slope of the bank. On completion of the work, in March 2023, 789 pots of native wetland plants, belonging to 21 species, were planted.

Site S6

Total area: 3.500 m²

Coordinates: 44°37'50"N 11°36'29"E

Elevation: 7-10 m a.s.l.

Location: Right bank and riparian strip of the Allacciante IV Circondario canal (Figure 14).

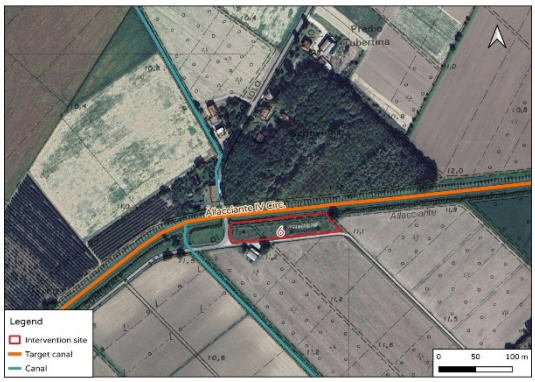

Figure 14 - Cartographic framing of S6.

Figure 15 – S6 after intervention.

S6 corresponds to the right bank of the Allacciante IV Circondario canal immediately downstream of the Via Dugliolo bridge (Figure 15). It occupies an intermediate position between the other intervention sites on the canal, lying 1.7 km from Site 5 and 2.8 km from Site 7. Situated in an entirely agricultural landscape, it is 1.3 km from Natura 2000 site IT4050023 - SCI-SPA “Biotopes and environmental restorations of Budrio and Minerbio”.

The intervention area extends for 130 m along the canal’s right bank. It also includes the adjoining plot bounded by the canal, Via Dugliolo and the unpaved Via Baraccano. This parcel, owned by the Renana Remediation Consortium, covers 3,500 m² and was cultivated by the neighbouring farmer until mid-2022. On the opposite bank a privately own ed area has been afforested with native tree species.

The short reach targeted for intervention is unembanked, owing to the relatively high elevation of the surrounding terrain. In November 2022, the bank of the canal was modified at this site by shifting the slope of the bank. In addition, a pond of 270 m^2 was created. On completion of the work, in March 2023, 241 pots of native wetland plants from 19 species were planted.

Site S7

Total area: 900 m²

Coordinates: 44°37'16"N 11°45'29"E

Elevation: 7-8 m a.s.l.

Location: Point of discharge of the Gallina Superiore canal into the Allacciante IV Circondario canal (Municipality of Budrio) (Figure 16).

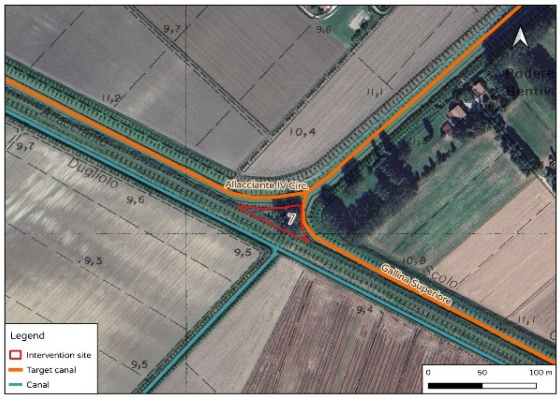

Figure 16 - Cartographic framing of S7.

Figure 17 – S7 after intervention.

S7 is at the confluence of Gallina Superiore and Allacciante IV Circondario canals (Figure 17), 600 m upstream of the Via Dugliolo bridge at the outskirts of the hamlet of the same name. It lies halfway between other two sites: 2.8 km upstream of S6 and 2.5 km downstream of S8. At 1 km west of the intervention area is Natura 2000 site IT4050023.

The intervention area corresponds to the sub-levee strip located at the confluence where the Gallina Superiore canal enters the Allacciante IV Circondario canal, affecting the left bank of the former and the right bank of the latter. This small parcel, owned by the Renana Remediation Consortium, has a total surface of 900 m², most of which is covered by dense spontaneous woody vegetation of habitat 92A0. The area lies below the crest of the surrounding embankments; being enclosed within the levees, it is subject to prolonged inundation during periods of heavy rainfall, thereby fostering ecological dynamics typical of lowland floodplain forests.

In November 2022, 80 m² pond was excavated at this site. In March 2023, 107 pots of 15 species of plants indigenous to wetland environments were planted along the banks of the pond.

Site S8

Total area: 380 m²

Coordinates: 44°36'20"N 11°35'13"E

Elevation: 9-11 m a.s.l.

Location: Point of discharge of the Cornamonda Nuova canal into the Gallina Superiore canal (Municipality of Budrio) (Figure 18).

Figure 18 - Cartographic framing of S8.

Figure 19 – S8 after intervention.

S8 is situated at the confluence where the Cornamonda Nuova canal enters the Gallina Superiore canal, south-east of the hamlet of Dugliolo (Figure 19). It lies 2.5 km from Site 7 and 2 km in a straight line from the boundary of Natura 2000 site IT4050023 - SCI-SPA “Biotopes and environmental restorations of Budrio and Minerbio”. The surrounding landscape is dominated by arable fields.

The intervention area corresponds to the wedge of level agricultural land at the junction of the two canals, which had been farmed until 2022 by the adjoining holding.

In November 2022, the banks of the canals were modified at this site by shifting the slope of the bank.

On completion of the work, in March 2023, 128 pots of native wetland plants from 15 species were planted.

Site S9

Total area: 9,800 m²

Coordinates: 44°40'48"N 11°36'48"E

Elevation: 9 m a.s.l.

Location: Bank situated between the left bank of the Botte canal and the right embankment of the Savena Abbandonato, a natural watercourse (Municipality of Baricella) (Figure 20).

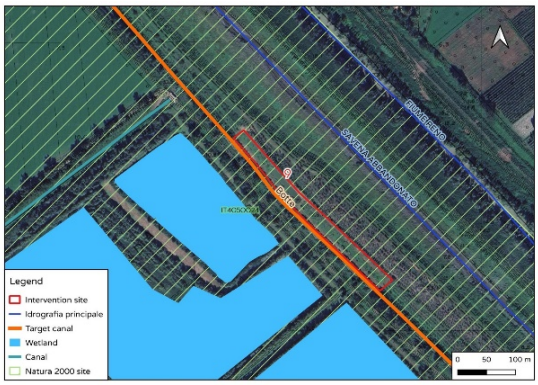

Figure 20 - Cartographic framing of S9.

Figure 21 – S9 after intervention.

S9 is the largest intervention area and is situated on the left bank of the Botte canal (Figure 21), inside and toward the northern boundary of Natura 2000 site IT4050024 - SCI-SPA “Biotopes and environmental restorations of Bentivoglio, San Pietro in Casale, Malalbergo and Baricella”. On the opposite bank lies the Gandazzolo Vecchia water retention basin, which comprises various wetlands.

The intervention area consists of a level bank segment 370 m long and 25 m wide between the left bank of the Botte canal and the right embankment of the Savena Abbandonato, a natural watercourse. The parcel covers 9,800 m² and, until 2021, was managed as a pulp-wood poplar plantation by the farm owned by Renana Remediation Consortium. The site lies below the crests of the surrounding levees; because it is enclosed within the embankments, the emergent area may experience prolonged inundation during heavy-rainfall periods, favouring ecological processes typical of lowland floodplain forests.

In July 2021, the bank of the canal was modified at this site by shifting the slope of the bank. In addition, a pond of 650 m² was created. On completion of the work, in March 2022, 825 pots of native wetland plants from 29 species were planted.

6 Materials and Methods

6.1 Water sampling and chemical and physical analysis

Water was monthly monitored between May 2020 and September 2024. Before the restoration activity, water monitoring of the canal was carried out upstream of the intervention site. Once the restoration was completed, canal water was monitored both upstream and downstream of the intervention site, as well as from the constructed ponds.

Restoration interventions based on Nature-Based Solutions (NBS) were implemented at eight sites in total. Four sites (S4, S6, S7, and S9) involved the creation of constructed ponds connected to the canals, while the remaining four (S1, S2, S5, and S8) were subject to canal bank reshaping interventions. All these sites were monitored following the same sampling protocol.

Although all four pond-creation sites were subject to the same type of intervention, they were analysed separately due to differences in canal water level dynamics. S4 and S9 are characterized by relatively stable water levels throughout the year, while S6 often dries out during the summer months and S7 experiences a significant drop in water level during winter, mainly due to the hydrological management of the canals.

According to Poesio et al. (2023), water levels in the canals of the Po Plain are actively managed and generally reduced from October to March (non-irrigation period, NIR) to ensure hydraulic safety, while remaining higher from April to September (irrigation period, IR) for agricultural use. However, not all canals are affected equally: in some canals, the water level drops drastically during NIR, whereas in others it remains more constant. Sites 4 and 9 fall into this latter category, allowing for a consistent seasonal comparison.

For this reason, only for sites 4 and 9 water data were presented and statistically analysed by season (summer/winter), while for sites 6 and 7 this distinction was not applicable due to the lack of comparable winter data.

In the field, water temperature (°C), pH, electrical conductivity (µS/cm), dissolved oxygen (mg/L), nitrate nitrogen (N-NO_3^-) (mg/L), and ammoniacal nitrogen (N-

NH_4^+) (mg/L) were measured using a multiparameter probe (Figure 22, Aquabrobe® 2000).

Figure 22 - In field water monitoring.

Water was sampled using a telescopic rod, placed in glass bottles, and then transported to the laboratory for chemical and physical analysis. Once in the laboratory, roughly 100 mL of each sample was filtered through Whatman 42 filter paper for the determination of total element concentrations.

The concentrations of several chemical parameters were evaluated in the laboratory, including:

- **Total element content determination**

The total amount of for example Al, Cu, Fe, P, etc. was measured by Inductively Coupled Plasma Optical Emission Spectrometry (ICP-OES, Arcos II, Kleve, Germany, Ameteck Spectro).

- **Determination of total organic carbon and total nitrogen**

The total organic carbon and total nitrogen contents were measured using a Shimadzu Total Organic Carbon TOC-V CPN.

- **Determination of suspended solids**

In weighed crucibles, 20 mL of unfiltered sample were added and placed in the oven at 105 °C. Once dried, they were weighed, and the suspended solid content was calculated by dividing the mass of solid particles within the crucibles by the volume of the samples used for the analysis (20 mL). The suspended solids content was obtained by calculating the difference in the weight of the pre- and post-oven crucibles and relating it to the sample volume.

6.2 Sediment sampling and chemical and physical analysis

Sediment was sampled twice a year: in December and July, between 2020 and 2024. Sediment samples were collected using an Ekman dredge (Figure 23), which allowed for the retrieval of a substrate column. The samples were then air-dried, sieved to remove coarse particles (>2 mm), and an aliquot was finely ground and stored in containers for subsequent analysis.

Figure 23 - Ekman dredge.

Chemical and physical analyses performed on the sediments included:

- **Determination of pH (ISO 10390) ed EC (ISO 11265)**

In 50 mL centrifuge tubes, 10 g of sample and 25 mL of distilled water were added. The suspension was shaken for 2 hours on a horizontal shaker, afterwards the pH was measured with a Crison pH meter and conductivity was determined with a CDM210 conductivity meter.

- **Determination of $CaCO_3$**

Through the use of the Dietrich-Frühling calcimeter, gas-volumetric determination of CO_2 was carried out by treating an aliquot finely ground sediment (~1g) with 5mL of hydrochloric acid (HCl, 6M).

- **Determination of particle size distribution**

The size classes used were based on the USDA classification system (Soil Survey Division Staff, 1993). The particle size distribution was determined using the 'pipette method.'

Briefly, 10 g of sediment was placed in 50 mL tubes, and 25 mL of deionized water and 10 mL of sodium hexametaphosphate solution were added. The resulting suspension was shaken for two hours to allow for the physical and physicochemical dispersion of the particles. Afterwards, the suspension was sieved through a 50-µm sieve to separate the sand (Ø > 50 µm) from the silty and clay fractions. The sand was collected in ceramic crucibles, dried at 105 °C, and then weighed. The silt and clay suspension was transferred into 1000 mL cylinders and made up to volume with distilled water.

In a temperature-controlled environment, the cylinders were shaken and left the silt fraction to settle. Then, 10 mL of suspension was taken up and transferred into weighed crucible. The crucible was placed in the oven at 105 °C overnight, allowed to cool in a desiccator, and finally weighed. The silt content was obtained by subtracting the sand and clay fractions to the total amount of sample used for the analysis.

- **Determination of total element content**

An aliquot of about 0.25 g of sediment was subjected to mineralization by digestion in aqua regia. Determination of the elements (for example Al, B, Be, etc.) in the samples was carried out by ICP.

- **Determination of total organic carbon and total nitrogen**

Sediments were weighed in silver capsules treated with acid to remove carbonates and analysed by a CN elemental analyser (Thermo Flash 2000, Thermo Fisher Scientific, USA). For the determination of stable isotopes ^{13}C and ^{15}N, a Delta C magnetic resonance mass spectrometer (IRMS) was used.

6.3 Vegetation survey

A transect-quadrat method was used to assess species composition and to estimate their percent-cover along the bank of canals and ponds. The transects 1.5 m width and 40 m long were laid parallel to the canals and the ponds. Within each transect, 4 plots 5 m long and 5 m far one each other were established. The vegetation survey was conducted in autumn and spring when most of the vascular plants flourish and the peak of vegetation occurs. The ground cover-abundance values (%) of all plant species located within each plot were determined by visual estimation according to the principles of the Braun-Blanquet method (Braun-Blanquet, 1928; 1964; Barkman et al., 1964; Damgaard, 2014). In addition, the species and cover were recorded for each plot.

Into groups based on expert knowledge of plant species autecology and of local vegetation. The groups were supposed to be used informally to distinguish between species that could indicate improved ecological conditions due to the reduction of embankment steepness and pond construction (i.e. aquatic or hygrophylus species) and species that are associated with disturbance caused by the works or surrounding land use or recruitment of invasive species. The groups resulted informative to analyse the vegetation dynamics due to the work and were maintained throughout the study. The groups are:

- **aquatic/hygrophilous species**: plants typical of aquatic/wetland environments (hydrophytes, helophytes) and hygrophilous species that would not occur in this type of environment without canals.
- **crops species**: plants usually cultivated in fields of neighbouring crops or weeds typical of crops or overgrown fields.
- **floodplain forest species**: species typical of Po Plain floodplain forests (*Quercus robur* woods, *Fraxinus* spp. woods…), mainly woody hygrophilous plants.
- **ruderal species**: nitrophilous large size species, living in disturbed areas, rich in available nitrogen in the soil or in canals' water.
- **invasive species**: introduced and invasive alien species.

- **ubiquitous species**: species colonizing multiple habitats affected by some kind of disturbance. These species are not associated to a specific habitat or nitrogen abundance but thrive everywhere they find idoneous conditions to grow.
- **pastures species**: species adapted to the disturbance of pastures (removal of above-ground biomass), which is actually similar to the disturbance caused by mowing along the canals.
- **unclassifiable species**: unidentified species (e.g., plant identified at genus-level only), that could not be associated to their habitats.

Based on this classification, vegetation data were elaborated to highlight both structural and compositional dynamics. For each transect and survey year, the total percentage cover of the different socio-ecological groups was calculated by summing the cover of all species belonging to the same group. Within each group, the dominant species were identified as those showing the highest relative cover, expressed as a percentage of the group total. This approach allowed us to track changes in vegetation structure and floristic composition before and after restoration interventions.

In addition, biodiversity indices were calculated to assess community-level responses. Margalef's Richness Index (Dm) was used to describe temporal changes in species richness, while Shannon's Diversity Index (H′) integrated both richness and evenness. These indices were applied to each site and year, enabling comparisons across sites and between canal and pond habitats.

This combined framework, ecological groups, dominant species, and diversity indices, provided the basis for interpreting vegetation dynamics and for relating vegetation changes to restoration works, flood events, and site-specific conditions.

6.4 Statistical Analysis and calculation

The collected data were analysed to assess both spatial (upstream, downstream, and pond) and temporal (year and pre/post restoration) changes in water and sediment properties. All statistical processing was conducted using RStudio software 4.2.3 Boxplots were used to show the median, interquartile range, and the presence of outliers, highlighting the distribution and variability of the data over time. The boxplots were built through the use of *ggplot2* and *boxplot* packages. Additionally, the mean and standard deviation were used to present certain data (e.g., pH, B, Ba, Fe, etc.).

Statistical analyses performed included:

- **Analysis of variance:** for each intervention site, the Kruskal-Wallis test was used to analyse the differences among the sampling years, seasons (autumn-winter and spring-summer), and sites (upstream, downstream, and pond). This approach was chosen due to the lack of normality and homoscedasticity of the data. The R package 'agricolae' was used for this analysis.

- **Determination of Sodium Adsorption Ratio (SAR)**

$$SAR = \frac{[Na^+]}{\sqrt{\frac{[Ca^{2+}] + [Mg^{2+}]}{2}}}$$

Na^+, Ca^{2+} and Mg^{2+} are total contents obtained by inductively coupled plasma optical emission spectrometry (ICP-OES) using a SPECTRO Analytical Instruments GmbH & Co. instrument (Kleve, Germany).

- **Shannon Index**

It proved to be a sensitive tool for detecting changes in community composition over time and across different sites. This sensitivity is particularly evident with respect to rare species, which, despite their low abundance, contribute

significantly to the overall index due to the mathematical formulation of H′. Its ability to incorporate both species richness and evenness within a single metric makes it widely applicable and valuable in ecological research (Magurran, 2004; Spellerberg & Fedor, 2003). In the context of this study, variations in the Shannon index across sites and years reflect the effects of hydrological changes and management interventions on biological diversity, highlighting its utility as a diagnostic and comparative tool.

$$H' = -\sum_{j=1}^{S} p_i \ln(pi)$$

Where:

- H' = Shannon diversity index (a measure of species diversity)
- S = total number of species (species richness)
- p_i = proportion of individuals belonging to species i
- n_i = number of individuals of species i
- N = total number of individuals of all species

- **Margalef's Richness Index**

It is an ecological measure used to quantify the species richness of a community, taking into account the total number of individuals sampled. This index is particularly useful for comparing biodiversity among communities with different sample sizes and ecosystems, as it normalizes species richness relative to total abundance (Sina & Zulkarnaen, 2018; Wang et al., 2023). However, it does not consider the evenness of individual distribution among species.

$$D_{Mg} = \frac{(S-1)}{\ln(N)}$$

Where:

- D_{Mg} = Margalef's species richness index
- S = total number of species observed
- N = total number of individuals of all species

To assess the temporal evolution of plant coverage, the “dominant species” approach was carried out. This approach was based on the identification of those plants species showing the highest coverage. In our case, we identified the “dominant species” for each *socio-ecological groups with an average coverage > 5% (McNellie et al., 2019; Pipenbaher, 2024; Westhoff & van der Maarel, 1978).* The decision to exclude socio-ecological groups with an average coverage < 5% is consistent with the Braun-Blanquet approach, which assigns unit values only to species reaching a minimum threshold of 5% cover.

However, such threshold was lowered to 1 % for the study sites with pond construction due to the more intense restoration activities that greatly reduced the vegetation coverage. Stacked bar charts were produced to illustrate the percentage composition of ecological groups for each site (S1, S2, S5, S8) from 2020 to 2024. These charts provide a visual synthesis of the coverage trends for each group, allowing for a quick identification of transitional phases, disturbance events, or re-equilibration processes.

7 Results and discussion

7.1 Influence of bank reshaping on water quality: Sites S1, S2, S5 and S8

The pH showed values ranging between 7.47 and 8.52 during the considered years (Table 2), though they remained within the typical range for surface waters (range 6.5-8.5) (Dewangan, S. K., et al., 2023; Bundschuh, M., et al., 2016).

In 2022 there is an increase in pH value probably related to reshaping of the banks that contributed to the mobilisation of alkaline elements present in the lithological material of the area.

In all sites, the lowest pH value was observed in 2020, when significant reductions of anthropogenic pressures were recorded due to restrictive measures linked to the COVID-19 pandemic, improving the quality of water bodies (Mohinuddin et al., 2023; Uddin et al., 2023). Conversely, the highest pH value was found in 2023 probably related to the heavy flooding occurred in May that transported mineral particles from the catchment area which is mostly characterized by alkaline lithology (Pavanelli and Selli, 2013; Davide et al., 2003). In support of this interpretation, Figure 24 shows the monthly average temperature and total precipitation recorded in the study area between January 2020 and December 2024. A clear peak in rainfall occurred in May and June 2023, when precipitation values were substantially higher than in the same months of previous years. These heavy rains caused flooding across the region, promoting intense surface runoff and soil erosion.

Such events likely contributed to change the concentration of several water parameters during 2023. In particular, the mobilisation of alkaline particles from the lithological matrix may explain the higher pH values, while the leaching of nutrients and the input of suspended sediments may have increased concentrations of nitrogen (Ntot), aluminium (Al), and iron (Fe).

These findings highlighted how extreme weather events can temporarily alter the chemical characteristics of canal water, even in systems where restoration interventions were implemented. Similar results were reported by several authors, who observed that flood events can mobilize nutrients and metals from

surrounding soils and sediments, increase suspended solids, and cause significant short-term changes in water chemistry (Chang ChiaJung, C. C., et al., 2020; Mishra, A. et al., 2021; Zhang, Y., 2024; Liu, Z. et al., 2024).

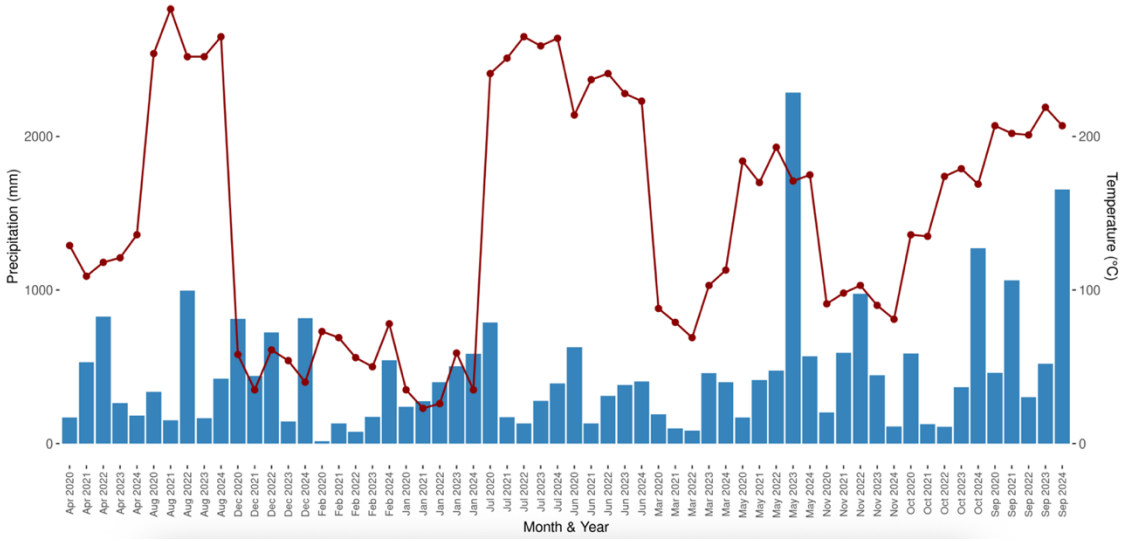

Figure 24 - Monthly average temperature and total precipitation in the study area (2020-2024)

Total nitrogen concentration (Ntot) tended to have higher values in 2022 and 2023 than in the other years (Table 3) and the lowest ones in 2020. As observed for pH, the lowest Ntot content in 2020 can be attributed to COVID-19 lockdown (Yunus et al., 2020; Sherman et al., 2023). The highest Ntot concentrations in 2022 might be related to reshaping of the banks that promoted the organic matter mineralization of the bank soil with consequent release of nutrient like nitrogen (Whalen, J. K., et al., 2000).

In 2023, the high Ntot content was driven by the increase of such nutrient in May. Specifically, this month was characterized by heavier rains than in May of the other studied years (ARPAE, 2025). Therefore, the more abundant rains may be promoted the leaching of nitrogen from the surrounding agricultural area in water (Mo, X., et al., 2022).

The concentrations of barium (Ba), magnesium (Mg), manganese (Mn), silicon (Si) and sulphur (S) did not show differences among the years (Table 4) suggesting their unresponsiveness to natural and man-based environmental changes (Alekseenko, V., & Alekseenko, A., 2014).

Table 2 - Mean ± standard deviation of water pH of canals subjected to bank reshaping. Within each column, different letters stand for significant differences among the means according to Kruskal-Wallis test ($p \leq 0.05$).

Year	Location	Site 1	Site 2	Site 5	Site 8
2020	Upstream	$7.47 \pm 0.09\ b$	$7.42 \pm 0.16\ d$	$7.79 \pm 0.23\ b$	$7.8 \pm 0.18\ b$
2021	Upstream	$7.90 \pm 0.48\ a$	$7.72 \pm 0.30\ bc$	$8.00 \pm 0.37\ b$	$8.10 \pm 0.38\ ab$
2022	Upstream	$7.60 \pm 0.20\ ab$	$7.63 \pm 0.33\ cd$	$8.23 \pm 0.37\ b$	
	Downstream	$7.61 \pm 0.21\ ab$	$7.55 \pm 0.21\ cd$		$8.05 \pm 0.37\ b$
2023	Upstream	$7.78 \pm 0.29\ a$	$8.01 \pm 0.14\ a$	$8.52 \pm 0.11\ a$	$8.23 \pm 0.24\ a$
	Downstream	$7.77 \pm 0.23\ a$	$7.93 \pm 0.19\ a$b	$8.48 \pm 0.14\ a$	$8.20 \pm 0.20\ a$
2024	Upstream	$7.58 \pm 0.54\ ab$	$7.61 \pm 0.29\ cd$	$7.90 \pm 0.29\ b$	$7.93 \pm 0.21\ b$
	Downstream	$7.60 \pm 0.48\ ab$	$7.62 \pm 0.24\ cd$	$7.98 \pm 0.29\ b$	$7.94 \pm 0.23\ ab$

Table 3 - Mean ± standard deviation of total nitrogen content of canals subjected to bank reshaping. Within each column, different letters stand for significant differences among the means according to Kruskal-Wallis test (p ≤ 0.05).

Year	Location	Site 1	Site 2	Site 5	Site 8
			mg L^{-1}		
2020	Upstream	$0.84 \pm 0.27\ c$	$0.78 \pm 0.30\ b$	$0.80 \pm 0.15\ c$	$1.28 \pm 0.45\ c$
2021	Upstream	$1.38 \pm 1.78\ bc$	$1.19 \pm 1.19\ b$	$1.00 \pm 0.20\ bc$	$1.09 \pm 0.44\ c$
2022	Upstream	$5.17 \pm 8.57\ ab$	$2.30 \pm 3.36\ b$	7.67 ± 10.77 bc	
	Downstream	$6.44 \pm 11.37\ a$	$2.38 \pm 4.03\ b$		6.03 ± 8.62 bc
2023	Upstream	$5.26 \pm 5.71\ ab$	$3.55 \pm 2.40\ a$	$8.49 \pm 11.40\ ab$	$4.81 \pm 8.35\ ac$
	Downstream	$5.46 \pm 6.08\ ab$	$3.22 \pm 2.08\ a$	$8.79 \pm 11.79\ ab$	$4.73 \pm 8.24\ ac$
2024	Upstream	$4.63 \pm 3.39\ b$	$3.19 \pm 1.45\ a$	$5.64 \pm 7.96\ a$	$3.09 \pm 2.02\ ab$
	Downstream	$4.62 \pm 3.41\ b$	$3.15 \pm 1.48\ a$	$5.55 \pm 7.97\ a$	$4.60 \pm 5.59\ a$

Table 4 - Mean ± standard deviation of boron (B), barium (Ba), magnesium (Mg), manganese (Mn), sulphur (S) and silicon (Si) contents of canals subjected to bank reshaping. Within each row, different letters stand for significant differences among the means according to Kruskal-Wallis test ($p \leq 0.05$).

Site	Parameter (mg L-1)	2020	2021	2022		2023		2024	
		Upstream	Upstream	Upstream	Downstream	Upstream	Downstream	Upstream	Downstream
S1	B	$0.18 \pm 0.08\ b$	$0.31 \pm 0.13\ a$	$0.36 \pm 0.20\ a$	$0.39 \pm 0.20\ a$	$0.24 \pm 0.11\ ab$	$0.23 \pm 0.09\ ab$	$0.19 \pm 0.07\ b$	$0.19 \pm 0.07\ b$
	Ba	$66.1 \pm 8.59\ ab$	$66.2 \pm 9.18\ b$	$77.6 \pm 11.3\ ab$	$80.7 \pm 14.1\ a$	$60.7 \pm 33.1\ ab$	$59.9 \pm 32.9\ ab$	$54.4 \pm 27.8\ b$	$54.9 \pm 28.1\ b$
	Mg	$14.6 \pm 1.68\ b$	$18.1 \pm 3.04\ ab$	$20.6 \pm 6.81\ ab$	$21.1 \pm 7.59\ ab$	$21.7 \pm 9.95\ a$	$21.7 \pm 6.01\ a$	$19.4 \pm 5.49\ ab$	$19.5 \pm 5.56\ ab$
	Mn	$52.1 \pm 38.6\ a$	$44.7 \pm 21.1\ a$	$55.4 \pm 60.3\ a$	$34.7 \pm 38.2\ a$	$33.7 \pm 24.9\ a$	$20.1 \pm 19.6\ a$	$29.6 \pm 25.7\ a$	$29.3 \pm 25.1\ a$
	S	$14.7 \pm 2.33\ b$	$20.4 \pm 5.83\ ab$	$26.5 \pm 17.2\ ab$	$25.6 \pm 15.2\ ab$	$21.9 \pm 5.82\ ab$	$22.1 \pm 5.74\ ab$	$25.1 \pm 10.75\ a$	$25.2 \pm 9.95\ a$
	Si	$0.91 \pm 0.15\ a$	$0.59 \pm 0.21\ b$	$0.52 \pm 0.25\ b$	$0.52 \pm 0.22\ b$	$0.62 \pm 0.54\ ab$	$0.60 \pm 0.54\ ab$	$0.70 \pm 0.49\ ab$	$0.69 \pm 0.47\ ab$
S2	B	$0.19 \pm 0.09\ c$	$0.30 \pm 0.16\ bc$	$0.40 \pm 0.17\ ab$	$0.36 \pm 0.16\ ac$	$0.22 \pm 0.07\ bc$	$0.22 \pm 0.06\ bc$	$4.55 \pm 7.13\ a$	$5.90 \pm 8.19\ a$
	Ba	$88.8 \pm 10.87\ a$	$103.8 \pm 14.4\ a$	$104.2 \pm 12.4\ a$	$96.9 \pm 20.3\ a$	$111.9 \pm 46.8\ a$	$109.4 \pm 46.3\ a$	$78.1 \pm 19.5\ a$	$80.3 \pm 19.2\ a$
	Mg	$16.3 \pm 1.78\ a$	$19.7 \pm 4.65\ a$	$21.6 \pm 7.75\ a$	$21.4 \pm 8.22\ a$	$24.2 \pm 11.4\ a$	$23.7 \pm 10.8\ a$	$22.3 \pm 16.4\ a$	$22.2 \pm 16.3\ a$
	Mn	$103.6 \pm 60.1\ a$	$182.7 \pm 233.6\ a$	$65.1 \pm 45.5\ ab$	$54.4 \pm 29.1\ ab$	$32.1 \pm 28.3\ b$	$29.9 \pm 38.2\ b$	$38.2 \pm 38.5\ b$	$50.2 \pm 54.3\ ab$
	S	$18.4 \pm 3.30\ a$	$25.8 \pm 13.8\ a$	$28.3 \pm 20.9\ a$	$28.3 \pm 21.1\ a$	$34.4 \pm 17.1\ a$	$35.2 \pm 18.3\ a$	$35.1 \pm 36.3\ a$	$34.6 \pm 36.3\ a$
	Si	$0.76 \pm 0.16\ a$	$0.68 \pm 0.38\ a$	$0.46 \pm 0.26\ a$	$0.48 \pm 0.23\ a$	$0.54 \pm 0.54\ a$	$0.55 \pm 0.54\ a$	$0.55 \pm 0.41\ a$	$0.56 \pm 0.40\ a$
S5	B	$0.12 \pm 0.11\ ab$	$0.08 \pm 0.04\ b$	$0.19 \pm 0.07\ a$		$0.12 \pm 0.06\ ab$	$0.12 \pm 0.06\ ab$	$0.13 \pm 0.08\ ab$	$0.13 \pm 0.08\ ab$
	Ba	$59.6 \pm 10.1\ a$	$55.8 \pm 7.95\ a$	$88.5 \pm 53.8\ a$		$80.1 \pm 58.5\ a$	$120.9 \pm 101.9\ a$	$63.5 \pm 17.5\ a$	$61.6 \pm 21.8\ a$
	Mg	$12.2 \pm 2.07\ b$	$14.3 \pm 2.15\ ab$	$18.7 \pm 7.98\ ab$		$19.6 \pm 6.99\ a$	$19.4 \pm 6.50\ a$	$17.2 \pm 6.50\ a$	$16.9 \pm 6.18\ a$
	Mn	$3.13 \pm 4.75\ c$	$9.45 \pm 8.09\ ac$	$8.60 \pm 7.85\ ac$		$4.93 \pm 2.37\ bc$	$6.42 \pm 4.22\ ac$	$19.5 \pm 21.5\ ab$	$27.8 \pm 39.4\ a$
	S	$13.2 \pm 0.83\ b$	$16.6 \pm 2.26\ ab$	$21.7 \pm 10.7\ ab$		$22.1 \pm 8.61\ a$	$21.8 \pm 8.15\ a$	$20.5 \pm 8.81\ a$	$20.2 \pm 7.92\ a$
	Si	$0.59 \pm 0.11\ a$	$0.59 \pm 0.10\ a$	$0.48 \pm 0.43\ a$		$0.44 \pm 0.51\ a$	$0.45 \pm 0.52\ a$	$0.81 \pm 0.34\ a$	$0.82 \pm 0.33\ a$
S8	B	$0.10 \pm 0.09\ b$	$0.09 \pm 0.06\ b$		$0.17 \pm 0.06\ b$	$0.11 \pm 0.08\ b$	$0.11 \pm 0.08\ b$	$0.71 \pm 1.33a$	$0.14 \pm 0.10\ a$
	Ba	$50.5 \pm 6.88\ b$	$52.9 \pm 10.2\ b$		$86.1 \pm 55.9\ ab$	$95.6 \pm 57.4\ a$	$82.9 \pm 57.5\ ab$	$82.1 \pm 53.2\ ab$	$84.2 \pm 46.2\ ab$
	Mg	$11.2 \pm 1.97\ b$	$13.4 \pm 1.25\ ab$		$21.1 \pm 10.2\ a$	$21.1 \pm 9.88\ a$	$20.8 \pm 9.74\ a$	$18.2 \pm 10.2\ ab$	$18.9 \pm 12.1\ ab$
	Mn	$15.3 \pm 30.7\ b$	$12.9 \pm 7.41\ ab$		$32.2 \pm 30.3\ a$	$48.2 \pm 50.2\ a$	$50.7 \pm 51.9\ a$	$32.6 \pm 17.0\ a$	$43.5 \pm 37.3\ a$
	S	$12.2 \pm 1.18\ a$	$14.9 \pm 1.79\ a$		$20.5 \pm 13.7\ a$	$19.6 \pm 11.8\ a$	$19.6 \pm 11.6\ a$	$16.2 \pm 6.71\ a$	$18.0 \pm 10.1\ a$
	Si	$0.61 \pm 0.14\ a$	$0.57 \pm 0.23\ a$		$0.71 \pm 0.52\ a$	$0.72 \pm 0.62\ a$	$0.73 \pm 0.62\ a$	$0.91 \pm 0.37\ a$	$0.88 \pm 0.34\ a$

In all sites the concentrations of aluminium (Al), ammoniacal nitrogen (N-NH_4) show similar trends (Figure 25, Figure 26, Figure 27 and Figure 28), with significant increases from 2022, when the canal banks were reshaped, although the trends of Al and N-NH_4 at site S5 were less evident compared to those observed at the other sites.

The increase of Al in 2022 and 2023 (Figure 25A, 26A, 27A and 28A) can be attributed to disturbance of soil and sediment during the restoration activities carried out on the banks. Aluminium, which is frequently present in a form bound to soil colloids, can be mobilized in the presence of erosive phenomena or physical alterations facilitating its release into water (Bache, B. W., 1986; Nordstrom, D. K., & Ball, J. W., 1986). However, we cannot exclude the influence of the intense precipitations occurred in those years which could have promoted erosive processes of the surrounding soils with consequent Al mobilization (Kopáček et al., 2009; Moon et al., 2011).

The increased N-NH_4 content (Figure 25B, 26B, 27B and 28B) observed in 2022 and 2024 might be due to the mineralization of soil organic matter (Marzi et al., 2020) boosted by the heavy soil tillage of the bank soil (Kristensen et al., 2003; Kabiri et al., 2016). While, the slight higher N-NH_4 content in 2024 could be attributed to the probably abundant use of N-based fertilizers to cope with the unfertile sediments deposited on agricultural lands during the flooding occurred in 2023 (De Feudis et al., 2024).

The P content did not show significant differences among the years with exception of S2 which showed a slight decrease after the restoration action. In this site, besides bank reshaping, a land use change was implemented through the re-naturalization of an agricultural area. This land use change may have contributed to reduce the P leaching from soil because of both reduction of P-based fertilizers and the role of vegetation to catch nutrients (McDowell et al., 2010; Stutter, M.I., et al., 2012). Although also site S8 underwent re-naturalization of a portion of a cropland, the absence of differences of P content in water can be attributed to much smaller area subjected to land use change compared with S2.

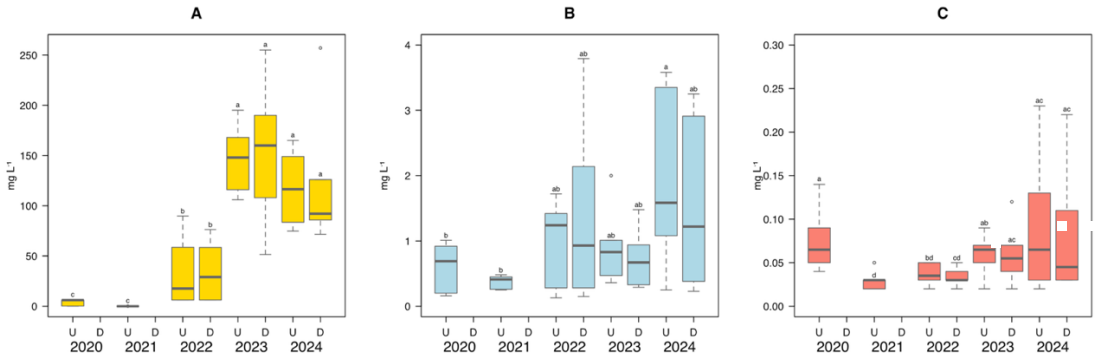

Figure 25 - Boxplot showing the aluminium (A), ammoniacal nitrogen (B) and phosphorus (C) concentrations in the water of site S1 for the years 2020-2024. Different letters stand for significant differences among the means according to Kruskal-Wallis test (p ≤ 0.05).

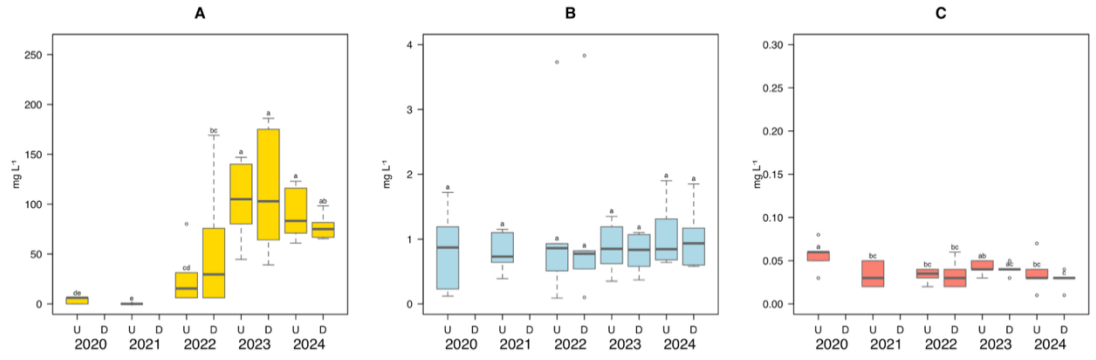

Figure 26 - Boxplot showing the aluminium (A), ammoniacal nitrogen (B) and phosphorus (C) concentrations in the water of site 2 for the years 2020-2024. Different letters stand for significant differences among the means according to Kruskal-Wallis test (p ≤ 0.05). U: upstream; D: downstream.

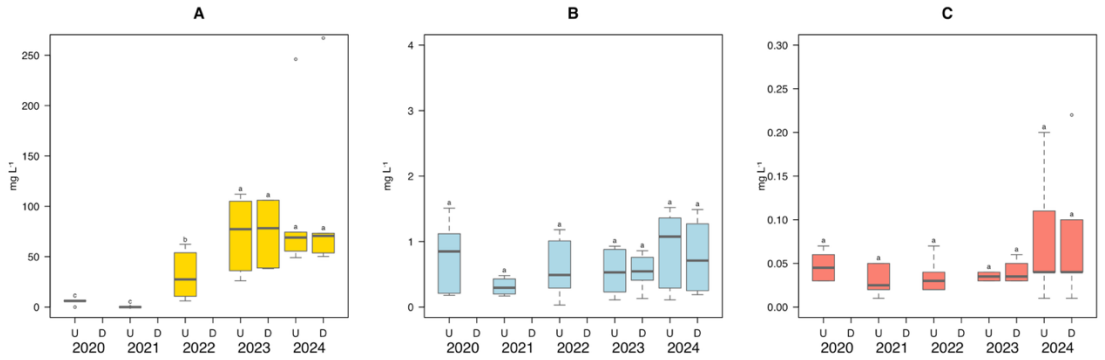

Figure 27 - Boxplot showing the aluminium (A), ammoniacal nitrogen (B) and phosphorus (C) concentrations in the water of site 5 for the years 2020-2024. Different letters stand for significant differences among the means according to Kruskal-Wallis test (p ≤ 0.05).

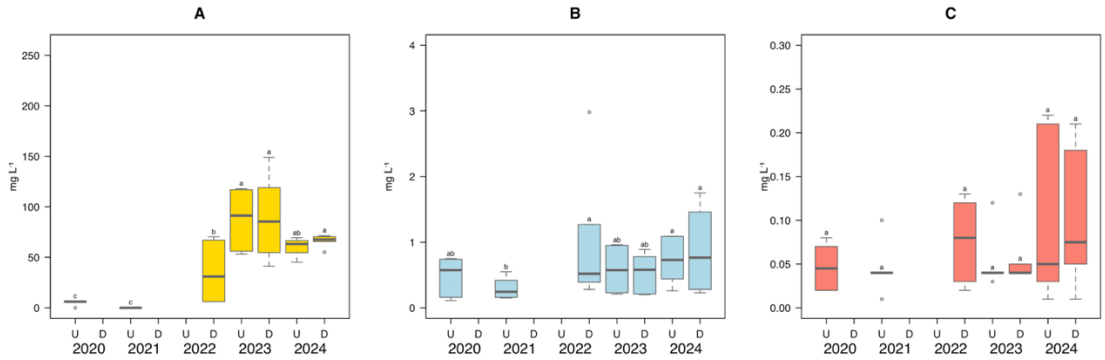

Figure 28 - Boxplot showing the aluminium (A), ammoniacal nitrogen (B) and phosphorus (C) concentrations in the water of site 8 for the years 2020-2024. Different letters stand for significant differences among the means according to Kruskal-Wallis test ($p \leq 0.05$).

The parameters related to salinity, electrical conductivity (EC) and sodium adsorption ratio (SAR), showed an increasing trend in the observed period (2020-2024), especially from 2022.

As shown in Figure 29B, 30B, 31B, 32B, at all sites, the EC progressively increased over the years, with higher average values in 2023 and 2024, indicating a gradual accumulation of dissolved salts in the system (Qiu, J., et al., 2023). This increase can be attributed to several factors:

- a reduction in dilution due to less frequent precipitation (Haygarth et al., 2005); the introduction of sea water in rivers due to the sea level rise and increase use fresh water for irrigation (Georgofili, 2024). In this context, it is important to mention that the considered study area is affected by sea water intrusion which negatively affect the quality of both surface and groundwater (Gaiolini et al., 2025; Buscaroli and Zannoni, 2010; Vittori Antisari et al., 2020);
- an increase in the intake of solutes from agricultural activities, especially fertilizers (Teatini, P., et al., 2005);
- the possible contribution of secondary drainage waters, as observed in agricultural environments subject to remediation (Vero et al., 2017).

At site S5, although an increasing trend in EC is observed, the values are lower compared to sites S1 and S2. This may be due to lower agricultural pressure or

greater efficiency in runoff and vertical percolation, which limits the accumulation of salts in the canal. The possible contribution of secondary drainage waters, as observed in agricultural environments subject to remediation (Vero et al., 2017). The SAR showed a progressive increase from 2021 with highest values in 2024 (Figure 29A, 30A, 31A, 32A). The increase of SAR may indicate both salinisation processes due to increased sodium and saline intrusion (Rengasamy & Olsson, 1991; Ayers & Westcot, 1985). At site S5, the SAR, although growing, shows lower values and greater inter-annual stability. While, at sites S2 and S8, the effects of the renaturalization initiated in 2022 may have helped to contain further increases.

However, it is important to mention that the considered study area is affected by sea water intrusion which negatively affect the quality of both surface and groundwater (Gaiolini et al., 2025; Buscaroli and Zannoni, 2010; Vittori Antisari et al., 2020).

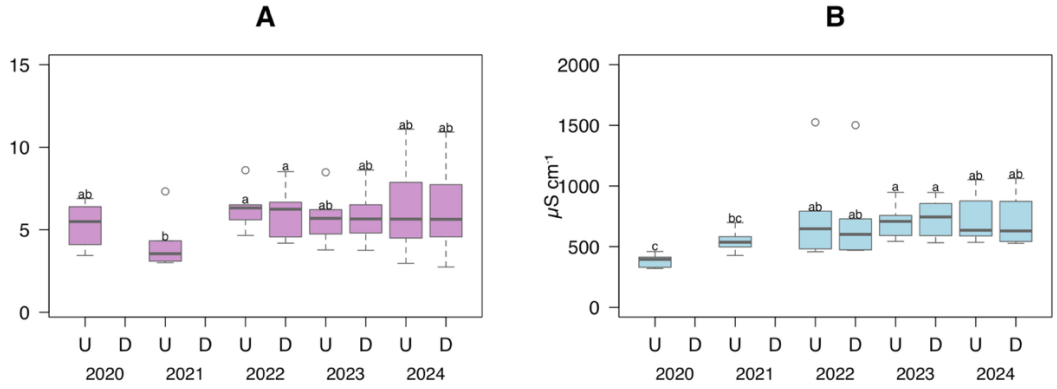

Figure 29 - Boxplot showing the sodium adsorption ratio (A) and electrical conductivity (B) in the water of site S1 for the years 2020-2024. Different letters stand for significant differences among the means according to Kruskal-Wallis test ($p \leq 0.05$). U: upstream; D: downstream.

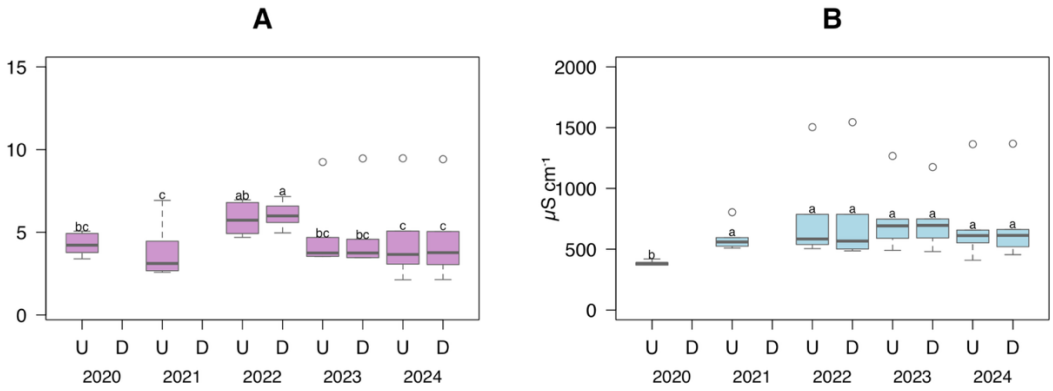

Figure 30 - Boxplot showing the sodium adsorption ratio (A) and electrical conductivity (B) in the water of site S2 for the years 2020-2024. Different letters stand for significant differences among the means according to Kruskal-Wallis test (p ≤ 0.05). U: upstream; D: downstream.

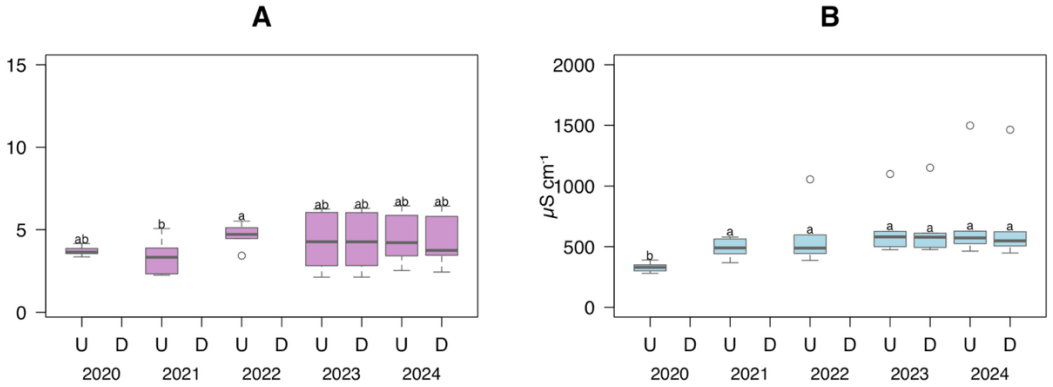

Figure 31 - Boxplot showing the sodium adsorption ratio(A) and electrical conductivity (B) in the water of site S5 for the years 2020-2024. Different letters stand for significant differences among the means according to Kruskal-Wallis test (p ≤ 0.05). U: upstream; D: downstream.

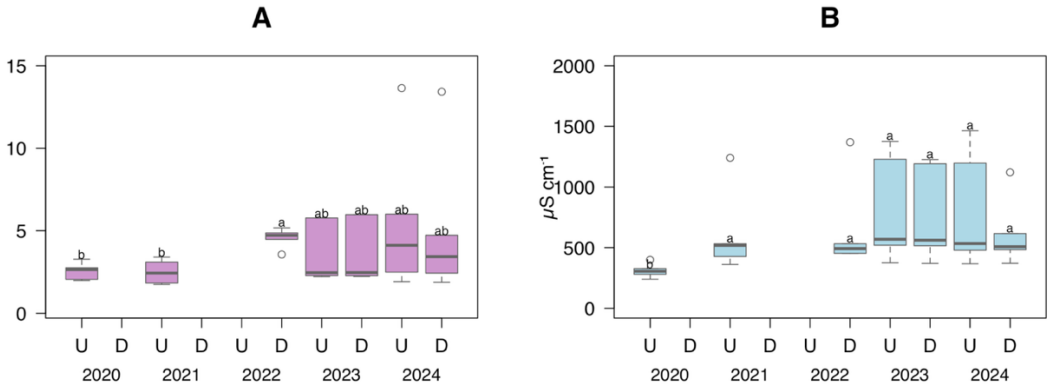

Figure 32 - Boxplot showing the sodium adsorption ratio(A) and electrical conductivity (B) in the water of site S8 for the years 2020-2024. Different letters stand for significant differences among the means according to Kruskal-Wallis test (p ≤ 0.05). U: upstream; D: downstream.

The contents for nitrate nitrogen ($N\text{-}NO_3^-$) (Figure 33A, 34A, 35A and 36A) and organic carbon (OC) (Figure 33B, 34B, 35B and 36B) showed the highest values in 2022. The increase of their concentrations in 2022 can be attributed to the restoration actions carried out in study sites.

Specifically, the reshaping of the banks through soil tillage might have promoted an intense mineralization of soil organic matter with consequent release of water-soluble organic carbon and nitrates. The observed dynamics is in line with literature, according to which disturbance events may temporarily increase nutrient and carbon loads in water bodies (Chen, Y., et al., 2015; Viaroli, P., et al., 2004).

At site 2, OC values tended to decrease more rapidly in 2023, suggesting a quicker response to post-intervention stabilization. While site 8 showed an intermediate behaviour. Since 2023 there was a decrease probably associated with the positive effect of renaturalisation, which favours the retention of carbon and nutrients in the soil and riparian vegetation (Zhu, G., et al., 2021; Kong, L., et al., 2023).

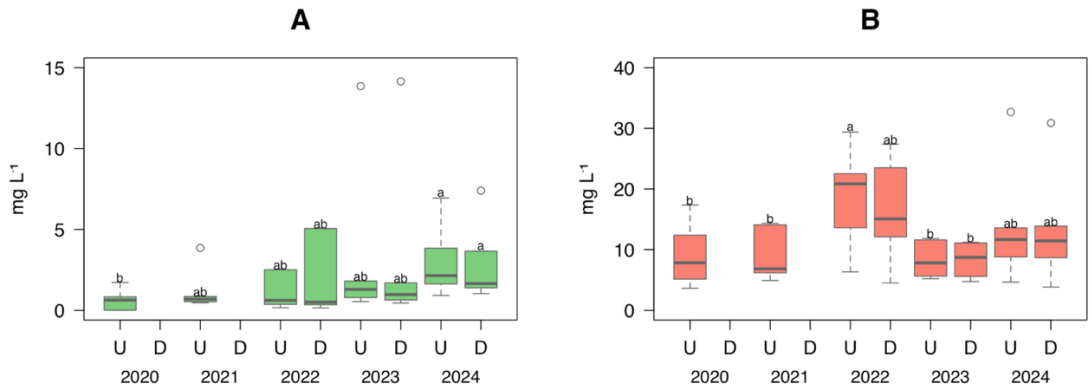

Figure 33 - Boxplot showing the nitrate nitrogen (A) e organic carbon (B) concentration in the water of site S1 for the years 2020-2024. Different letters stand for significant differences among the means according to Kruskal-Wallis test ($p \leq 0.05$). U: upstream; D: downstream.

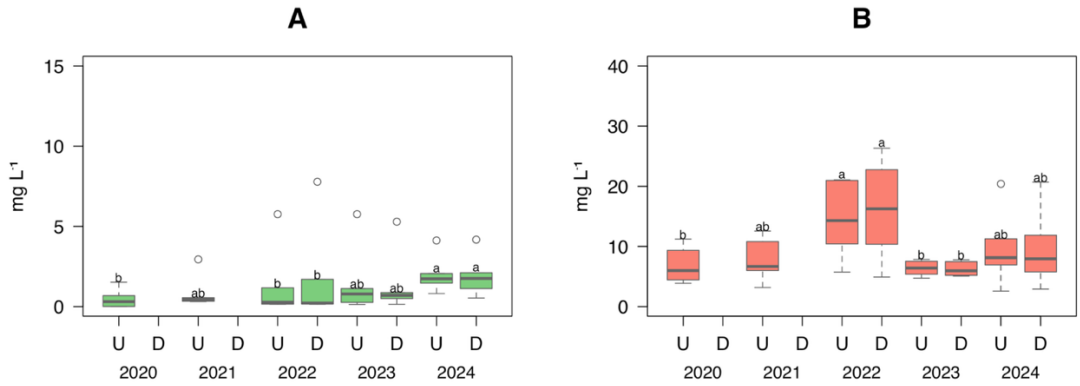

Figure 34 - Boxplot showing the nitrate nitrogen (A) e organic carbon (B) concentration in the water of site S2 for the years 2020-2024. Different letters stand for significant differences among the means according to Kruskal-Wallis test (p ≤ 0.05). U: upstream; D: downstream.

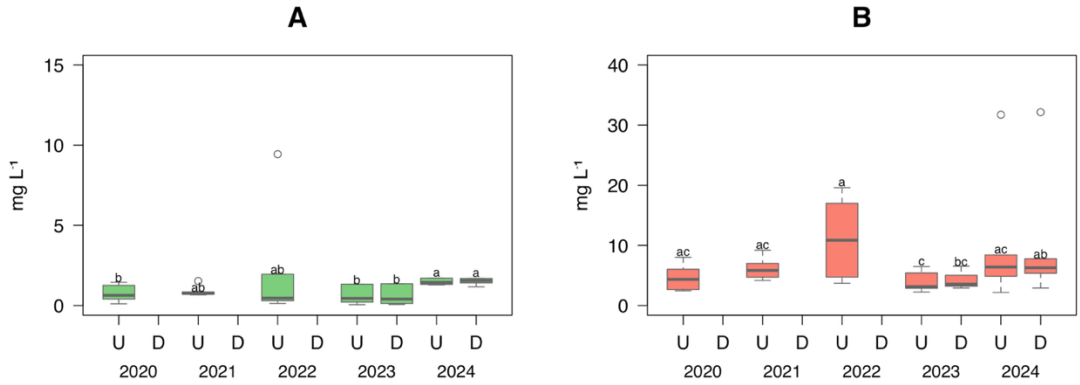

Figure 35 - Boxplot showing the nitrate nitrogen (A) e organic carbon (B) concentration in the water of site S5 for the years 2020-2024. Different letters stand for significant differences among the means according to Kruskal-Wallis test (p ≤ 0.05). U: upstream; D: downstream.

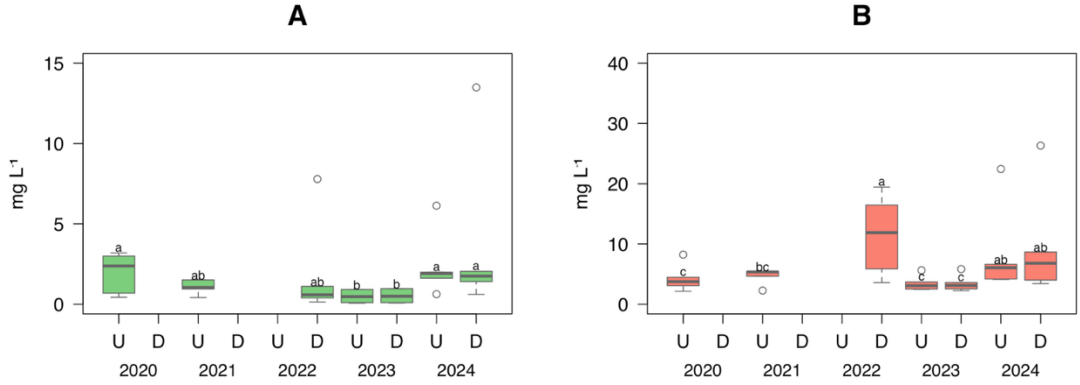

Figure 36 - Boxplot showing the nitrate nitrogen (A) e organic carbon (B) concentration in the water of site S8 for the years 2020-2024. Different letters stand for significant differences among the means according to Kruskal-Wallis test (p ≤ 0.05). U: upstream; D: downstream.

In all study sites, the dissolved oxygen (DO) content did not show significant differences over time ad showing values ranging between 7 and 9 mg L^{-1} (Figure 37, Figure 38, Figure 39 and Figure 40) which were in line with the DO content of European rivers (Feio et al., 2014; Williams and Boorman, 2012; Csábrági et al., 2019; Sánchez et al., 2007). The lack of differences among the years might be due to the numerous pumping systems characterizing the canal network which promote water oxygenation. Moreover, the limited presence of aquatic vegetation in certain sections and the absence of prolonged stagnation may have contributed to preventing summer hypoxia events, making dissolved oxygen a relatively stable parameter within the analysed canals (Miranda, L. E., & Hodges, K. B., 2000).

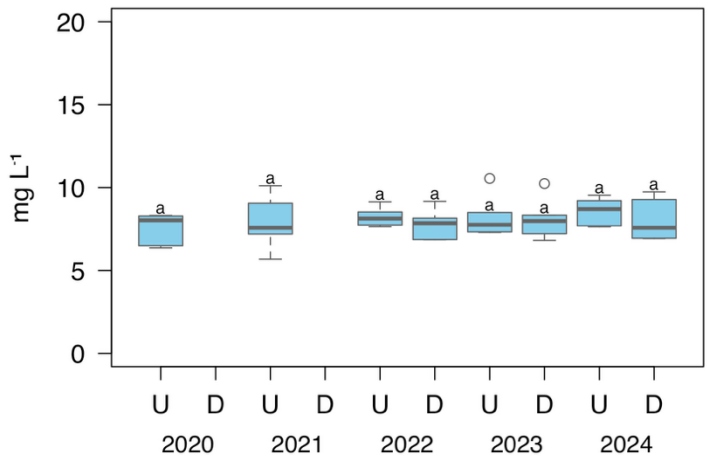

Figure 37 - Boxplot showing the dissolved oxygen concentration in the water of site S1 for the years 2020-2024. Different letters stand for significant differences among the means according to Kruskal-Wallis test ($p \leq 0.05$). U: upstream; D: downstream.

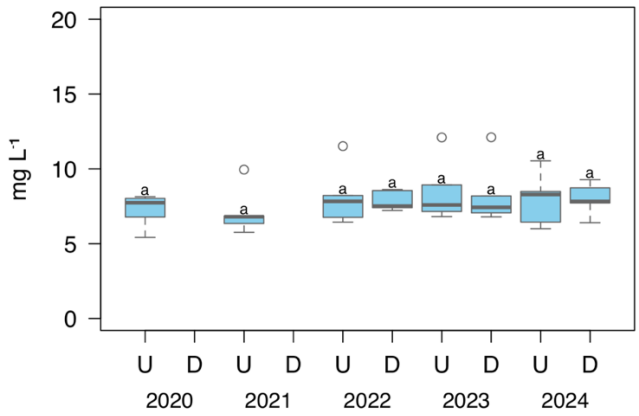

Figure 38 - Boxplot showing the dissolved oxygen concentration in the water of site S2 for the years 2020-2024. Different letters stand for significant differences among the means according to Kruskal-Wallis test ($p \leq 0.05$). U: upstream; D: downstream.

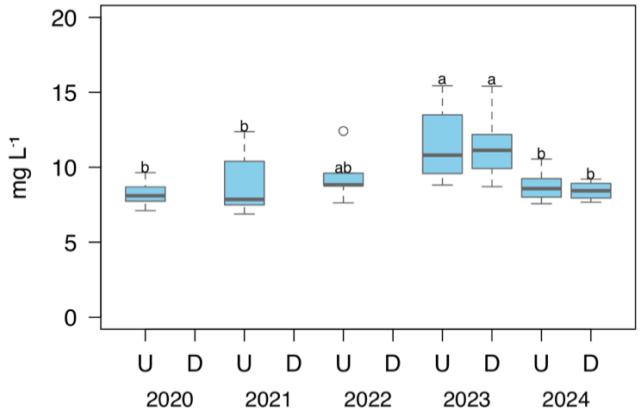

Figure 39 - Boxplot showing the dissolved oxygen concentration in the water of site S5 for the years 2020-2024. Different letters stand for significant differences among the means according to Kruskal-Wallis test ($p \leq 0.05$). U: upstream; D: downstream.

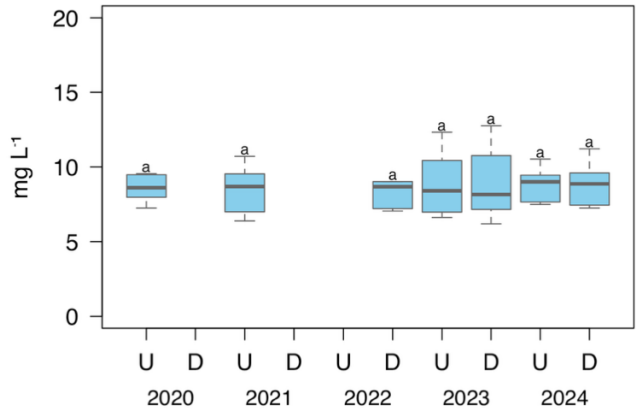

Figure 40 - Boxplot showing the dissolved oxygen concentration in the water of site S8 for the years 2020-2024. Different letters stand for significant differences among the means according to Kruskal-Wallis test ($p \leq 0.05$). U: upstream; D: downstream.

Concerning iron (Fe) and copper (Cu) concentrations in S1 (Figure 41A and 41B, respectively), in 2020 both metals showed the highest values. This fact can be attributed to the steep bank which might have promoted the introduction within the canal of soil particles resulting from water runoff enriched of Fe and Cu (Laubel et al., 2003; Bąk et al., 2013). However, while Cu did not show differences between 2021 and 2024, Fe content showed an increase in 2023 which could be attributed to the flood occurred in May 2023 because of the heavy erosion processes that took place (Cánovas et al., 2008).

At S2, Fe concentrations (Figure 42A) were elevated in 2020 and 2023, confirming the sensitivity of this parameter to erosion episodes and the transport of particles from the soil. Cu (Figure 42B) exhibited greater interannual variability, though without any significant trends, and remained, on average, at lower levels than those observed at S1 (Quinton, J. N., & Catt, J. A., 2007). The partial renaturalisation carried out in 2022 may have contributed to a reduction in copper inputs from surface runoff. At S5, both Fe and Cu (Figures 43A and 43B, respectively) remained at consistently low and stable levels throughout the observation period, suggesting a lower susceptibility to erosion-driven inputs or a different composition of the surrounding soils. At site S8, Fe (Figure 44A) followed a pattern similar to that of S1, with high concentrations in 2020 and an increase in 2023, indicating a strong influence of flood events on iron mobilisation. In contrast, Cu (Figure 44B) showed a slight decline from 2020 onwards, likely associated with the reduction in agricultural activities following the land-use change implemented in 2022.

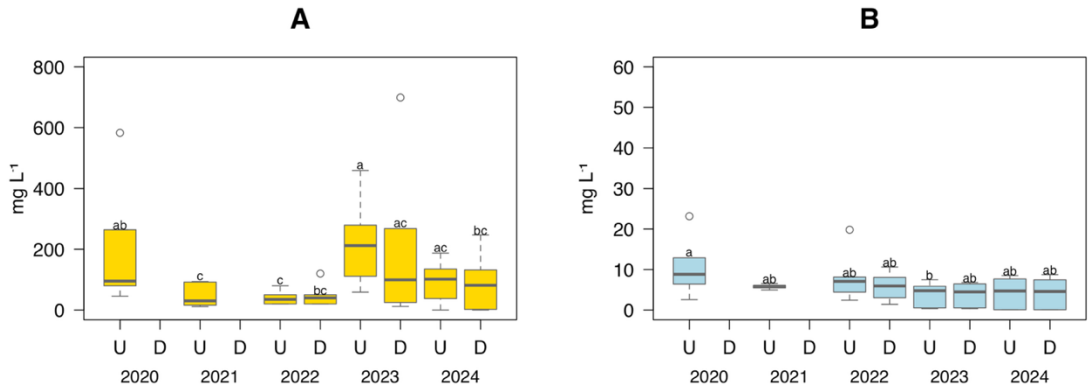

Figure 41 - Boxplot showing the iron (A) and copper (B) concentration in the water of site S1 for the years 2020-2024. Different letters stand for significant differences among the means according to Kruskal-Wallis test (p ≤ 0.05). U: upstream; D: downstream

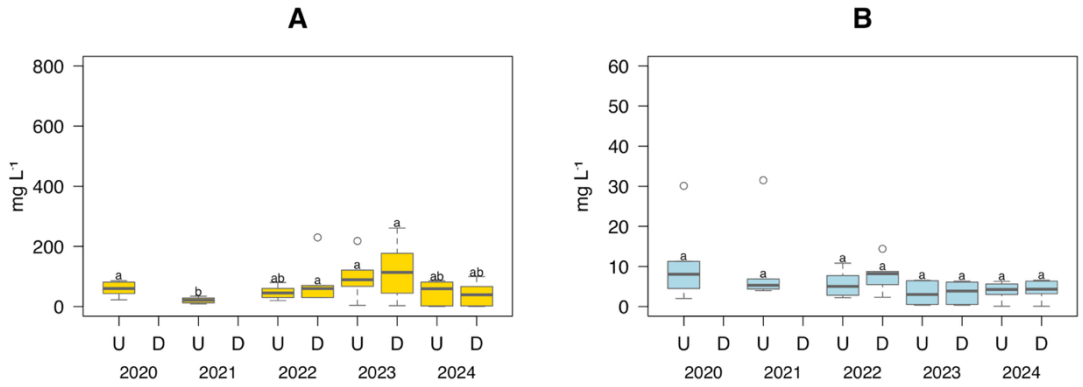

Figure 42 - Boxplot showing the iron (A) and copper (B) concentration in the water of site S2 for the years 2020-2024. Different letters stand for significant differences among the means according to Kruskal-Wallis test (p ≤ 0.05). U: upstream; D: downstream.

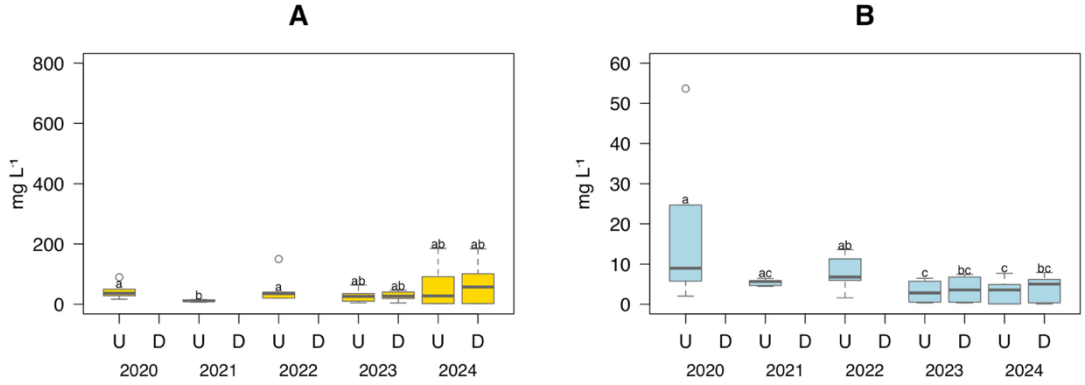

Figure 43 - Boxplot showing the iron (A) and copper (B) concentration in the water of site S5 for the years 2020-2024. Different letters stand for significant differences among the means according to Kruskal-Wallis test (p ≤ 0.05). U: upstream; D: downstream.

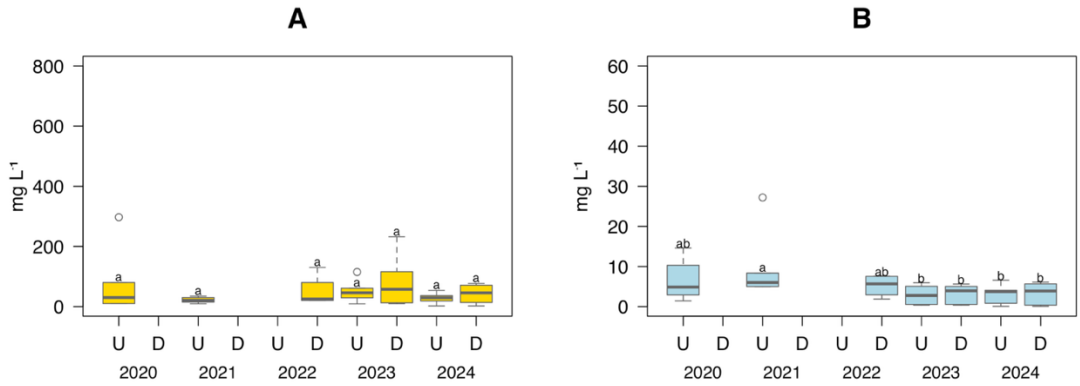

Figure 44 - Boxplot showing the iron (A) and copper (B) concentration in the water of site S8 for the years 2020-2024. Different letters stand for significant differences among the means according to Kruskal-Wallis test ($p \leq 0.05$). U: upstream; D: downstream.

Overall, the differences between upstream and downstream sampling points are not statistically significant for most parameters. However, some trends suggest a gradual accumulation of nutrients and salts in the terminal part of the analysed tract, especially for parameters such as Ntot, P and SAR. This may reflect the combined effect of canal transport and morphology.

Data suggest that the requalification measures have contributed to the containment of the most extreme variations in water quality. However, intense and flooding meteor events such as those in 2022 and 2023 temporarily affected some parameters, particularly those related to nutrient transport and sediment dynamics.

7.2 Influence of ponds on water quality of sandy sites: Sites S6 and S7

The pH values ranged between 7.81 and 8.69 over the study period (Table 5). Except for certain values recorded in 2023, the pH generally falls within the optimal range for surface waters (6.5–8.5) (Dewangan et al., 2023; Bundschuh et al., 2016). The higher pH measured in 2023 than in the other years may be associated with intense rainfall and flood events, which caused the transport of

mineral particles from surrounding areas predominantly characterized by alkaline lithologies (Ponting et al., 2021; Davide et al., 2003).
The lowest values were recorded in 2020 at both sites, likely due to reduced human activities resulting from the COVID-19 lockdowns. This led to a general improvement in surface water quality, as also reported in the literature (Mohinuddin et al., 2023; Uddin et al., 2023).

Total nitrogen concentrations (Ntot) showed significant spatial and temporal variability during the study period, ranging between 0.77 and 7.52 mg L^{-1} (Table 6). The lowest concentrations were observed in 2020, while the highest values occurred in 2023 and 2024. The low Ntot concentrations in 2020 are likely attributable to the reduction in anthropogenic activities during the COVID-19 lockdowns, which temporarily improved water quality (Liu et al., 2022).
In 2023, a marked increase in Ntot was observed, coinciding with the high rainfall that occurred throughout the year that likely intensified nutrient runoff from surrounding agricultural land, particularly from fertilized soils, facilitating the transport of nitrogen compounds into the canals (Skidmore et al., 2023).
In 2024, a slight decrease in total nitrogen concentrations was recorded, although values were higher than those measured in 2020 and 2021. The slight decrease observed between 2023 and 2024 can be attributed to the lower rainfalls in the latter than in the former. However, the still high Ntot content might be attributed to the probably intense fertilization to cope with the damages caused to cropland soils by floods in 2023. Indeed, the floods on the one hand eroded the topsoil and on the other hand deposited unfertile sediments.
Noteworthy, ponds of both S6 and S7 showed lower Ntot contents than the neighbor canal suggesting the potential capacity of these NBSs to reduce the nutrient load of the water (Shen et al., 2021).
At both sites, manganese concentrations (Table 7) showed a marked increase in the ponds, reaching high levels, particularly in 2023 and 2024. This increase is attributed to anoxic conditions in the pond sediments, which promote the reduction of manganese oxides and the subsequent release of Mn^{2+} into the

overlying water. Such processes are typical in stagnant environments with high levels of organic matter decomposition (Froelich et al., 1979).

Sulphur content (Table 6) exhibited an increasing trend over time, with higher values recorded in the ponds compared to the canal reaches. This pattern may result from organic matter mineralization and sulphate reduction under anoxic conditions typical of stagnant sediments (Fenchel et al., 1995).

Magnesium and silicon concentrations (Table 7) were slightly higher in the ponds, suggesting potential release from sediments or reduced dilution due to stagnation. Finally, boron and barium concentrations (Table 7) remained relatively stable across ponds and canal reaches, with no significant differences. This suggests that the vegetated ponds did not exert a substantial influence on the distribution of these elements.

Table 5 - Mean ± standard deviation of water pH of canals subjected to pond creation. Within each column, different letters stand for significant differences among the means according to Kruskal-Wallis test ($p \leq 0.05$).

Year	Location	Site 6	Site 7
2020	Upstream	$7.95 \pm 0.25\,b$	$8.05 \pm 0.32\,b$
2021	Upstream	$8.04 \pm 0.45\,b$	$8.00 \pm 0.38\,b$
2022	Upstream	$7.85 \pm 0.27\,b$	$8.00 \pm 0.34\,b$
2023	Upstream	$8.49 \pm 0.14\,a$	$8.51 \pm 0.24\,a$
	Pond	$8.57 \pm 0.16\,a$	$8.69 \pm 0.47\,a$
	Downstream	$8.54 \pm 0.12\,a$	$8.46 \pm 0.29\,a$
2024	Upstream	$8.11 \pm 0.30\,b$	$8.06 \pm 0.28\,b$
	Pond		$7.81 \pm 0.21\,b$
	Downstream	$8.10 \pm 0.27\,b$	$8.05 \pm 0.24\,b$

Table 6 - Mean ± standard deviation of total nitrogen content of canals subjected to pond creation. Within each column, different letters stand for significant differences among the means according to Kruskal-Wallis test ($p \leq 0.05$).

Year	Location	Site 6	Site 7
		mg L^{-1}	
2020	Upstream	$0.77 \pm 0.11\ d$	$0.94 \pm 0.41\ c$
2021	Upstream	$0.91 \pm 0.19\ cd$	$1.71 \pm 1.64\ bc$
2022	Upstream	$3.13 \pm 5.57\ b$d	$3.50 \pm 6.47\ bc$
2023	Upstream	$7.51 \pm 10.5\ a$	$5.59 \pm 8.98\ ab$
	Pond	$1.84 \pm 1.71\ bc$	$4.25 \pm 7.12\ bc$
	Downstream	$7.53 \pm 10.1\ a$	$5.22 \pm 8.64\ a$b
2024	Upstream	$5.86 \pm 7.57\ ab$	$6.02 \pm 7.93\ a$
	Pond		$3.08 \pm 3.53\ bc$
	Downstream	$5.73 \pm 7.75\ ab$	$6.13 \pm 8.23\ a$

Table 7 - Mean ± standard deviation of boron (B), barium (Ba), magnesium (Mg), manganese (Mn), sulphur (S) and silicon (Si) contents of canals subjected to pond creation. Within each row, different letters stand for significant differences among the means according to Kruskal-Wallis test ($p \leq 0.05$).

Site	Parameter (mg L-1)	2020	2021	2022		2023			2024		
		Upstream	Upstream	Upstream	Downstream	Upstream	Pond	Downstream	Upstream	Pond	Downstream
S6	B	$0.04 \pm 0.03\ c$	$0.08 \pm 0.03\ b$	$0.16 \pm 0.11\ b$		$0.11 \pm 0.06\ b$	$0.11 \pm 0.05\ b$	$0.11 \pm 0.03\ b$	$0.11 \pm 0.08\ a$		$0.11 \pm 0.08\ a$
	Ba	$50.1 \pm 23.1\ a$	$54.5 \pm 9.24\ a$	$60.3 \pm 12.3\ a$		$58.8 \pm 26.1\ a$	$69.7 \pm 14.7\ a$	$59.1 \pm 25.1\ a$	$63.2 \pm 19.8\ a$		$58.5 \pm 18.2\ a$
	Mg	$11.1 \pm 2.70\ b$	$14.1 \pm 1.89\ ab$	$15.5 \pm 4.85\ a$		$18.7 \pm 6.83\ a$	$15.6 \pm 3.50\ a$	$18.6 \pm 6.89\ a$	$17.3 \pm 7.14\ a$		$17.0 \pm 6.72\ a$
	Mn	$1.03 \pm 2.53\ c$	$7.65 \pm 3.96\ ab$	12.5 ± 15.1 ab		$4.90 \pm 3.39\ bc$	$8.72 \pm 8.25\ ab$	$4.80 \pm 3.19\ ac$	$13.3 \pm 11.1\ ab$		$13.5 \pm 10.4\ a$
	S	$12.9 \pm 1.50\ c$	$16.2 \pm 1.90\ bc$	$17.3 \pm 8.26\ bc$		21.5 ± 9.15 ab	$24.8 \pm 7.24\ a$	21.3 ± 8.69 ab	$20.6 \pm 8.82\ ab$		20.5 ± 8.53 ab
	Si	0.49 ± 0.15 ac	$0.60 \pm 0.11\ ab$	$0.48 \pm 0.31\ ac$		$0.44 \pm 0.46\ bc$	$0.20 \pm 0.25\ c$	$0.44 \pm 0.46\ bc$	$0.83 \pm 0.33\ a$		$0.82 \pm 0.31\ a$
S7	B	$0.11 \pm 0.07\ b$	$0.08 \pm 0.04\ b$		$0.17 \pm 0.12\ b$	$0.11 \pm 0.06\ b$	$0.13 \pm 0.04\ b$	$0.11 \pm 0.06\ b$	$0.57 \pm 0.34\ a$	$0.72 \pm 0.39\ a$	$0.56 \pm 0.33\ a$
	Ba	55.5 ± 9.23 ab	$46.9 \pm 7.49\ b$		$58.7 \pm 13.3\ ab$	$48.3 \pm 33.8\ b$	$77.3 \pm 78.6\ ab$	$48.2 \pm 33.0\ b$	$58.6 \pm 17.4\ ab$	$78.3 \pm 26.0\ a$	$60.6 \pm 17.4\ ab$
	Mg	$12.2 \pm 2.24\ a$	$13.9 \pm 2.10\ a$		$16.2 \pm 6.08\ a$	$19.2 \pm 9.42\ a$	$17.2 \pm 4.98\ a$	$19.2 \pm 9.17\ a$	$16.8 \pm 7.67\ a$	$14.2 \pm 3.55\ a$	$16.9 \pm 7.85\ a$
	Mn	$2.80 \pm 3.99\ c$	$7.08 \pm 3.83\ bc$		18.4 ± 22.7 ab	$19.3 \pm 19.1\ ab$	$35.6 \pm 45.5\ ab$	$16.1 \pm 17.3\ b$	$13.3 \pm 5.90\ ab$	$39.9 \pm 31.9\ a$	$13.0 \pm 7.28\ ab$
	S	$13.1 \pm 1.37\ b$	$16.0 \pm 2.02\ ab$		$18.1 \pm 10.3\ ab$	$21.1 \pm 9.90\ a$	$17.0 \pm 6.62\ ab$	$21.2 \pm 9.81\ a$	$20.3 \pm 10.2\ a$	19.1 ± 9.81 ab	$20.4 \pm 9.80\ a$
	Si	0.59 ± 0.14 ab	$0.51 \pm 0.22\ ab$		$0.50 \pm 0.31\ ab$	$0.45 \pm 0.45\ ab$	$0.34 \pm 0.40\ b$	$0.44 \pm 0.45\ ab$	$0.77 \pm 0.34\ a$	$0.61 \pm 0.36\ ab$	$0.77 \pm 0.33\ a$

At both sites, aluminium (Al) concentration (Figures 45A and 46A) increased since the year of pond construction (2022), with generally higher values in ponds than in the canals. The increase of Al content starting from pond construction might be attributed to both erosion processes and intense organic matter mineralization (Olivares-Rieumont et al., 2005; Li et al., 2022; Jones, 2004) due to vegetation removal during site preparation. While the higher Al content in ponds than in the canals might be attributed to the absence of dilution effect.

Generally, $N\text{-}NH_4$ concentrations showed higher values after pond construction than 2020 and 2021 (Figure 45B and 46B). Such higher values can be attributed to the intense organic matter mineralization and vegetation removal in 2022, heavy rains in 2023 and abundant use of N-based fertilizers in 2024 (Marzi et al., 2020). No differences occurred between water of ponds and that of the canals, which could be attributed to ammonia oxidation performed by several bacteria harbouring in stagnant water bodies like ponds and lakes (Qiu and Liu, 2025).

Phosphorus (P) concentrations at Sites 6 and 7 (Figures 45C and 46C) remained relatively low, with values between 0.02 and 0.13 mg L^{-1} and without any significant differences between canals and ponds.

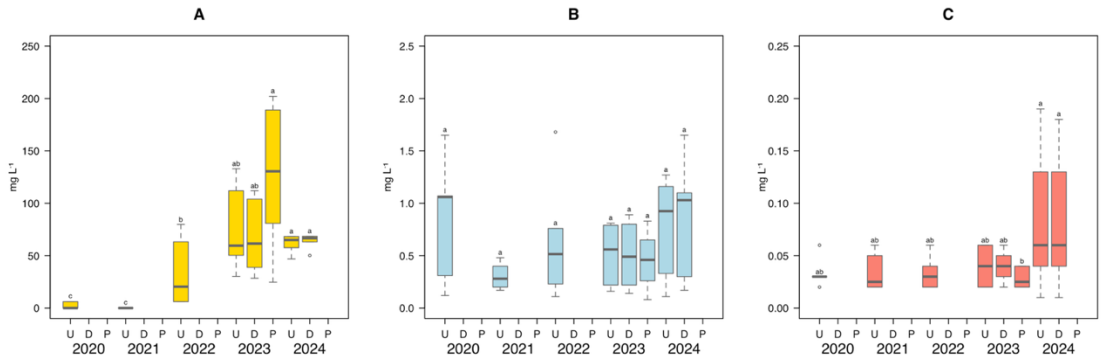

Figure 45 - Boxplot showing the Al (A), $N\text{-}NH_4$ (B) e phosphorus (C) concentration in canal water upstream (U) and downstream (D) the intervention site and pond water (P) of site 6 for the years 2020-2024. For each parameter, different letters stand for significant differences among the means according to Kruskal-Wallis test ($p \leq 0.05$).

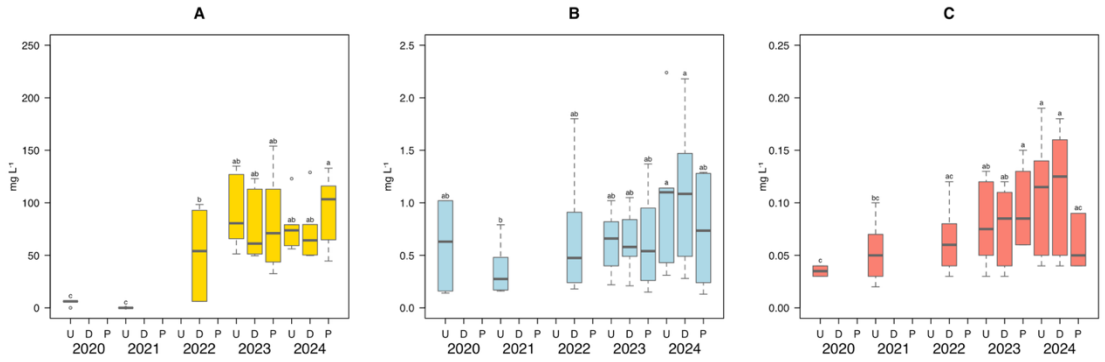

Figure 46 - Boxplot showing the Al (A), N-NH_4 (B) e phosphorus (C) concentration in canal water upstream (U) and downstream (D) the intervention site and pond water (P) of site 7 for the years 2020-2024. For each parameter, different letters stand for significant differences among the means according to Kruskal-Wallis test ($p \leq 0.05$).

Electrical conductivity (Figures 47B and 48B) increased steadily over time at both sites. In 2023 and 2024, values exceeded 1000 µS/cm in both canal and pond. The increase was more pronounced in the canal, probably due to the progressive accumulation of dissolved salts linked to agricultural runoff and saline intrusion. Initially, the ponds appeared to act as buffering compartments; however, by 2023–2024, EC values in the ponds were comparable to or even higher than those in the canal, likely as a result of evaporation and limited water exchange. The pond at Site 6 tends to dry out for most of the year, favouring salt concentration through evaporation. In contrast, the pond at site 7 maintains more stable water levels, allowing for greater dilution of salts. This behaviour is consistent with observations by Haygarth et al. (2005), who noted that reduced rainfall and increased evaporation can lead to higher salinity in surface waters. SAR (Figures 47A and 48A) also followed an increasing trend, with the highest values observed in the canals. Ponds exhibited lower SAR values, suggesting a potential role of vegetation in maintaining cationic balance. Notably, site 7 features finer soil texture, which better retains moisture and slows down salinization processes, while site 6 is characterized by sandy, more permeable substrate with reduced cation retention capacity. Studies such as Rengasamy & Olsson (1991) have highlighted the importance of soil texture in salinity and sodicity dynamics.

Differences in agricultural management practices (crop type, fertilization, irrigation) in the surrounding areas may also have contributed to variations in dissolved salt inputs across the two systems. Bellafiore et al. (2021) reported that fertilizer use can significantly influence water salinity in agricultural settings.

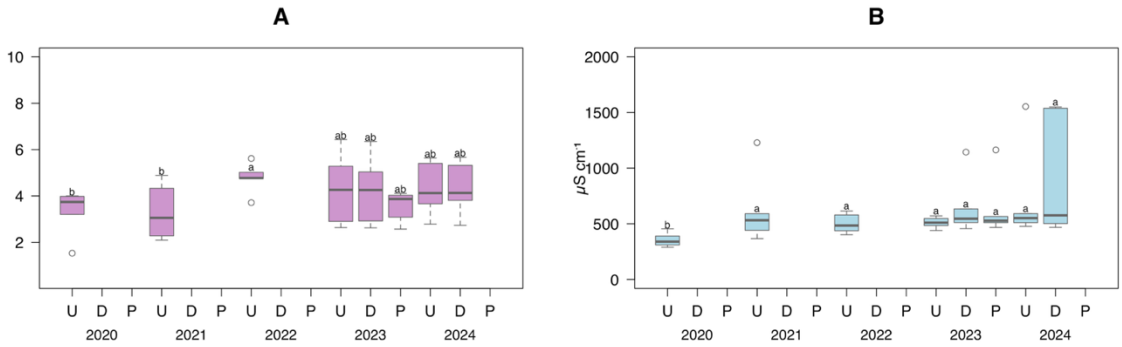

Figure 47 - Boxplot showing the sodium adsorption ratio (A) and electrical conductivity (B) of canal water upstream (U) and downstream (D) the intervention site and pond water (P) of site 6 for the years 2020-2024. For each parameter, different letters stand for significant differences among the means according to Kruskal-Wallis test (p ≤ 0.05).

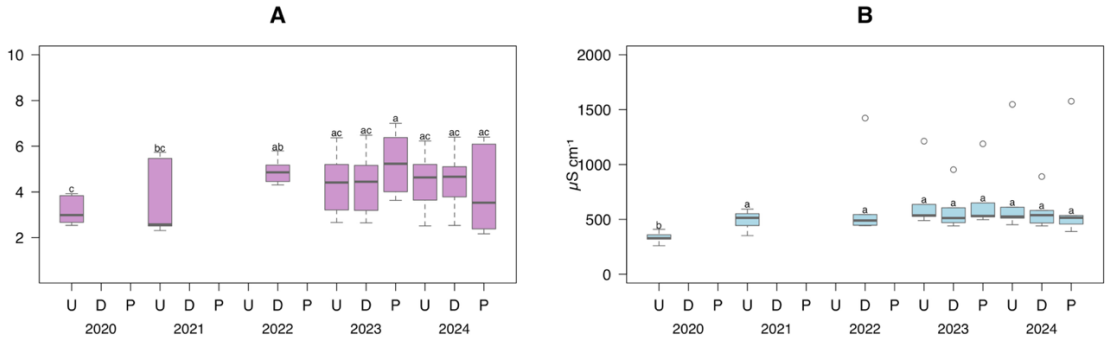

Figure 48 - Boxplot showing the sodium adsorption ratio (A) and electrical conductivity (B) of canal water upstream (U) and downstream (D) the intervention site and pond water (P) of site 7 for the years 2020-2024. For each parameter, different letters stand for significant differences among the means according to Kruskal-Wallis test (p ≤ 0.05).

Nitrate nitrogen concentrations (Figures 49A and 50A) at both sites increased starting in 2022, with high values observed between 2023 and 2024, particularly

in the ponds. At Site 6, values exceeded 3 mg L^{-1} in 2024, while Site 7 recorded lower, yet still elevated, values compared to the pre-intervention period.
This trend may be due to several factors:

- the presence of ponds, which in their early phase had not yet achieved full biological equilibrium and may have contributed to nutrient release from decomposing newly planted vegetation (Kadlec & Wallace, 2009);
- intense rainfall in 2023, which caused the accumulation of nitrates from the runoff of fertilizers applied to surrounding agricultural soils (Zhu et al., 2021).

Sites 6 and 7 showed distinct dynamics in terms of NO_3^- accumulation. At Site 6 (Figure 49A), significantly higher nitrate levels were observed in the pond (P) than in the canal (U and D) from 2023 onwards, consistent with a system subject to seasonal drying. In contrast, Site 7 showed more uniform and stable behaviour (Figure 50A), with generally lower and more homogeneous concentrations across the site, confirming the greater efficiency of this pond.
Organic carbon (OC) concentrations (Figures 49B and 50B) also increased between 2022 and 2023, especially in the pond at Site 6, where values exceeded 7 mg L^{-1}. Unlike sites with mechanical bank reshaping, where OC increased was linked to post-disturbance mineralization, in Sites 6 and 7, the increase appears to be associated with:

- release of organic matter from decomposing vegetation within the ponds;
- lack of water exchange during low-flow periods, which intensifies the concentration of dissolved fractions.

In 2024, a slight decrease in OC concentrations was observed, particularly at Site 7, suggesting possible system stabilization and improved carbon retention capacity, in line with observations from studies on mature constructed wetlands (Chen et al., 2015; Kong et al., 2023).

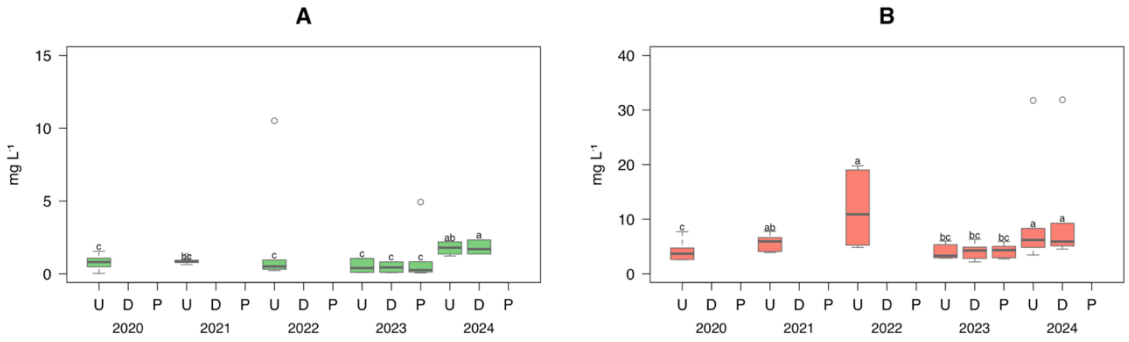

Figure 49 - Boxplot showing the N-NO_3 (A) and organic carbon (B) concentration in canal water upstream (U) and downstream (D) the intervention site and pond water (P) of site 6 for the years 2020-2024. For each parameter, different letters stand for significant differences among the means according to Kruskal-Wallis test ($p \leq 0.05$).

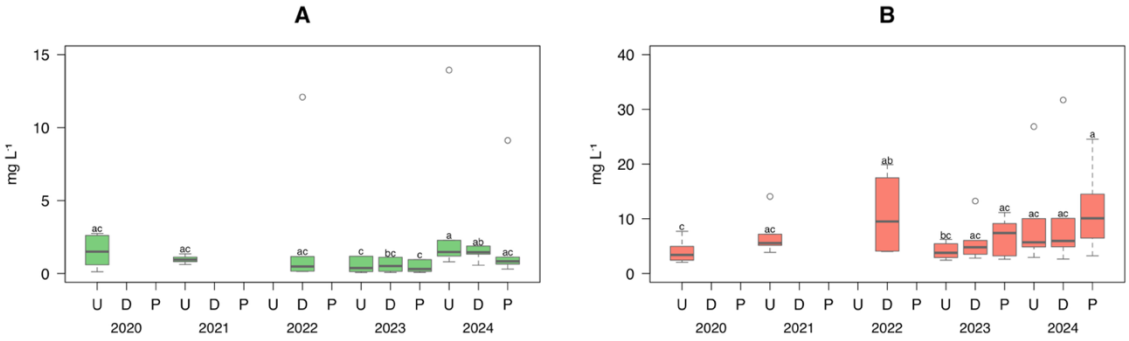

Figure 50 - Boxplot showing the NO_3- (A) e organic carbon (B) concentration in canal water upstream (U) and downstream (D) the intervention site and pond water (P) of site 7 for the years 2020-2024. For each parameter, different letters stand for significant differences among the means according to Kruskal-Wallis test ($p \leq 0.05$).

Site 6 exhibited highly variable dissolved oxygen (DO) concentrations (Figure 51). Values were low in the early years but rose significantly in the pond from 2022 onward, exceeding 200 mg L^{-1}. These values might be linked to temporary supersaturation conditions caused by intense photosynthetic activity. Such concentrations were not observed in the canal, where DO remained more stable. These fluctuations may be attributed to:

- drying and rewetting cycles in the pond, altering the oxygen balance;
- massive oxygen production by macrophytes or algae;
- potential imbalances in biogeochemical processes due to hydrological instability.

In contrast, Site 7 showed a much more stable DO pattern (Figure 52). Average pond values consistently ranged between 8 and 12 mg L^{-1}, similar to those in the canal. The absence of extreme values and reduced interannual variability indicate a more balanced system, likely favoured by:

- greater hydrological stability of the pond;
- well-structured aquatic vegetation, ensuring oxygenation through photosynthesis;
- more continuous water exchange compared to Site 6.

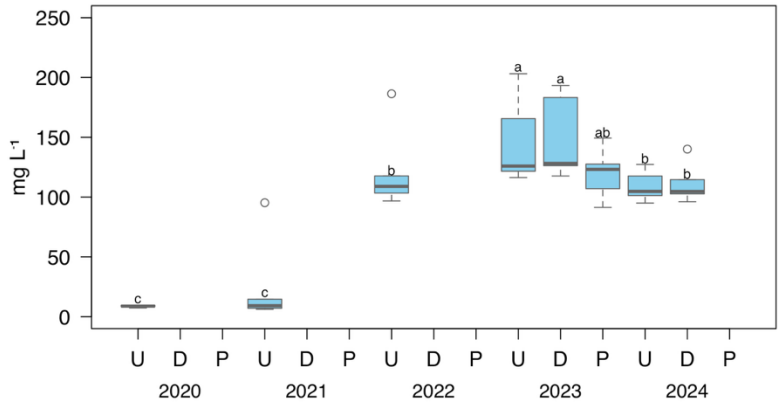

Figure 51 - Boxplot showing the dissolved oxygen concentration in canal water upstream (U) and downstream (D) the intervention site and pond water (P) of site 6 for the years 2020-2024. For each parameter, different letters stand for significant differences among the means according to Kruskal-Wallis test ($p \leq 0.05$).

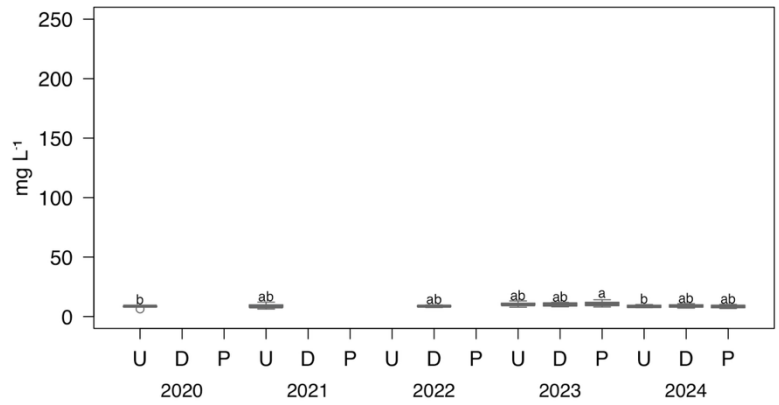

Figure 52 - Boxplot showing the dissolved oxygen concentration in canal water upstream (U) and downstream (D) the intervention site and pond water (P) of site 7 for the years 2020-2024. different letters stand for significant differences among the means according to Kruskal-Wallis test ($p \leq 0.05$).

Data on iron (Fe) and copper (Cu) concentrations at sites 6 and 7 (Figures 53 and 54) showed considerable interannual and spatial variability, with differences between canals and ponds depending on local hydrology, erosion processes, and system evolution.

Iron concentrations were highly variable, with peaks recorded in 2020 and 2023, both in the canals and during certain pond sampling campaigns. These peaks may be linked to erosion processes that mobilize iron bound to the solid fraction of the soil, particularly during heavy rainfall or flood events (Cánovas et al., 2008). In the ponds, Fe values were generally lower or comparable to those in the canal, suggesting a partial attenuation effect. This effect may result from:

- adsorption by submerged and emergent vegetation;
- local redox processes in stagnant sediments, which can immobilize part of the iron in insoluble forms (Sigg et al., 2000).

However, in some years (2023), high values were also observed in the ponds, likely due to surface runoff following extreme weather events.

Copper showed more variable behaviour than iron, with more pronounced interannual fluctuations. The highest Cu concentrations were generally observed during the early years of monitoring (2020–2021). These values may be attributed to:

- copper release from agricultural soils during the initial monitoring phase;
- limited maturity of the phytoremediation system, which may have temporarily favoured metal accumulation in the aquatic compartments.

From 2022 onward, Cu concentrations tended to decrease, particularly in the ponds, indicating improved retention efficiency by vegetation and sediments, consistent with observations from natural or semi-natural water treatment systems (Zhao et al., 2021).

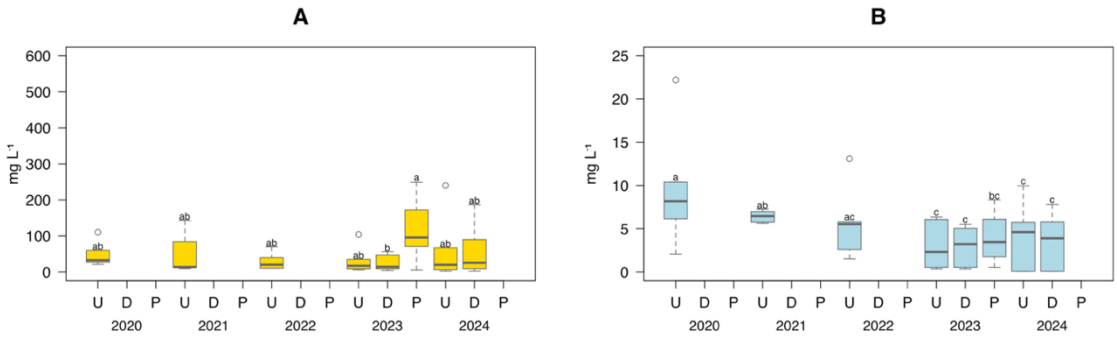

Figure 53 - Boxplot showing the Fe (A) and Cu (B) concentration in canal water upstream (U) and downstream (D) the intervention site and pond water (P) of site 6 for the years 2020-2024. For each parameter, different letters stand for significant differences among the means according to Kruskal-Wallis test ($p \leq 0.05$).

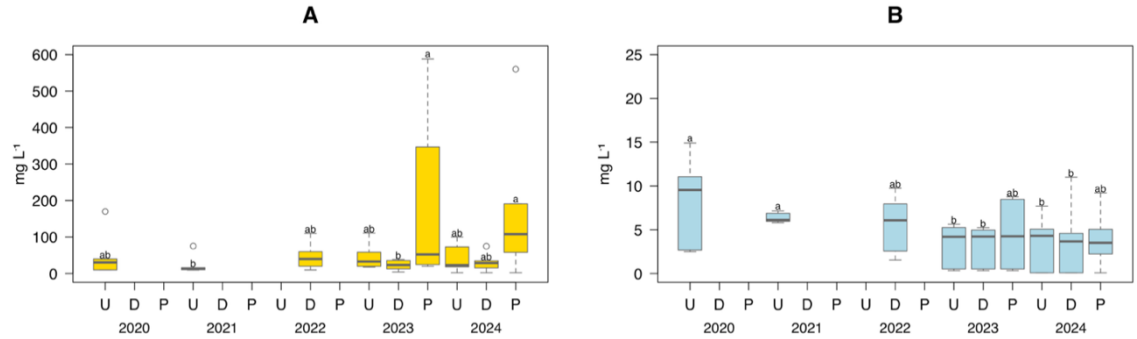

Figure 54 - Boxplot showing the Fe (A) and Cu (B) concentration in canal water upstream (U) and downstream (D) the intervention site and pond water (P) of site 7 for the years 2020-2024. For each parameter, different letters stand for significant differences among the means according to Kruskal-Wallis test ($p \leq 0.05$).

All these results highlight the importance of long-term monitoring of these interconnected systems to assess their effectiveness in retaining metals and improving water quality.

7.3 Influence of ponds on water quality of clay sites: Sites S4 and S9

The pH showed values ranging between 7.58 and 8.38 during the considered years (Table 8), which are in line with typical range for surface waters (range 6.5-8.5) (Dewangan, S. K., et al., 2023; Bundschuh, M., et al., 2016).

The higher pH values observed in the pond waters could be partly caused by the alkaline ions release from the pond bed (Capuano, R. M., et al., 2020) since it is made up of subsoil particles enriched of alkaline elements naturally present within the soil particles and/or received by translocation from the upper soil horizons.

However, we cannot exclude that the higher pH values in pond than in the canal might also be caused by intense photosynthesis by algae or macrophytes. Indeed, when algae and macrophytes photosynthesise, they consume carbon dioxide (CO_2) from water. Since CO_2 dissolved in water usually forms carbonic acid (H_2CO_3), which acidify water, if plants remove great amount of CO_2 during photosynthesis, the amount of H_2CO_3 is reduced. As a result, the water becomes less acidic, i.e. more alkaline, and thus the pH increases (Wetzel, R. G., 2001). This phenomenon is marked in the summer period for the ponds, which could be attributed to the higher algae/macrophytes-to-water ratio in the ponds than in the canals. In contrast, in winter the lower photosynthetic activity and higher dilution due to rainfall lead to a slight decrease in pH, as observed in other studies in wetlands and phytodepuration systems (Kadlec, R. H., & Wallace, S. D., 2009; Wetzel R. G., 2001).

Total nitrogen (Ntot) content showed high seasonal and spatial variability (Table 9). In 2020 and 2021, the Ntot concentrations ranged from 1.28 to 3.83 mg L^{-1} for Site 4 and from 1.26 to 3.08 mg L^{-1} for Site 9, with a slight increase in winter. At site S4, a strong increase (5.23 mg L^{-1}) was observed starting from the winter of 2022 and reaching the highest values in winter of 2024 (14.38 mg L^{-1}) in the downstream section of the canal. Unlike site S4, a weaker increase of Ntot content was observed in S9 reaching values of 8.12 and 6.98 mg L^{-1} upstream and downstream, respectively, in winter 2024. Hence, the present results would

suggest the lack of effects carried out by the ponds on the Ntot content of the water.

In both study sites, the Ntot content showed seasonal changes with higher values in wintertime. The increase of Ntot content in winter could be associated with higher erosive phenomena and leaching during the winter than in spring and summer seasons.

Noteworthy, the pond of both study sites showed lower Ntot contents than the canal (1.00-1.95 mg L^{-1}) and did not show temporal variation likely due to effective Ntot removal through phytodepuration processes. Therefore, the pond of both sites seems to be NBSs with the capacity to contain water nitrogen load, particularly in the summer months due to the intense vegetative activities, which is consistent with previous studies carried out in wetlands (Kadlec, R. H., & Wallace, S. D., 2009).

At both sites, the ponds showed generally higher concentrations of manganese (Mn) and barium (Ba) (Table 10 and Table 11) especially in the winter months, indicating favourable conditions for the accumulation of metals in water of environments characterized by negligible water exchange. In details, at site S9, a marked increase of Ba content was observed in the pond in 2024, but such increase was not found in the canal, suggesting limited hydraulic connectivity. Unlike site S9, at site S4, the concentrations of some elements in the canal (such as Mg, S and Si) tended do not change over time. However, also in this case the pond construction did not affect the quality of canal water.

Overall, our findings would indicate that the influence of ponds on canals can vary significantly depending on site, seasonality and degree of hydrological connection.

Table 8 - Mean ± standard deviation of water pH of canals subjected to pond creation. Within each column, different letters stand for significant differences among the means according to Kruskal-Wallis test ($p \leq 0.05$). Summer: from April to September; Winter: from October to March.

Year	Season	Location	Site 4	Site 9
2020	Summer	Upstream	$7.71 \pm 0.21\ f$	$7.58 \pm 0.06\ f$
	Winter	Upstream	$7.81 \pm 0.08\ ef$	7.63 ± 0.09 ef
2021	Summer	Upstream	$7.86 \pm 0.26\ ef$	$7.72 \pm 0.26\ df$
	Winter	Upstream	$7.96 \pm 0.20\ bf$	$7.97 \pm 0.17\ bd$
2022	Summer	Upstream	$7.75 \pm 0.16\ ef$	$7.79 \pm 0.16\ cf$
		Downstream	$7.86 \pm 0.15\ df$	$7.82 \pm 0.18\ ce$
		Pond	$8.12 \pm 0.21\ ab$	$8.35 \pm 0.34\ a$
	Winter	Upstream	$7.81 \pm 0.39\ ef$	$7.82 \pm 0.34\ ce$
		Downstream	$7.79 \pm 0.26\ ef$	$7.80 \pm 0.37\ cf$
		Pond	$7.98 \pm 0.42\ be$	$8.13 \pm 0.29\ ab$
2023	Summer	Upstream	$8.06 \pm 0.09\ ac$	$7.88 \pm 0.06\ bc$
		Downstream	$7.97 \pm 0.07\ be$	$8.05 \pm 0.21\ bd$
		Pond	$8.34 \pm 0.15\ a$	$8.17 \pm 0.25\ ab$
	Winter	Upstream	8.00 ± 0.05 be	$8.05 \pm 0.13\ ab$
		Downstream	$8.03 \pm 0.13\ bd$	$8.10 \pm 0.07\ ab$
		Pond	$8.38 \pm 0.22\ a$	$8.19 \pm 0.24\ a$
2024	Summer	Upstream	$7.81 \pm 0.26\ ef$	$7.82 \pm 0.20\ bd$
		Downstream	$7.88 \pm 0.22\ cf$	$7.80 \pm 0.18\ ce$
		Pond	$8.06 \pm 0.30\ bd$	$7.83 \pm 0.19\ bd$
	Winter	Upstream	$7.94 \pm 0.10\ bf$	$7.95 \pm 0.09\ bd$
		Downstream	$7.99 \pm 0.17\ bf$	$7.99 \pm 0.21\ bd$
		Pond	8.00 ± 0.03 be	$8.06 \pm 0.14\ cf$

Table 9 - Mean ± standard deviation of total nitrogen content of canals subjected to pond creation. Within each column, different letters stand for significant differences among the means according to Kruskal-Wallis test ($p \leq 0.05$). Summer: from April to September; Winter: from October to March.

Year	Season	Location	Site 4	Site 9
			mg L^{-1}	
2020	Summer	Upstream	$1.28 \pm 0.36\,h$	$1.44 \pm 0.59\,eg$
	Winter	Upstream	$1.83 \pm 0.50\,fh$	$1.89 \pm 0.50\,df$
2021	Summer	Upstream	$1.39 \pm 0.54\,h$	$1.26 \pm 0.66\,fg$
	Winter	Upstream	$3.83 \pm 1.46\,af$	$3.08 \pm 1.21\,bd$
2022	Summer	Upstream	$2.26 \pm 2.26\,gh$	$1.43 \pm 0.61\,eg$
		Downstream	$2.30 \pm 2.26\,gh$	$1.31 \pm 0.56\,fg$
		Pond	$1.00 \pm 0.36\,h$	$0.72 \pm 0.18\,g$
	Winter	Upstream	$5.23 \pm 2.29\,ad$	$4.41 \pm 1.66\,ac$
		Downstream	$4.20 \pm 1.89\,ae$	$3.90 \pm 1.62\,ac$
		Pond	$1.95 \pm 0.76\,gh$	$1.56 \pm 0.88\,fg$
2023	Summer	Upstream	$4.20 \pm 4.41\,dg$	$4.47 \pm 3.84\,ad$
		Downstream	$4.11 \pm 4.47\,cg$	$4.00 \pm 3.79\,ad$
		Pond	$3.83 \pm 4.18\,eg$	$3.66 \pm 3.46\,ce$
	Winter	Upstream	$5.50 \pm 1.72\,ac$	$5.18 \pm 2.01\,ab$
		Downstream	$5.47 \pm 1.55\,ab$	$6.32 \pm 5.78\,ab$
		Pond	$2.72 \pm 0.95\,dg$	$4.14 \pm 4.68\,ef$
2024	Summer	Upstream	$5.05 \pm 4.11\,ae$	$3.64 \pm 1.41\,ac$
		Downstream	$5.29 \pm 4.10\,af$	$2.70 \pm 1.73\,ac$
		Pond	$4.21 \pm 3.95\,bg$	$4.24 \pm 1.32\,ce$
	Winter	Upstream	$10.78 \pm 5.96\,a$	$8.12 \pm 3.76\,a$
		Downstream	$14.38 \pm 11.05\,a$	$6.98 \pm 4.16\,a$
		Pond	$1.49 \pm 0.42\,gh$	$5.10 \pm 2.91\,ab$

Table 10 - Mean ± standard deviation of boron (B), barium (Ba), magnesium (Mg), manganese (Mn), sulphur (S) and silicon (Si) contents in water and pond of site S4. Within each column, different letters stand for significant differences among the means according to Kruskal-Wallis test ($p \leq 0.05$). Summer: from April to September; Winter: from October to March.

Year	Season	Location	B	Ba	Mg	Mn	S	Si
					mg L-1			
2020	Summer	Upstream	$0.13 \pm 0.09\ g$	$59.2 \pm 17.2\ eg$	$12.6 \pm 5.07\ g$	$53.5 \pm 46.8\ cf$	$17.2 \pm 6.48\ e$	$0.64 \pm 0.22\ ae$
	Winter	Upstream	$0.13 \pm 0.01\ g$	$68.0 \pm 8.73\ bg$	$20.7 \pm 2.93\ cf$	$96.1 \pm 16.0\ ac$	$28.8 \pm 1.61 ad$	$0.98 \pm 0.04\ a$
2021	Summer	Upstream	$0.37 \pm 0.13\ bd$	$65.2 \pm 5.97\ dg$	$17.3 \pm 2.71\ fg$	$53.3 \pm 30.4\ ce$	$22.5 \pm 4.47\ de$	$0.72 \pm 0.18\ ad$
	Winter	Upstream	$0.67 \pm 0.32\ ac$	$59.4 \pm 10.4\ fg$	$20.1 \pm 3.58\ df$	$129.3 \pm 85.9\ a$	$31.6 \pm 5.01\ ac$	$0.59 \pm 0.24\ ae$
2022	Summer	Upstream	$0.36 \pm 0.21\ b$	$75.8 \pm 10.5\ ae$	$18.3 \pm 4.34\ eg$	$52.3 \pm 50.9\ ce$	$23.5 \pm 9.28\ de$	$0.53 \pm 0.24\ ce$
		Downstream	$0.32 \pm 0.21\ eg$	$75.6 \pm 9.40\ ae$	$18.1 \pm 4.04\ eg$	$51.9 \pm 45.4\ ce$	$23.3 \pm 8.80\ de$	$0.52 \pm 0.25\ ce$
		Pond	$0.44 \pm 0.26\ bd$	$62.0 \pm 12.4\ eg$	$20.8 \pm 4.09\ cf$	$13.2 \pm 13.8\ f$	$29.8 \pm 13.21\ be$	$0.40 \pm 0.28\ de$
2022	Winter	Upstream	$0.28 \pm 0.34\ fg$	$57.3 \pm 13.5\ fg$	$20.3 \pm 4.99\ cf$	$126.1 \pm 57.0\ ac$	$32.8 \pm 9.54\ ad$	$0.84 \pm 0.30\ ad$
		Downstream	$0.14 \pm 0.02\ g$	$58.2 \pm 12.6\ fg$	$20.6 \pm 4.55\ cf$	$116.8 \pm 77.8\ ac$	$32.5 \pm 9.02\ ad$	$0.82 \pm 0.31\ ac$
		Pond	$0.16 \pm 0.03\ fg$	$75.7 \pm 16.3\ ad$	$25.5 \pm 1.48\ ad$	$38.1 \pm 18.6\ df$	$46.4 \pm 17.34\ ab$	$0.59 \pm 0.25\ ce$
2023	Summer	Upstream	$0.16 \pm 0.04\ eg$	$60.0 \pm 10.1\ bg$	$22.0 \pm 5.31\ bf$	$53.3 \pm 46.2\ ce$	$26.2 \pm 5.83\ be$	$0.61 \pm 0.53\ ae$
		Downstream	$0.16 \pm 0.04\ eg$	$60.8 \pm 30.4\ bg$	$22.2 \pm 5.20\ bf$	$57.9 \pm 43.7\ bd$	$26.2 \pm 5.68\ be$	$0.61 \pm 0.52\ ae$
		Pond	$0.22 \pm 0.04\ eg$	$75.2 \pm 77.1\ cg$	$24.1 \pm 5.85\ ad$	$26.4 \pm 35.0\ df$	$28.3 \pm 6.81\ bd$	$0.30 \pm 0.46\ e$
2023	Winter	Upstream	$0.14 \pm 0.03\ fg$	$73.4 \pm 13.2\ af$	$25.0 \pm 5.96\ ad$	$114.8 \pm 61.2\ ab$	$31.6 \pm 10.5\ ad$	$0.73 \pm 0.14\ ad$
		Downstream	$0.15 \pm 0.03\ fg$	$73.7 \pm 11.3\ af$	$24.8 \pm 5.51\ ad$	$114.7 \pm 56.4\ a$	$31.6 \pm 11.2\ ad$	$0.73 \pm 0.14\ ad$
		Pond	$0.16 \pm 0.03\ eg$	$90.6 \pm 23.7\ ac$	$27.1 \pm 4.42\ ab$	$17.4 \pm 16.7\ df$	$32.3 \pm 13.1\ ad$	$0.58 \pm 0.38\ ae$
2024	Summer	Upstream	$0.15 \pm 0.08\ a$	$74.8 \pm 9.94\ ae$	$23.9 \pm 9.09\ bf$	$42.0 \pm 34.3\ df$	$33.8 \pm 18.4\ bd$	$0.92 \pm 0.28\ ab$
		Downstream	$0.15 \pm 0.08\ a$	$78.9 \pm 11.4\ ac$	$24.7 \pm 9.15\ ae$	$41.1 \pm 32.9\ df$	$33.3 \pm 18.8\ bd$	$0.90 \pm 0.29\ ba$
		Pond	$0.15 \pm 0.05\ ab$	$48.7 \pm 35.8\ g$	$21.0 \pm 5.22\ cf$	$19.6 \pm 30.0\ ef$	$25.8 \pm 8.16\ ce$	$0.53 \pm 0.48\ be$
2024	Winter	Upstream	$0.20 \pm 0.03\ bd$	$82.9 \pm 12.8\ ac$	$32.5 \pm 6.47\ a$	$138.0 \pm 36.1 a$	$52.6 \pm 12.0\ a$	$0.70 \pm 0.20\ ae$
		Downstream	$0.20 \pm 0.03\ bd$	$85.8 \pm 12.4\ ab$	$32.8 \pm 6.20\ a$	$135.3 \pm 32.7\ a$	$52.4 \pm 12.1\ a$	$0.71 \pm 0.22\ ae$
		Pond	$0.17 \pm 0.01\ ce$	$89.4 \pm 5.66\ a$	$24.5 \pm 0.81\ ad$	$25.6 \pm 18.1\ df$	$27.4 \pm 2.68\ be$	$0.46 \pm 0.38\ ce$

Table 11 - Mean ± standard deviation of boron (B), barium (Ba), magnesium (Mg), manganese (Mn), sulphur (S) and silicon (Si) contents in water and pond of site S9. Within each column, different letters stand for significant differences among the means according to Kruskal-Wallis test ($p \leq 0.05$). Summer: from April to September; Winter: from October to March.

Year	Season	Location	B	Ba	Mg	Mn	S	Si
2020	Summer	Upstream	$0.16 \pm 0.08\ eh$	$73.0 \pm 4.17\ a$	$14.9 \pm 0.57\ d$	$107.4 \pm 119.3\ bd$	$20.4 \pm 1.85\ d$	$0.81 \pm 0.16\ a$
	Winter	Upstream	$0.09 \pm 0.01\ h$	$64.7 \pm 10.1\ ab$	$26.0 \pm 1.24\ bd$	$125.4 \pm 44.2\ ac$	$25.7 \pm 0.68\ ad$	$0.78 \pm 0.04\ ac$
2021	Summer	Upstream	$0.34 \pm 0.11\ ab$	$76.5 \pm 10.6\ a$	$18.4 \pm 1.21\ ac$	$126.8 \pm 34.2\ ac$	$25.0 \pm 2.02\ de$	$0.70 \pm 0.22\ ac$
	Winter	Upstream	$0.59 \pm 0.28\ c$	$72.4 \pm 16.8\ a$	$21.0 \pm 7.34\ ab$	$144.6 \pm 53.33\ ac$	$32.2 \pm 9.83\ bd$	$0.62 \pm 0.17\ ac$
2022	Summer	Upstream	$0.28 \pm 0.19\ cf$	$73.8 \pm 14.7\ a$	$14.7 \pm 3.25\ cd$	$111.4 \pm 52.1\ ac$	$19.4 \pm 4.70\ d$	$0.46 \pm 0.29\ bc$
		Downstream	$0.28 \pm 0.19\ cf$	$76.0 \pm 14.9\ a$	$14.7 \pm 3.21\ d$	$115.8 \pm 60.9\ ac$	$19.7 \pm 4.78\ d$	$0.47 \pm 0.31\ ac$
		Pond	$0.39 \pm 0.29\ ac$	$44.1 \pm 10.6\ a$	$17.1 \pm 3.68\ ad$	$89.6 \pm 10.5\ cd$	$19.4 \pm 6.06\ d$	$0.33 \pm 0.20\ c$
2022	Winter	Upstream	0.23 ± 0.27 eh	$70.3 \pm 12.6\ a$	$19.7 \pm 1.92\ ab$	$191.2 \pm 59.3\ a$	$31.7 \pm 3.95\ ab$	$0.73 \pm 0.32\ ac$
		Downstream	$0.10 \pm 0.03\ gh$	$62.4 \pm 25.3\ ab$	$19.6 \pm 1.84\ ab$	$196.0 \pm 59.4\ a$	$31.7 \pm 4.57\ ab$	$0.62 \pm 0.44\ ac$
		Pond	$0.13 \pm 0.04\ eh$	$49.5 \pm 13.2\ a$	$19.4 \pm 1.27\ ac$	$131.6 \pm 105.6\ ac$	$27.2 \pm 8.14\ ad$	$0.52 \pm 0.42\ ac$
2023	Summer	Upstream	$0.17 \pm 0.04\ cg$	$97.4 \pm 46.1\ a$	$21.1 \pm 5.48\ ac$	$126.3 \pm 79.0\ ab$	$28.2 \pm 7.52\ ad$	$0.73 \pm 0.68\ ac$
		Downstream	$0.21 \pm 0.05\ eg$	$91.9 \pm 51.0\ a$	$20.4 \pm 5.45\ ab$	$80.12 \pm 50.6\ ac$	$23.4 \pm 7.92\ ad$	$0.67 \pm 0.62\ ac$
		Pond	$0.14 \pm 0.03\ ad$	$76.9 \pm 27.5\ a$	$19.8 \pm 5.83\ ab$	$100.7 \pm 83.1\ d$	$25.7 \pm 5.48\ cd$	$0.51 \pm 0.54\ ac$
2023	Winter	Upstream	$0.13 \pm 0.02\ eh$	$79.7 \pm 6.87\ a$	$23.1 \pm 4.74\ a$	$147.5 \pm 78.6\ ac$	$31.2 \pm 9.77\ ac$	$0.61 \pm 0.16\ ac$
		Downstream	$0.17 \pm 0.03\ eh$	$80.2 \pm 7.52\ a$	$21.8 \pm 5.56\ a$	$117.0 \pm 10.5\ ac$	$27.9 \pm 13.0\ ac$	$0.49 \pm 0.11\ ac$
		Pond	$0.14 \pm 0.02\ eg$	$72.5 \pm 9.58\ a$	$24.1 \pm 5.11\ a$	$97.6 \pm 50.6\ d$	$30.9 \pm 7.93\ bd$	$0.71 \pm 0.23\ ae$
2024	Summer	Upstream	$0.14 \pm 0.08\ dh$	$75.5 \pm 20.8\ a$	$20.8 \pm 9.67\ ac$	$117.7 \pm 28.0\ ac$	$28.5 \pm 15.5\ ad$	$0.82 \pm 0.22\ ab$
		Downstream	$0.17 \pm 0.04\ eh$	$78.6 \pm 13.2\ a$	$21.1 \pm 7.28\ ac$	$91.7 \pm 61.6\ ac$	33.9 ± 11.5 ad	$0.66 \pm 0.37\ ab$
		Pond	$0.11 \pm 0.06\ cf$	$68.3 \pm 14.0\ a$	$17.3 \pm 6.68\ ab$	$118.7 \pm 33.8\ bd$	$22.7 \pm 9.24\ ac$	$0.92 \pm 0.17\ ac$
2024	Winter	Upstream	$0.17 \pm 0.07\ bf$	$93.5 \pm 26.7\ a$	$29.8 \pm 11.3\ a$	$223.6 \pm 120.7\ a$	$48.3 \pm 20.2\ a$	$0.61 \pm 0.27\ ac$
		Downstream	$0.12 \pm 0.05\ cg$	$87.3 \pm 30.1\ a$	$19.4 \pm 7.79\ a$	$232.8 \pm 149.0\ a$	$33.7 \pm 13.7\ a$	$0.69 \pm 0.16\ ac$
		Pond	$0.21 \pm 0.02\ fh$	$106.6 \pm 12.5\ a$	$35.5 \pm 3.02\ ad$	$217.3 \pm 117.7\ a$	$57.4 \pm 7.84\ ac$	$0.52 \pm 0.26\ ac$

Aluminium showed an increasing trend since 2022 (Figure 55A and Figure 56A), with higher average concentrations recorded during the summer periods compared to winter ones. In site S4, for example, a concentration of 4.1 mg L^{-1} was measured in summer 2020, rising to 52.4 mg L^{-1} in summer 2022. The higher Al content in summer than in winter was likely associated to the mobilisation of the metal from sediments promoted by rising temperatures (Bache, B. W., 1986; Nordstrom, D. K., & Ball, J. W., 1986). The ponds exhibited significantly higher aluminium concentrations than the canals, suggesting greater accumulation due to prolonged water residence time and stronger interaction with sediments. These findings are consistent with previous studies reporting aluminium mobilisation under stagnant and anoxic conditions (Davison, W., 1993; Tipping, E., et al., 2002).

Ammoniacal nitrogen (N-NH_4) showed a more pronounced seasonal pattern than interannual variation, with higher average concentrations recorded during winter, without significant differences from 2020 to 2023 (Figure 55B and Figure 56B). In site S4, the N-NH_4 concentration increased from 0.87 mg L^{-1} in summer 2020 to 1.34 mg L^{-1} in summer 2022. This pattern is consistent with reduced microbial activity during the colder months, which limits nitrification processes, as well as with lower plant biomass. Conversely, lower concentrations were observed during summer, suggesting effective transformation of ammonium into nitrate due to both the activity of nitrifying microorganisms and the nutrient uptake by aquatic vegetation (Anthonisen, A. C., et al., 1976).

Phosphorus (P) content showed lower values in the ponds compared to the canals (Figure 55C and Figure 56C). These results would suggest that the ponds play a key role in phosphorus removal, likely through phytoremediation processes (Kadlec, R. H., & Wallace, S. D., 2009). However, both ponds and canals did not show significant seasonal and interannual differences.

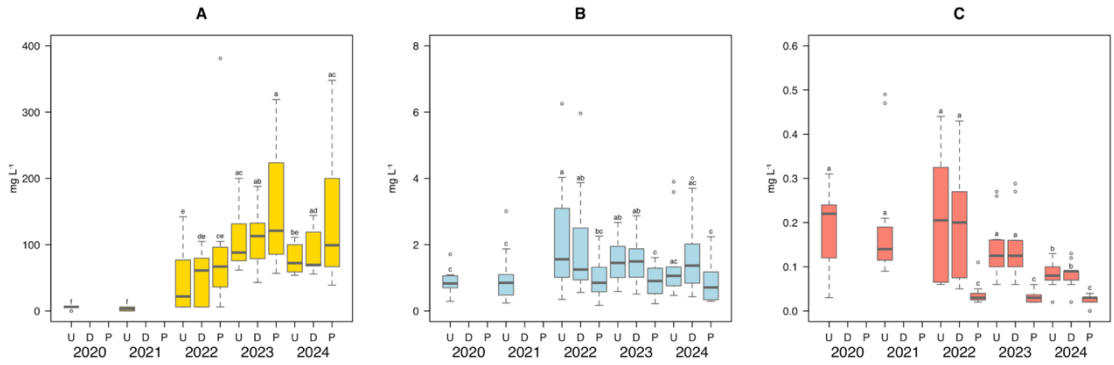

Figure 55 - Boxplot showing the Al (A), N-NH4 (B) e phosphorus (C) concentration in canal water upstream (U) and downstream (D) the intervention site and pond water (P) of site 4 for the years 2020-2024. For each parameter, different letters stand for significant differences among the means according to Kruskal-Wallis test ($p \leq 0.05$).

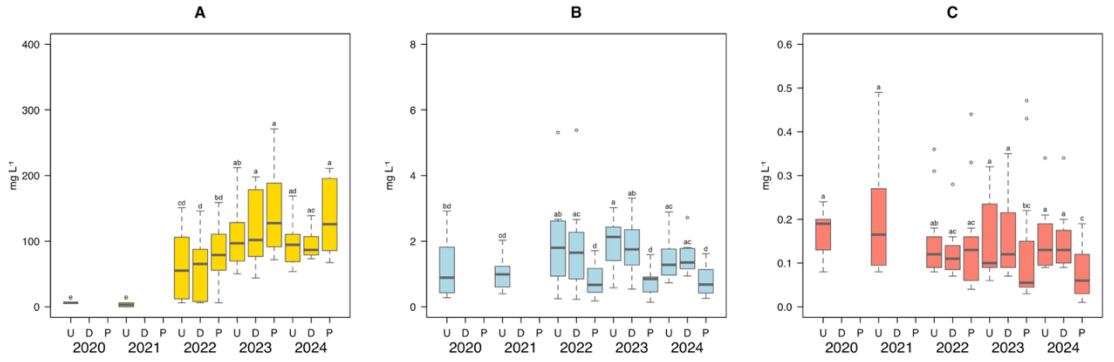

Figure 56 - Boxplot showing the Al (A), N-NH_4 (B) e phosphorus (C) concentration in canal water upstream (U) and downstream (D) the intervention site and pond water (P) of site 9 for the years 2020-2024. For each parameter, different letters stand for significant differences among the means according to Kruskal-Wallis test ($p \leq 0.05$).

At both sites, electrical conductivity (EC) showed higher values in the canals than in the ponds (Figures 57A and 58A) likely due to the removal of nutrients by the vegetation harboured within ponds.

The Sodium Adsorption Ratio (SAR) showed different dynamics between the two sites (Figures 57B and 58B). At site 4, SAR values were higher in the pond than in the canal, while the opposite trend was observed at site 9, with higher values in the canal. This different behaviour ca be attributed to the greater water

stagnation in the pond of S4 than in that of S9 which could have contributed to Na accumulation in the former than in latter (Richards, L. A., 1954).

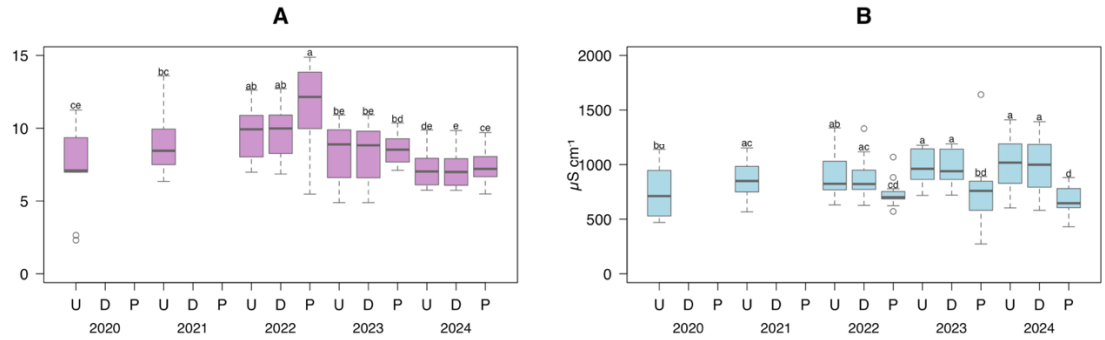

Figure 57 - Boxplot showing the sodium adsorption ratio (A) and electrical conductivity (B) of canal water upstream (U) and downstream (D) the intervention site and pond water (P) of site 4 for the years 2020-2024. For each parameter, different letters stand for significant differences among the means according to Kruskal-Wallis test (p ≤ 0.05).

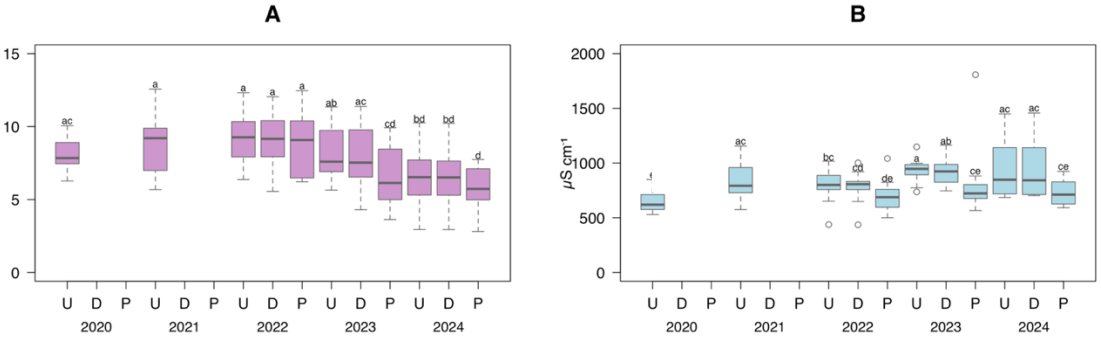

Figure 58 - Boxplot showing the sodium adsorption ratio (A) and electrical conductivity (B) of canal water upstream (U) and downstream (D) the intervention site and pond water (P) of site 9 for the years 2020-2024. For each parameter, different letters stand for significant differences among the means according to Kruskal-Wallis test (p ≤ 0.05).

Nitrate nitrogen (N-NO_3) content showed lower values in the ponds compared to the canals (Figure 59A and Figure 60A). While the water of the canals did not show seasonal differences, ponds showed higher N-NO_3 contents in winter than in the summer. The absence of seasonal differences in the canals can be attributed to the continuous inflow of fresh water which could have masked the influence of surrounding environment (i.e., fertilization) on such parameter.

Conversely, because of the negligible water exchange, the lower N-NO_3 content in summer than in winter for the ponds can be attributed to plant uptake and denitrification processes which are promoted by the higher temperatures (Messer, et al., 2017). In addition, ponds showed a slight reduction in N-NO_3 concentrations from 2021 to 2023. which would confirm the role of ponds in nitrogen removal processes (Vymazal, J., 2007).

Organic carbon (OC) (Figure 59B and Figure 60B) content showed an opposite trend compared to N-NO_3, with generally higher values in the ponds than in the canals, particularly at site 4. The OC enrichment observed within the ponds can be due to the accumulation within them of organic material that reaches pond water by erosion processes and plant residues (Wetzel, R. G., 2001). Conversely, the canal water did not accumulate OC due to the continuous water flow all over the year. The high availability of organic carbon may also support biological processes such as denitrification, in which nitrate is reduced through microbial activity using organic matter as a substrate, further explain the lower N-NO_3 concentrations in the ponds than in the canal (Mitsch, W. J., & Gosselink, J. G., 2015; Kadlec, R. H., & Wallace, S. D., 2009). Ponds therefore act as carbon accumulation environments (Bastviken, D., et al., 2004).

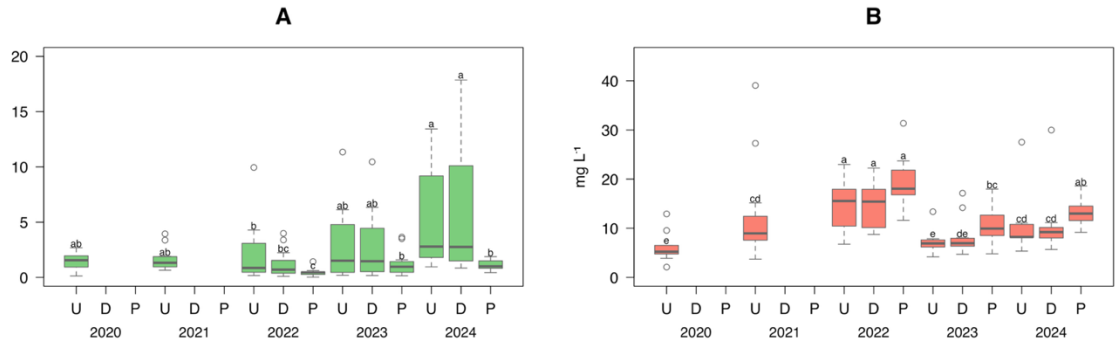

Figure 59 - Boxplot showing the N-NO_3 (A) and organic carbon (B) concentration in canal water upstream (U) and downstream (D) the intervention site and pond water (P) of site 4 for the years 2020-2024. For each parameter, different letters stand for significant differences among the means according to Kruskal-Wallis test ($p \leq 0.05$).

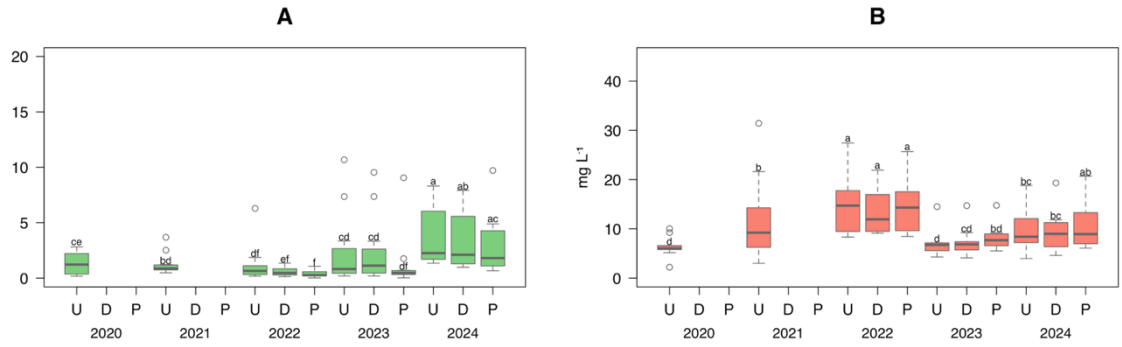

Figure 60 - Boxplot showing the N-NO_3 (A) and organic carbon (B) concentration in canal water upstream (U) and downstream (D) the intervention site and pond water (P) of site 9 for the years 2020-2024. For each parameter, different letters stand for significant differences among the means according to Kruskal-Wallis test ($p \leq 0.05$).

Dissolved oxygen (DO) content showed generally high values, with averages exceeding 9 mg L^{-1} in both canals and ponds (Figure 61 and Figure 62). In both study sites, no differences occurred between pond and canal despite the greater water stagnation in the former than in the latter which could have been counterbalanced by oxygenation provided through the algal community grow within water of ponds (Mara, D. D., & Pearson, H. W., 1998). It was interesting to observe that in ponds and canals, the DO content showed higher values in winter than in summer period which could be attributed to the lower temperature which promotes gas solubility in water and the lower aquatic vegetation activity which lowered the root respiration (Kadlec, R. H., & Wallace, S. D. 2009).

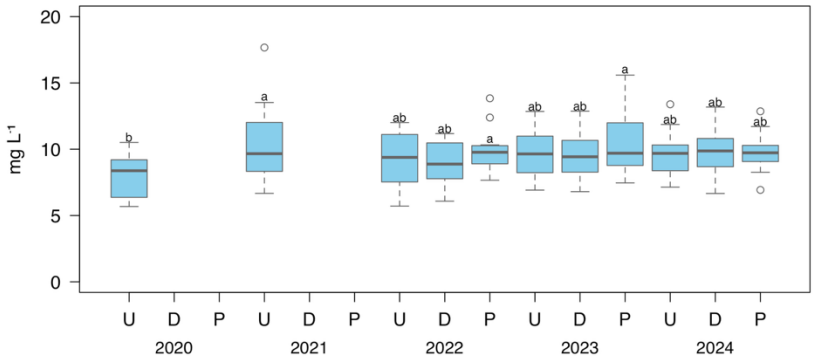

Figure 61 - Boxplot showing the dissolved oxygen concentration in canal water upstream (U) and downstream (D) the intervention site and pond water (P) of site 4 for the years 2020-2024. For each parameter, different letters stand for significant differences among the means according to Kruskal-Wallis test ($p \leq 0.05$).

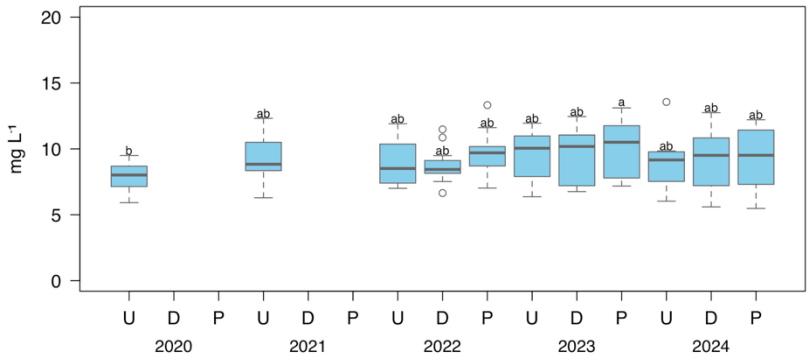

Figure 62 - Boxplot showing the dissolved oxygen concentration in canal water upstream (U) and downstream (D) the intervention site and pond water (P) of site 9 for the years 2020-2024. For each parameter, different letters stand for significant differences among the means according to Kruskal-Wallis test ($p \leq 0.05$).

Iron (Fe) and copper (Cu) did not show significant differences among the seasons and the years (Figure 63 and Figure 64). Some differences occurred between ponds and canals with higher concentrations in the former than in the latter likely due to water stagnation and the presence of organic matter (Baken, S., et al., 2011).

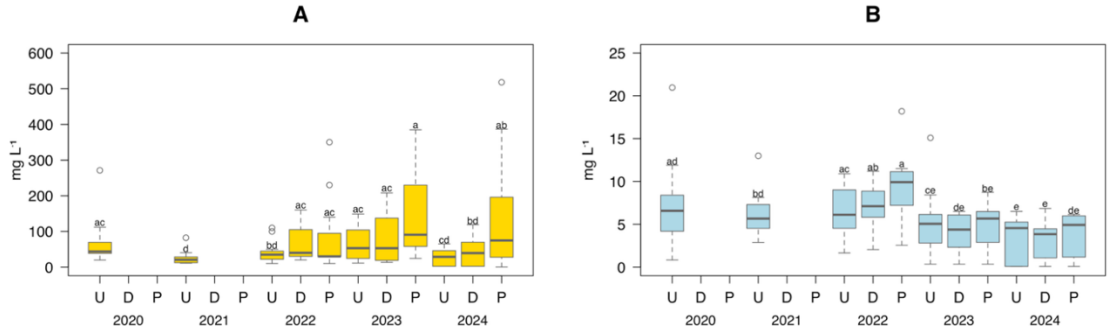

Figure 63 - Boxplot showing the Fe (A) and Cu (B) concentration in canal water upstream (U) and downstream (D) the intervention site and pond water (P) of site 4 for the years 2020-2024. For each parameter, different letters stand for significant differences among the means according to Kruskal-Wallis test ($p \leq 0.05$).

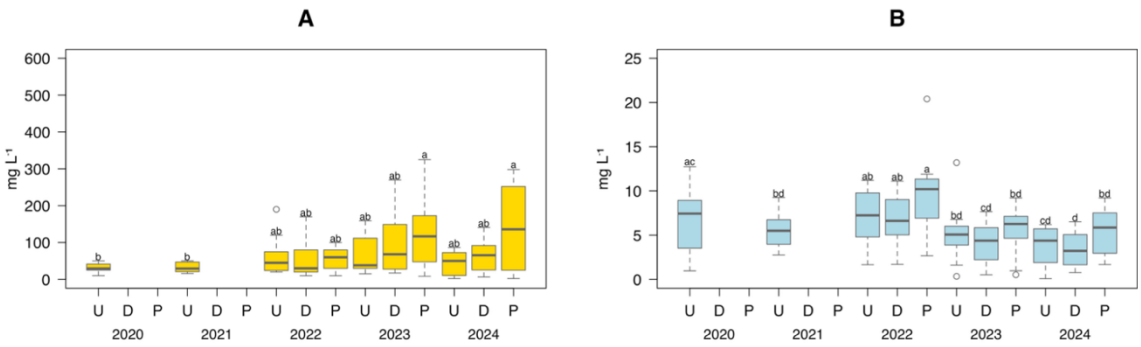

Figure 64 - Boxplot showing the Fe (A) and Cu (B) concentration in canal water upstream (U) and downstream (D) the intervention site and pond water (P) of site 9 for the years 2020-2024. For each parameter, different letters stand for significant differences among the means according to Kruskal-Wallis test ($p \leq 0.05$).

Overall, these results confirm that the construction of ponds represents an effective strategy for improving water quality, although continuous monitoring is necessary to assess the potential long-term effects of metal accumulation. However, this type of intervention has not appeared to significantly affect the water quality of the canals, likely due to the relatively small size of the ponds compared to the canals themselves.

7.4 Influence of bank reshaping on bed sediment features of sites S1, S2, S5 and S8

The pH trend (Table 12) in the sediments of the analysed sites shows some variability over the five-year period 2020–2024, with higher values recorded between 2021 and 2022, followed by a downward trend in the subsequent two years. Between 2020 and 2022, the mean pH increased significantly at all sites, reaching average values between 8.15 and 8.25 in S1 and S2, suggesting a temporary rise in alkalinity (Capuano, R. M., et al., 2020). However, in 2023 and 2024, a significant decrease in pH was observed, with values dropping to 7.20 in S1 and 7.38 in S8, reversing the trend observed immediately after the intervention. The initial pH increase could be attributed to the effects of bank reshaping carried out in 2022, which likely promoted greater sediment

oxygenation and reduced organic matter accumulation, conditions known to temporarily increase pH (Reddy, K. R., & Delaune, R. D., 2008).

The lack of correlation with $CaCO_3$ content (R^2 = 0.002) suggests that the pH variation was not primarily controlled by the presence of carbonates, but rather by dynamic environmental factors, such as organic matter decomposition, redox cycles, and seasonal water flows (Mitsch, W. J., & Gosselink, J. G., 2015). For example, for sites S2 and S5, while the $CaCO_3$ content decreased after the intervention, the pH value did not show any change. However, it was interesting to observe that the reduction of $CaCO_3$ content after the bank reshaping was observed only in S2 and S5. This fact can be attributed to the larger surface area addressed for the intervention in S2 and S5 than in S1 and S8 which might have promoted a higher accumulation of soil particles by erosion processes from the surrounding area. In fact, it is recognized the lower amount of carbonates into topsoil than subsoil due to decarbonation processes (Khalidy, R., et al., 2024; De Ros, A., et al., 2025).

Table 12 - Mean ± standard deviation of pH and the concentrations of calcium carbonate ($CaCO_3$). Within each column and site, different letters stand for significant differences among the means according to Kruskal-Wallis test ($p \leq 0.05$). Pre and post are for before and after intervention activity, respectively.

Site	Period	pH	CaCO3
			$g\,Kg^{-1}$
S1	pre	$7.78 \pm 0.25\ a$	$154 \pm 8\ a$
	post	7.85 ± 0.45 a	$141 \pm 19\ a$
S2	pre	$7.82 \pm 0.20\ a$	$176 \pm 23\ a$
	post	7.99 ± 0.33 a	$149 \pm 13\ b$
S5	pre	$8.01 \pm 0.31\ a$	$204 \pm 17\ a$
	post	7.99 ± 0.43 a	$186 \pm 5.8\ b$
S8	pre	$7.79 \pm 0.19\ a$	$200 \pm 13\ a$
	post	7.78 ± 0.42 a	$202 \pm 14\ a$

The particle size distribution showed significant variations between the pre- and post-intervention periods for S1, S2 and S5 (Figure 65). Specifically, both in S2 and S5, the bank reshaping increased the amount of finer particles within sediments likely due to the more intense erosion processes related to the larger

surface area that underwent intervention activities. It was interesting to observe that the bed sediment of sites S2 and S5 enriched of silty particles because of the weaker aggregation capacity of such particles promoting their erosion (Chang, T. S., et al., 2006; Forsberg, P. L., et al., 2018). Conversely, in S1 an increase of the sandy fraction and a reduction of silt and clay were observed post-intervention. This fact can be attributed to the flooding occurred in May 2023 which caused an increase of water flow within the canal promoting the resuspension and transport of the finer mineral particles (Park, J., & Hunt, J. R., 2018).

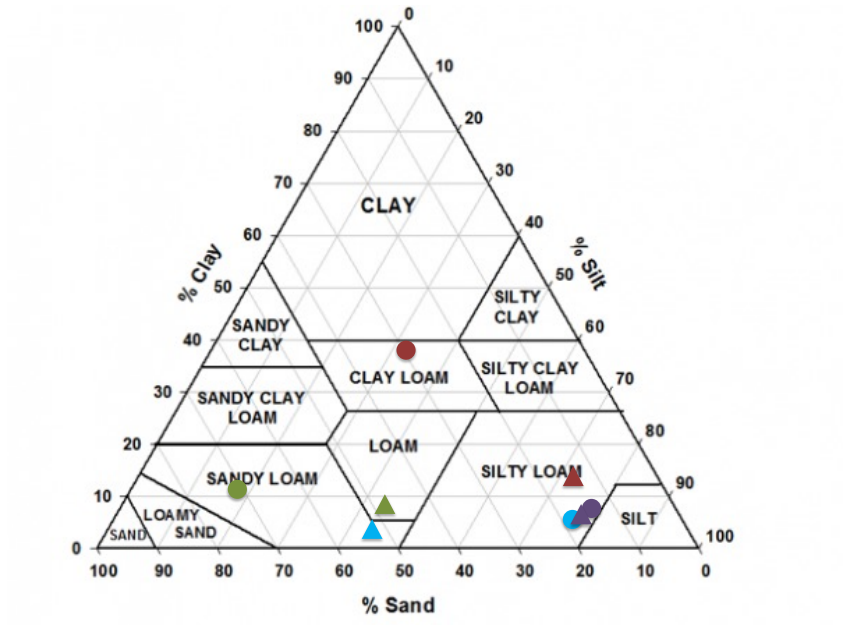

Figure 65 - Soil texture classification of sediment samples before (circles) and after (triangles) the intervention, based on the USDA soil texture triangle. Blue: S1; Purple: S2; Green; S5; Burgundy: S8.

The total amounts of boron (B), barium (Ba), zinc (Zn), manganese (Mn) and sulphur (S) generally did not show significant differences between pre and post intervention (Table 13). Few differences occurred in S1, S2 and S8 where the concentrations of such elements decreased after the intervention suggesting a slight positive effect of bank reshaping on bed sediment quality. No differences were found in S5 which can be attributed to the high amount of sandy mineral particles which do not allow the accumulation of nutrients because of their lower

cation exchange capacity compared with the finer mineral particles (Sukitprapanon, T. S., et al., 2020).

Table 13 - Mean ± standard deviation of boron (B), barium (Ba), magnesium (Mg), manganese (Mn), sulphur (S) and silicon (Si) concentrations. Within each row, different letters stand for significant differences among the means according to Kruskal-Wallis test (p ≤ 0.05). Pre and post are for before and after intervention activity, respectively.

Site	Parameter (mg L-1)	Period	
		Pre	Post
S1	**B**	$78 \pm 7\ a$	$37 \pm 21\ b$
	Ba	167 ± 17 a	119 ± 29 b
	Mn	0.7 ± 0.04 a	0.7 ± 0.1 a
	S	$1.4 \pm 0.5\ a$	$0.7 \pm 0.3\ b$
	Zn	$114 \pm 22\ a$	$103 \pm 29\ a$
S2	**B**	$67 \pm 29\ a$	$52 \pm 15\ b$
	Ba	185 ± 17 a	135 ± 13 a
	Mn	0.7 ± 0.08 a	0.7 ± 0.1 a
	S	$0.9 \pm 0.6\ a$	$0.7 \pm 0.3\ a$
	Zn	$95 \pm 6\ a$	$92 \pm 14\ b$
S5	**B**	$31 \pm 11\ a$	$22 \pm 10\ a$
	Ba	120 ± 24 a	97 ± 24 a
	Mn	0.6 ± 0.04 a	0.6 ± 0.09 a
	S	$0.4 \pm 0.1\ a$	$0.4 \pm 0.1\ a$
	Zn	$91 \pm 25\ a$	$96 \pm 31\ a$
S8	**B**	$49 \pm 10\ a$	$27 \pm 15\ b$
	Ba	160 ± 27 a	125 ± 18 b
	Mn	0.7 ± 0.08 a	0.6 ± 0.09 a
	S	$0.9 \pm 0.4\ a$	$1.2 \pm 0.3\ a$
	Zn	$97 \pm 15\ a$	$109 \pm 16\ a$

Concerning the EC, the results showed that the reshaping of the banks had no significant impact on the electrical conductivity of the sediments. The persistence of high values at some sites (more than 800 µS/cm) (Figure 66, Figure 67, Figure 68 and Figure 69) could be linked to external phenomena, such as agricultural inputs and drainage, which are not directly modifiable through physical intervention on the banks. For instance, the application of fertilizers and the use of drainage systems in adjacent agricultural lands can lead to increased leaching

of salts and nutrients into nearby water bodies, thereby elevating the EC of sediments (Zhang et al., 2023; Kadlec & Wallace, 2009). According to previous studies, conductivity tends to respond slowly to physical changes in the system and is significantly influenced by climatic conditions and surrounding land use (Kadlec & Wallace, 2009). This is consistent with findings from a recent study conducted in the Chi-Mun River Basin (Thailand), where agricultural expansion and urbanization were associated with increased EC values, especially during the dry season due to reduced flow and salt concentration (Pakoksung et al., 2025).

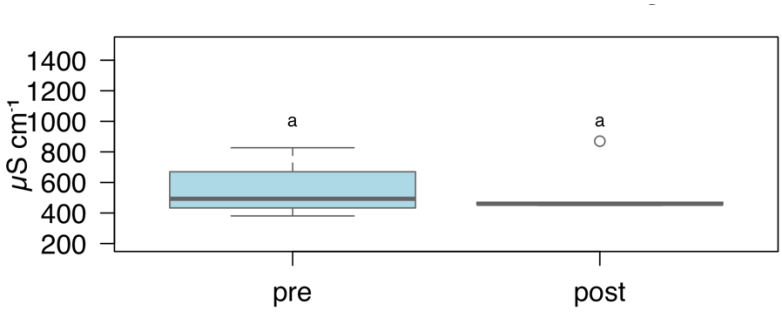

Figure 66 - Boxplot showing the electrical conductivity value before (pre) and after (post) intervention activity in site S1. Different letters stand for significant differences among the means according to Kruskal-Wallis test ($p \leq 0.05$).

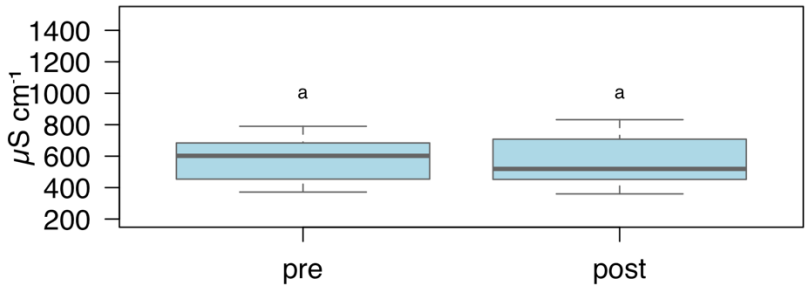

Figure 67 - Boxplot showing the electrical conductivity value before (pre) and after (post) intervention activity in site S2. Different letters stand for significant differences among the means according to Kruskal-Wallis test ($p \leq 0.05$).

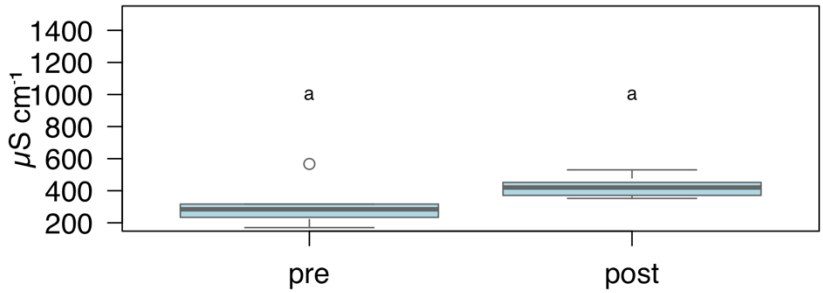

Figure 68 - Boxplot showing the electrical conductivity value before (pre) and after (post) intervention activity in site S5. Different letters stand for significant differences among the means according to Kruskal-Wallis test ($p \leq 0.05$).

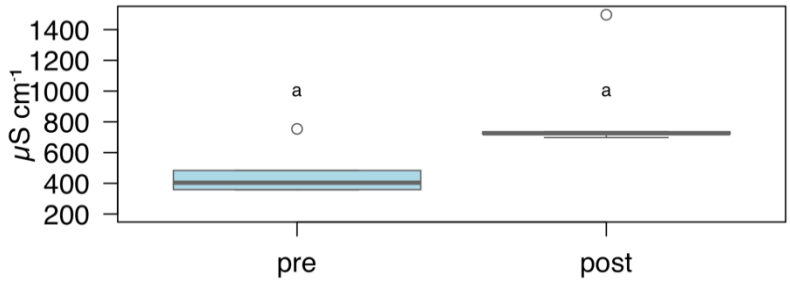

Figure 69 - Boxplot showing the electrical conductivity value before (pre) and after (post) intervention activity in site S8. Different letters stand for significant differences among the means according to Kruskal-Wallis test ($p \leq 0.05$).

The bank reshaping intervention generally did not cause changes of Ca, Na, Mg, and K concentrations in the sediments, suggesting a limited and localised impact on the chemical composition of the substrate (Figure 70, Figure 71, Figure 72 and Figure 73). The slight decrease in Ca and K contents at some sites (especially in S1 and S2) could reflect a dilution or dispersion effect following the morphological reorganisation of the banks. For Na and Mg, the absence of clear trends or the presence of small fluctuations would indicate that the intervention did not have a significant direct impact on these elements, which appeared to be more dependent on the input of water from external sources.

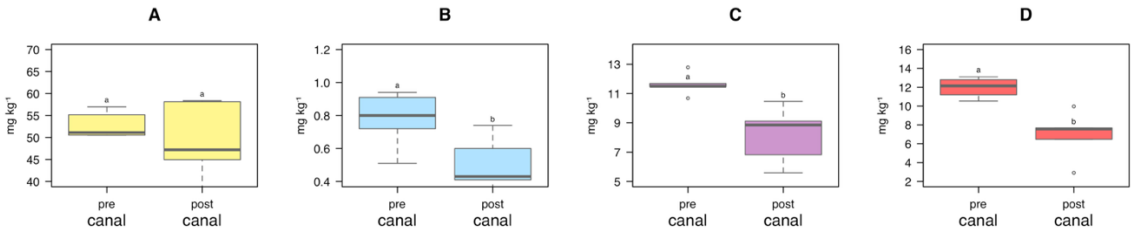

Figure 70 - Boxplot showing calcium (A), sodium (B), magnesium (C) and potassium (D) concentrations before (pre) and after (post) intervention activity in sediments at site S1. For each parameter, different letters stand for significant differences among the means according to Kruskal-Wallis test ($p \leq 0.05$).

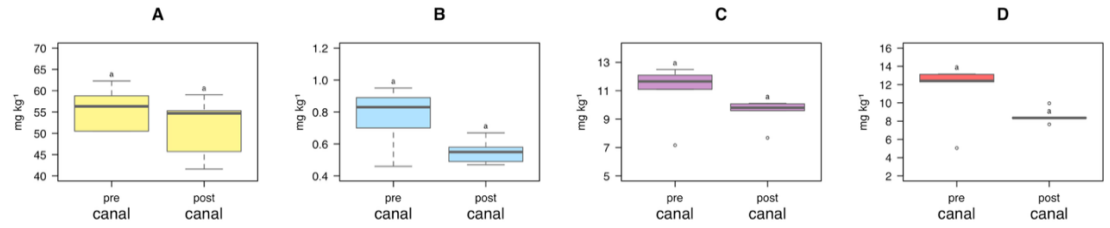

Figure 71 - Boxplot showing calcium (A), sodium (B), magnesium (C) and potassium (D) concentrations before (pre) and after (post) intervention activity in sediments at site S2. For each parameter, different letters stand for significant differences among the means according to Kruskal-Wallis test ($p \leq 0.05$).

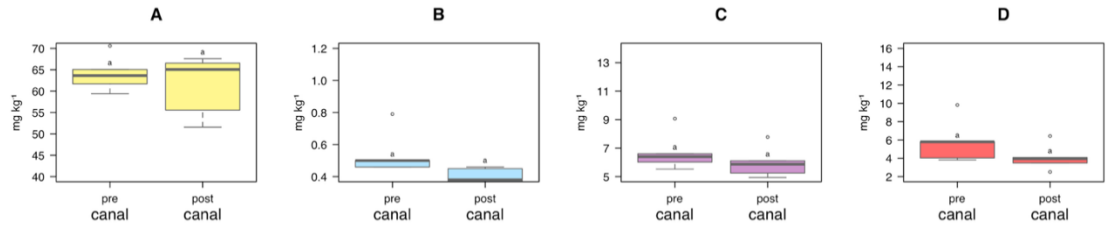

Figure 72 - Boxplot showing calcium (A), sodium (B), magnesium (C) and potassium (D) concentrations before (pre) and after (post) intervention activity in sediments at site S5. For each parameter, different letters stand for significant differences among the means according to Kruskal-Wallis test ($p \leq 0.05$).

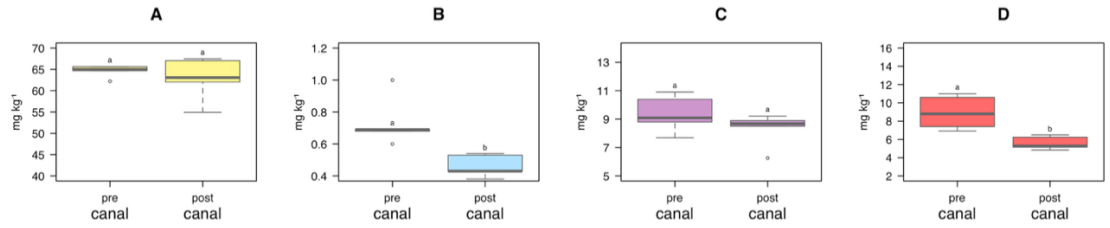

Figure 73 - Boxplot showing calcium (A), sodium (B), magnesium (C) and potassium (D) concentrations before (pre) and after (post) intervention activity in sediments at site S8. For each parameter, different letters stand for significant differences among the means according to Kruskal-Wallis test ($p \leq 0.05$).

With regard to iron (Fe) and copper (Cu) concentrations in sediments, our findings showed the absence of significant differences between pre and post intervention (Figure 74, Figure 75, Figure 76 and Figure 77). Conversely, the Al content showed lower values after intervention with exception of site S5 where no differences were found. The reduction of Al content could be interpreted as positive effect of bank reshaping on the chemical quality of the sediment since it is recognized as a potentially phytotoxic element in acidic or reduced environments (Delhaize, E., & Ryan, P. R., 1995).

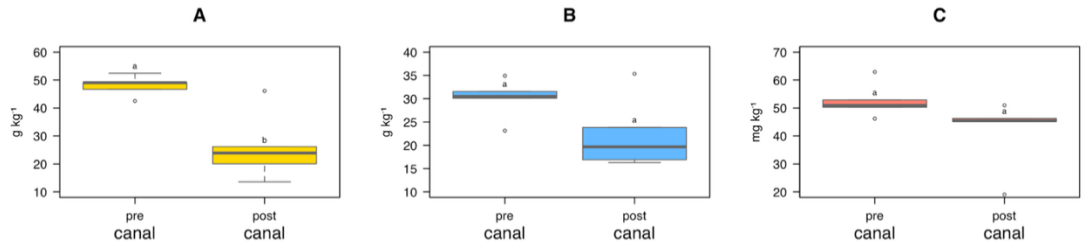

Figure 74 - Boxplot showing the *aluminium* (A), *i*ron (B) and copper (C) concentration*s before (pre) and after (post) intervention activity in sediments at site S1. For each parameter, different letters stand for significant differences among the means according to Kruskal-Wallis test (p ≤ 0.05).*

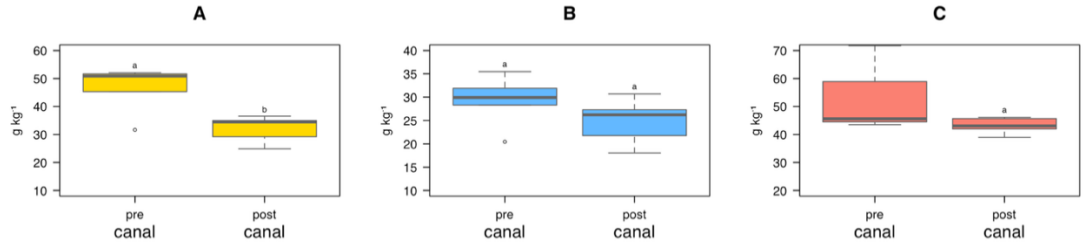

Figure 75 - Boxplot showing the aluminium (A), iron (B) and copper (C) concentrations before (pre) and after (post) intervention activity in sediments at site S2. For each parameter, different letters stand for significant differences among the means according to Kruskal-Wallis test (p ≤ 0.05).

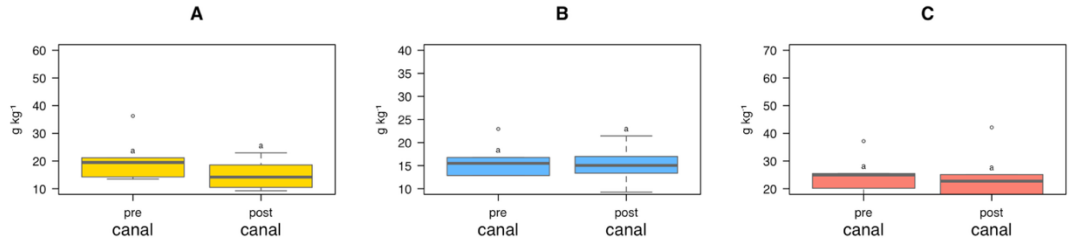

Figure 76 - Boxplot showing the aluminium (A), iron (B) and copper (C) concentrations before (pre) and after (post) intervention activity in sediments at site S5. For each parameter, different letters stand for significant differences among the means according to Kruskal-Wallis test (p ≤ 0.05).

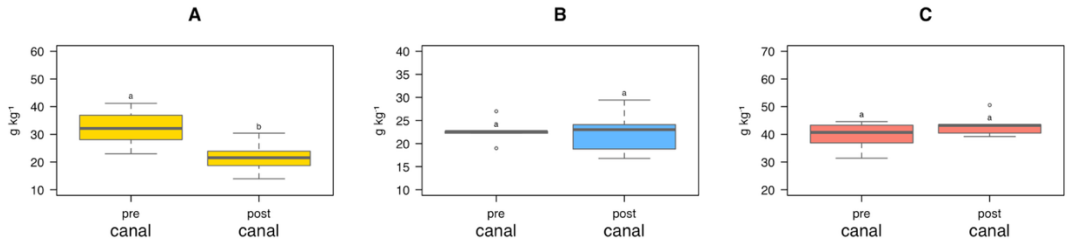

Figure 77 - Boxplot showing the aluminium (A), iron (B) and copper (C) concentrations before (pre) and after (post) intervention activity in sediments at site S8. For each parameter, different letters stand for significant differences among the means according to Kruskal-Wallis test (p ≤ 0.05).

Phosphorus (P) is an essential but potentially limiting nutrient in aquatic ecosystems, and its behaviour in sediments is strongly influenced by redox factors, the presence of hydroxyl metals (such as Fe and Al), the particle size of the substrate, and the amount of organic matter (Reddy, K. R., & Delaune, R. D., 2008). However, the restoration activity carried out in sites S1, S2, S5 and S8 did not affect the total content of P in bed sediments (Figure 78, Figure 79, Figure 80 and Figure 81).

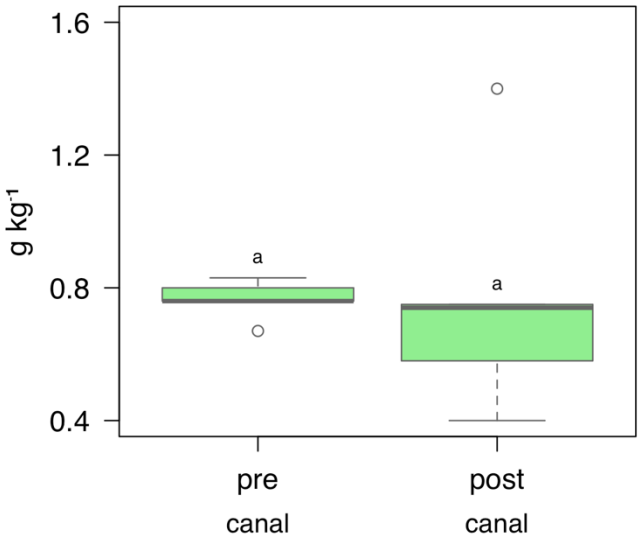

Figure 78 - Boxplot showing phosphorus concentration before (pre) and after (post) intervention activity in sediments at site S1. For each parameter, different letters stand for significant differences among the means according to Kruskal-Wallis test (p ≤ 0.05).

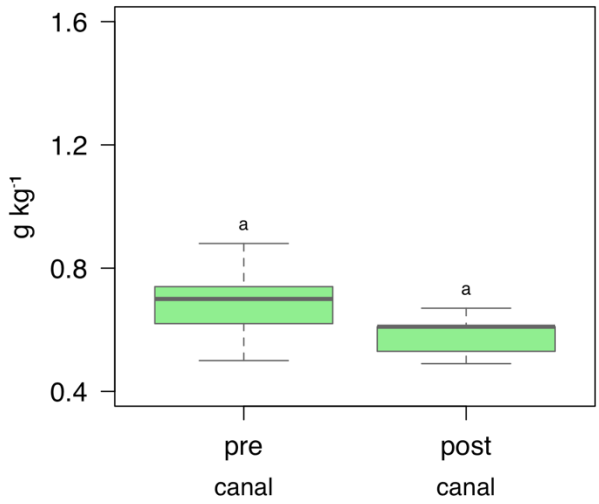

Figure 79 - Boxplot showing phosphorus concentration before (pre) and after (post) intervention activity in sediments at site S2. For each parameter, different letters stand for significant differences among the means according to Kruskal-Wallis test ($p \leq 0.05$).

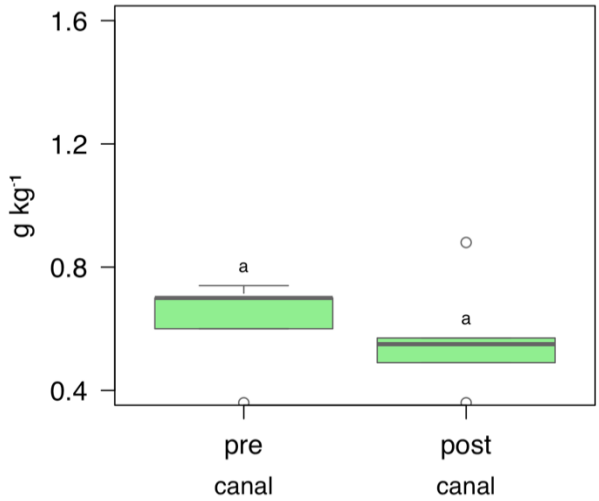

Figure 80 - Boxplot showing phosphorus concentration before (pre) and after (post) intervention activity in sediments at site S5. For each parameter, different letters stand for significant differences among the means according to Kruskal-Wallis test ($p \leq 0.05$).

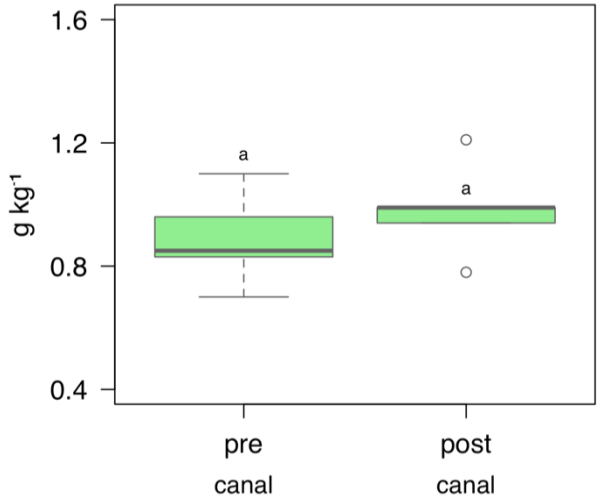

Figure 81 - Boxplot showing phosphorus concentration before (pre) and after (post) intervention activity in sediments at site S8. For each parameter, different letters stand for significant differences among the means according to Kruskal-Wallis test ($p \leq 0.05$).

Despite the different soil particle distribution of the bed sediments, no differences of total organic C were observed between pre and post intervention which would indicate the unresponsiveness of such feature at bank reshaping. Unlike organic C, the total N content showed some differences at sites S2 and S8 (Figure 83 and Figure 85). Specifically, an increase of total N content was observed after the bank reshaping.

However, no changes of C:N ratio were found. The lack of differences about C:N ratio would indicate a quite similar organic matter quality reaching the study sites and that such organic material undergoes similar decomposition processes in the considered sites.

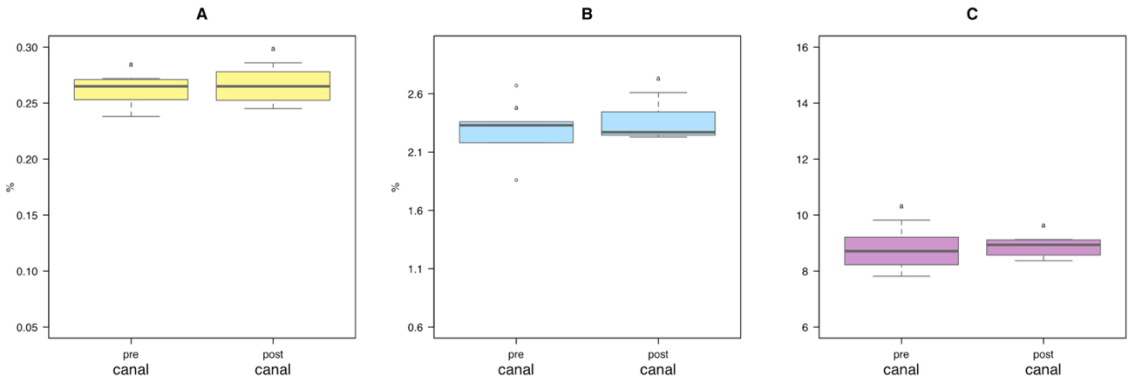

Figure 82 - Boxplot showing the concentrations of total nitrogen (A) and organic carbon (B), and C:N ratio (C) before (pre) and after (post) intervention activity in sediments at site S1. For each parameter, different letters stand for significant differences among the means according to Kruskal-Wallis test (p ≤ 0.05).

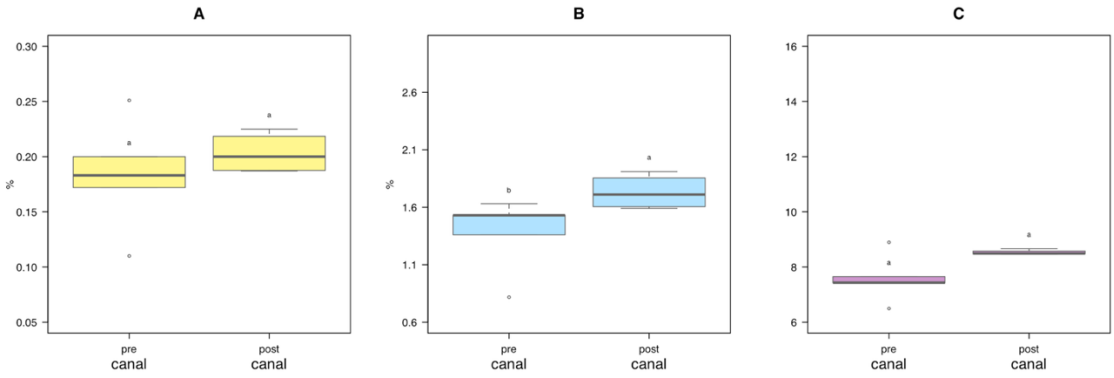

Figure 83- Boxplot showing the concentrations of total nitrogen (A) and organic carbon (B), and C:N ratio (C) before (pre) and after (post) intervention activity in sediments at site S2. For each parameter, different letters stand for significant differences among the means according to Kruskal-Wallis test (p ≤ 0.05).

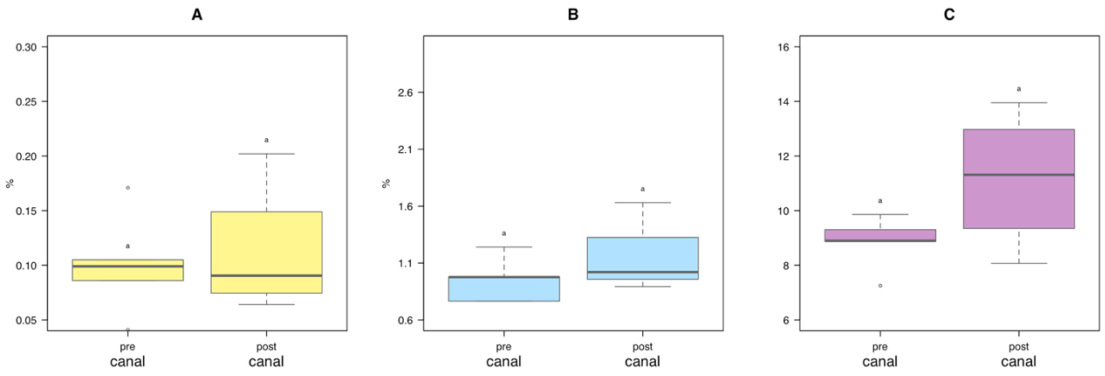

Figure 84 - Boxplot showing the concentrations of total nitrogen (A) and organic carbon (B), and C:N ratio (C) before (pre) and after (post) intervention activity in sediments at site S5. For each parameter, different letters stand for significant differences among the means according to Kruskal-Wallis test (p ≤ 0.05).

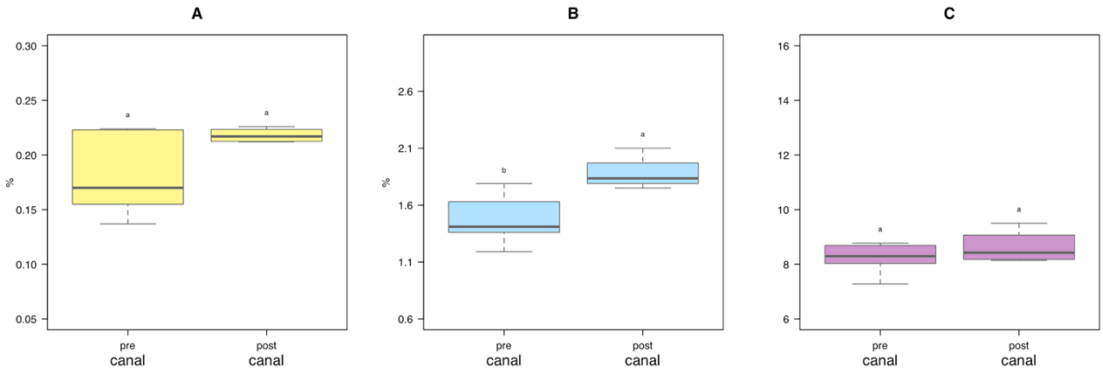

Figure 85 - Boxplot showing the concentrations of total nitrogen (A) and organic carbon (B), and C:N ratio (C) before (pre) and after (post) intervention activity in sediments at site S8. For each parameter, different letters stand for significant differences among the means according to Kruskal-Wallis test (p ≤ 0.05).

7.5 Influence of ponds on sediments quality of silty sites: Sites S6 and S7

The pH value in the sediments of S6 and S7 (Table 14) did not change over time and showed little variation between canals and ponds. In the canals, the pH ranged between 7.6 and 8.0, whereas slightly higher pH values were observed within ponds (7.8-8.2). The content of calcium carbonate ($CaCO_3$) was similar between canals and ponds. These findings would suggest that the balance between carbonate input, precipitation and dissolution was not substantially altered by the intervention (Mitsch, W. J., & Gosselink, J. G., 2015).

Table 14 - Mean ± standard deviation of pH and the concentration of calcium carbonate ($CaCO_3$). Within each column and site, different letters stand for significant differences among the means according to Kruskal-Wallis test (p ≤ 0.05). Pre: before pond construction; post: after pond construction.

Site	Location	Period	pH	CaCO3
				$g\,Kg^{-1}$
S6	Canal	pre	$7.84 \pm 0.21\ a$	$191 \pm 17\ a$
		post	8.00 ± 0.59 a	$187 \pm 12\ a$
	Pond		8.12 ± 0.36 a	$194 \pm 18\ a$
S7	Canal	pre	$7.88 \pm 0.26\ a$	$177 \pm 11\ b$
		post	8.17 ± 0.38 a	$173 \pm 14\ b$
	Pond		7.80 ± 0.41 a	$159 \pm 17\ a$

The analysis of sediment texture in S6 and S7 (Figure 86) showed substantial differences between canals and ponds, attributable to the combined effects of morphology, hydrodynamic conditions, and depositional processes induced by the creation of ponds in 2022.

In the canals of both sites, sediments showed a relatively coarser texture, with a higher percentage of the sandy fraction compared to the silt and clay fractions. Sediments from the canal at S6 showed a sandy-silty texture, with a more pronounced sand content compared to S7, where sediments were relatively finer. This pattern can be explained by the higher hydrodynamic energy within the canals, which promotes the transport and removal of finer particles, allowing the selective deposition of heavier and coarser materials (Nichols, M. M., 1999; Walling, D. E., & Collins, A. L., 2008).

The resuspension dynamics, typical of canals under continuous flow, further contributed to maintaining a coarser texture by limiting the stable accumulation of silt and clay, which are particularly sensitive to flow velocity (Wetzel, A., & Unverricht, D., 2020).

On the contrary, in the ponds constructed at both sites, sediment texture evolved towards a clear increase in the silt and clay fractions and a corresponding decrease in the sand fraction. In particular, sediments from the pond at S6 showed a predominantly silty-clayey texture, with high percentages of silt (over 60%) and clay (above 20%) particles.

The finer texture observed in the ponds has important implications for the chemical quality of sediments: silty-clayey sediments have a much greater specific surface area compared to sandy sediments, increasing their ability to adsorb nutrients, contaminants, and organic matter (Wagai, R., et al., 2020). This makes ponds particularly effective as "traps" for nutrients such as phosphorus and nitrogen, as well as for potentially toxic metals like zinc and copper, which tend to bind to colloidal surfaces or to organic matter associated with fine sediments (Kadlec, R. H., & Wallace, S. D., 2009).

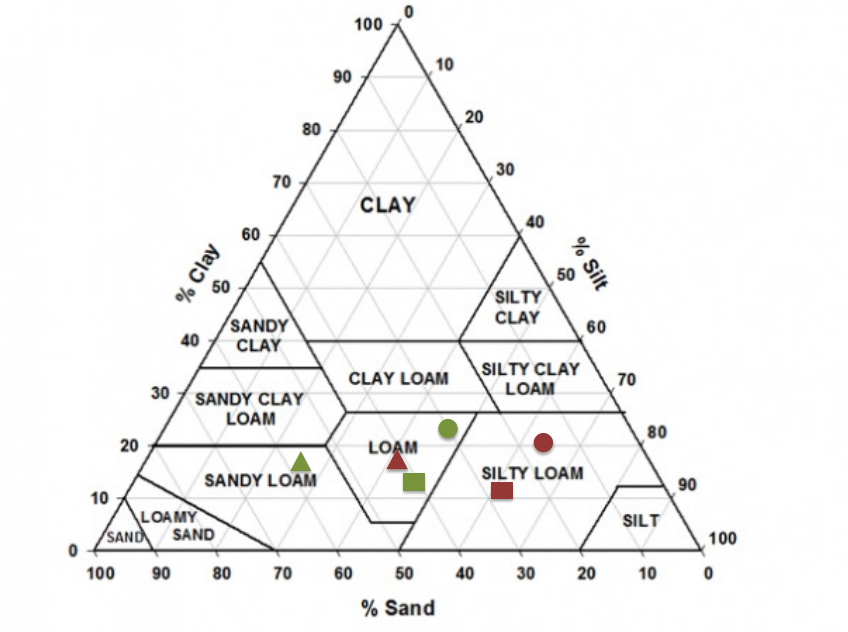

Figure 86 - Sediment texture classification based on the USDA soil texture triangle. Circles represent canal sediments before the intervention, triangles represent canal sediments after the intervention, and rectangles represent pond sediments. *Burgundy: S6; Green: S7.*

The concentrations of boron and barium (Table 15) were slightly higher in the pond sediments compared to the canals in S7, while in S6 the observed differences were minimal. The greater accumulation in the ponds can be explained by the sedimentation of fine particles and organic matter, which tend to retain these elements (Wagai, R., et al., 2020).

Zinc concentrations were higher in the pond at S7 compared to the canal, although the differences were not statistically significant. Conversely, in S6, Zn concentrations were significantly higher in the canal than in the pond. This difference may reflect varying dynamics of fine sediment and organic matter accumulation, which influence Zn retention. Manganese concentrations did not show differences between canals and ponds, while sulphur content showed lower values in the pond than in the canal at S6, but higher values in the pond than in the canal for S7. This different behaviour between the two sites might be attributed to the smaller dimension of pond S7 which might promote eutrophic conditions with consequent accumulation of sulphur (Zawiska et al., 2023; Holmer and Storkholm, 2001).

Table 15 - Mean ± standard deviation of concentrations of boron (B), barium (Ba), manganese (Mn), sulphur (S) and zinc (Zn). Within each row, different letters stand for significant differences among the means according to Kruskal-Wallis test (p ≤ 0.05). Pre: before pond construction; post: after pond construction.

Site	Parameter	Location & Period		
		Canal pre	Canal post	Pond
S6	**B**	$42 \pm 6\ a$	$29 \pm 13\ ab$	$24 \pm 5\ b$
	Ba	140 ± 29 a	95 ± 28 ab	117 ± 15 b
	Mn	0.5 ± 0.06 a	0.6 ± 0.1 a	0.6 ± 0.06 a
	S	$0.7 \pm 0.1\ a$	$0.5 \pm 0.2\ ab$	$0.4 \pm 0.1\ b$
	Zn	$174 \pm 154\ a$	$74 \pm 29\ b$	$69 \pm 6\ b$
S7	**B**	$36 \pm 9\ a$	$35 \pm 17\ a$	$25 \pm 9\ a$
	Ba	130 ± 36 a	135 ± 42 a	160 ± 46 a
	Mn	0.6 ± 0.08 a	0.6 ± 0.1 a	0.6 ± 0.06 a
	S	$0.4 \pm 0.2\ a$	$0.4 \pm 0.3\ a$	$0.8 \pm 0.9\ a$
	Zn	$94 \pm 30\ a$	$87 \pm 13\ a$	$144 \pm 60\ a$

In both sites, the electrical conductivity (EC) values did not show significant differences between canal and pond, as well as before and after pond construction (Figure 87 and Figure 88)

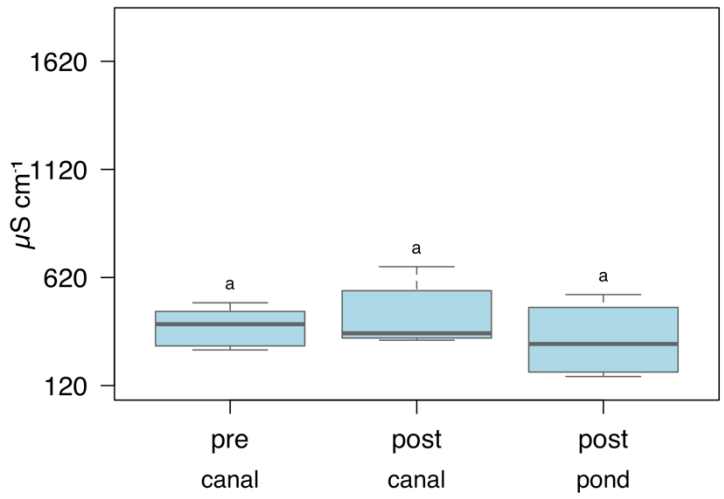

Figure 87 - Boxplot showing the electrical conductivity value in the sediments of canal before (pre) and after (post) intervention, and of pond at site S6. Different letters above the boxes indicates statistical differences according to Kruskal-Wallis test (p ≤ 0.05).

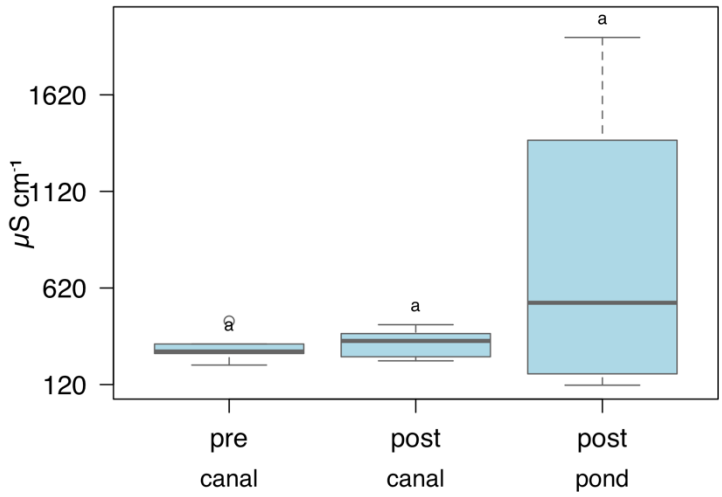

Figure 88 - Boxplot showing the electrical conductivity value in the sediments of canal before (pre) and after (post) intervention, and of pond at site S7. Different letters above the boxes indicates statistical differences according to Kruskal-Wallis test ($p \leq 0.05$).

Regarding Ca, Mg, K, and Na concentrations, some differences occurred only at S6 (Figure 89). In particular, both the canal and the pond sediments after the intervention showed lower Na and K concentrations compared to the pre-intervention canal sediments. This decrease may be explained by the partial removal or disturbance of the surface sediment layer during restoration activities, which likely led to the loss of more soluble and weakly bound elements such as Na and K (Steinman et al., 2022). Additionally, the sandy substrate of the pond, characterized by low cation exchange capacity, prevented their accumulation in the sediments (Kabata-Pendias, 2011).

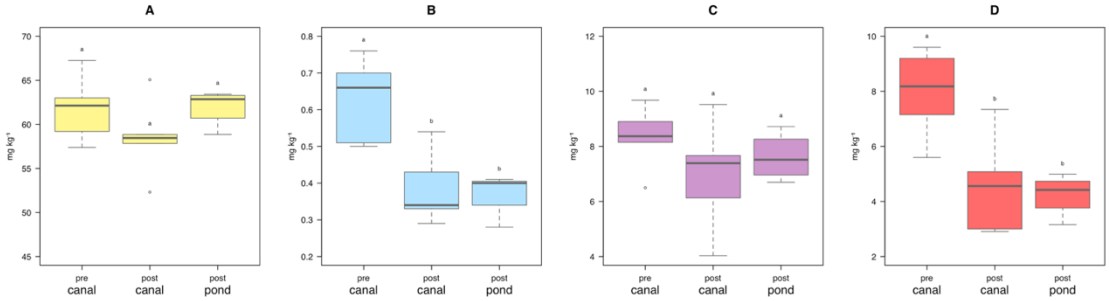

Figure 89 - Boxplot showing the calcium (A), sodium (B), magnesium (C) and potassium (D) concentrations in sediments of canal before (pre) and after (post) intervention, and of pond at site S6. Different letters above the boxes indicates statistical differences according to Kruskal-Wallis test ($p \leq 0.05$).

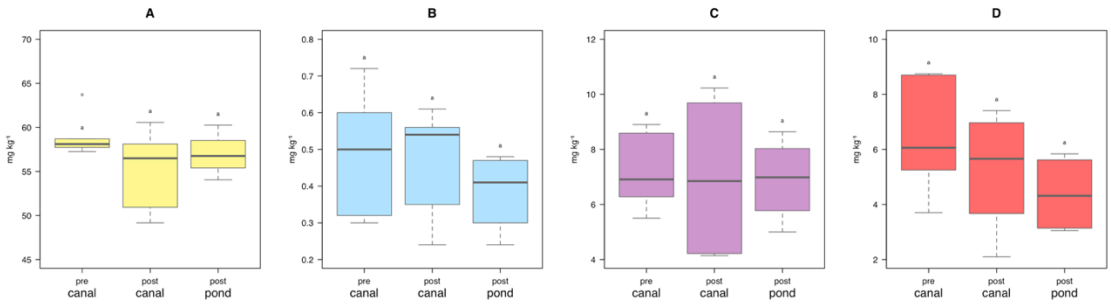

Figure 90 - Boxplot showing the calcium (A), sodium (B), magnesium (C) and potassium (D) concentrations in sediments of canal before (pre) and after (post) intervention, and of pond at site S7. Different letters above the boxes indicates statistical differences according to Kruskal-Wallis test ($p \leq 0.05$).

At both sites, aluminium and iron concentrations did not show differences between pond and canal (Figure 91 and Figure 92), as well as, between the sediments sampled before and after the pond construction. Some differences occurred for copper content at site S6 showing lower values in the pond than in the canal. Unlike site S6, as observed for Zn content, in S7 the Cu content did not show differences likely due to the different hydrodynamic conditions in the S7 pond, which promote the accumulation of fine sediments and organic matter, thereby enhancing metal retention (Kabata-Pendias, 2011; Huang et al., 2020). Moreover, reduced water flow in the pond environment can lead to more anoxic conditions, which are known to influence the geochemical mobility and binding of trace metals such as copper (Förstner & Wittmann, 2012).

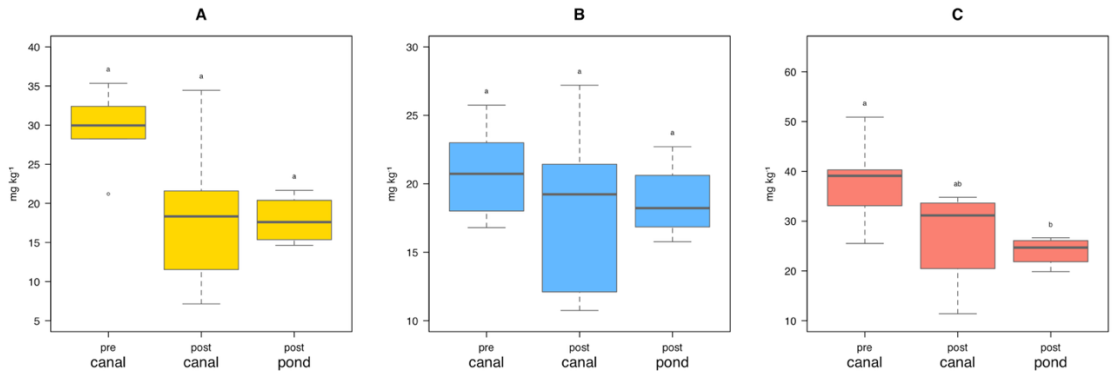

Figure 91 - Boxplot showing the aluminium (A), iron (B) and copper (C) concentrations in the sediment of canal before (pre) and after (post) intervention, and of pond at site S6. Different letters above the boxes indicates statistical differences according to Kruskal-Wallis test ($p \leq 0.05$).

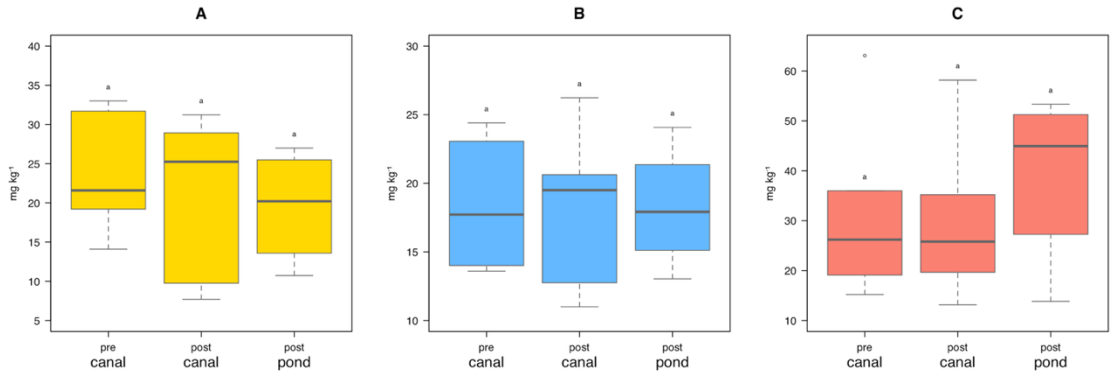

Figure 92 - Boxplot showing the aluminium (A), iron (B) and copper (C) concentration in the sediment of canal before (pre) and after (post) intervention, and of pond at site S7. Different letters above the boxes indicates statistical differences according to Kruskal-Wallis test ($p \leq 0.05$).

Regarding phosphorus, while in S6 its concentration decreased after the pond construction, in S7 no differences were found among pond, the canal before the intervention and the canal after the intervention (Figure 93 and Figure 94). Such different behaviour might be attributed to the smaller dimension of the pond in S7 than in S6 which likely prevented any positive effect of the used NBS on sediment quality improvement.

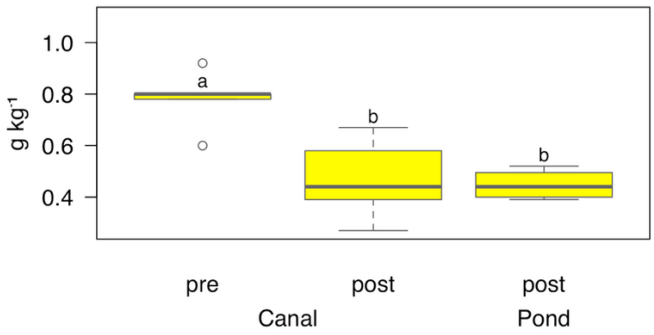

Figure 93 - Boxplot showing the phosphorus concentration in the sediment of canal before (pre) and after (post) intervention, and of pond at site S6. Different letters above the boxes indicates statistical differences according to Kruskal-Wallis test ($p \leq 0.05$).

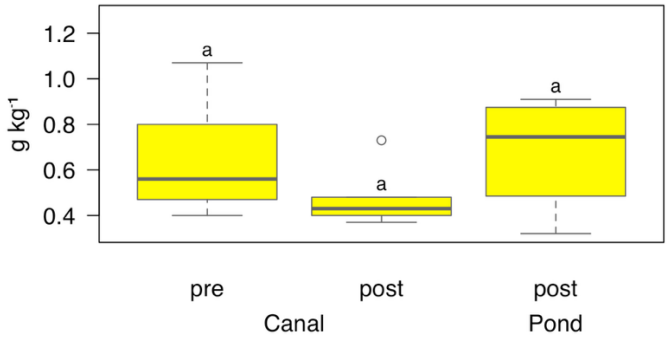

Figure 94 - Boxplot showing the phosphorus concentration in the sediment of canal before (pre) and after (post) intervention, and of pond at site S7. Different letters above the boxes indicates statistical differences according to Kruskal-Wallis test ($p \leq 0.05$).

Similar to phosphorus, while in S6 both the organic C and total N concentration showed lower values in the pond and in the canal after the intervention than in the canal before the intervention (Figure 95A and Figure 95B), a lack of differences was observed in S7 (Figure 96A and Figure 96B). These findings would suggest a weaker role of small ponds on sediment quality improvement compared to large ponds. The C:N ratio (Figure 95C and Figure 96C) remained relatively similar between canals and ponds (around 8–9), indicating a similar organic matter origin and dynamics in both sites.

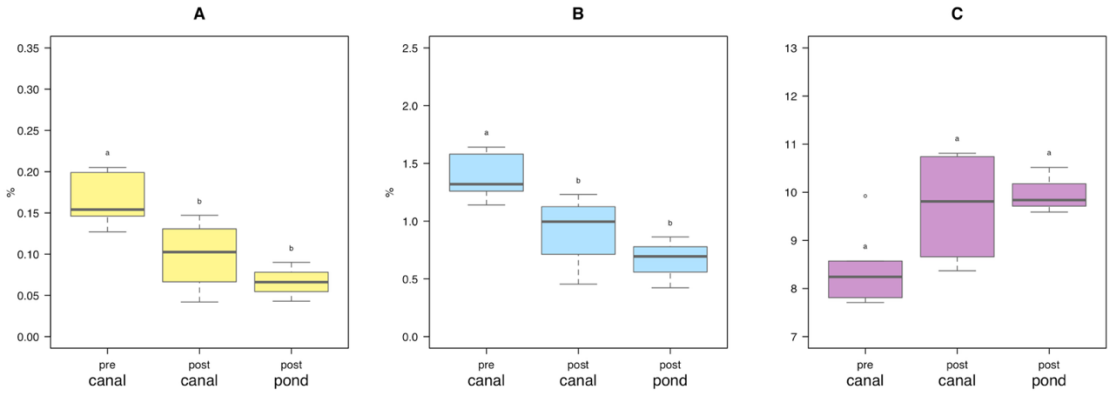

Figure 95 - Boxplot showing the concentrations of nitrogen (A) and organic carbon (B), and C:N ratio (C) in the sediment of canal before (pre) and after (post) intervention, and of pond at site S6. Different letters above the boxes indicates statistical differences according to Kruskal-Wallis test ($p \leq 0.05$).

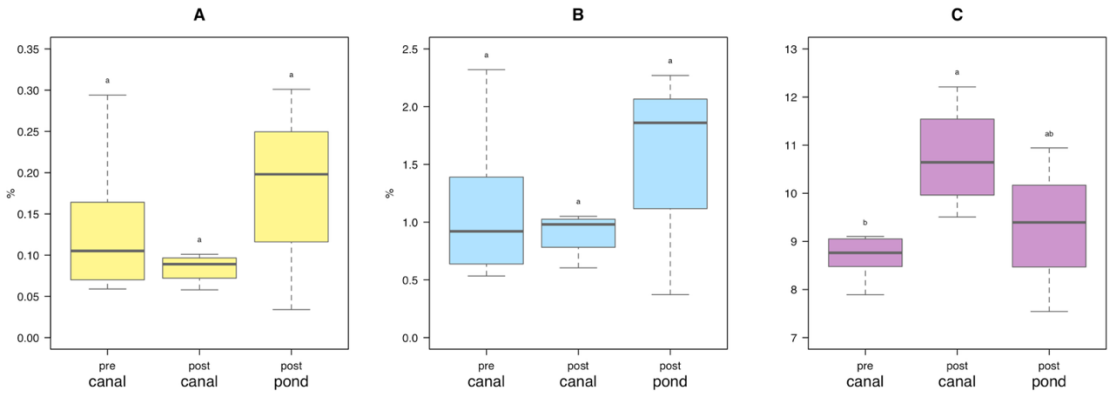

Figure 96 - Boxplot showing the concentrations of nitrogen (A) and organic carbon (B), and C/N ratio (C) in the sediment of canal before (pre) and after (post) intervention, and of pond at site S7. Different letters above the boxes indicates statistical differences according to Kruskal-Wallis test ($p \leq 0.05$).

7.6 Influence of ponds on sediments quality of clay sites: Sites S4 and S9

In S4 and S9, pH values were slightly alkaline, ranging from 7.5 to 8.1 (Table 16). Pond sediments exhibited slightly higher pH values compared to the canals, although the differences were not statistically significant. This pattern may reflect more stable redox conditions in the stagnant environment of the ponds or a lower degree of microbial acidification. In stagnant systems such as ponds, the limited availability of oxygen reduces aerobic microbial activity, which is often responsible for the production of organic acids during the decomposition of organic matter (Chen et al., 2025).

The carbonate content ($CaCO_3$) was high across all samples, with mean values exceeding 13% in S9 and 17% in S4 (Table 16). In S9, pond sediments showed carbonate enrichment compared to the canals, while in S4 the differences were not statistically significant. The observed accumulation in S9 may be linked to carbonate precipitation processes promoted by alkaline and reducing conditions, which are often characteristic of stagnant sedimentary environments (Zhu & Dittrich, 2016).

Table 16 - Mean ± standard deviation of pH and the concentration of calcium carbonate ($CaCO_3$). Within each column and site, different letters stand for significant differences among the means according to Kruskal-Wallis test ($p \leq 0.05$). Pre: before pond construction; post: after pond construction.

Site	Location	Period	pH	CaCO3
				$g\,Kg^{-1}$
S4	Canal	pre	$7.76 \pm 0.23\ a$	$177 \pm 17\ a$
		post	7.51 ± 0.53 a	$170 \pm 12\ a$
	Pond		8.11 ± 0.46 a	$175 \pm 18\ a$
S9	Canal	pre	$7.76 \pm 0.26\ a$	$131 \pm 11\ b$
		post	7.76 ± 0.38 a	$130 \pm 14\ b$
	Pond		8.00 ± 0.41 a	$160 \pm 17\ a$

Sediment texture analysis in S4 and S9 revealed marked differences between canals and ponds (Figure 97). In the canals of both sites, sediments exhibited a generally coarser texture than ponds, dominated by the sand fraction.

In S4, canal sediments were classified as sandy-silty, with a clear predominance of sand (~69%), followed by silt (23%) and clay (8%). A similar pattern was observed in S9, with average proportions of 63% sand, 26% silt, and 11% clay. This distribution confirms the influence of higher hydrodynamic energy in the canals, which promotes the resuspension and downstream transport of finer particles, allowing for the selective deposition of coarser grains (Nichols, 1999; Walling & Collins, 2008).

The fluvial dynamics and turbulence associated with continuous flow help maintain a sand-dominated texture in canals, limiting the accumulation of silt and clay fractions particularly sensitive to flow velocity (Wetzel & Unverricht, 2020). This behaviour is consistent with what was observed in S6 and S7, underscoring the role of the hydrodynamic regime in shaping sediment grain-size composition.

In contrast, the ponds in S4 and S9 exhibited a significantly finer texture, with enrichment in the silt and clay fractions. In S4, compared to the canal, the pond showed a lower sand content (45%), and higher contents of silt (39%) and clay (16%) particles. A similar distribution was found in S9 showing lower sand content (41%), higher silt content (43%), and similar clay content (16%) compared with the canal. The reduced hydraulic energy typical of ponds

promotes the settling of finer particles, leading to the accumulation of silty and clayey sediments.

From a functional standpoint, the accumulation of fine-grained material in the ponds increases the specific surface area of the sediments, thereby enhancing their ability to adsorb nutrients, contaminants, and organic matter (Wagai et al., 2020). In this context, ponds may act as natural filtration systems, capable of retaining phosphorus, nitrogen, and potentially toxic metals associated with the colloidal and organic sediment fractions (Kadlec & Wallace, 2009).

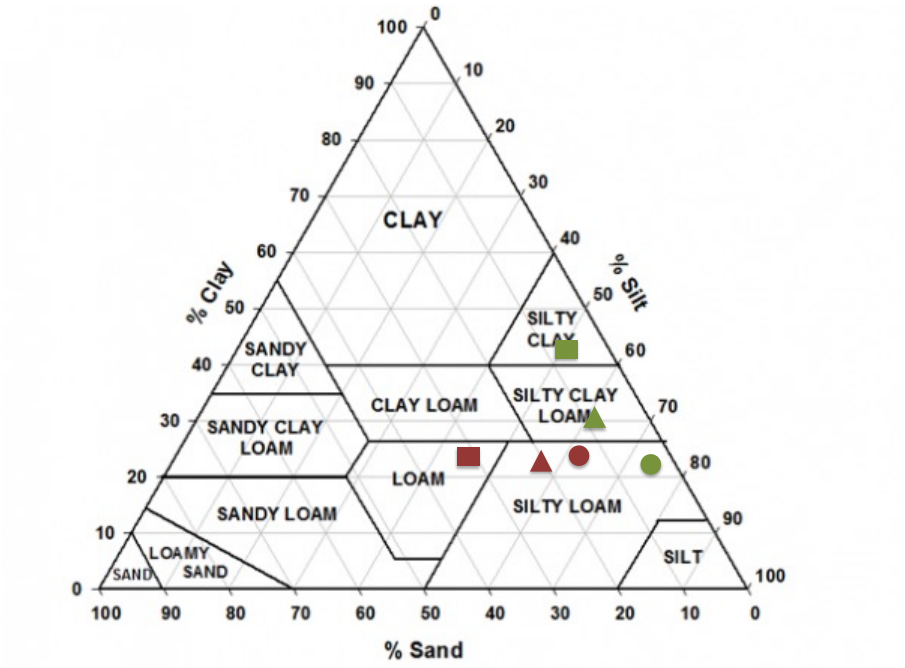

Figure 97 - Sediment texture classification based on the USDA soil texture triangle. Circles represent canal sediments before the intervention, triangles represent canal sediments after the intervention, and rectangles represent pond sediments after the intervention. Site 9 is represented in green, while site 4 is shown in burgundy.

At both sites, the concentrations of boron and barium (Table 17) showed the highest values within the canal before pond construction. While manganese and sulphur concentrations showed the lowest values within the ponds. These findings would suggest a potential effect of enhanced retention in the ponds, likely associated with the presence of fine sediment fractions and organic matter, as previously observed in S6 and S7 (Wagai et al., 2020).

Table 17 - Mean ± standard deviation of concentrations of boron (B), barium (Ba), manganese (Mn), sulphur (S) and zinc (Zn). Within each row, different letters stand for significant differences among the means according to Kruskal-Wallis test (p ≤ 0.05). Pre: before pond construction; post: after pond construction.

Site	Parameter	Location & Period		
		Canal pre	Canal post	Pond
S4	**B**	$71 \pm 7\ a$	$41 \pm 16\ b$	$37 \pm 19\ b$
	Ba	180 ± 21 a	116 ± 12 b	111 ± 9 b
	Mn	0.7 ± 0.06 a	0.7 ± 0.09 a	0.5 ± 0.08 b
	S	$1.3 \pm 0.3\ a$	$1.5 \pm 0.2\ a$	$0.5 \pm 0.2\ b$
	Zn	$131 \pm 20\ a$	$140 \pm 31\ a$	$85 \pm 17\ b$
S9	**B**	$46 \pm 2\ a$	$46 \pm 4\ b$	$53 \pm 7\ b$
	Ba	73 ± 7 a	64 ± 64 a	40 ± 0.8 b
	Mn	0.6 ± 0.08 a	0.6 ± 0.1 a	0.6 ± 0.06 a
	S	$0.4 \pm 0.2\ b$	$0.6 \pm 0.3\ b$	$0.7 \pm 0.9\ b$
	Zn	$94 \pm 30\ b$	$87 \pm 13\ b$	$128 \pm 60\ a$

The electrical conductivity (EC) of sediments exhibited relatively high values at both sites (Figure 98 and Figure 99), reflecting a certain degree of salinity in the deposited material and a potential influence from canal water.

In S4, EC values in the canal increased from the pre-intervention condition (around 650 µS cm⁻¹) to the post-intervention condition (median approximately 900 µS cm⁻¹), and then decreased in the pond, returning to levels similar to the initial condition (600–650 µS cm⁻¹). In S9, a slightly different pattern was observed: EC values gradually increased from pre- to post-intervention and were slightly higher in the pond compared to the initial canal condition. However, at both sites these differences among the three compartments were not statistically significant.

The lack of significant variation between canals and ponds may reflect a balance between the accumulation of dissolved ions in the sediments and dilution processes associated with water inputs. Ponds may function as temporary stagnation zones, favouring salt accumulation but also subject to dilution phenomena resulting from water exchange with the canal or rainfall events (Wang et al., 2025).

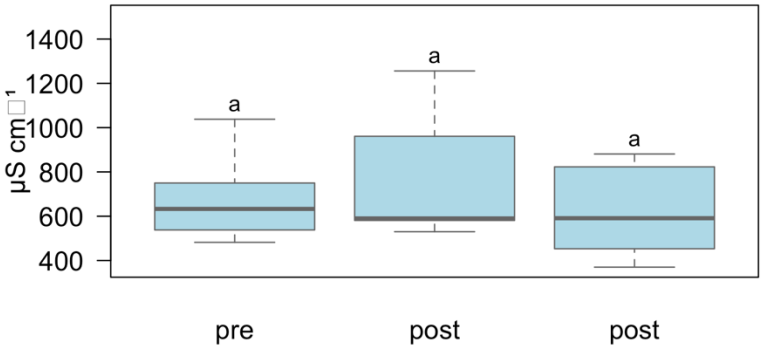

Figure 98 - Boxplot showing the electrical conductivity value in the sediments of canal before (pre) and after (post) intervention, and of pond at site S4. Different letters above the boxes indicates statistical differences according to Kruskal-Wallis test (p ≤ 0.05).

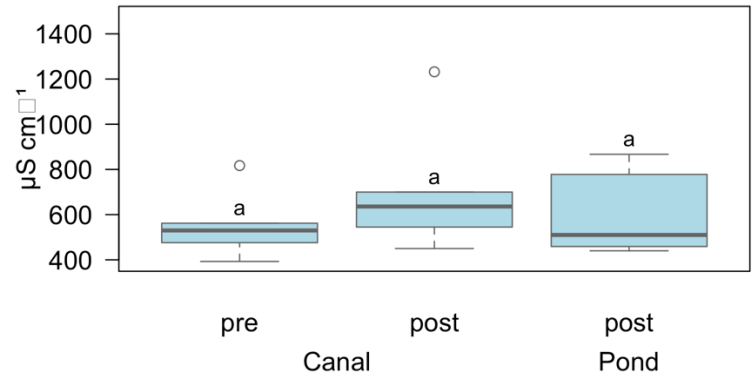

Figure 99 - Boxplot showing the electrical conductivity value in the sediments of canal before (pre) and after (post) intervention, and of pond at site S9. Different letters above the boxes indicates statistical differences according to Kruskal-Wallis test (p ≤ 0.05).

The analysis of Ca, Na, Mg and K revealed substantial differences between the canal and pond compartments, with occasionally divergent trends between the two sites (Figure 100 and Figure 101). Sediments of pond and canal after the intervention activity showed generally lower contents of Ca, Na, Mg and K compared to the sediments of canal before the intervention suggesting a positive effect of the NBS on nutrient loads in sediments. We can hypothesize that the intense vegetative activities occurring around the ponds prevented nutrient accumulation within their sediments, which is consistent with previous studies carried out in wetlands (Kadlec, R. H., & Wallace, S. D., 2009). Since, the fairly

high dimension of such ponds and their connection with the canal, such positive effect was observed also within the canal after the pond construction.

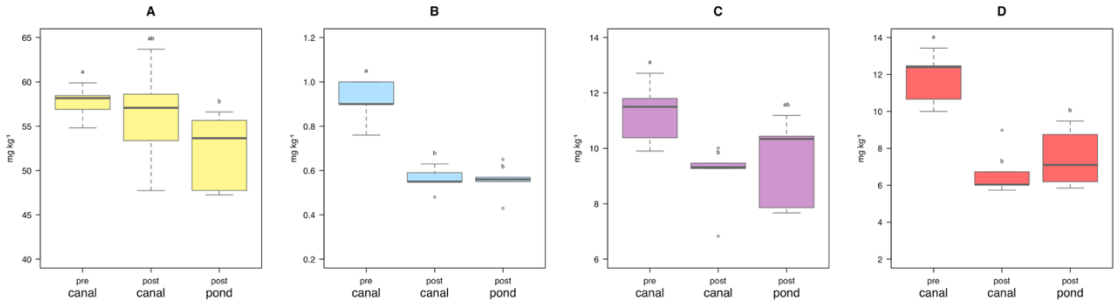

Figure 100 - Boxplot showing the calcium (A), sodium (B), magnesium (C) and potassium (D) concentrations in sediments of canal before (pre) and after (post) intervention, and of pond at site S4. Different letters above the boxes indicates statistical differences according to Kruskal-Wallis test (p ≤ 0.05).

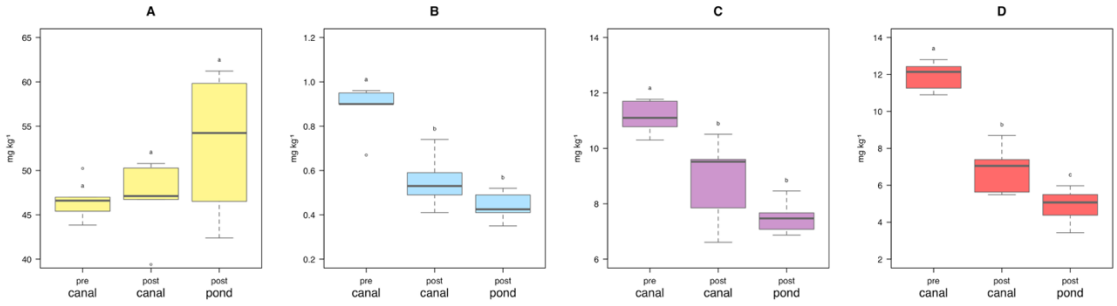

Figure 101 - Boxplot showing the calcium (A), sodium (B), magnesium (C) and potassium (D) concentrations in sediments of canal before (pre) and after (post) intervention, and of pond at site S9. Different letters above the boxes indicates statistical differences according to Kruskal-Wallis test (p ≤ 0.05).

The analysis of aluminium (Al), iron (Fe), and copper (Cu) concentrations in the sediments of sites S4 (Figure 102) and S9 (Figure 103) revealed significant differences between canals and ponds. In S4, aluminium content showed a clear decrease from pre- to post-intervention conditions in the canal. Concentrations were initially high in the pre-intervention canal (approximately 50 g/kg), then dropped in the post-intervention canal (30 g/kg). Also, the Al content in pond resulted to be lower than in the canal before the intervention.

In S9, the trend was even more pronounced compared to S4 with a progressive and significant decrease in Al from the pre- to the post-intervention canal, and further into the pond (from approximately 55 to 20 g/kg).

Iron (Fe) concentrations in S4 remained relatively stable across compartments, with only a slight decrease in the pond. In contrast, S9 exhibited a clear decrease in Fe from the pre-intervention canal to the pond, with statistically significant differences.

Regarding copper (Cu) content, both sites showed the lowest values within the ponds (35 mg/kg and 45 mg/kg at S4 and S9, respectively). This trend contrasts with observations in sites S6 and S7, where copper tended to accumulate in the ponds. Such a difference may be related to lower organic matter availability or the different sediment texture in the ponds of S4 and S9, which could reduce the retention capacity for Cu, a metal typically associated with the colloidal and organic fractions (Zhang et al., 2021; Sparks, 2003).

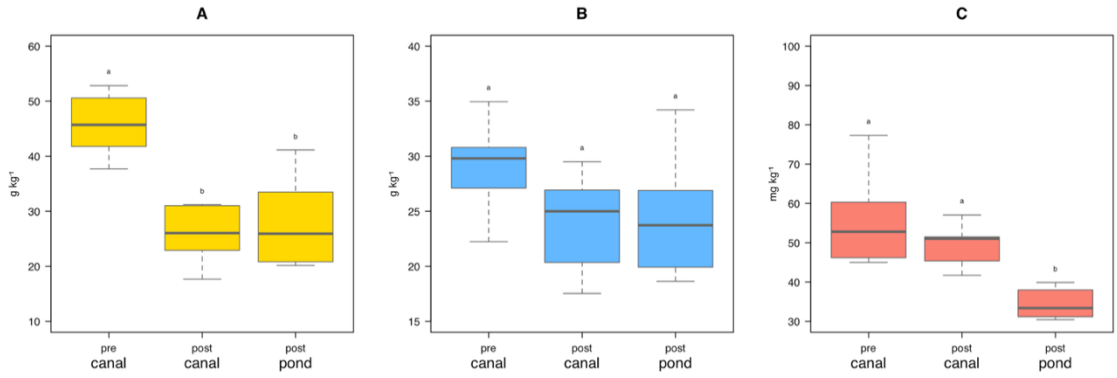

Figure 102 - Boxplot showing the aluminium (A), iron (B) and copper (C) concentrations in the sediment of canal before (pre) and after (post) intervention, and of pond at site S4. Different letters above the boxes indicates statistical differences according to Kruskal-Wallis test ($p \leq 0.05$).

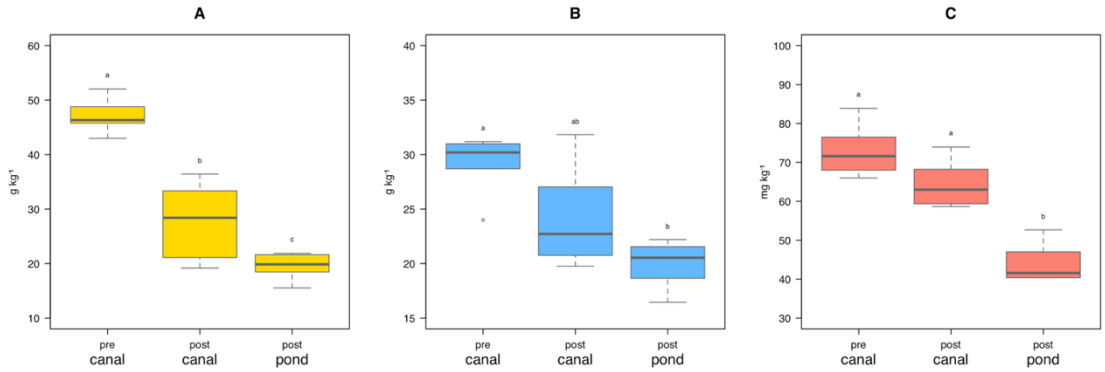

Figure 103 - Boxplot showing the aluminium (A), iron (B) and copper (C) concentrations in the sediment of canal before (pre) and after (post) intervention, and of pond at site S9. Different letters above the boxes indicates statistical differences according to Kruskal-Wallis test ($p \leq 0.05$).

At both sites, the pond construction generally decreased the phosphorus content within the sediments.

The reduction in phosphorus concentrations in the ponds may be attributed to more reducing redox conditions in the ponds that favour phosphorus mobilization into the dissolved phase. In reducing environments, phosphorus release from sediments is frequently observed due to the dissolution of Fe–P complexes, particularly the reduction of Fe^{3+}, as described by Wang et al. (2023).

These dynamics contrast with those observed in S6 and S7, where ponds promoted phosphorus accumulation due to a greater presence of silt-clay fractions and organic matter. The data therefore suggest a site-specific response to the intervention, with reduced effectiveness of the S4 and S9 ponds as phosphorus traps.

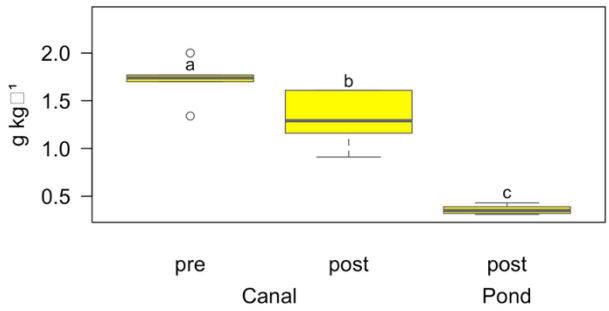

Figure 104 - Boxplot showing the phosphorus concentration in the sediment of canal before (pre) and after (post) intervention, and of pond at site S4. Different letters above the boxes indicates statistical differences according to Kruskal-Wallis test ($p \leq 0.05$).

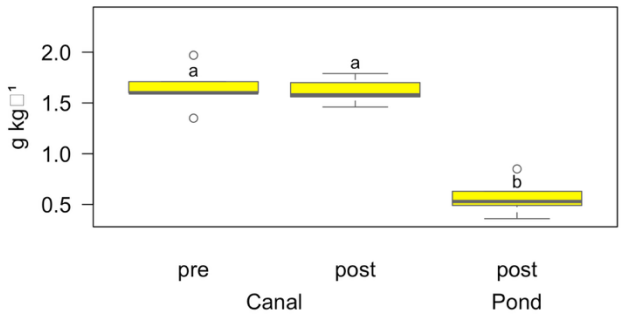

Figure 105 - Boxplot showing the phosphorus concentration in the sediment of canal before (pre) and after (post) intervention, and of pond at site S9. Different letters above the boxes indicates statistical differences according to Kruskal-Wallis test ($p \leq 0.05$).

In S4, nitrogen concentrations remained stable between the pre- and post-intervention canals but showed a significant decrease in the pond (Figure 106A). Organic carbon (OC) followed a similar pattern, increasing in the post-intervention canal but exhibiting a marked decline in the pond (Figure 106B). These results suggest that, in S4, pond sediments did not support the stable accumulation of organic matter and nitrogen, in contrast to what was observed in S6 and S7. This behaviour may be related to a lower deposition of fine material or to the intense degradation of organic matter under reducing and stagnant conditions, as highlighted by Song et al. (2023), who emphasized the strong influence of redox processes and hydrodynamics on OC preservation in sediments.

The C:N ratio, an indicator of organic matter quality, did not show significant variation between compartments in S4, with average values around 9–10 (Figure 106C). This suggests that the nature of the organic matter remained similar across compartments, despite quantitative differences in OC and N.

In S9, the dynamics were more pronounced: both nitrogen and OC contents showed a clear decreasing trend from the pre-intervention canal to the pond, with statistically significant reductions (Figure 107A and B). The C:N ratio also declined from the pre-intervention canal to the pond (from approximately 9.5 to 8.5), although the differences were not statistically significant (Figure 107C). This again pointed out the preferential degradation of labile organic matter, associated with limited stabilization in pond sediments (Casal-Porras et al., 2022).

These findings indicate that, in both S4 and S9, ponds did not function as preferential accumulation zones for organic matter and nitrogen, unlike in S6 and S7. This may be due to differences in sediment texture, hydrological dynamics, organic matter availability, or the frequency and intensity of transport flows. In particular, the lack of enrichment in the pond compartments may reflect a lower efficiency in organic particle sedimentation, or environmental conditions that favour post-depositional degradation of organic matter, as discussed by Alongi (1998) in reference to low-energy environments.

In addition, the similarity in the C:N ratio implies that the organic inputs to the sites have a fairly uniform quality and undergo analogous degradation dynamics in the investigated areas.

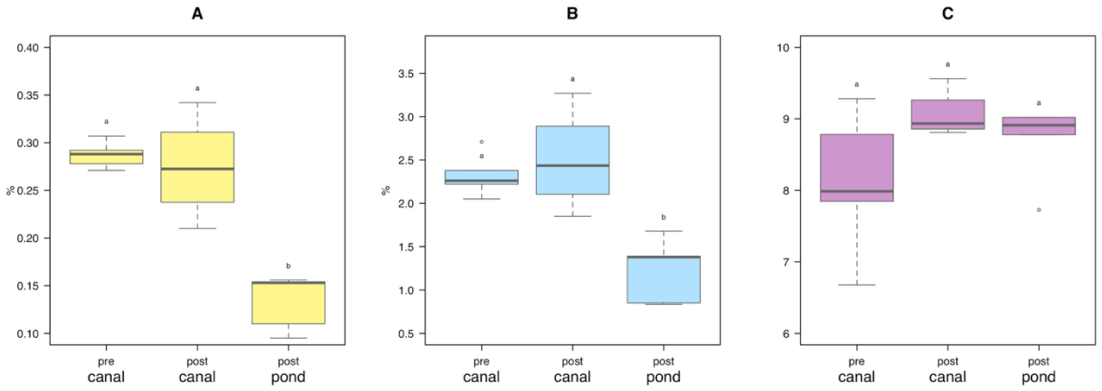

Figure 106 - Boxplot showing the concentrations of nitrogen (A) and organic carbon (B), and C:N ratio (C) in the sediment of canal before (pre) and after (post) intervention, and of pond at site S4. Different letters above the boxes indicates statistical differences according to Kruskal-Wallis test ($p \leq 0.05$).

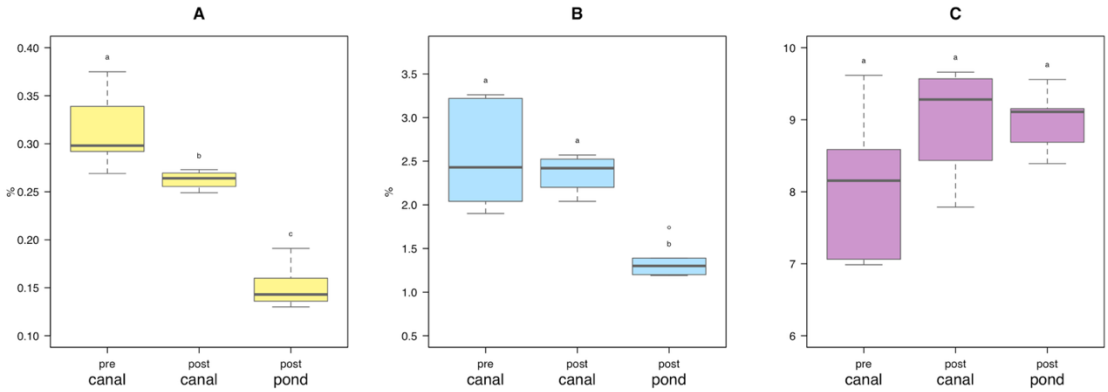

Figure 107 - Boxplot showing the concentrations of nitrogen (A) and organic carbon (B), and C:N ratio (C) in the sediment of canal before (pre) and after (post) intervention, and of pond at site S9. Different letters above the boxes indicates statistical differences according to Kruskal-Wallis test ($p \leq 0.05$).

Overall, the results suggest that the effectiveness of ponds as retention environments for nutrients and metals is highly dependent on the local hydrogeomorphological context (Noe et al., 2013).

In S4 and S9, the post-intervention sedimentary and hydrological conditions did not appear to promote a marked accumulation of elements in pond sediments, in contrast to what was observed in S6 and S7.

8 Vegetation changes before and after restoration: a cross-site overview

The monitoring of vegetation between 2020 and 2024 highlights distinct shifts in species composition and ecological structure associated with the restoration works carried out in the canals and ponds of the study area. Before the interventions (2020–2021), vegetation was generally dominated by aquatic and hygrophilous species, particularly *Phragmites australis* and *Carex riparia*, which reflected relatively stable hydrological conditions and the persistence of riparian habitats along canal banks. Ruderal and crop-related species were present only locally and at low cover, while bare soil was generally limited, indicating relatively continuous plant cover.

After the implementation of restoration measures in 2022, a marked transition was observed across most sites. In particular, the coverage of aquatic and hygrophilous species declined, while bare soil increased substantially, especially in 2022–2023. These patterns were accompanied by the expansion of ruderal, crop-related, and ubiquitous species, which are typically associated with disturbed and nutrient-rich environments (Chytrý, M., et al., 2008; Pyšek, P., et al., 2009). The strong flood event of spring 2023 further amplified these dynamics, mechanically removing established vegetation, delaying recolonization processes, and favouring opportunistic taxa adapted to unstable substrates (Bornette, G., & Puijalon, S., 2011; Gurnell, A. M., et al., 2001).

Despite these short-term signs of disturbance, the vegetation surveys in 2023–2024 also revealed an overall increase in species richness and the first signs of ecological diversification, particularly in the newly created ponds. Hygrophilous species such as pioneer woody taxa like *Populus alba* were observed colonizing bare substrates, suggesting the onset of successional processes. These dynamics point to a transitional stage, where vegetation has not yet reached structural stability but is progressing toward more heterogeneous assemblages (Corenblit, D., et al., 2007; Palmer, M. A., et al., 2010).

A comparison of vegetation cover and species richness before (2020–2021) and after restoration (2022–2024) shows that interventions initially reduced vegetation cover but also increased floristic diversity in the medium term.

- Before restoration (2020–2021): all monitored sites were dominated by aquatic and hygrophilous vegetation, mainly *Phragmites australis* and *Carex riparia*, which together often exceeded 70–80% of total cover. Bare soil was generally below 10%, and ruderal or crop-related species were rare. Overall species richness was relatively low, with communities composed of few dominant taxa.
- After restoration (2022–2024): the reshaping of canal banks and creation of ponds caused an immediate increase in bare soil (often >40%) and a decline in aquatic/hygrophilous species. In sites S1, S2, S5, and S8, ruderal and crop species expanded, reflecting unstable substrates and external agricultural pressure. In S4 and S9, pond creation promoted colonization by *Carex riparia* and ruderal taxa, though S9 was more affected by the 2023 flood and the persistence of the invasive shrub *Amorpha fruticosa*. In S6 and S7, newly created ponds supported the establishment of heterogeneous assemblages, including hygrophilous species and pioneer woody taxa, although vegetation cover remained discontinuous.

Taken together, these results indicate that restoration produced both negative short-term effects (loss of cover, dominance of disturbance-tolerant taxa, increase in bare soil) and positive medium-term trends (higher species richness, initiation of successional processes, greater ecological heterogeneity in ponds).

9 Ecological role of vegetation and methodological approach to floristic analysis

The vegetation plays a key role in defining the ecological characteristics of canals and associated wetland areas. The diversity and abundance of plant species are reliable indicators of environmental quality, hydrological conditions, and the effectiveness of ecological restoration measures.

In site S1, vegetation was initially dominated by aquatic/hygrophilous species (up to ~89% in 2021), followed by a marked decrease in 2022, coinciding with the bank reshaping (Figure 108). In 2023 and 2024, vegetation coverage decreased, while bare soil increased significantly (reaching over 40% in 2023) suggesting a delayed recolonization and ongoing substrate instability (Figure 108).

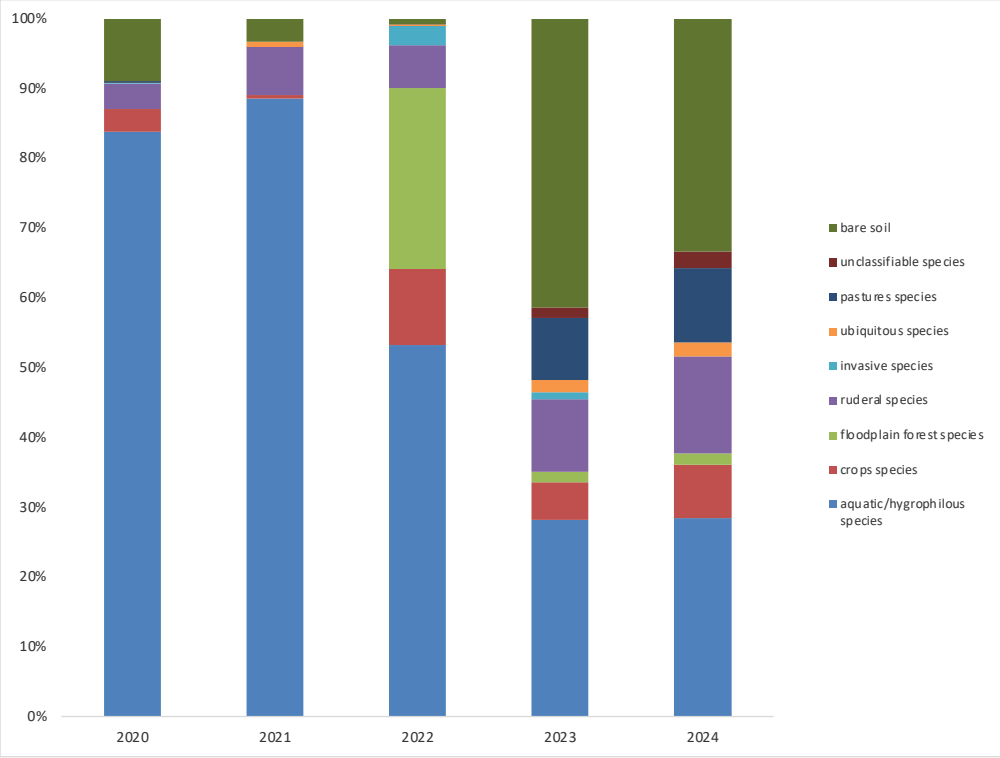

Figure 108 - Soil coverage (%) of the socioecological groups of vegetation in site S1 from 2020 to 2024. Restoration works (bank reshaping and planting) were carried out in 2022.

In site S2, the initial dominance of aquatic/hygrophilous species (~80%) persisted until 2021 but declined sharply after the 2022 intervention. This shift was

accompanied by a substantial increase in bare soil (~48% in 2022), along with a rise in ruderal and ubiquitous species. In 2023, bare soil remained high, suggesting a disturbed and ecologically unstable environment (Figure 109).

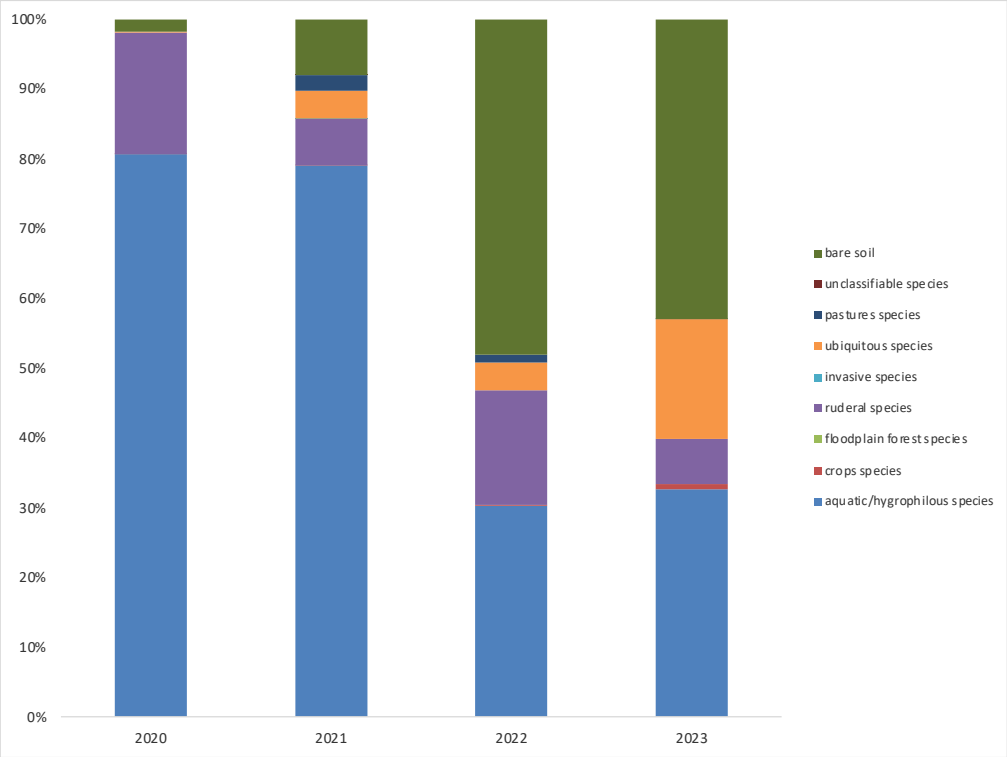

Figure 109 - Soil coverage (%) of the socioecological groups of vegetation in site S2 from 2020 to 2023. Restoration works (bank reshaping and planting) were carried out in 2022.

In site S5, aquatic/hygrophilous species dominated in 2020 and 2022, but showed lower coverage in 2021 and 2023 with consequent increase of bare soil (up to ~63%). The temporary decline in 2021 can be linked to the bed reworking of the canal carried out that year, which stimulated the germination of aquatic species from the seed bank and led to a short-term enrichment of the vegetation. However, such pioneer aquatic taxa typically disappear in the following phases of succession, explaining the subsequent reduction. In 2022, the restoration activity promoted a new phase of colonization, whereas in 2023 the flood disturbance caused another sharp decline (Figure 110).

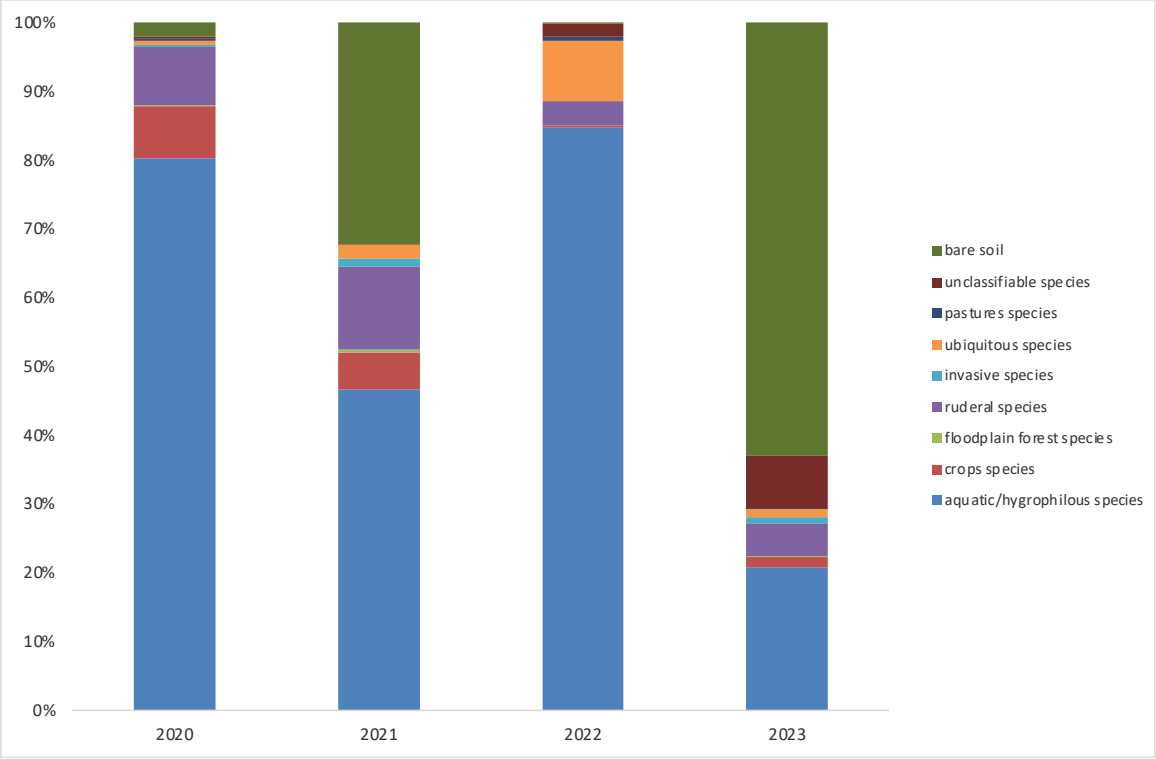

Figure 110 - Soil coverage (%) of the socioecological groups of vegetation in site S5 from 2020 to 2023. Restoration works (bank reshaping and planting) were carried out in 2022.

In site S8, ruderal and aquatic species dominated the vegetation in 2020–2022. Following the 2022 intervention, bare soil increased sharply (up to ~52% in 2023), while most ecological groups declined, suggesting reduced vegetation cover and delayed recovery (Figure 111).

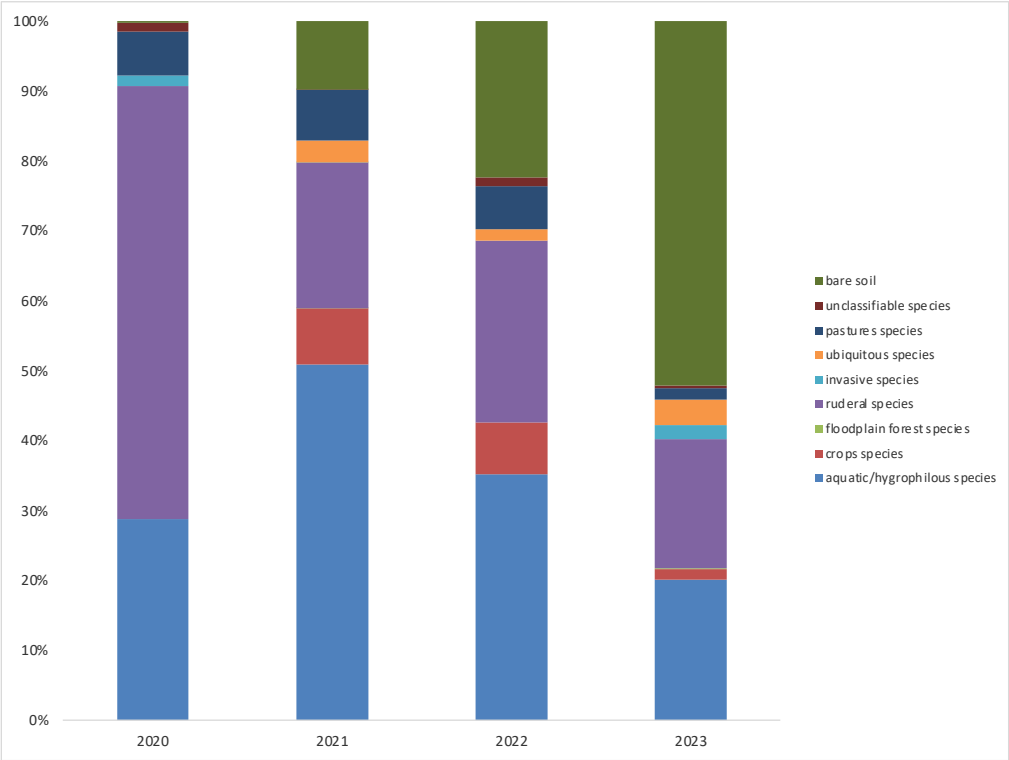

Figure 111 - Soil coverage (%) of the socioecological groups of vegetation in site S8 from 2020 to 2023. Restoration works (bank reshaping and planting) were carried out in 2022.

The significant increase in bare soil observed in 2023 across the various sites can be attributed to the flood events that affected the study area. The sudden and prolonged high flows that occurred during the spring of 2023 likely led to mechanical vegetation removal, inhibited the germination of annual species, and altered the physic-chemical properties of the substrate, rendering it less suitable for plant colonization (Bornette & Puijalon, 2011; Gurnell et al., 2001). These processes may explain the sharp reduction in vegetation cover and the reappearance of ruderal or ubiquitous species, typically associated with the early phases of ecological recolonization.

9.1 Effects of bank reshaping on vegetation in sites S1, S2, S5, and S8: analysis by ecological groups

The plant species coverage exhibited distinct trends over time, especially before and after 2022, the year when bank reshaping was implemented (Table 18). Aquatic and hygrophilous species are known to reflect local hydrological conditions and the physic-chemical quality of water and sediments (Bornette, G., & Puijalon, S., 2011; Merritt, D. M., et al., 2010). Their abundance is generally associated with well-functioning wetland systems; however, excessive dominance of a few taxa, such as *Phragmites australis*, may also indicate low plant diversity or unstable successional stages.

In contrast, ruderal and crop-related species, often nitrophilous and disturbance-tolerant, tend to expand in areas subject to hydromorphological alteration, eutrophication, or soil instability (Chytrý et al., 2008; Pyšek et al., 2009). This was observed in several sites, such as S5 and S8, where taxa like *Anisantha sterilis (syn. Bromus sterilis)*, *Carduus sp.*, and *Rubus fruticosus coll.* became dominant within their respective groups, especially after the 2022 restoration and the 2023 flood event.

Although invasive species did not reach high overall coverage, their sporadic occurrence, combined with the widespread presence of opportunistic ruderal and crop species, confirms a vegetation composition shaped by repeated disturbances and potentially reduced resilience. These dynamics underscore the importance of long-term monitoring to assess the success of restoration actions and the trajectory of vegetative re-establishment.

At site S1, both in 2020 and 2021 the aquatic and hygrophilous species covered most of the bank, but in 2020 such socio ecological group showed as dominant species *Phragmites australis* (a perennial helophytic herb common in wetlands, indicative of stable hydrological conditions but also adaptable to moderate disturbance) accounting for 45.6 % of the socioecological group, while in 2021 the dominant species was *Carex riparia* (a perennial hygrophilous species typical of banks and areas with variable moisture) accounting for 68.3 %. In the following years, *P. australis* was again the dominant species, with 47.2% in 2022 and 33.3% in 2023, confirming its high stress tolerance and its ability to grow and

spread even in disturbed environments (Grime, J. P., 2001; Bornette, G., & Puijalon, S., 2011). In contrast, *C. riparia* is a species that frequently colonizes temporarily exposed soils or marginal hydrological conditions typical of transitional riparian zones (Ellenberg, H., & Leuschner, C., 2010). *Carex riparia*, with a relative abundance of 81.4% in 2020 and 84% in 2021, was also the dominant aquatic and hygrophilous species in site S2.

In site S5, the aquatic and hygrophilous group was mainly represented by *Phragmites australis*, accounting for 68.6% in 2020 and 64.6% in 2021. After 2022, the coverage increased to 84.7%, then dropped to 20.7% in 2023. Also, in site S8 the *Phragmites australis* was the dominant species within the aquatic and hygrophilous socioecological group, with 81.8% coverage in 2020. After 2022, a decline was observed, reaching 35.9% in 2023, associated with an increase in bare soil (52.1%).

Ruderal species are plants typically associated with anthropogenic disturbance, poor quality soils, road margins, abandoned agricultural areas, and artificial banks. These species colonize unstable environments rapidly due to opportunistic growth strategies, high seed production, and short life cycles (Grime, J. P., 2001; Chytrý et al., 2008).

In floodplains strongly affected by canalization, their presence is often interpreted as an indicator of ecological disturbance, although some species may play a beneficial role in the initial stabilization of soils and in the early development of riparian vegetation (Aguiar, F. C., et al., 2009).

In site S1, ruderal species progressively increased from 3.5% in 2020 to 13.9% in 2024. *Urtica dioica* dominated in 2021 (80.3%), followed by *Carduus* sp., which reached 98.4% in 2022 and remained present in 2023 (33.2%). In 2024, a replacement by *Mummenhoffia alliacea* (24.7%) was observed, an annual nitrophilous species typically grows on fresh and marginal soils. All these species, characterized by high disturbance tolerance and preference for nutrient-rich substrates, reflect unstable conditions and suggest an opportunistic vegetation response to mechanical disturbances or fluctuations in soil moisture (Chytrý et al., 2008; Pyšek et al., 2009).

In site S2, *Rubus fruticosus* coll., a perennial shrub typical of eutrophic and disturbed environments, accounted for 17.4% of the total coverage of ruderal species in 2020. A decrease was observed in 2021 (6.6%), followed by an increase after the reshaping intervention (16.4% in 2022). The persistent presence of *Rubus fruticosus* coll. indicates ongoing substrate disturbance and eutrophic conditions, typical of post-intervention or erosion-prone environments (Pyšek et al., 2009; Chytrý et al., 2008).

In site S5, the coverage of ruderal ecological group showed low values in 2020 (8.5%) and in 2021 (12.1%). In both years, the dominant species was *Anisantha sterilis*, an annual grass of arable fields and disturbed soils, accounting for 88.2% and 47.7% of the ruderal group's total coverage, respectively. In the following years (2022–2023), the group experienced a sharp decline reaching a total coverage less than 5%, suggesting a temporary reduction in the environmental conditions favourable to this pioneer and nitrophilous species, typical of nutrient-rich and disturbed soils (Chytrý et al., 2008; Pyšek et al., 2009).

In site S8, the group was consistently dominated by *Rubus* sp., which represented more than 60% of the group's coverage in each year, indicating persistent disturbance and nutrient-rich soils (Chytrý et al., 2008; Pyšek et al., 2009).

Crop species observed during the surveys do not represent a natural component of riparian or aquatic flora but rather reflect the direct influence of the surrounding agricultural landscape on the artificial canals. Their presence within the monitoring transects is often the result of seed drift, surface runoff, or edge effects due to the absence of buffer strips between cultivated fields and water bodies (Fischer, R. A., & Fischenich, J. C., 2000; Correll, D. L., 2005). These species do not provide ecological benefits to fluvial ecosystems and may compete with native pioneer species during the early stages of colonization. However, their occurrence can serve as an indirect indicator of agricultural pressure.

In site S5, the group reached 7.7% coverage in 2020 and 5.4% in 2021, with *Elymus repens* (a perennial grass thriving in overgrown fields and at the

margin of crops or roads) as the dominant species, accounting for 98% and 99.5% of the group's coverage, respectively. This perennial species, typical of agricultural margins and disturbed soils, is known for its persistence and regenerative capacity through rhizomes. In site S8, *E. repens* also showed high percentages in 2021 (89.9%). After 2022, the dominant species became *Bromus hordeaceus* (a tufted annual grass, common in dry meadows, roadsides, and disturbed soils; indicative of pioneer environments with low vegetative cover), which accounted for 66.4% of the socioecological group.

Ubiquitous species are characterized by a broad ecological amplitude and the ability to colonize a wide range of environments, tolerating broad gradients of moisture, nutrients, and disturbance (Grime, J. P., 2001).
Their presence in riparian and canalized environments is not necessarily a negative indicator; however, marked dominance may reflect environmental simplification and low specialization of the plant community (Cottenie, K., 2005). Their presence in 2022 and 2023, at sites S2 and S5, can be interpreted as the result of intermediate ecological conditions, typical of transitional contexts. In these cases, disturbances related to the bank reshaping intervention and the flood may have created microhabitats favourable to the colonization by generalist species. These occurrences indicate an unstable but not fully degraded phase of the system, characterized by partially stabilized substrates and the availability of open ecological niches not yet occupied by specialized vegetation. The ubiquitous socioecological group of S2 was dominated by *Holcus lanatus*, a grass species typical of moist and semi-natural meadows, but also able to colonize disturbed or fertilized soils due to its high ecological plasticity and competitive strategies that promote its spread (Grime, J. P., 2001). While in site S5 the major ubiquitous species was *Cynodon dactylon*, a perennial grass commonly found in disturbed environments. Its post-flood presence is indicative of structural simplification.

Pasture species observed within the transects are not part of the typical flora of natural aquatic or riparian habitats but instead originate from adjacent semi-

natural environments such as permanent grasslands, agricultural edges, and open herbaceous areas. Their presence on the banks of the artificial canals is generally promoted by grazing or mowing. These species are adapted to frequent removal of the aboveground biomass and/or have evolved structural defences against herbivores (i.e. spines) or to exploit herbivores for seed dispersal (i.e. hooks and structures firmly anchoring fruits to animal coat), with partially stabilized substrates and low-intensity maintenance. In such contexts, herbaceous and shrubby species associated with pasture environments can colonize margins and exposed surfaces, indicating a transition toward more heterogeneous plant communities. Although not structural elements of riparian vegetation, their presence can represent a signal of ecological transition or a response to intermediate conditions between degradation and renaturalization. Pasture species are mostly herbaceous plants, primarily grasses or legumes, commonly found in open environments such as permanent grasslands and areas subject to moderate disturbance, like canal margins or low-management zones. Their presence in artificial canals is indicative of an intermediate successional stage, where the substrate is partially stabilized and some continuity of herbaceous cover is observed. These species require relatively stable hydromorphological conditions and moderate nutrient availability, indicating an evolution toward more heterogeneous but still transitional environments.

In site S1, *Prunus spinosa*, a pioneer spiny shrub typical of woodland margins, accounted for more than 87% of the group in 2023 and 2024. The presence of *Prunus spinosa* would suggest the beginning of a succession toward more later success stages, likely favoured by the reduced intensity of bank maintenance.

In site S8, *Galium mollugo* (perennial herbaceous species, widespread in stable mesophilous grasslands, pastures, and roadsides; its presence is indicative of partially stabilized environments with moderate disturbance and good water availability) reached 100% of the group in 2021–2022, with a decrease observed in 2023.

Overall, the vegetation analysis in sites S1, S2, S5, and S8 showed a strong influence of bank reshaping interventions (2022) and the flood event (2023) on

the composition and structure of plant communities. Aquatic and hygrophilous species, initially dominant in all sites, experienced a progressive decline, especially in the two years following the intervention, indicating a possible alteration of hydromorphological balance and a loss of stable habitats.

The low percentage of coverage (<5%) for most ecological groups in sites can be attributed to a combination of factors related to environmental disturbances and hydrological changes. After the bank reshaping intervention in 2022 and the flood event in 2023, the sites underwent significant changes in water regime and soil structure. These changes likely created unsuitable conditions for many plant species, reducing both the diversity and coverage of various ecological groups. In particular, the alteration of hydrology may have led to prolonged periods of flooding or, conversely, drought conditions, both of which are detrimental to many riparian species. Furthermore, the observed increase in bare soil in the study sites suggests reduced substrate stability, which can hinder the establishment and growth of plants. These combined factors contribute to the low vegetation coverage observed across the different ecological groups.

However, an increase in ruderal, ubiquitous, and crop species was observed, ecological groups typically associated with disturbed environments, unstable substrates, or nutrient-rich soils. The spread of species such as *Rubus fruticosus*, *Urtica dioica*, and *Cynodon dactylon* reflects the onset of chronic disturbance conditions and an early successional phase in plant community development.

Despite some signs of recolonization, the results would suggest that plant communities remain in an unstable and fragmented state. The increase in bare soil across all sites, especially in 2023, supports the hypothesis of an incomplete ecological transition, where the loss of structuring species has not yet been offset by the establishment of a functionally mature composition.

These findings highlight the importance of long-term monitoring to evaluate the effectiveness of renaturalization interventions and to inform corrective actions aimed at supporting biodiversity and ecosystem resilience in canal systems.

Table 18 - Abundance of the dominant species within each socioecological group at sites S1, S2, S5 and S8 between 2020 and 2024. The scientific name of the dominant species is between brackets. The socioecological groups showing a total coverage less than 5 % (< 5 %) were not considered. The group "unclassifiable species" includes species that cannot be attributed with certainty to a specific socio-ecological group. NF: Not found.

SITE	YEAR	ECOLOGICAL GROUP %							
		aquatic/hygrophilous species	crops species	floodplain forest species	ruderal species	invasive species	ubiquitous species	pastures species	unclassifiable species
S1	2020	45,6 (Phragmites australis)	<5%	<5%	<5%	<5%	<5%	<5%	<5%
S2		81,4 (Carex riparia)	<5%	NF	57 (Rubus fruticosus coll.)	NF	<5%	NF	NF
S5		68,6 (Phragmites australis)	98 (Elymus repens)	<5%	88,2 (Anisantha sterilis)	<5%	<5%	<5%	<5%
S8		81,8 (Phragmites australis)	NF	NF	96,5 (Rubus sp.)	<5%	NF	100 (Galium mollugo)	<5%
S1	2021	68,3 (Carex riparia)	<5%	NF	80,3 (Urtica dioica)	<5%	<5%	NF	NF
S2		84 (Carex riparia)	<5%	NF	43,1 (Rubus fruticosus coll.)	<5%	<5%	<5%	<5%
S5		64,6 (Phragmites australis)	99,5 (Elymus repens)	<5%	47,7 (Anisantha sterilis)	<5%	<5%	<5%	<5%
S8		74,6 (Phragmites australis)	89,9 (Elymus repens)	<5%	39,9 (Rubus sp.)	<5%	<5%	100 (Galium mollugo)	<5%
S1	2022	47,2 (Phragmites australis)	96,8 (Brassica nigra)	100 (Symphytum officinale)	98,4 (Carduus sp.)	<5%	<5%	<5%	<5%
S2		55,8 (Carex riparia)	<5%	NF	42,8 (Rubus fruticosus coll.)	<5%	<5%	<5%	NF
S5		94,3 (Phragmites australis)	<5%	<5%	<5%	NF	70,2 (Holcus lanatus)	<5%	<5%
S8		95,7 (Phragmites australis)	66,4 (Bromus hordeaceus)	NF	67,3 (Rubus sp.)	<5%	<5%	77,4 (Galium mollugo)	<5%
S1	2023	33,3 (Phragmites australis)	46,6 (Brassica nigra)	<5%	33,2 (Carduus sp.)	<5%	<5%	88,4 Prunus spinosa (plantule)	<5%
S2		29,7(Carex riparia)	<5%	NF	88,2 (Rubus fruticosus coll.)	<5%	51,5 (Cynodon dactylon)	NF	NF
S5		73,9 (Phragmites australis)	<5%	<5%	<5%	<5%	<5%	<5%	71,9 (Equisetum sp.)
S8		35,9 (Phragmites australis)	<5%	<5%	61,1 (Rubus sp.)	<5%	<5%	<5%	<5%
S1	2024	32,7 (Phragmites australis)	37,3 (Brassica nigra)	<5%	24,7 (Mummenhoffia alliacea)	NF	<5%	87,7 Prunus spinosa (plantule)	<5%
S2									
S5					no data				
S8									

9.2 Effects of ponds on vegetation in sites S6 and S7

In sites S6 and S7, the creation of ponds resulted in changes in floristic composition and vegetation dynamics between 2020 and 2024 (Table 19). This NBS was applied to enhance water quality and biodiversity by increasing environmental heterogeneity and promoting natural phytoremediation processes. Stacked bar charts illustrate the evolution of ecological group composition in the canal (Figure 112 and Figure 113) and the pond (Figure 114 and Figure 115) for both sites. In site S6, the canal was consistently dominated by aquatic and hygrophilous species, particularly *Phragmites australis*, indicating stable hydrological conditions and reduced anthropogenic pressure after the intervention. The pond, which was unvegetated after its construction, showed an increase in ruderal and hygrophilous species from 2023 onwards, suggesting the onset of colonization dynamics. In site S7, the canal showed the ruderal species as second most abundant socioecological group (range between 8-20%) across all years, while the pond exhibited greater ecological heterogeneity with the coexistence of multiple functional groups. However, in both sites, vegetation cover in the pond remained structurally discontinuous, highlighting an early successional stage with on-going stabilization processes. Although the applied NBS modified the coverage of the socioecological groups, it increased the bare soil showing values of 54% and 9% for the bank canal of site S6 and S7, respectively, and values of 81% and 47% or the pond of sites S6 and S7, respectively.

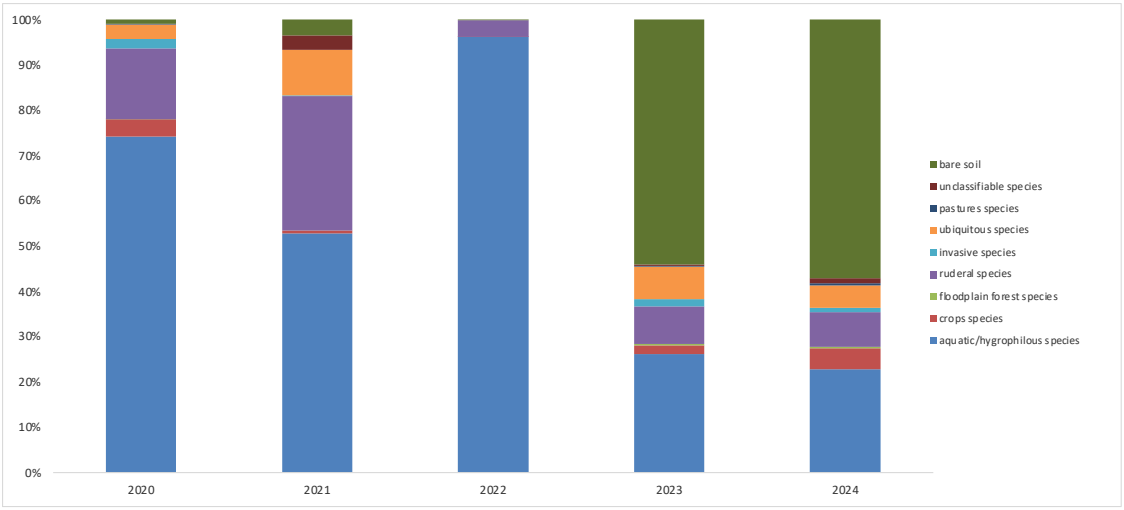

Figure 112 - Soil coverage (%) of the socioecological groups of vegetation in S6 canal from 2020 to 2024. Restoration works (bank reshaping and planting) were carried out in 2022. In 2022, restoration work was carried out (pond creation).

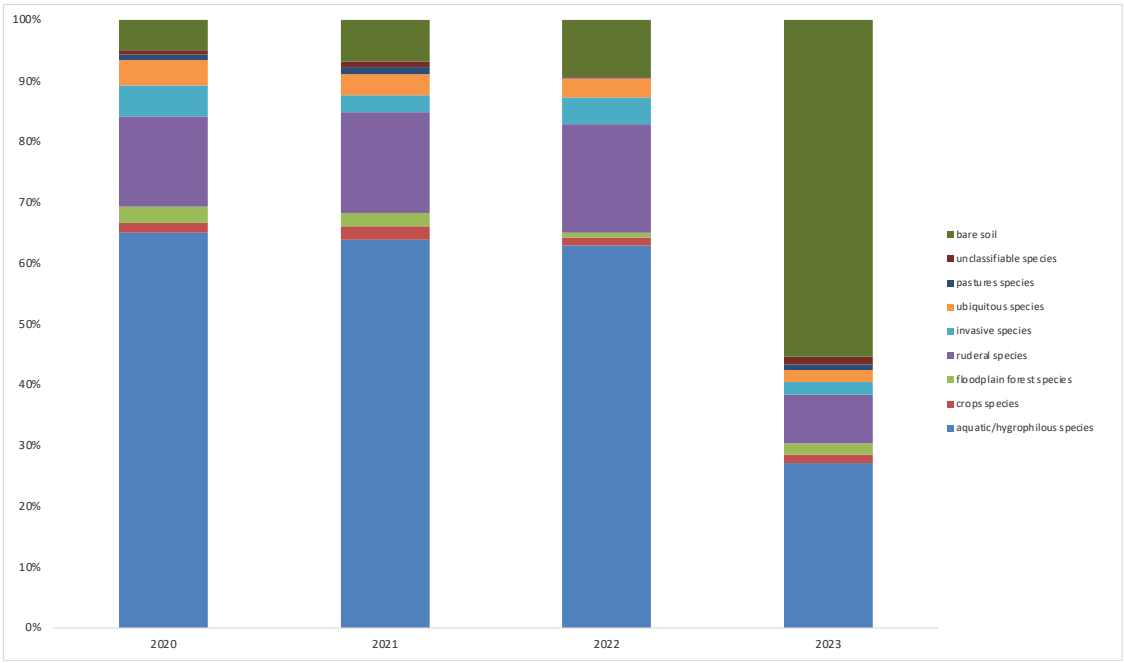

Figure 113 - Soil coverage (%) of the socioecological groups of vegetation in S7 canal from 2020 to 2023. In 2022, restoration work was carried out (pond creation).

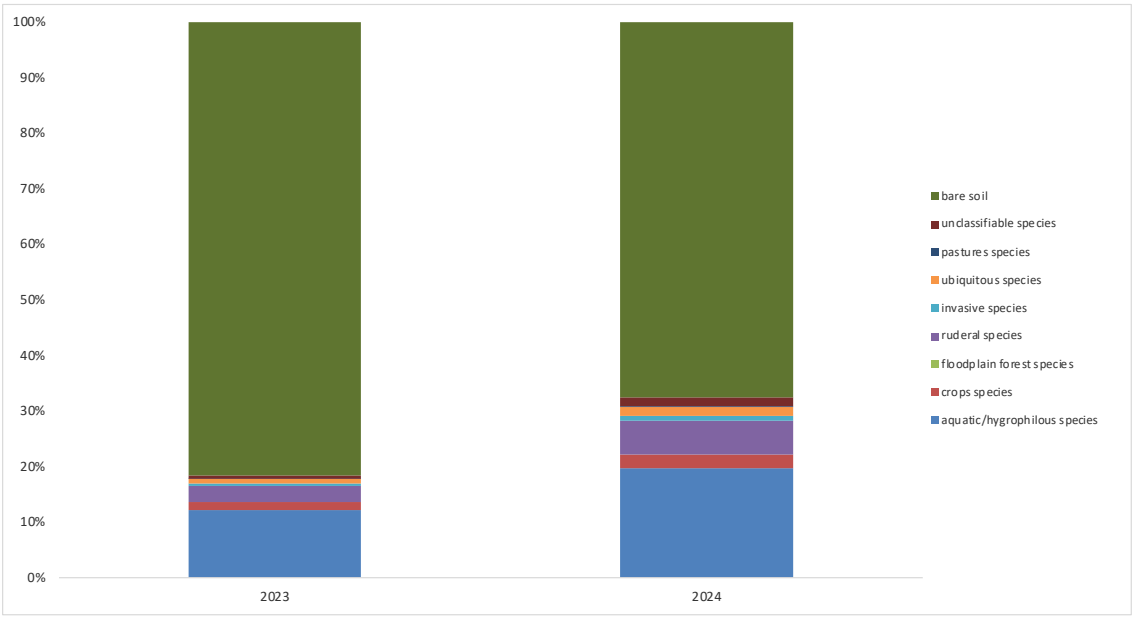

Figure 114 - Soil coverage (%) of the socioecological groups of vegetation in S6 pond in 2023 and 2024.

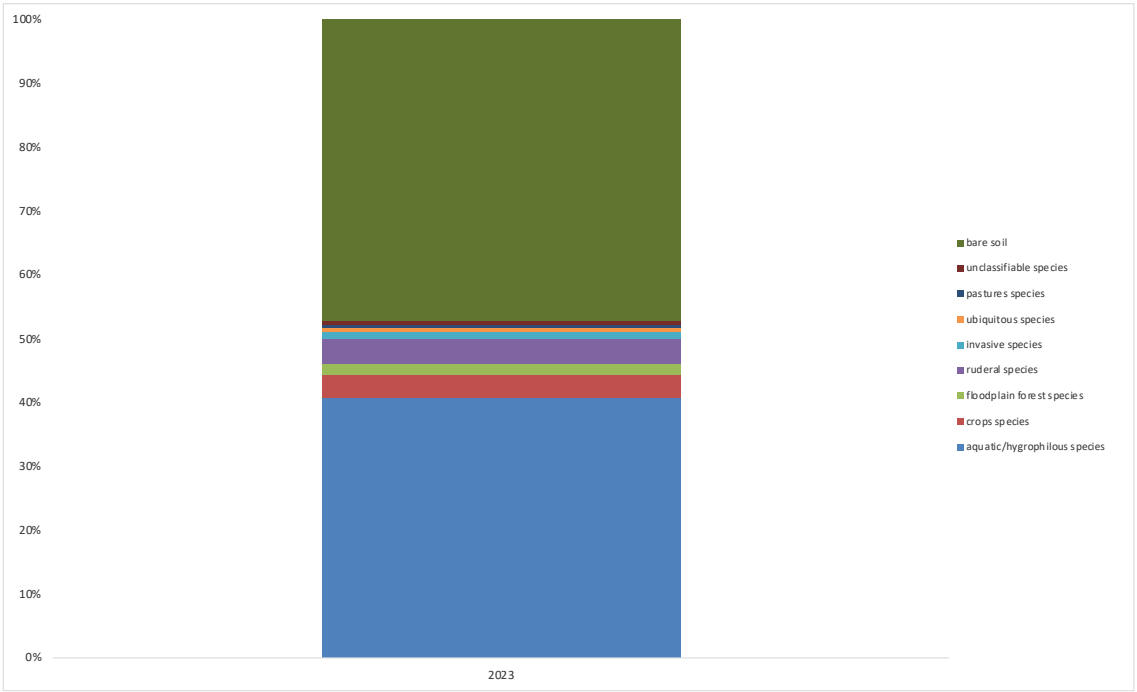

Figure 115 - Soil coverage (%) of the socioecological groups of vegetation in S7 pond in 2023.

In the canal of site S6, aquatic and hygrophilous species maintained a dominant role until 2022, with *Phragmites australis* exceeding 90% of the group's cover in 2020 (94.3%), 2021 (92.5%), and 2022 (99.1%) (Table 19). *P. australis* is a

perennial helophytic herb widely found in wetlands, known for its high ecological plasticity: it tolerates both stable hydrological conditions and moderate disturbance, forming dense stands thanks to its clonal propagation (Grime, 2001; Bornette & Puijalon, 2011). Following the intervention, its coverage decreased to 99.1% in 2022 to 71.0% in 2024, suggesting that the disturbance event negatively impacted vegetation stability. In the pond, aquatic species were represented in 2023 and 2024 by *Populus alba* (19.0% and 17.3%, respectively), a fast-growing pioneer tree typical of riparian environments. *P. alba* tolerates short-term flooding and sandy or silty soils, contributing to bank stabilization and initiating succession towards shrub-dominated formations (Corenblit & Steiger, 2024).

In the canal of site S7, *P. australis* was identified at lower percentages compared to S6 (33.8% in both 2020 and 2021) and was no longer observed after 2022. This pattern likely reflects more variable hydrological conditions and greater substrate instability. Another species identified in the S7 canal was *Equisetum telmateia*, which accounted for 31.8% of the hygrophilous group. It is a rhizomatous perennial fern typical of moist, nutrient-rich soils, often found along ditches, canals, and wet banks. Its presence indicates continuous water availability and low competition from shrubs or trees (Ellenberg & Leuschner, 2010; Pignatti et al., 2017). However, its absence in the following years may be related to intervention of creation of the pond.

In the pond, *P. australis* was identified in 2023 (26.6%) but was no longer observed in 2024. However, this absence does not necessarily indicate unsuitable conditions for perennial hygrophilous species, as other taxa such as *Populus alba* became dominant, suggesting a shift in the successional trajectory rather than a general decline in habitat suitability.

The socioecological group of ruderal species showed notable site-specific variability. In the canal of site S7, *Rubus* sp. consistently dominated throughout the entire period with coverage values exceeding 50% of the total coverage of ruderal group, indicating persistent disturbance and nutrient-rich substrates. *Rubus* sp. is a genus of perennial pioneer shrubs that are highly tolerant to stress and eutrophication, capable of rapidly colonizing unstable or

abandoned environments such as embankments, roadsides, and artificial canals. Its dominance is often associated with slowed or arrested ecological succession, due to soil disturbance, nutrient accumulation, or the absence of tree competitors (Pyšek et al., 2009).

In contrast, in the canal of site S6, *Urtica dioica* reached 99.7% of the ruderal group in 2021, while *Rubus* sp. became dominant in 2023 with 94.4%. *U. dioica* is a perennial nitrophilous herbaceous species, indicative of recent mechanical disturbances and high nitrogen availability in the soil (Grime, 2001).

In the S6 pond, the group was mostly represented in 2023 by *Helminthotheca echioides* (62.1%), an annual or biennial herbaceous species typical of nutrient-rich soils that are temporarily exposed due to water level fluctuations, and in 2024 by *Equisetum ramosissimum* (32.3%), a rhizomatous perennial fern widespread in dry and sandy environments, indicative of prolonged soil exposure resulting from reduced water retention and well-drained substrates (Pignatti et al., 2017).

In the S7 pond, *Urtica dioica* reached 70.9% of the group in 2023, confirming the prevalence of disturbed and nutrient-rich environments.

In site S6, crop species exhibited a limited and discontinuous presence over time. They were absent in the canal until 2023, when *Convolvulus arvensis* was identified in the pond accounting for 47.6% total coverage of crop species and rising to 49.8% in 2024. This perennial, climbing, and nitrophilous herbaceous species is commonly associated with agricultural and disturbed environments, such as field edges, and its presence may reflect either residual agricultural pressure or recolonization promoted by mechanical disturbances (Grime, 2001; Holm et al., 1997).

In site S7, *Cirsium arvense* dominated the crop species group in the pond in 2023, accounting for 75.3% of such socioecological group. Although not strictly a cultivated species, it is often considered a weed in intensive agricultural systems and is indicative of disturbed and nutrient-rich soils. Its appearance suggests highly eutrophic conditions or bare soil, typical of the early stages of recolonization (Chytrý et al., 2008; Pyšek et al., 2009).

The low coverage observed for this group in most of the years can be interpreted as a sign of limited direct agricultural influence. However, the episodic appearance of synanthropic species, that is, plant species that thrive in environments heavily influenced by human activity, in specific years, such as 2023, may be attributed to disturbance events that favoured seed dispersal along the margins and in temporarily unvegetated areas, offering suitable conditions for the establishment of these opportunistic taxa.
Examples include *Convolvulus arvensis* and *Cirsium arvense*, which are commonly found in agricultural margins and disturbed soils.

For the group of ubiquitous species, it was observed that in the canal of site S6, *Stellaria* sp. dominated in 2021 (99.7%), while *Plantago lanceolata* reached 57.9% in 2023 and 60.0% of the total coverage by ubiquitous group in 2024, indicating an intermediate successional stage. In the pond, by contrast, *Polygonum aviculare* represented 22.2% of the group in 2023 and 50.0% in 2024. In the canal of site S7, these species were scarcely represented, while in the pond in 2023 *Polygonum aviculare* and other ubiquitous taxa were observed at low percentages (0.68% coverage for the ecological group).
The presence of these species reflects intermediate stages of ecological succession, where recent disturbances have modified the pre-existing community, but recolonization processes are already underway. *Stellaria* sp. (Caryophyllaceae), typical of cool and disturbed soils, indicates early recolonization phases. *Plantago lanceolata*, a cosmopolitan perennial species, tolerates compacted and nitrogen-rich soils, suggesting partial substrate stabilization. *Polygonum aviculare*, a nitrophilous annual species, is indicative of anthropogenic and compacted habitats. Their presence is common in transitional artificial environments and may indicate semi-stabilized conditions and the availability of ecological niches not yet occupied by specialized species (Grime, 2001; Ellenberg & Leuschner, 2010).

The vegetation analysis in sites S6 and S7 confirms that the creation of ponds has, in the short-term, promoted the establishment of more heterogeneous and structured plant communities compared to adjacent canals. In particular:

- in the ponds, a progressive replacement of bare soil and ruderal species by hygrophilous, ubiquitous, and forest groups was observed, indicating an active ecological succession and improved microenvironmental conditions.
- crop species appeared only sporadically, suggesting a limited direct influence from agricultural activity after the intervention, but also a persistent vulnerability of the systems to seed dispersal or mechanical disturbance.

Overall, the results suggest that ponds can offer a concrete opportunity for rewilding in canalized contexts, contributing to floristic diversification and microhabitat stabilization. However, long-term monitoring will be necessary to assess the actual capacity of these interventions to support biodiversity and promote the resilience of artificial riparian ecosystems over time.

Table 19 - Abundance of the dominant species within each socioecological group at sites S6 and S7 between 2020 and 2024. The scientific name of the dominant species is between brackets. The socioecological groups showing a total coverage less than 5 % for the bank canal (< 5 %) and 1% for the pond (<1%) were not considered. The group "unclassifiable species" includes species that cannot be attributed with certainty to a specific ecological group. NF: No data.

SITE	YEAR	Location	ECOLOGICAL GROUP %							
			aquatic/hygrophilous species	crops species	floodplain forest species	ruderal species	invasive species	ubiquitous species	pastures species	unclassifiable species
S6	2020	Canal	*94,3 (Phragmites australis)*	*<5%*	*<5%*	*48,2 (Urtica dioica)*	*<5%*	*<5%*	*<5%*	*NF*
	2021		*92,5 (Phragmites australis)*	*<5%*	*NF*	*99,7 (Urtica dioica)*	*<5%*	*99,7 (Stellaria sp.)*	*NF*	*<5%*
	2022		*99,1 (Phragmites australis)*	*<5%*	*NF*	*<5%*	*NF*	*NF*	*NF*	*NF*
	2023		*79,9 (Phragmites australis)*	*<5%*	*<5%*	*94,4 (Rubus sp.)*	*<5%*	*57,9 (Plantago lanceolata)*	*<5%*	*<5%*
	2024		*71,0 (Phragmites australis)*	*<5%*	*<5%*	*28,6 (Trifolium fragiferum)*	*<5%*	*60,0 (Plantago lanceolata)*	*<5%*	*<5%*
	2023	Pond	*21,7 (Populus alba)*	*47,6 (Convolvulus arvensis)*	*NF*	*62,1 (Helminthotheca echioides)*	*<1%*	*22,2 (Polygonum aviculare)*	*NF*	*<1%*
	2024		*17,3 (Populus alba)*	*49,8 (Convolvulus arvensis)*	*NF*	*32,3 (Equisetum ramosissimum)*	*<1%*	*50,0 (Polygonum aviculare)*	*<1%*	*62,50 (Salix sp.)*
S7	2020	Canal	*33,8 (Phragmites australis)*	*<5%*	*<5%*	*71,5 (Rubus sp.)*	*<5%*	*<5%*	*<5%*	*100 (Brachypodium sp.)*
	2021		*33,8 (Phragmites australis)*	*<5%*	*<5%*	*70,5 (Rubus sp.)*	*<5%*	*<5%*	*<5%*	*<5%*
	2022		*31,8 (Equisetum telmateia)*	*<5%*	*<5%*	*58,7 (Rubus sp.)*	*<5%*	*<5%*	*<5%*	*<5%*
	2023		*27,6 (Populus alba)*	*<5%*	*<5%*	*56,9 (Rubus sp.)*	*<5%*	*<5%*	*<5%*	*<5%*
	2024					no data				
	2023	Pond	*26,7 (Phragmites australis)*	*75,1 (Cirsium arvense)*	*99,6 (Symphytum officinale)*	*70,9 (Urtica dioica)*	*<1%*	*<1%*	*<1%*	*<1%*
	2024					no data				

9.3 Effects of ponds on vegetation in sites S4 and S9

In sites S4 and S9, the creation of ponds in late 2021 and the flood event of 2023 led to distinct changes in floristic composition and vegetation dynamics between 2020 and 2024. This nature-based solution (NBS) was implemented to improve water quality and biodiversity by increasing habitat heterogeneity and promoting spontaneous colonization processes.

Stacked bar charts illustrate the evolution of ecological group composition in the canal (Figure 116 and Figure 117) and the pond (Figure 118 and Figure 119) at both sites. In site S4, the canal remained largely dominated by aquatic and hygrophilous species, particularly *Phragmites australis*, suggesting relatively stable hydrological conditions. The pond, unvegetated after its construction, exhibited progressive colonization from 2022 onward, with the establishment of *Carex riparia* and other hygrophilous and ruderal species, indicating the onset of a transition toward more structured vegetation.

In site S9, the canal was initially dominated by *Phragmites australis*, but its cover significantly declined after the 2023 flood, which likely disrupted substrate stability and local hydrology. At the same time, the pond exhibited high cover of ruderal (*Rubus* sp.) and ubiquitous species (*Hypericum perforatum*, *Potentilla reptans*), indicating ecological instability and opportunistic recolonization following disturbance. The persistent dominance of the invasive shrub *Amorpha fruticosa* in the canal throughout the study period further reflected the degraded condition of the riparian zone.

Although the implementation of NBSs modified the composition of ecological groups, it did not immediately lead to dense vegetation cover in the ponds. Bare soil percentages remained high in 2023, particularly in site S9, where the flood likely delayed colonization. In contrast, the pond in site S4 exhibited a more gradual and functional recovery of vegetation, suggesting higher site-specific resilience.

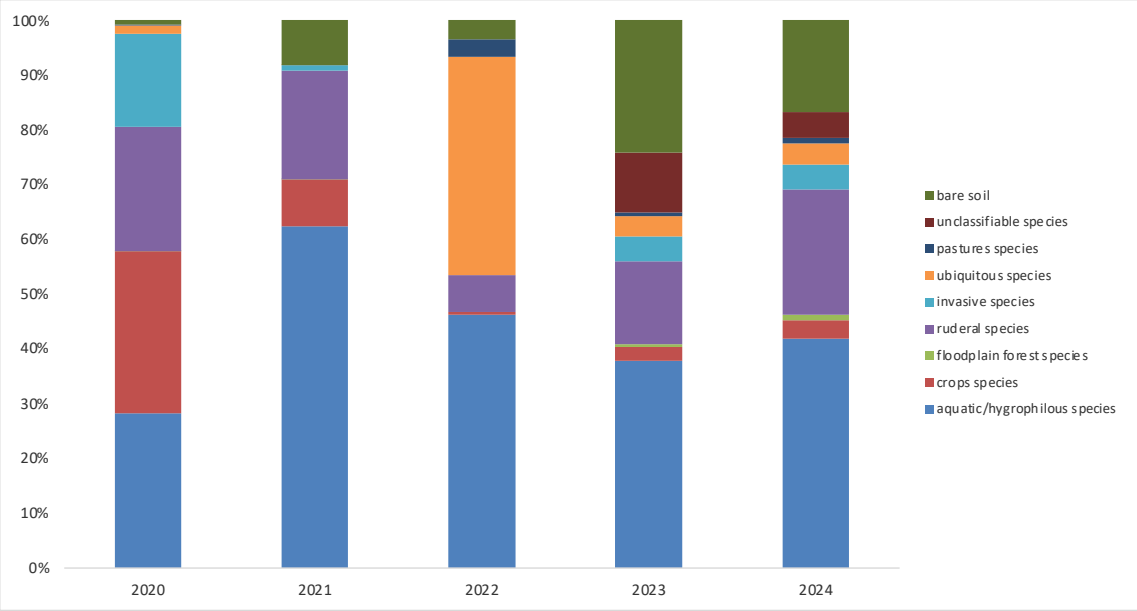

Figure 116 - Soil coverage (%) of the socioecological groups of vegetation in S4 canal from 2020 to 2024. In 2022, restoration work was carried out (pond creation).

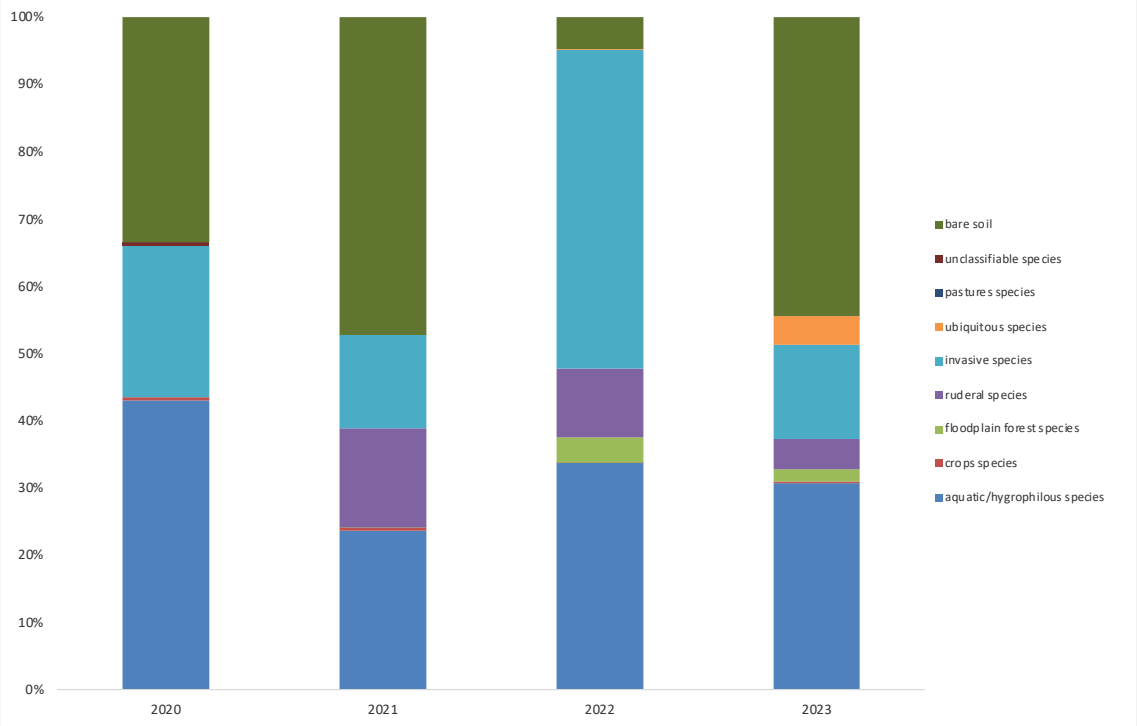

Figure 117 - Soil coverage (%) of the socioecological groups of vegetation in S9 canal from 2020 to 2023. In 2022, restoration work was carried out (pond creation).

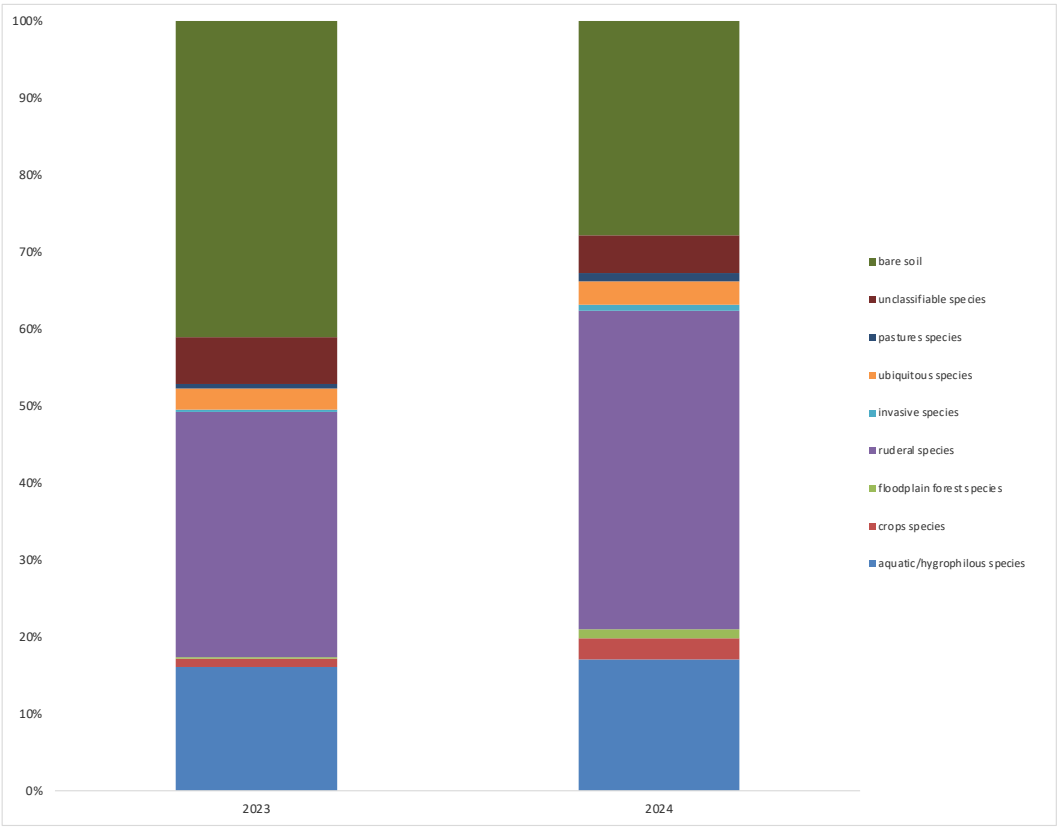

Figure 118 - Soil coverage (%) of the socioecological groups of vegetation in S4 pond in 2023 and 2024.

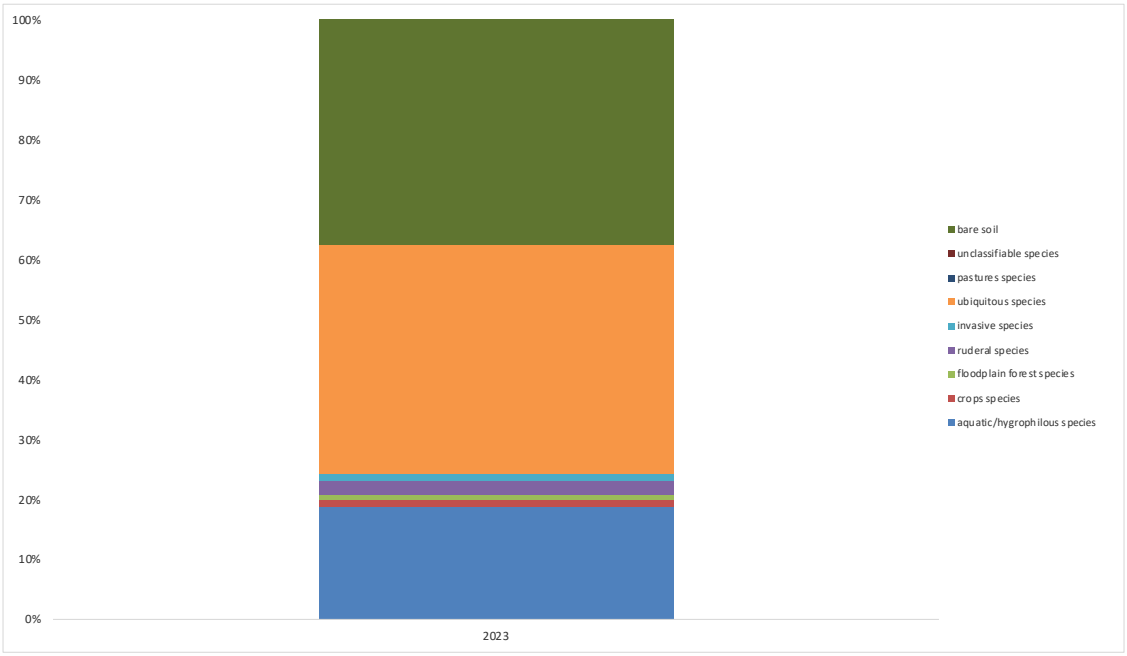

Figure 119 - Soil coverage (%) of the socioecological groups of vegetation in S9 pond in 2023.

In both canals (S4 and S9), *Phragmites australis* was the most abundant among the aquatic species, accounting for 80.5 and 89.7 % of the aquatic and hygrophilous socioecological group in 2020 and 2023, respectively, in site S4 (Table 20). In site S9, *Phragmites australis* has been the dominant species until 2022, accounting for 73.8% of the aquatic and hygrophilous socioecological group but showed a significant decline in 2023 (47.9%) and was no longer present in 2024. In the pond of site S9 *Phragmites australis* reached values of 85.6% in 2023. In contrast, in the pond of site S4, *Carex riparia* was the dominant species in 2023 (87.6%) and 2024 (78.5%). These changes may reflect the impact of the 2023 flood, which altered the local hydrological regime and site conditions.

In site S4, *Amorpha fruticosa*, a shrub-like invasive species native to North America, typical of disturbed riparian habitats and indicative of high nutrient availability (Brunel et al., 2010), was identified exclusively in 2020, when it accounted for 99.9% invasive socioecological group. In subsequent years, its presence drastically declined to less than 5%. This sharp reduction may be attributed to the increased abundance of more structured and competitive hygrophilous species such as *Phragmites australis*, which likely limited *A. fruticosa* through competition for light and space. Additionally, the construction of the pond may have altered the hydrological dynamics of the area, making the canal environment less suitable for the persistence of this invasive species.
The rapid decline of *A. fruticosa* in S4 could be interpreted as a positive signal of functional recovery of the canal, marked by the gradual replacement of invasive dominance with species more consistent with the natural evolution of riparian vegetation.
In contrast, in site S9, *Amorpha fruticosa* remained the dominant species throughout the entire monitoring period, with cover values reaching up to 100%, reflecting persistent disturbance conditions and reduced ecological resilience.

Ruderal species exhibited a marked presence and distinct dynamics between the two sites, reflecting differences in disturbance regimes and nutrient availability. In

site S4, the canal was initially dominated by *Urtica dioica* (55.4% in 2020 and 96.7% in 2021), while in 2022 *Anisantha sterilis* became prevalent (56.6%). In the pond, *Hirschfeldia incana* progressively expanded during 2023 and 2024, reaching up to 31.2% of the ruderal socioecological group. This Brassicaceae species is characteristic of temporarily exposed and nutrient-rich soils and suggests the early colonization of bare substrates following pond construction and the onset of recolonization processes.

In site S9, *Urtica dioica* maintained high values in the canal from 2020 to 2022 (up to 72%) but subsequently disappeared, likely as a consequence of the 2023 flood event, which altered the hydrological regime and habitat conditions. In the pond, a progressive establishment of *Rubus* sp. was observed, reaching 51.7% of the ruderal group in 2024. The dominance of *Rubus* suggests a slowed successional trajectory, where disturbance has favoured the establishment of stress-tolerant species in the absence of competitive woody vegetation (Pyšek et al., 2009; Chytrý et al., 2008).

Crop species were observed sporadically in sites S4 and S9, yet their presence provides relevant insights into anthropogenic pressures and the effects of disturbance events. In the canal of site S4, *Elymus repens* was dominant in 2020 (99.7%) and 2021 (99.4%), reflecting a strong influence of agricultural practices in the surrounding areas. This perennial grass, commonly found along the edges of cultivated fields, is known for its rhizomatous propagation and ability to colonize disturbed, nutrient-rich soils (Holm, et al., 1991). After 2022, the species was no longer observed, suggesting a reduction in direct agricultural pressure and in the extent of abandoned or fallow land in the surrounding area, which may have limited its persistence.

In site S9, crop species were exclusively identified in the pond. *Echinochloa crus-galli*, an annual synanthropic and nitrophilous grass, was dominant in 2023 (99.8%), while *Avena sterilis* reached 26.6% of crop socioecological group in 2024. Both species are commonly associated with intensive farming systems and moist, disturbed soils. Their appearance may be linked to the 2023 flood event, which could have facilitated seed dispersal from surrounding farmland into the

pond, creating favourable conditions for establishment in temporarily unvegetated areas. The absence of these species in previous years supports the hypothesis that they act as opportunistic colonizers, associated with specific and episodic disturbance events.

Ubiquitous species, tolerant of a wide range of ecological conditions, were primarily identified in the pond of site S9 and, to a lesser extent, in the pond of site S4. In 2021, *Plantago lanceolata* accounted for 37.6% of the ubiquitous socioecological group in the canal of S4, suggesting a transitional stage characterized by partially stabilized substrates and available nutrients. *P. lanceolata* is a cosmopolitan perennial species typical of compacted or disturbed habitats, often colonizing simplified environments undergoing recolonization (Grime, J. P., 2001; Ellenberg, H., & Leuschner, C., 2010). In the pond of S9, *Hypericum perforatum* exhibited high cover values in 2023 (69.7%) and 2024 (54.5%), while *Potentilla reptans* accounted for 90.7% of ubiquitous plant species in 2023. Both species are perennial herbs with high ecological plasticity (Grime, J. P., 2001), indicative of semi-open and partially consolidated habitats, often associated with fertile soils and moderate disturbance (Ellenberg, H., & Leuschner, C., 2010). Their presence reflects conditions of dynamic equilibrium, in which the vegetation is evolving toward more structured communities, although the influence of recent disturbances persists (Pignatti et al., 2017).

Unclassified species were mostly identified in site S9, both in the canal and in the pond, with cover values reaching up to 98.5% (*Equisetum* sp.). This genus of non-flowering vascular plants, often difficult to identify in the absence of reproductive structures, is typical of humid environments subject to fluctuating water levels. Their abundance indicates early successional stages, with high microenvironmental variability and plant communities still undergoing structural stabilization (Pignatti et al., 2017; Bornette & Puijalon, 2011). The prevalence of undetermined taxa may reflect the difficulty of identifying plants observed at early developmental stages, which often lack clear diagnostic traits, do not reach flowering (whose traits are most informative for taxonomy), or belong to

taxonomic complexes with frequent hybridization producing individuals with intermediate, non-distinctive characters.

Despite some signs of recolonization, the vegetation dynamics observed in sites S4 and S9 reflect divergent post-intervention trajectories. In S4, the progressive establishment of *Carex riparia* and other perennial species in the pond suggests a gradual stabilization process and the onset of structured plant communities. Conversely, in S9, the 2023 flood appears to have disrupted previous successional stages, promoting the dominance of ruderal and invasive species in both canal and pond habitats. The sharp decline of *Phragmites australis* and the increase in *Amorpha fruticosa* and bare soil in the canal point to a loss of ecological equilibrium.

These contrasting patterns suggest that, while site S4 is progressing toward increased ecological complexity, site S9 remains unstable with discontinuous vegetation cover. The results emphasize the need for long-term monitoring to assess the resilience of restored riparian systems and to guide site-specific adaptive management strategies aimed at sustaining biodiversity and ecological functionality in artificial canals.

Table 20 - Abundance of the dominant species within each socioecological group at sites S4 and S9 between 2020 and 2024. The scientific name of the dominant species is between brackets. The socioecological groups showing a total coverage less than 5 % for the bank canal (< 5 %) and 1% for the pond (<1%) were not considered. The group "unclassifiable species" includes species that cannot be attributed with certainty to a specific ecological group. NF: No data.

SITE	YEAR	Location	ECOLOGICAL GROUP %							
			aquatic/hygrophilous species	crops species	floodplain forest species	ruderal species	invasive species	ubiquitous species	pastures species	unclassifiable species
S4	2020	Canal	*66,7 (Cornus sanguinea)*	*87,5 (Papaver rhoeas)*	*<5%*	*<5%*	*66,7 (Cyperus erythorizos)*	*<5%*	*<5%*	*98,9 (Liliaceae sp.)*
	2021		*83,6 (Rorippa palustris)*	*93,7 (Papaver rhoeas)*	*<5%*	*95 (Ballota nigra)*	*90,4 (Cyperus erythorizos)*	*98,9 (Plantago major)*	*<5%*	*<5%*
	2022		*70,5 (Rorippa palustris)*	*<5%*	*NF*	*100 (Melissa officinalis)*	*37,1 (Erigeron canadensis)*	*100 (Bellis perennis)*	*<5%*	*50 (Crataegus sp.)*
	2023		*37,8 (Cornus sanguinea)*	*76 (Elymus repens)*	*NF*	*<5%*	73 (Cyperus erythorizos)	*<5%*	*<5%*	*<5%*
	2024		*82,9 (Cornus sanguinea)*	*<5%*	*NF*	*<5%*	*82,9 (Cyperus erythorizos)*	*84,2 (Plantago major)*	*<5%*	*<5%*
	2023	Pond	*80,2 (Rorippa palustris)*	*32,3 (Sonchus arvensis)*	*<1%*	*64,2 (Colchicum lusitanum)*	*<1%*	*<1%*	*<1%*	*51,6 (Plantago major)*
	2024		*67,3 (Rorippa palustris)*	*39,4 (Sonchus arvensis)*	<1%	*61,9 (Colchicum lusitanum)*	*90,9 (Erigeron canadensis)*	*64,9 (Plantago major)*	*63,8 (Prunus padus)*	*29,5 (Lathyrus sp.)*
S9	2020	Canal	*91,8 (Cornus sanguinea)*	*<5%*	*NF*	90,3 (Dactylis glomerata)	*95,7 (Cyperus erythorizos)*	*<5%*	*<5%*	*NF*
	2021		*96,3 (Cornus sanguinea)*	*<5%*	*<5%*	96,6 (Dactylis glomerata)	*<5%*	*<5%*	*<5%*	*99,7 (Liliaceae sp.)*
	2022		*97,2 (Cornus sanguinea)*	*<5%*	*NF*	*96,6 (Dactylis glomerata)*	*99,5 (Cyperus erythorizos)*	*<5%*	*<5%*	*100 (Liliaceae sp.)*
	2023		*76,3 (Cornus sanguinea)*	*<5%*	*<5%*	*26,7 (Rumex conglomeratus)*	*85,8 (Cyperus erythorizos)*	*42,8 (Holcus lanatus)*	*<5%*	*<5%*
	2024		no data							
	2023	Pond	*40,3 (Cornus sanguinea)*	*52,9 (Camelina sativa)*	*NF*	*32,5 (Rumex conglomeratus)*	*92,4 (Cyperus erythorizos)*	*95,8 (Bellis perennis)*	*48,8 (Silene vulgaris)*	*<1%*
	2024		no data							

9.4 Comparative synthesis of vegetation responses to restoration

Across the monitored sites, restoration interventions triggered consistent short-term responses but also revealed divergent ecological trajectories depending on the type of intervention, hydrological regime, and local environmental context.

In canals where bank slopes were reshaped, vegetation cover decreased markedly after the interventions, with a strong increase in bare soil and a decline in aquatic and hygrophilous species that had dominated the pre-restoration stage. Opportunistic ruderal and crop-related species rapidly colonized the newly exposed substrates, reflecting mechanical disturbance and high nutrient availability. These dynamics indicate an early successional stage, characterized by instability and dominance of generalist taxa, while signs of recolonization by more structured vegetation remained limited by 2024.

In sites where ponds were constructed, colonization dynamics were more heterogeneous. Initially unvegetated, the ponds progressively hosted hygrophilous, ruderal, and ubiquitous species, with occasional establishment of pioneer woody taxa. While vegetation cover remained discontinuous, species richness increased, suggesting that ponds may act as nuclei of diversification and create microhabitats that complement the adjacent canals. However, trajectories differed: in S4, the progressive establishment of *Carex riparia* and the decline of invasive *Amorpha fruticosa* suggested positive recovery, whereas in S9, ruderal and invasive taxa persisted, reflecting lower resilience and the strong effect of the 2023 flood.

The comparison between pre- and post-restoration phases highlights that the interventions initially reduced vegetation cover and shifted composition toward disturbance-tolerant taxa. Yet, the overall number of species increased after restoration, especially in ponds, indicating the onset of successional processes. The flood of 2023 further modified these dynamics, accentuating vegetation loss in some sites but also creating opportunities for recolonization. These results point to a trade-off between short-term disturbance and medium-term

diversification, a pattern widely reported in floodplain restoration projects (Palmer, M. A., et al., 2010; Kail, J., et al., 2015; Muhar, S., et al., 2016;).

In highly anthropogenic floodplains such as the Po Plain, restoration is constrained by hydrological regulation and intensive land use. Under these conditions, stable floodplain forest communities cannot establish, and vegetation trajectories are likely to converge toward reed-dominated assemblages (*Phragmites australis*) or mixed ruderal-hygrophilous mosaics. These communities, although simplified, provide relevant ecosystem services such as bank stabilization, nutrient retention, and habitat provision. The monitoring results suggest that NBS can enhance floristic diversity and create opportunities for recolonization, but their full ecological potential can only be assessed in the long term, once successional processes stabilize and the interaction with water and sediment quality is fully developed.

10 Plant species richness and evenness through biodiversity indices

Margalef's Richness Index (Dm) has practical applications in various areas of ecological monitoring, particularly in the context of environmental restoration (Gamito, S., 2010). Such index is usually used to (Wijnhoven, S., et al., 2023):

- monitor the effectiveness of environmental restoration interventions.
- assess the advancement of the ecological recovery processes.
- make comparison within and between sites.
- verify the effectiveness of management and conservation actions.

Instead, Shannon's Diversity Index (H') allows for the assessment not only of species richness, but also of the evenness in the abundance of individuals among species (Roswell, M., et al., 2021). The use of both indices enables a more comprehensive evaluation of biodiversity, by integrating information on both species' composition and community structure (Sharashy, O., 2022).

The analysis of Dm over the study period showed distinct temporal trends in species richness across the monitored sites (Table 21). In site S1, a progressive increase in Dm was observed from 2020 (Dm = 4) to 2024 (Dm = 8), reflecting a continuous enrichment of the plant community following restoration interventions. Similarly, site S8 showed a steady increase in richness, from 4 in 2020 to 8 in 2023, suggesting positive effects of environmental conditions or management actions on plant community richness. However, the Shannon Index values in these sites showed slight changes (between 1 and 2), indicating that the increase in species richness was not accompanied by improved evenness in species abundance. This would suggest that, although the number of species increased, the communities remained dominated by a few prevalent species.

Site S2 displayed a more fluctuating pattern, with Dm values ranging from 4 to 6. The increase in 2022 (Dm = 6) is followed by a slight decline in 2023 (Dm = 5), possibly reflecting interannual variability or a limited effect of restoration actions. In contrast, site S5 showed a high level of species richness in 2020 (Dm = 11) likely due to pre-existing floristic diversity, followed by a marked decline in the

subsequent years, reaching a value of 4 in 2023. This trend may be attributed to disturbance events or competitive exclusion phenomena, as also reflected by the persistently low Shannon Index values.

Table 21 – Biodiversity indices (Shannon and Margalef) for sites S1, S2, S5, and S8 from 2020 to 2024. Values of S correspond to the mean number of species recorded per year, while N indicates the mean α-richness per year used in the Margalef formula. This data refers to the reshaping works of the canal bank.

Site	Year	Mean n° of plant species (S)	Mean α-richness (N)	Shannon Index	Margalef Index
S1	2020	8	9	1	4
	2021	9	10	1	4
	2022	13	17	2	6
	2023	17	20	2	7
	2024	23	27	2	8
S2	2020	6	8	1	4
	2021	9	11	1	5
	2022	15	19	1	6
	2023	11	14	2	5
S5	2020	28	39	1	11
	2021	7	10	1	5
	2022	14	19	1	7
	2023	9	11	2	4
S8	2020	5	8	1	4
	2021	8	11	1	5
	2022	13	16	1	6
	2023	16	22	2	8

Sites S6 and S7 exhibited distinct trends in Margalef's Richness Index (Table 22). In site S6, a sharp decline in species richness was observed in the canal after 2020 (Dm = 19), with values dropping to 4 in both 2021 and 2022. A moderate recovery followed in 2023 and 2024 (Dm = 6 and 7, respectively), likely reflecting the gradual recolonization by plant species after the hydromorphological stabilization of the area. In the pond of S6, Dm values were slightly lower (5 and 7 in 2023 and 2024, respectively) but followed a trend similar to that of the canal, suggesting a complementary role of the pond in enhancing local biodiversity. However, the Shannon Index remained between 1 and 2 in both habitats,

indicating that despite the increase in species richness, evenness in species distribution remained limited, likely due to the dominance of a few pioneer species during the early recolonization stage.

In contrast, site S7 displayed a more stable trajectory. The canal maintained relatively high species richness over time, with Dm values ranging from 5 to 10 between 2020 and 2023. In 2023, both the canal and the pond reached Dm = 8, indicating a balanced distribution of species richness across the two habitats. This pattern may reflect better hydrological connectivity between the pond and the canal, or more favourable ecological conditions for vegetation development. However, the Shannon Index remained around 2, suggesting a slight but positive trend toward improved evenness in community structure.

Overall, both sites showed signs of biodiversity recovery after pond creation, albeit with different temporal dynamics. Despite being recently established, these environments demonstrate a clear potential to enhance local plant richness.

Table 22 - Biodiversity indices (Shannon and Margalef) for sites S6 and S7 from 2020 to 2024. Values of S correspond to the mean number of species recorded per year, while N indicates the mean α-richness per year used in the Margalef formula. This data refers to the canals and the pond.

Site	Location	Year	Mean n° of plant species (S)	Mean α-richness (N)	Shannon Index	Margalef Index
S6	Canal	2020	19	25	1	19
		2021	3	5	1	4
		2022	6	8	0	4
		2023	12	15	2	6
	Pond		7	10	2	5
		2024	14	19	2	7
S7	Canal	2020	10	13	1	10
		2021	9	12	1	5
		2022	11	15	1	6
		2023	19	25	2	8
	Pond		16	23	2	8

In site S4, the over time changes of Dm values were negligible with values ranging between 5 and 6 from 2020 to 2024 (Table 23). This would indicate a consistent level of species richness throughout the monitoring period, with no

substantial increase following the intervention. In the pond, richness was slightly lower starting in 2023 (Dm = 4), but reached 6 in 2024, suggesting a possible delayed colonization effect or improved hydrological connectivity. Shannon Index values (equal to 2 in both years) further confirm the stability in the structure of the plant community.

Site S9 exhibited a gradual increase in canal species richness over time (Table 23), with Dm rising from 5 in 2020 and 2021, to 6 in 2022 and 7 in 2023. This positive trend suggests that restoration efforts may have promoted a progressive enrichment of the plant community. In contrast, the pond in site S9 recorded a lower Dm value (4) and a Shannon Index value of 1, potentially due to limited hydrological connectivity or the impact of the 2023 flood, which may have hindered the establishment and distribution of plant species.

Overall, both sites displayed moderate levels of species richness following pond creation, with slightly better values observed in the canal habitats.

Table 23 – Biodiversity indices (Shannon and Margalef) for sites S4 and S9 from 2020 to 2024. Values of S correspond to the mean number of species recorded per year, while N indicates the mean α-richness per year used in the Margalef formula. This data refers to the canals and the pond.

Site	Location	Year	Mean n° of plant species (S)	Mean α-richness (N)	Shannon Index	Margalef Index
S4	Canal	2020	13	18	1	6
		2021	7	10	1	5
		2022	12	14	2	5
		2023	10	13	2	5
	Pond		8	10	2	4
		2024	12	16	2	6
S9	Canal	2020	8	11	1	5
		2021	5	9	0	5
		2022	9	14	1	6
		2023	12	18	2	7
	Pond		7	9	1	4

The combined use of Margalef's Richness Index and Shannon's Diversity Index provided a more comprehensive understanding of plant biodiversity dynamics across the monitored sites. Margalef's Index effectively highlighted the

temporal increase in species richness at several locations (i.e., sites S1 and S8), indicating a growing number of plant species over time. However, the Shannon Index remained relatively stable (typically between 1 and 2), suggesting that evenness in species distribution did not significantly improve.

The different behaviour showed by the two indices would indicate that, although the number of species increased, plant communities continued to be dominated by a few prevalent species. Therefore, the integration of both indices enabled a more nuanced interpretation, capturing both the enrichment in species composition and the internal structural dynamics of the communities. This dual approach is particularly valuable for evaluating not only the quantitative response (species richness), but also the ecological quality and stability of plant communities.

The joint analysis suggests that the restoration interventions have indeed enhanced species richness across the sites but have not yet produced a more even distribution of individuals among species. This may be due to the relatively short time study since the interventions or the need for additional management measures to foster greater ecological balance.

Previous studies have shown that species richness often increases rapidly after restoration, while improvements in evenness occur more slowly, being influenced by factors such as interspecific competition and habitat stability. In the studied wetlands, however, evenness is further constrained by the dominance of *Phragmites australis*, a species that tends to form stable climax stands and characterizes many surrounding wetlands in the Po Plain, so a substantial increase in the Shannon index is not expected (Crouzeilles et al., 2016). Consequently, it is common to observe an increase in Dm without a corresponding rise in H′ during the early stages of post-restoration succession.

11 Conclusions

The research conducted has highlighted the potential of bank reshaping and pond construction in improving the environmental quality of artificial canals embedded in a highly anthropized floodplain landscape. Through the 5-years monitoring of water, bed sediments and vegetation, this study provided a detailed assessment of the effects of the applied NBSs on such resources.

The data collected between 2020 and 2024 indicate that both NBSs triggered measurable ecological responses, although the intensity and duration of these effects varied depending on local conditions and external factors such as extreme weather events and land use. Bank reshaping proved particularly effective in promoting the establishment of a rich riparian vegetation, which likely contributed, at least partially, to the reduction of nutrient and sediment inputs from adjacent agricultural areas. However, the positive effects on water quality were in some cases temporary or obscured by interannual variability linked to intense meteorological events, such as the floods of 2023.

Similarly, the construction of ponds connected to the canals, especially in sites with sandy substrates such as S6 and S7, fostered local plant biodiversity and improved water quality through phytoremediation processes. Nonetheless, the effectiveness of these interventions was strongly influenced by hydrological dynamics, particularly in cases where ponds are subject to seasonal drying, as in sites S6 and S7. In sites with more stable hydrological regimes, such as S4 and S9, the positive effects of the applied NBS were more evident and consistent, with improvements recorded in water parameters such as pH, EC, SAR and nutrient concentrations.

From a broader perspective, this study confirms the role of artificial canals not only as hydraulic infrastructures but also as potential ecological corridors capable of supporting biodiversity and contributing to the delivery of ecosystem services. However, the capacity of these systems to provide such services is strongly influenced by management practices, territorial context and the frequency of extreme climate events.

Vegetation data show an increase in hygrophilous plant species in the intervention sites suggesting that spontaneous renaturalization dynamics aligned

with conservation goals. However, the persistent presence of ruderal and invasive species underscores the importance of continuous maintenance and long-term adaptive management.

Sediment analyses further reinforced the relevance of renaturalization interventions in modulating the input and accumulation of elements such as aluminium, phosphorus and nitrogen. While some parameters exhibited a degree of resilience, others were sensitive to both restoration actions and external environmental pressures. The observed increase in salinity indicators, such as electrical conductivity (EC) and sodium adsorption ratio (SAR), over time, particularly in sites S1, S2 and S8, highlights an emerging risk linked to saltwater intrusion. These sites are located in low-lying areas of the Po Plain that are affected by groundwater over-extraction for irrigation purposes and reduced freshwater inputs, which together facilitate the inland movement of saline water fronts from coastal areas or deep aquifers.

Overall, the study emphasizes the importance of a site-specific, long-term and multidisciplinary approach to floodplain restoration. Restoration interventions should be designed not only based on ecological criteria but also taking into account local pedological and hydrological characteristics, land use and future climate scenarios. The combination of physic-chemical and biological indicators used in this work proved to be an effective tool for evaluating the outcomes of restoration actions and guiding adaptive management strategies.

In conclusion, this study provides robust evidence in support of the use of Nature-Based Solutions to improve the ecological quality of artificial water bodies in agricultural floodplain contexts. However, their success depends on integrated territorial governance, continuous monitoring and the ability to adapt strategies in response to evolving environmental conditions. The results contribute to expanding the scientific knowledge base necessary for the sustainable planning and management of floodplains in Europe and beyond.

References

Abbas, N., Butt, T., Ahmad, M., Deeba, F., & Hussain, N. (2021). Phytoremediation potential of Typha latifolia and water hyacinth for removal of heavy metals from industrial wastewater. *N. Chemistry International*, *7*(2), 103-111.

Acreman, M. C., & Holden, J. (2013). How wetlands affect floods. *Wetlands*, 33(5), 773-786.

Aguiar, F. C., Ferreira, M. T., Albuquerque, A., Rodríguez-González, P., & Segurado, P. (2009). Structural and functional responses of riparian vegetation to human disturbance: performance and spatial scale-dependence. *Fundamental and Applied Limnology*, *175*(3), 249.

Akhtar, N., Syakir Ishak, M. I., Bhawani, S. A., & Umar, K. (2021). Various natural and anthropogenic factors responsible for water quality degradation: A review. *Water*, *13*(19), 2660.

Alekseenko, V., & Alekseenko, A. (2014). The abundances of chemical elements in urban soils. *Journal of Geochemical Exploration*, *147*, 245-249.

Almaaitah, T., Appleby, M., Rosenblat, H., Drake, J., & Joksimovic, D. (2021). The potential of Blue-Green infrastructure as a climate change adaptation strategy: a systematic literature review. *Blue-Green Systems*, *3*(1), 223-248.

Amoros, C., & Bornette, G. (2002). Connectivity and biocomplexity in waterbodies of riverine floodplains. Freshwater Biology, 47(4), 761–776.

Amorosi A. & Farina M. (1995) - Large-scale architecture of a thrust-related alluvial complex from subsurface data: the Quaternary succession of the Po Basin in the Bologna area (northern Italy). Giornale di geologia, 57: 3-16

Amorosi A., Asioli A., Bondesan M., Cibin U., Colalongo M.L., Correggiari A., Pasini G., Preti D., Roveri M., Sarti G., Severi P., Stefani M., Trincardi F., Vaiani S.C. & Vincenzi S. (2000) – Dalle conoidi pedemontane al mare aperto: l'architettura stratigrafica tardo-quaternaria dell'Adriatico settentrionale e della pianura costiera emiliano-romagnola. Atti del convegno: Le Pianure Conoscenza e salvaguardia, 191- 194.

Amorosi A., Centineo M.C., Colalongo M.L., Pasini G., Sarti G. & Vaiani S.C. (2003) - Facies architecture and latest Pleistocene-Holocene depositional history of the Po Delta (Comacchio area), Italy. Journal of Geology, 111: 39-56.

Amorosi A., Colalongo M.L., Fiorini F., Fusco F., Pasini G., Vaiani S.C. & Sarti G. (2004) – Palaeogeographic and palaeoclimatic evolution of the Po Plain from 150-ky core records. Global and Planetary Change, 40: 55-78.

Amorosi A., Colalongo M.L., Fusco F., Pasini G. & Fiorini F. (1999b) - Glacio-eustatic control of continental-shallow marine cyclicity from Late Quaternary deposits of the south-eastern Po Plain (Northern Italy). Quaternary Research, 52: 1-13.

Amorosi A., Colalongo M.L., Pasini G. & Preti D. (1999a) - Sedimentary response to Late Quaternary sea-level changes in the Romagna coastal plain (Northern Italy). Sedimentology, 46: 99-121.

Anthonisen, A. C., Loehr, R. C., Prakasam, T. B. S., & Srinath, E. G. (1976). *Inhibition of nitrification by ammonia and nitrous acid*. Journal of the Water Pollution Control Federation, 48(5), 835–852.

Appelo, C.A.J., & Postma, D. (2005). *Geochemistry, Groundwater and Pollution*. CRC Press.

Ayers, R. S., & Westcot, D. W. (1985). *Water quality for agriculture*. FAO Irrigation and Drainage Paper 29.

Bache, B. W. (1986). Aluminium mobilization in soils and waters. *Journal of the Geological Society*, *143*(4), 699-706.

Bajocco, S., de Angelis, A., & Salvati, L. (2012). A satellite-based green index as a proxy for vegetation cover quality in a Mediterranean region. Ecological Indicators, 23, 578–587.

Baken, S., Degryse, F., Verheyen, L., Merckx, R., & Smolders, E. (2011). *Metal complexation properties of organic matter: Comparison of different models and experimental data*. Environmental Science & Technology, 45(19), 7467–7474.

Ball, T. (2008). Management approaches to floodplain restoration and stakeholder engagement in the UK: a survey. Ecohydrology & Hydrobiology, 8(2-4), 273-280.

Banas, D., Marin, B., Skraber, S., Chopin, E. I. B., & Zanella, A. (2010). Copper mobilization affected by weather conditions in a stormwater detention system receiving runoff waters from vineyard soils (Champagne, France). *Environmental Pollution*, *158*(2), 476-482.

Barbier, E. B., Hacker, S. D., Kennedy, C., Koch, E. W., Stier, A. C., & Silliman, B. R. (2011). *The value of estuarine and coastal ecosystem services*. Ecological Monographs, 81(2), 169-193.

Barbosa, A., Martín, B., Hermoso, V., Arévalo-Torres, J., Barbière, J., Martínez-López, J., ... & Iglesias-Campos, A. (2019). Cost-effective restoration and conservation planning in Green and Blue Infrastructure designs. A case study on the Intercontinental Biosphere Reserve of the Mediterranean: Andalusia (Spain)–Morocco. *Science of the Total Environment*, *652*, 1463-1473.

Barkman J.J., Doing H. & Segal S., 1964. Kritische Bemerkungen und Vorschläge zur quantitativen Vegetationsanalyse. Acta Bot. Neerl., 13: 394-419.

Barlow, P. M., & Reichard, E. G. (2010). Saltwater intrusion in coastal regions of North America. *Hydrogeology Journal*, *18*(1), 247-260.

Bartole, R. (1995). The North Tyrrhenian–Northern Apennines post-collisional system: constraints for a geodynamic model. *Terra Nova*, *7*(1), 7-30.

Bastiani, M. (2011). Contratti di fiume. Pianificazione strategica e partecipata dei bacini idrografici. Approcci, esperienze, casi studio. Palermo: Dario Flaccovio Editore.

Bastviken, D., Cole, J. J., Pace, M. L., & Tranvik, L. J. (2004). *Methane emissions from lakes: Dependence of lake characteristics, two regional assessments, and a global estimate*. Global Biogeochemical Cycles, 18(4), GB4009.

Bellafiore, D., Ferrarin, C., Maicu, F., Manfè, G., Lorenzetti, G., Umgiesser, G., ... & Levinson, A. V. (2021). Saltwater intrusion in a Mediterranean delta under a changing climate. *Journal of Geophysical Research: Oceans*, *126*(2), e2020JC016437.

Bellafiore, D., Ferrarin, C., Maicu, F., Manfè, G., Lorenzetti, G., Umgiesser, G., ... & Levinson, A. V. (2021). Saltwater intrusion in a Mediterranean delta under a changing climate. *Journal of Geophysical Research: Oceans*, *126*(2), e2020JC016437.

Benjankar, R., Egger, G., Jorde, K., Goodwin, P., & Glenn, N. F. (2011). Dynamic floodplain vegetation model development for the Kootenai River, USA. Journal of Environmental Management, 92(12), 3058–3070.

Biggs, J., Von Fumetti, S., & Kelly-Quinn, M. (2017). The importance of small waterbodies for biodiversity and ecosystem services: implications for policy makers. *Hydrobiologia*, *793*, 3-39.

Biswal, B. K., & Balasubramanian, R. (2022). Constructed wetlands for reclamation and reuse of wastewater and urban stormwater: A review. *Frontiers in Environmental Science*, *10*, 836289.

Blann, K. L., Anderson, J. L., Sands, G. R., & Vondracek, B. (2009). Effects of agricultural drainage on aquatic ecosystems: a review. *Critical reviews in environmental science and technology*, *39*(11), 909-1001.

Blum, M. D., & Törnqvist, T. E. (2000). Fluvial responses to climate and sea-level change: a review and look forward. Sedimentology, 47, 2-48.

Blüthgen, N., Dormann, C. F., Prati, D., Klaus, V. H., Kleinebecker, T., Hölzel, N., ... & Weisser, W. W. (2012). A quantitative index of land-use intensity in grasslands: Integrating mowing, grazing and fertilization. *Basic and Applied Ecology*, *13*(3), 207-220.

Bolpagni, R., Laini, A., Stanzani, C., & Chiarucci, A. (2018). Aquatic plant diversity in Italy: Distribution, drivers and strategic conservation actions. *Frontiers in Plant Science*, *9*, 116.

Bornette, G., & Puijalon, S. (2011). Response of aquatic plants to abiotic factors: a review. *Aquatic sciences*, *73*, 1-14

Brandolini, F., & Cremaschi, M. (2018). The impact of late Holocene flood management on the Central Po plain (Northern Italy). *Sustainability*, *10*(11), 3968.

Braun-Blanquet J. 1928. Planzensoziologie. Grundzüge der Vegetationskunde. Berlin: Springer. 330 pp.

Braun-Blanquet J. 1964. Planzensoziologie. Grundzüge der Vegetationskunde. Wien/New York: Springer. XIV + 845 pp.

Brunel, S., Branquart, E., Fried, G., Van Valkenburg, J., Brundu, G., Starfinger, U., ... & Baker, R. (2010). The EPPO prioritization process for invasive alien plants. *EPPO bulletin*, *40*(3), 407-422.
Brunel, S., Schrader, G., Brundu, G., & Fried, G. (2010). Emerging invasive alien plants for the Mediterranean Basin. *EPPO bulletin*, *40*(2), 219-238.

Bruno, L., Amorosi, A., Curina, R., Severi, P., & Bitelli, R. (2013). Human–landscape interactions in the Bologna area (northern Italy) during the mid–late Holocene, with focus on the Roman period. *The Holocene*, *23*(11), 1560-1571.
Bryson, C. T., & DeFelice, M. S. (Eds.). (2010). *Weeds of the midwestern United States and central Canada* (Vol. 44). Athens, GA: University of Georgia Press.

Bundschuh, M., Weyers, A., Ebeling, M., Elsaesser, D., & Schulz, R. (2016). Narrow pH range of surface water bodies receiving pesticide input in Europe. *Bulletin of environmental contamination and toxicology*, *96*, 3-8.
Buscaroli, A., & Zannoni, D. (2010). Influence of ground water on soil salinity in the San Vitale Pinewood(Ravenna- Italy). *Agrochimica*, *54*(5), 303-320.
Camacho-Cristóbal, J. J., Rexach, J., & González-Fontes, A. (2008). Boron in plants: deficiency and toxicity. *Journal of Integrative Plant Biology*, 50(10), 1247–1255.
Cánovas, C. R., Hubbard, C. G., Olías, M., Nieto, J. M., Black, S., & Coleman, M. L. (2008). Hydrochemical variations and contaminant load in the Río Tinto (Spain) during flood events. *Journal of Hydrology*, *350*(1-2), 25-40.
Capuano, R. M., & Jones, C. R. (2020). Cation exchange in groundwater-chemical evolution and prediction of paleo-groundwater flow: a natural-system study. *Water Resources Research*, *56*(8), e2019WR026318.
Casal-Porras, I., de Los Santos, C. B., Martins, M., Santos, R., Pérez-Lloréns, J. L., & Brun, F. G. (2022). Sedimentary organic carbon and nitrogen stocks of intertidal seagrass meadows in a dynamic and impacted wetland: Effects of coastal infrastructure constructions and meadow establishment time. *Journal of Environmental Management*, *322*, 115841.

Casanova, M. T., & Brock, M. A. (2000). How do depth, duration and frequency of flooding influence the establishment of wetland plant communities?. *Plant ecology*, *147*(2), 237-250.

Cattaneo, A., & Steel, R. J. (2003). Transgressive deposits: a review of their variability. *Earth-Science Reviews*, *62*(3-4), 187-228

Centamore E., Deiana G., Micarelli A. et al. (1986). Il Trias-Paleogene delle Marche. In: E. CENTAMORE e G. DEIANA (Eds.), La geologia delle Marche. Studi Geologici Camerti, Vol. Spec. (1986), 9-27.

Chang ChiaJung, C. C., Huang ChinPao, H. C., Chen ChiaYang, C. C., & Wang GenShuh, W. G. (2020). Assessing the potential effect of extreme weather on water quality and disinfection by-product formation using laboratory simulation.

Chang, T. S., Joerdel, O., Flemming, B. W., & Bartholomä, A. (2006). The role of particle aggregation/disaggregation in muddy sediment dynamics and seasonal sediment turnover in a back-barrier tidal basin, East Frisian Wadden Sea, southern North Sea. *Marine Geology*, *235*(1-4), 49-61.

Chapman, D. (1996). Water Quality Assessments: A Guide to Use of Biota, Sediments and Water in Environmental Monitoring (2nd ed.). CRC Press.

Chavan, P. V., & Dennett, K. E. (2008). Wetland simulation model for nitrogen, phosphorus, and sediments retention in constructed wetlands. *Water, air, and soil Pollution*, *187*, 109-118.

Chen, M., Ma, L. Q., Harris, W. G. (2019). Distribution of cadmium, copper, lead and zinc in soils and sediments. *Environmental Pollution*, 124(1), 3–10.

Chen, Y., et al. (2015). "Soil disturbance and nitrate leaching following land use change and restoration in a subtropical wetland." *Ecological Engineering*, 83, 307–316.

Chen, Y., Li, D., Liu, S., Zhang, Y., Yan, X., Song, X., ... & Hou, J. (2025). Long-term effects of dead algal deposition on sediment surfaces: Behavior of endogenous phosphorus release in sediments. *Water Research*, *268*, 122742.

Chen, Y., Song, X., Zhang, Z., Shi, P., & Tao, F. (2015). Simulating the impact of flooding events on non-point source pollution and the effects of filter strips in an intensive agricultural watershed in China. *Limnology*, *16*, 91-101.

Choi, C., Berry, P., & Smith, A. (2021). The climate benefits, co-benefits, and trade-offs of green infrastructure: A systematic literature review. *Journal of Environmental Management*, *291*, 112583.

Chytrý, M., Jarošík, V., Pyšek, P., Hájek, O., Knollová, I., Tichý, L., & Danihelka, J. (2008). Separating habitat invasibility by alien plants from the actual level of invasion. *Ecology*, *89*(6), 1541-1553.

Chytrý, M., Maskell, L. C., Pino, J., Pyšek, P., Vilà, M., Font, X., & Smart, S. M. (2008). Habitat invasions by alien plants: a quantitative comparison among Mediterranean, subcontinental and oceanic regions of Europe. *Journal of Applied Ecology*, *45*(2), 448-458.

Chytrý, M., Pyšek, P., Tichý, L., Knollová, I., & Danihelka, J. (2005). Invasions by alien plants in the Czech Republic: a quantitative assessment across habitats. *Preslia*, *77*(4), 339-354.

Ciszewski, D., & Grygar, T. M. (2016). A review of flood-related storage and remobilization of heavy metal pollutants in river systems. *Water, Air, & Soil Pollution*, *227*, 1-19.

Clerici, N., & Vogt, P. (2013). Ranking European regions as providers of structural riparian corridors for conservation and management purposes. *International Journal of Applied Earth Observation and Geoinformation*, *21*, 477-483.

Cleveland, C. C., Wieder, W. R., Reed, S. C., & Townsend, A. R. (2020). Experimental drought in a tropical rainforest increases soil carbon dioxide losses to the atmosphere. *Proceedings of the National Academy of Sciences*, 107(35), 15571–15574.

CNR – Consiglio Nazionale delle Ricerche. (2019). *Impatto dei cambiamenti climatici sulle risorse idriche italiane*.

Cohen-Shacham, E., Walters, G., Janzen, C., & Maginnis, S. (Eds.). (2016). *Nature-Based Solutions to Address Global Societal Challenges*. IUCN.

Conrad, S. R., Santos, I. R., White, S. A., Hessey, S., & Sanders, C. J. (2020). Elevated dissolved heavy metal discharge following rainfall downstream of intensive horticulture. *Applied Geochemistry*, *113*, 104490.

Consorzio della Bonifica Renana 1909-1979. Forni Editore. 9-23.

Corenblit, D., & Steiger, J. (2024). Fluvial biogeomorphological feedbacks from plant traits to the landscape: Lessons from selected French rivers in line with AM Gurnell's influential contribution. *River Research and Applications*, *40*(6), 1012-1030.

Corenblit, D., Steiger, J., Gurnell, A. M., Tabacchi, E., & Roques, L. (2009). Control of sediment dynamics by vegetation as a key function driving biogeomorphic succession within fluvial corridors. *Earth Surface Processes and Landforms: The Journal of the British Geomorphological Research Group*, *34*(13), 1790-1810.

Corenblit, D., Tabacchi, E., Steiger, J., & Gurnell, A. M. (2007). Reciprocal interactions and adjustments between fluvial landforms and vegetation dynamics in river corridors: a review of complementary approaches. *Earth-Science Reviews*, *84*(1-2), 56-86.

Correll, D. L. (2005). Principles of planning and establishment of buffer zones. *Ecological Engineering*, *24*(5), 433-439.

Costanza, R., R. D'Arge, R. de Groot, S. Farber, M. Grasso, B. Hannon, K. Limburg, S. Naeem, R. V. O'Neill, J. Paruelo, R. G. Raskin, P. Sutton & M. van den Belt, 1997. The value of the world's ecosystem services and natural capital. Nature 387: 253–260.

Costanza, R., R. de Groot, P. Sutton, S. van der Ploeg, S. J. Anderson, I. Kubiszewski, S. Farber & R. K. Turner, 2014. Changes in the global value of ecosystem services. Global Environmental Change 26: 152–158.

Cottenie, K. (2005). Integrating environmental and spatial processes in ecological community dynamics. *Ecology letters*, *8*(11), 1175-1182.

Cremaschi, M. (1978). L'evoluzione di un tratto di pianura Padana (prov. Reggio e Parma) in rapporto agli insediamenti ed alla struttura geologica tra il XV sec. a. C. ed il sec. XI d. C. *Archeologia medievale*, *5*, 542.

Cremonini, L., Randi, P., Fazzini, M., Nardino, M., Rossi, F., & Georgiadis, T. (2024). Causes and impacts of flood events in Emilia-Romagna (Italy) in May 2023. *Land*, *13*(11), 1800.
Crouzeilles, R., Curran, M., Ferreira, M. S., Lindenmayer, D. B., Grelle, C. E., & Rey Benayas, J. M. (2016). A global meta-analysis on the ecological drivers of forest restoration success. *Nature communications*, *7*(1), 11666.

Csábrági, A., Molnár, S., Tanos, P., Kovács, J., Molnár, M., Szabó, I., & Hatvani, I. G. (2019). Estimation of dissolved oxygen in riverine ecosystems: Comparison of differently optimized neural networks. *Ecological Engineering*, *138*, 298-309.
Curtis, D. R., & Campopiano, M. (2014). Medieval land reclamation and the creation of new societies: Comparing Holland and the Po Valley, c. 800–c. 1500. *Journal of Historical Geography*, *44*, 93-108.
Custodio, E. (2010). Coastal aquifers of Europe: an overview. *Hydrogeology Journal*, *18*(1), 269.

Dallai D., Buldrini F., Fanti E., Tonelli F., Zampighi C., Conte L., Ferrari C., Managlia A. (2014a).
Davison, W. (1993). *Iron and manganese in lakes*. Earth-Science Reviews, 34(2), 119–163.
De Groot, R., L. Brander, S. van der Ploeg, R. Costanza, F. Ber- nard, L. Braat, M. Christie, N. Crossman, A. Ghermandi, L. Hein, S. Hussain, P. Kumar, A. McVittie, R. Portela, L. C. Rodriguez, P. ten Brink & P. van Beukering, 2012. Global estimates of the value of ecosystems and their services in monetary units. Ecosystem Services 1: 50–61.
De Ros, A., Piccoli, I., Sartori, L., Portelli, B., Serra, G., Dal Ferro, N., & Morari, F. (2025). Advancing soil texture and organic carbon spatial variability assessment: Integrating proximal γ-ray spectroscopy and electromagnetic induction via data fusion for site-independent analysis. *Catena*, *254*, 108980.
De Steven, D., Faulkner, S. P., Keeland, B. D., Baldwin, M. J., McCoy, J. W., & Hughes, S. C. (2015). Understory vegetation as an indicator for floodplain forest

restoration in the Mississippi River Alluvial Valley, USA. *Restoration Ecology*, *23*(4), 402-412.

Deng, P., Yi, Q., Zhang, J., Wang, C., Chen, Y., Zhang, T., & Shi, W. (2022). Phosphorous partitioning in sediments by particle size distribution in shallow lakes: from its mechanisms and patterns to its ecological implications. *Science of the Total Environment*, *814*, 152753.

Denny P. (1994). Biodiversity & wetlands. Wetlands Ecology and Management 3: 55-61.

Dewangan, S. K., Toppo, D. N., & Kujur, A. (2023). Investigating the impact of pH levels on water quality: An experimental approach. *International Journal for Research in Applied Science and Engineering Technology*, *11*(9), 756-759.

Dolejš, M., Raška, P., Kohnová, S., Schinke, R., Warachowska, W., Thaler, T., & Kočický, D. (2022). On the right track of flood planning policy? Land uptake in Central-European floodplains (1990–2018). *Landscape and Urban Planning*, *228*, 104560.

Dotterweich, M. (2008). The history of soil erosion and fluvial deposits in small catchments of central Europe: deciphering the long-term interaction between humans and the environment—a review. *Geomorphology*, *101*(1-2), 192-208.

Dudgeon, D., Arthington, A. H., Gessner, M. O., Kawabata, Z. I., Knowler, D. J., Lévêque, C., ... & Sullivan, C. A. (2006). Freshwater biodiversity: importance, threats, status and conservation challenges. *Biological reviews*, *81*(2), 163-182.

EEA (2018) European freshwater: Why should we care about floodplains? Briefing No. 14/2018.

Egertson, C. J., Kopaska, J. A., & Downing, J. A. (2004). A century of change in macrophyte abundance and composition in response to agricultural eutrophication. *Hydrobiologia*, *524*, 145-156.

Ellenberg, D., & Mueller-Dombois, D. (1974). *Aims and methods of vegetation ecology* (Vol. 547). New York: Wiley.

Ellenberg, H., & Leuschner, C. (2010). *Vegetation Mitteleuropas mit den Alpen: in ökologischer, dynamischer und historischer Sicht* (Vol. 8104). Utb.

England, J., Angelopoulos, N., Cooksley, S., Dodd, J., Gill, A., Gilvear, D., ... & Wilkes, M. A. (2021). Best practices for monitoring and assessing the ecological response to river restoration. *Water*, *13*(23), 3352.

European Environment Agency (2011). Green Infrastructure and territorial cohesion. Technical Report N° 18/2011. Copenhagen, https://www.eea.europa.eu/publications/green-infrastructure-and-territorial-cohesion/at_download/file

Farabegoli, E. (2004). *Introduzione all'analisi dei depositi alluvionali quaternari del margine appenninico-padano: Il fiume Savio*. Federal Emergency Management Agency (FEMA). (s.d.). *Unità 1: Inondazioni e gestione delle pianure alluvionali*. Recuperato da https://www.fema.gov/pdf/floodplain/nfip_sg_unit_1.pdf

Feio, M. J., Aguiar, F. C., Almeida, S. F. P., Ferreira, J., Ferreira, M. T., Elias, C., ... & Vieira, C. (2014). Least disturbed condition for European Mediterranean rivers. *Science of the total environment*, *476*, 745-756.

Fenchel, T., & Finlay, B. J. (1995). *Ecology and evolution in anoxic worlds*. Oxford University Press.

Feng, W., Ng, Z. Y., Chen, H., Zhang, J., Xu, D., He, Y., ... & Dang, L. (2024). Calcium ion deposition with precipitated calcium carbonate: Influencing factors and mechanism exploration. *Processes*, *12*(4), 629.

Ferronato, C., Vianello, G., & Vittori Antisari, L. (2015). Heavy metal risk assessment after oxidation of dredged sediments through speciation and availability studies in the Reno river basin, Northern Italy. *Journal of Soils and Sediments*, *15*, 1235-1245.

Fischer, R. A., & Fischenich, J. C. (2000). *Design recommendations for riparian corridors and vegetated buffer strips*. Army engineer waterways experiment station vicksburg ms engineer research and development center.

Fletcher, C. S., Gurney, G., & Douglass, D. (2013). *Nature-based solutions for disaster risk reduction and climate change adaptation*. *Environmental Science & Policy*, 33, 10-22.

Floodplains improve the water quality of rivers (2022) retrieved 30 December 2024 from https://phys.org/news/2022-09-floodplains-quality-rivers.html

Fookes, P. G., & Higginbottom, I. E. (1975). The classification and description of near-shore carbonate sediments for engineering purposes. *Geotechnique*, *25*(2), 406-411.

Forsberg, P. L., Skinnebach, K. H., Becker, M., Ernstsen, V. B., Kroon, A., & Andersen, T. J. (2018). The influence of aggregation on cohesive sediment erosion and settling. *Continental Shelf Research*, *171*, 52-62.

Förstner, U., & Wittmann, G. T. W. (2012). *Metal Pollution in the Aquatic Environment*. Springer Science & Business Media.

Fraaije R.G.A., Poupin C., Verhoeven J.T.A. and Soons M.B. (2019). Functional responses of aquatic and riparian vegetation to hydrogeomorphic restoration of channelized lowland streams and their valleys. Journal of Applied Ecology 56: 1007–1018

Froelich, P., Klinkhammer, G. P., Bender, M. A. A., Luedtke, N. A., Heath, G. R., Cullen, D., ... & Maynard, V. (1979). Early oxidation of organic matter in pelagic sediments of the eastern equatorial Atlantic: suboxic diagenesis. *Geochimica et Cosmochimica Acta*, *43*(7), 1075-1090.

Früh-Müller, A., Wegmann, M., & Koellner, T. (2015). Flood exposure and settlement expansion since pre-industrial times in 1850 until 2011 in north Bavaria, Germany. Regional Environmental Change, 15(1), 183–193. https://doi.org/10.1007/s10113-014-0633-9

Fu, Z., Wang, P., Sun, J., Lu, Z., Yang, H., Liu, J., ... & Li, T. (2020). Composition, seasonal variation, and salinization characteristics of soil salinity in the Chenier Island of the Yellow River Delta. *Global Ecology and Conservation*, *24*, e01318.

Funk, A., Martínez-López, J., Borgwardt, F., Trauner, D., Bagstad, K. J., Balbi, S., Magrach, A., Villa, F., & Hein, T. (2019). Identification of conservation and restoration priority areas in the Danube River based on the multi-functionality of river-floodplain systems. Science of the Total Environment, 654, 763–777.

Gaiolini, M., Colombani, N., Chierici, V., Montanari, L., & Mastrocicco, M. (2025). Numerical Modelling of Groundwater Level and Salinity Evolution in a Low-Lying Coastal Area Under Intensive Agricultural Activity. *Water Resources Management*, *39*(4), 1747-1761.

Gamito, S. (2010). Caution is needed when applying Margalef diversity index. *Ecological Indicators*, *10*(2), 550-551.

Garzanti E, Doniglioni C., Vezzoli G., Andò S. 2010, Orogenic belts and orogenic sediment provenance.

Gennai, M., Gabellini, A., Viciani, D., Venanzoni, R., Dell'Olmo, L., Giunti, M., ... & Foggi, B. (2021). The floodplain woods of Tuscany: towards a phytosociological synthesis. *Plant Sociology*, *58*, 1-28.

Gibling, M. R. (2018). River systems and the Anthropocene: a Late Pleistocene and Holocene timeline for human influence. *Quaternary*, *1*(3), 21.

Goldberg, S. (2005). *Soil Chemistry and Mineralogy: Cation Exchange Processes*. In: Encyclopedia of Soils in the Environment. Elsevier.

Gori, B., Pezzi, G., Brundu, G., Ceschin, S., Palella, E., Alessandrini, A., ... & Lambertini, C. (2023). Invasion trends of aquatic Ludwigia hexapetala and L. peploides subsp montevidensis (Onagraceae) in Italy based on herbarium records and global datasets.

Greggio, N., Giambastiani, B. M., Campo, B., Dinelli, E., & Amorosi, A. (2018). Sediment composition, provenance, and Holocene paleoenvironmental evolution of the Southern Po River coastal plain (Italy). *Geological Journal*, *53*(3), 914-928.

Grime, J. P. (2001). Plant strategies, vegetation processes, and ecosystem properties.

Grime, J. P. (2006). *Plant strategies, vegetation processes, and ecosystem properties*. John Wiley & Sons.england

Guerrero, J., Mahmoud, A., Alam, T., Chowdhury, M. A., Adetayo, A., Ernest, A., & Jones, K. D. (2020). Water quality improvement and pollutant removal by two regional detention facilities with constructed wetlands in South Texas. *Sustainability*, *12*(7), 2844.

Gumiero, B., Rinaldi, M., Belletti, B., Lenzi, D., & Puppi, G. (2015). Riparian vegetation as indicator of channel adjustments and environmental conditions: the case of the Panaro River (Northern Italy). *Aquatic sciences*, *77*, 563-582.

Gupta, D., Ranjan, R. K., Parthasarathy, P., & Ansari, A. (2021). Spatial and seasonal variability in the water chemistry of Kabar Tal wetland (Ramsar site), Bihar, India: multivariate statistical techniques and GIS approach. *Water Science and Technology*, *83*(9), 2100-2117.

Gurnell, A. (2014). Plants as river system engineers. *Earth Surface Processes and Landforms*, *39*(1), 4-25.

Gurnell, A. M., & Grabowski, R. C. (2016). Vegetation–hydrogeomorphology interactions in a low-energy, human-impacted river. *River Research and Applications*, *32*(2), 202-215.

Gurnell, A. M., Petts, G. E., Hannah, D. M., Smith, B. P., Edwards, P. J., Kollmann, J., ... & Tockner, K. (2001). Riparian vegetation and island formation along the gravel-bed Fiume Tagliamento, Italy. *Earth Surface Processes and Landforms: The Journal of the British Geomorphological Research Group*, *26*(1), 31-62.

Han, Y., Huang, Q., He, C., Fang, Y., Wen, J., Gao, J., & Du, S. (2020). The growth mode of built-up land in floodplains and its impacts on flood vulnerability. Science of the Total Environment, 700, 134462. https://doi.org/10.1016/j.scitotenv.2019.134462

Harvolk, S., Symmank, L., Sundermeier, A., Otte, A., & Donath, T. W. (2014). Can artificial waterways provide a refuge for floodplain biodiversity? A case study from North Western Germany. *Ecological Engineering*, *73*, 31-44.

Hassan, S. S., & Taseer, F. (2018) Water Quality Index (WQI) as an Indicator of Water Pollution: A Review. Environmental Science and Pollution Research, 25(6): 5510-5517.

Hassett, M. C., & Steinman, A. D. (2022). Wetland restoration through excavation: Sediment removal results in dramatic water quality improvement. *Land*, *11*(9), 1559.

Haygarth, P. M., Condron, L. M., Heathwaite, A. L., Turner, B. L., & Harris, G. P. (2005). The phosphorus transfer continuum: Linking source to impact with an interdisciplinary and multi-scaled approach. *Science of the Total Environment*, 344(1-3), 5–14.

Haygarth, P., Turner, B. L., Fraser, A., Jarvis, S., Harrod, T., Nash, D., ... & Beven, K. (2004). Temporal variability in phosphorus transfers: classifying concentration–discharge event dynamics. *Hydrology and Earth System Sciences*, *8*(1), 88-97.

Hein, T., Schwarz, U., Habersack, H., Nichersu, I., Preiner, S., Willby, N., & Weigelhofer, G. (2016). Current status and restoration options for floodplains along the Danube River. Science of the Total Environment, 543, 778–790.

Holm, L. G., Plucknett, D. L., Pancho, J. V., & Herberger, J. P. (1991). *The World's Worst Weeds: Distribution and Biology*. Malabar, FL: Krieger Publishing Company.

Holmer, M., & Storkholm, P. (2001). Sulphate reduction and sulphur cycling in lake sediments: a review. *Freshwater Biology*, *46*(4), 431-451.

Howarth, R. W., & Marino, R. (2006). Nitrogen as the limiting nutrient in coastal marine ecosystems: Implications for managing nutrient inputs. Ecological Applications, 16(6), 2035-2048.

Hsu, L. C., Huang, C. Y., Chuang, Y. H., Chen, H. W., Chan, Y. T., Teah, H. Y., ... & Tzou, Y. M. (2016). Accumulation of heavy metals and trace elements in fluvial sediments received effluents from traditional and semiconductor industries. *Scientific reports*, *6*(1), 34250.

Huang, Z., Liu, C., Zhao, X., Dong, J., & Zheng, B. (2020). Risk assessment of heavy metals in the surface sediment at the drinking water source of the Xiangjiang River in South China. *Environmental Sciences Europe*, *32*, 1-9.

Hughes, F. M. R., Colston, A., & Mountford, J. O. (2005). Restoring riparian ecosystems: The challenge of accommodating variability and designing restoration trajectories. Ecology and Society, 10(1). http://www.ecologyandsociety.org/vol10/iss1/art12/.

Hughes, F. M., & Rood, S. B. (2003). Allocation of river flows for restoration of floodplain forest ecosystems: a review of approaches and their applicability in Europe. *Environmental Management*, *32*(1), 12-33.

Hughes, F. M., Moss, T., & Richards, K. S. (2008). Uncertainty in riparian and floodplain restoration. In S. Darby & D. Sear (Eds.), River restoration:

managing the uncertainty in restoring physical habitat. (Vol. 79, pp. 94–119). Chichester, England: John Wiley & Sons, Ltd.

ISPRA – Istituto Superiore per la Protezione e la Ricerca Ambientale. (2015). *Rapporto 234/15: Modello geologico della Pianura Padana centro-orientale*.

ISPRA – Istituto Superiore per la Protezione e la Ricerca Ambientale. (2022). *Rapporto sullo stato dell'ambiente: Acque e suolo*.

ISPRA – Istituto Superiore per la Protezione e la Ricerca Ambientale. (2009). *Note illustrative della Carta Geologica d'Italia – Foglio 222:*

J.D. Pérez-Gutiérrez, J.O. Paz, M.L.M. Tagert Seasonal water quality changes in on-farm water storage systems in a south-central U.S. agricultural watershed. Agric. Water Manag., 187 (2017), pp. 131-139

Jakubínský, J., Prokopova, M., Raška, P., Salvati, L., Bezak, N., Cudlín, O., ... & Lepeška, T. (2021). Managing floodplains using nature-based solutions to support multiple ecosystem functions and services. Wiley Interdisciplinary Reviews: Water, 8(5), e1545.

Janke, B. D., Finlay, J. C., Taguchi, V. J., & Gulliver, J. S. (2022). Hydrologic processes regulate nutrient retention in stormwater detention ponds. *Science of the Total Environment*, *823*, 153722.

Jones, J. A. A. (2004). Implications of natural soil piping for basin management in upland Britain. *Land Degradation & Development*, *15*(3), 325-349.

Jose, S. (2009). Agroforestry for ecosystem services and environmental benefits: An overview. *Agroforestry Systems*, 76(1), 1-10.

Kabata-Pendias, A. (2011). *Trace Elements in Soils and Plants* (4th ed.). CRC Press.

Kabiri, V., Raiesi, F., & Ghazavi, M. A. (2016). Tillage effects on soil microbial biomass, SOM mineralization and enzyme activity in a semi-arid Calcixerepts. *Agriculture, Ecosystems & Environment*, *232*, 73-84.

Kabisch, N., Korn, H., Stadler, J., & Bonn, A. (Eds.). (2016). *Nature-Based Solutions to Climate Change Adaptation in Urban Areas: Linkages between Science, Policy and Practice*. Springer.

Kadlec, R. H., & Wallace, S. D. (2009). *Treatment Wetlands* (2nd ed.). CRC Press.

Kadlec, R. H., & Wallace, S. D. (2009). *Treatment Wetlands*. CRC Press.

Kail, J., Arle, J., & Jähnig, S. C. (2012). Limiting factors and thresholds for macroinvertebrate assemblages in European rivers: empirical evidence from three datasets on water quality, catchment urbanization, and river restoration. *Ecological Indicators*, *18*, 63-72.

Kail, J., Brabec, K., Poppe, M., & Januschke, K. (2015). The effect of river restoration on fish, macroinvertebrates and aquatic macrophytes: A meta-analysis. *Ecological Indicators*, *58*, 311-321.

Kanianska, R., Varga, J., Benková, N. et al. Floodplain soils contamination assessment using the sequential extraction method of heavy metals from past mining activities. Sci Rep 12, 2927 (2022). https://doi.org/10.1038/s41598-022-06929-7

Kendall, J. (1912). XCVI. The solubility of calcium carbonate in water. *The London, Edinburgh, and Dublin Philosophical Magazine and Journal of Science*, *23*(138), 958-976.

Kent, M. (2011). *Vegetation description and data analysis: a practical approach*. John Wiley & Sons.

Khalidy, R., Chiang, Y. W., & Santos, R. M. (2024). Tracking pedogenic carbonate formation and migration in agricultural soils amended with crushed wollastonite ore-Evidence from field trials.

Kietzka, G. J., Pryke, J. S., Gaigher, R., & Samways, M. J. (2021). Webs of well-designed conservation corridors maintain river ecosystem integrity and biodiversity in plantation mosaics. *Biological Conservation*, *254*, 108965.

Kingsford, R. T. (2000). Ecological impacts of dams, water diversions and river management on floodplain wetlands in Australia. *Austral Ecology*, *25*(2), 109-127.

Knox, R. L., Morrison, R. R. & Wohl, E. E. A river ran through it: Floodplains as America's newest relict landform. Sci. Adv. 8, eabo1082 (2022)

Koebel, J. W., & Kenner, S. (1999). "Restoring the Kissimmee River ecosystem." Restoration Ecology, 7(4), 273-285.

Kong, L., et al. (2023). "Performance and microbial community structure in a constructed wetland treating agricultural drainage water." *Journal of Environmental Management*, 336,

Kong, L., Zhang, L., Wang, Y., & Huang, Z. (2023). Impact of ecological restoration on the physicochemical properties and bacterial communities in alpine mining area soils. *Microorganisms*, *12*(1), 41.

Kopáček, J., Hejzlar, J., Kaňa, J., Norton, S. A., Porcal, P., & Turek, J. (2009). Trends in aluminium export from a mountainous area to surface waters, from deglaciation to the recent: effects of vegetation and soil development, atmospheric acidification, and nitrogen-saturation. *Journal of Inorganic Biochemistry*, *103*(11), 1439-1448.

Kothari, N. (1988). Groundwater, iron and manganese an unwelcome trio. *Water Engineering and Management;(USA)*, *135*(2).

Kristensen, H. L., Debosz, K., & McCarty, G. W. (2003). Short-term effects of tillage on mineralization of nitrogen and carbon in soil. *Soil Biology and Biochemistry*, *35*(7), 979-986.

Kummu, M., Tes, S., Yin, S., Adamson, P., Józsa, J., Koponen, J., ... & Sarkkula, J. (2014). Water balance analysis for the Tonle Sap Lake–floodplain system. *Hydrological Processes*, *28*(4), 1722-1733.

L'erbario della Bonifica. Un progetto per la conoscenza del territorio e della biodiversità vegetale nei canali della Bonifica Burana (Emilia orientale). Museologia Scientifica Memorie 11: 188–194.

Latella, M., Bertagni, M. B., Vezza, P., & Camporeale, C. (2020). An integrated methodology to study riparian vegetation dynamics: From field data to impact modeling. *Journal of Advances in Modeling Earth Systems*, *12*(8), e2020MS002094.

Laubel, A., Kronvang, B., Hald, A. B., & Jensen, C. (2003). Hydromorphological and biological factors influencing sediment and phosphorus loss via bank erosion in small lowland rural streams in Denmark. *Hydrological processes*, *17*(17), 3443-3463.

Lavorel, S., McIntyre, S., Landsberg, J., & Forbes, T. D. A. (1997). Plant functional classifications: from general groups to specific groups based on response to disturbance. *Trends in Ecology & Evolution*, *12*(12), 474-478.

Lavorel, S., Rochette, C., & Lebreton, J. D. (1999). Functional groups for response to disturbance in Mediterranean old fields. *Oikos*, 480-498.

Li, K. W., Lu, H. L., Nkoh, J. N., Hong, Z. N., & Xu, R. K. (2022). Aluminum mobilization as influenced by soil organic matter during soil and mineral acidification: A constant pH study. *Geoderma*, *418*, 115853.

Liu, D., Yang, H., Thompson, J. R., Li, J., Loiselle, S., & Duan, H. (2022). COVID-19 lockdown improved river water quality in China. *Science of the Total Environment*, *802*, 149585.

Liu, Y., Jiang, M., Lu, X., Lou, Y., & Liu, B. (2017). Carbon, nitrogen and phosphorus contents of wetland soils in relation to environment factors in Northeast China. *Wetlands*, *37*(1), 153-161.

Liu, Z., Song, L., Wang, Y., Zhang, D., Liang, J., Song, Y., ... & Zhao, Z. (2024). Impact of extreme rainfall and flood events on harmful cyanobacterial communities and ecological safety in the Baiyangdian Lake Basin, China. *Science of The Total Environment*, *956*, 177287.

Lorito, S., Calabrese, L., Perini, L., & Cibin, U. (2010). Uso del suolo della costa. *Il Sistema Mare-Costa dell'Emilia-Romagna; Perini, L., Calabrese, L., Eds*, 109-118.

Maes, J., & Jacobs, S. (2017). Nature-based solutions for Europe's sustainable development. *Conservation letters*, *10*(1), 121-124.

Maiti, K., & Roy, A. (2021). Iron-Mediated organic matter preservation in the Mississippi river-influenced shelf sediments. *Journal of Geophysical Research: Biogeosciences*, *126*(4), e2020JG006089.

Mandarino, A., Maerker, M., & Firpo, M. (2019). Channel planform changes along the Scrivia River floodplain reach in northwest Italy from 1878 to 2016. *Quaternary Research*, *91*(2), 620-637.

Mansour, H., Ahmed, S. A., Zaghloul, A., Kabary, H., & Nassar, H. F. (2024). Seasonal variation effect on water quality and sediments criteria and its influence

on soil pollution: Fayoum Governorate, Egypt. *Environmental Sciences Europe*, *36*(1), 132.

Mara, D. D., & Pearson, H. W. (1998). Design manual for waste stabilization ponds in Mediterranean countries. *Water Science and Technology*, 38(2), 1–13.

Marchetti, M. (2002). Environmental changes in the central Po Plain (northern Italy) due to fluvial modifications and anthropogenic activities. *Geomorphology*, *44*(3-4), 361-373.

Marzi, M., Shahbazi, K., Kharazi, N., & Rezaei, M. (2020). The influence of organic amendment source on carbon and nitrogen mineralization in different soils. *Journal of Soil Science and Plant Nutrition*, *20*, 177-191.

Mays, P. A., & Edwards, G. S. (2001). Comparison of heavy metal accumulation in a natural wetland and constructed wetlands receiving acid mine drainage. *Ecological Engineering*, 16(4), 487–500.

McFarlane, D., et al. (2015). Integrated stormwater management and water sensitive urban design in Melbourne. *Australian Journal of Water Resources*, 19(3), 235-245.

McNellie, M. J., Dorrough, J., & Oliver, I. (2019). Species abundance distributions should underpin ordinal cover-abundance transformations. *Applied Vegetation Science*, *22*(3), 361-372.

Merritt, D. M., Scott, M. L., LeRoy Poff, N., Auble, G. T., & Lytle, D. A. (2010). Theory, methods and tools for determining environmental flows for riparian vegetation: riparian vegetation-flow response guilds. *Freshwater Biology*, *55*(1), 206-225.

Messer, T. L., Burchell II, M. R., Birgand, F., Broome, S. W., & Chescheir, G. (2017). Nitrate removal potential of restored wetlands loaded with agricultural drainage water: A mesocosm scale experimental approach. *Ecological Engineering*, *106*, 541-554.

Messer, T. L., Burchell II, M. R., Grabow, G. L., & Osmond, D. L. (2012). Groundwater nitrate reductions within upstream and downstream sections of a riparian buffer. *Ecological Engineering*, *47*, 297-307.

Michael, H. A., Russoniello, C. J., & Byron, L. A. (2013). Global assessment of vulnerability to sea-level rise in topography-limited and recharge-limited coastal groundwater systems. *Water Resources Research*, *49*(4), 2228-2240.

Michalik, A., & Tekielak, T. (2013). The relationship between bank erosion, local aggradation and sediment transport in a small Carpathian stream. *Geomorphology*, *191*, 51-63.

Millennium ecosystem assessment, M. E. A. (2005). *Ecosystems and human well-being* (Vol. 5, p. 563). Washington, DC: Island press.

Minhas, P. S., & Sharma, D. R. (2006). *Irrigation with saline water and management strategies*. Agricultural Water Management, 84(1-2), 17–26.

Miranda, L. E., & Hodges, K. B. (2000). Role of aquatic vegetation coverage on hypoxia and sunfish abundance in bays of a eutrophic reservoir. *Hydrobiologia*, *427*(1), 51-57.

Mishra, A., Alnahit, A., & Campbell, B. (2021). Impact of land uses, drought, flood, wildfire, and cascading events on water quality and microbial communities: A review and analysis. *Journal of Hydrology*, *596*, 125707.

Mitsch, W. J., & Gosselink, J. G. (2015). *Wetlands* (5th ed.). John Wiley & Sons.

Mo, X., Peng, H., Xin, J., & Wang, S. (2022). Analysis of urea nitrogen leaching under high-intensity rainfall using HYDRUS-1D. *Journal of Environmental Management*, *312*, 114900.

Mohanavelu, A., Naganna, S. R., & Al-Ansari, N. (2021). Irrigation induced salinity and sodicity hazards on soil and groundwater: An overview of its causes, impacts and mitigation strategies. *Agriculture*, *11*(10), 983.

Molle, P., et al. (2008). French experience with constructed wetlands for wastewater treatment. *Water Science and Technology*, 58(10), 1-7.

Montanarella, L., & Panagos, P. (2015). "The relevance of sustainable soil management within the European Green Deal." *Environmental Sciences Europe, 27*(1), 1-6.

Montanari I., Buldrini F., Bolpagni R., Laini A., Dalla Vecchia A., De Bernardini N., Campione L., Naiman R.J., Décamps H. (1997). The ecology of interfaces: Riparian zones. Annual Review of Nazioni Unite - UNESCO. (2018). *Rapporto*

mondiale delle Nazioni Unite sullo sviluppo delle risorse idriche 2018: Soluzioni basate sulla natura per la gestione dell'acqua. UNESCO. Traduzione italiana.

Montanari, I., Buldrini, F., Bolpagni, R., Laini, A., Dalla Vecchia, A., De Bernardini, N., ... & Chiarucci, A. (2020). Role of irrigation canal morphology in driving riparian flora in over-exploited catchments. *Community Ecology*, *21*, 121-132.

Moon, S., Page Chamberlain, C., Blisniuk, K., Levine, N., Rood, D. H., & Hilley, G. E. (2011). *Climatic control of denudation in the deglaciated landscape of the Washington Cascades, Nat. Geosci., 4, 469–473*.

Muhar, S., Januschke, K., Kail, J., Poppe, M., Schmutz, S., Hering, D., & Buijse, A. D. (2016). Evaluating good-practice cases for river restoration across Europe: context, methodological framework, selected results and recommendations. *Hydrobiologia*, *769*(1), 3-19.

Nair, P. K. R. (2011). Agroforestry systems in floodplain agriculture: A case study from the Niger River Delta. *Agroforestry Systems*, 82(3), 215-229.

Native Plant Trust. (2024). *Rorippa palustris (common yellow-cress)*. Retrieved from https://gobotany.nativeplanttrust.org/species/rorippa/palustris/

Nehring, S., & Kolthoff, D. (2011). The invasive water primrose Ludwigia grandiflora(Michaux) Greuter & Burdet(Spermatophyta: Onagraceae) in Germany: First record and ecological risk assessment. *Aquatic invasions*, *6*(1), 83-89.

Nguyen, T. T., Meurk, C., Benavidez, R., Jackson, B., & Pahlow, M. (2021). The effect of blue-green infrastructure on habitat connectivity and biodiversity: a case study in the Ōtākaro/Avon River catchment in Christchurch, New Zealand. *Sustainability*, *13*(12), 6732.

Nichols, M. M. (1989). Sediment accumulation rates and relative sea-level rise in lagoons. *Marine geology*, *88*(3-4), 201-219.

Noe, G. B., Hupp, C. R., & Rybicki, N. B. (2013). Hydrogeomorphology influences soil nitrogen and phosphorus mineralization in floodplain wetlands. *Ecosystems*, *16*(1), 75-94.

Nordstrom, D. K., & Ball, J. W. (1986). The geochemical behavior of aluminum in acidified surface waters. *Science*, *232*(4746), 54-56.

Nowak, D. J., Hirabayashi, S., Bodine, A., & Greenfield, E. (2014). *Tree and forest effects on air quality and human health in the United States*. Environmental Pollution, 193, 119-129.

Olivares-Rieumont, S., De la Rosa, D., Lima, L., Graham, D. W., Borroto, J., Martínez, F., & Sanchez, J. (2005). Assessment of heavy metal levels in Almendares River sediments—Havana City, Cuba. *Water research*, *39*(16), 3945-3953.

Ostrowska, A., & Porębska, G. (2015). Assessment of the C/N ratio as an indicator of the decomposability of organic matter in forest soils. *Ecological Indicators*, *49*, 104-109.

P. Shi, Y. Zhang, Z.B. Li, P. Li, G.C. Xu Influence of land use and land cover patterns on seasonal water quality at multi-spatial scales Catena, 151 (2017), pp. 182-190

Paillex, A., Dolédec, S., Castella, E., & Mérigoux, S. (2009). Large river floodplain restoration: Predicting species richness and trait responses to the restoration of hydrological connectivity. Journal of Applied Ecology, 46, 250–258.

Pakoksung, K., Inseeyong, N., Chawaloesphonsiya, N., Punyapalakul, P., Chaiwiwatworakul, P., Xu, M., & Chuenchum, P. (2025). Seasonal dynamics of water quality in response to land use changes in the Chi and Mun River Basins Thailand. *Scientific Reports*, *15*(1), 7101.

Palmer, M. A., Menninger, H. L., & Bernhardt, E. (2010). River restoration, habitat heterogeneity and biodiversity: a failure of theory or practice?. *Freshwater biology*, *55*, 205-222.

Pant, H. K., Reddy, K. R., & Lemon, E. (2002). Phosphorus retention capacity of root bed media of sub-surface flow constructed wetlands. *Ecological Engineering*, 19(1), 89–105.

Park, J., & Hunt, J. R. (2018). Modeling fine particle dynamics in gravel-bedded streams: Storage and re-suspension of fine particles. *Science of the Total Environment*, *634*, 1042-1053.

Pasini P. (1925). La Bonifica Renana. Brochure descrittiva. Pubblicata su: Penning, E., Peñailillo Burgos, R., Mens, M., Dahm, R., & de Bruijn, K.

(2023). *Nature-based solutions for floods AND droughts AND biodiversity: Do we have sufficient proof of their functioning? Cambridge Prisms: Water, 1, e11*.
Peipoch, M., Brauns, M., Hauer, F. R., Weitere, M., & Valett, H. M. (2015). Ecological simplification: human influences on riverscape complexity. *BioScience*, *65*(11), 1057-1065.
Pérez-Gutiérrez, J. D., Paz, J. O., & Tagert, M. L. M. (2017). Seasonal water quality changes in on-farm water storage systems in a south-central US agricultural watershed. *Agricultural Water Management*, *187*, 131-139.
Pipenbaher, N. (2024). A link between species abundance and plant strategies for semi-natural dry grasslands. *Plants*, *13*(16, članka 2260).
Plants For A Future (PFAF). (2024). Cyperus longus. Retrieved from https://pfaf.org/user/plant.aspx?latinname=Cyperus+longus

Poesio, C., De Feudis, M., Morsolin, A., Lambertini, C., Zambonelli, A., Falsone, G., & Vittori Antisari, L. (2023). Exploring the canal environment in terms of water, bed sediments and vegetation in a reclaimed floodplain of Northern Italy. *Science of the Total Environment, 871*, 161953.
Poldini, L., Vidali, M., Castello, M., & Sburlino, G. (2020). A novel insight into the remnants of hygrophilous forests and scrubs of the Po Plain biogeographical transition area (Northern Italy). *Plant Sociology*, *57*(2), 17-69.
Ponting, J., Kelly, T. J., Verhoef, A., Watts, M. J., & Sizmur, T. (2021). The impact of increased flooding occurrence on the mobility of potentially toxic elements in floodplain soil–A review. *Science of the Total Environment*, *754*, 142040.
Pradit, S., Shazili, N. A. M., Towatana, P., & Saengmanee, W. (2016). Trace metals, grain size and organic matter in sediment from a coastal area of Thailand and Malaysia. *Aquatic Ecosystem Health & Management*, *19*(4), 345-354.
Pyšek, P., Jarošík, V., Hulme, P. E., Kühn, I., Wild, J., Arianoutsou, M., ... & Winter, M. (2010). Disentangling the role of environmental and human pressures on biological invasions across Europe. *Proceedings of the National Academy of Sciences*, *107*(27), 12157-12162.
Pyšek, P., Jarošík, V., Pergl, J., Randall, R., Chytrý, M., Kühn, I., ... & Sádlo, J. (2009). The global invasion success of Central European plants is related to

distribution characteristics in their native range and species traits. *Diversity and Distributions*, *15*(5), 891-903.

Qiu, J. G., & Liu, S. J. (2025). Dirammox (direct ammonia oxidation) to nitrogen (N2): discovery, current status, and perspectives. *Current Opinion in Microbiology*, *83*, 102565.

Qiu, J., Shen, Z., & Xie, H. (2023). Drought impacts on hydrology and water quality under climate change. *Science of the total environment*, *858*, 159854

Quinton, J. N., & Catt, J. A. (2007). Enrichment of heavy metals in sediment resulting from soil erosion on agricultural fields. *Environmental science & technology*, *41*(10), 3495-3500.

Rajib, A., Zheng, Q., Golden, H. E., Wu, Q., Lane, C. R., Christensen, J. R., ... & Nardi, F. (2021). The changing face of floodplains in the Mississippi River Basin detected by a 60-year land use change dataset. *Scientific Data*, *8*(1), 271.

Raymond, C. M., Frantzeskaki, N., Kabisch, N., Berry, P., Breil, M., Nita, M. R., ... & Calfapietra, C. (2017). A framework for assessing and implementing the co-benefits of nature-based solutions in urban areas. *Environmental science & policy*, *77*, 15-24.

Raymond, C., Horton, R. M., Zscheischler, J., Martius, O., AghaKouchak, A., Balch, J., ... & White, K. (2020). Understanding and managing connected extreme events. *Nature climate change*, *10*(7), 611-621.

Reddy, K. R., & Delaune, R. D. (2008). *Biogeochemistry of Wetlands: Science and Applications*. CRC Press.

Reddy, K. R., DeLaune, R. D., & Inglett, P. W. (2022). *Biogeochemistry of wetlands: science and applications*. CRC press.

Reid, A. J., Carlson, A. K., Creed, I. F., Eliason, E. J., Gell, P. A., Johnson, P. T., ... & Cooke, S. J. (2019). Emerging threats and persistent conservation challenges for freshwater biodiversity. *Biological reviews*, *94*(3), 849-873.

Rengasamy, P., & Olsson, K. A. (1991). Sodicity and soil structure. *Soil Research*, *29*(6), 935-952.

RER (2008). Regione Emilia-Romagna, Carta geologica, 1:25.000 - Ambienti deposizionali e litologie - 50k, a cura di Martini, A.

RER (2021). Regione Emilia-Romagna, Catalogo dei suoli 2020/2021, a cura di Tarocco, P., & Aprea, A.

RER (2023). Regione Emilia-Romagna. Coperture vettoriali uso del suolo di dettaglio.

Revenga, C., Campbell, I., Abell, R., De Villiers, P., & Bryer, M. (2005). Prospects for monitoring freshwater ecosystems towards the 2010 targets. Philosophical Transactions of the Royal Society B: Biological Sciences, 360(1454), 397-413.

Rhoades, J.D. (1982). "Salinity and Sodicity." In "Salinity and Drainage," pp. 93-114. Edited by R.D. Hillel.

Richards, L. A. (Ed.). (1954). *Diagnosis and Improvement of Saline and Alkali Soils*. U.S. Department of Agriculture Handbook No. 60, Washington, D.C.: U.S. Government Printing Office.

Riis, T., & Sand-Jensen, K. (2001). Historical changes in species composition and richness accompanying perturbation and eutrophication of Danish lowland streams over 100 years. *Freshwater Biology*, *46*(2), 269-280.

Rosolem, C. A., Calonego, J. C., & Foloni, J. S. S. (2005). Leaching of nitrate and ammonium from cover crop straws as affected by rainfall. *Communications in Soil Science and Plant Analysis*, *36*(7-8), 819-831.

Roswell, M., Dushoff, J., & Winfree, R. (2021). A conceptual guide to measuring species diversity. *Oikos*, *130*(3), 321-338.

Ruangpan, L., Vojinovic, Z., Plavšić, J., Curran, A., Rosic, N., Pudar, R., ... & Brdjanovic, D. (2024). Economic assessment of nature-based solutions to reduce flood risk and enhance co-benefits. *Journal of Environmental Management*, *352*, 119985.

Salehi Sarvak, A. H., Almodaresi, S. A., Deh-Abadi, A. M., Shishehbore, M. R., Kangazian, A. H., & Jamali, A. A. (2025). Calcium carbonate sediment corrosion and formation investigation in drinking water distribution network in Sough City, Iran. *Scientific Reports*, *15*(1), 2548.

Salvati, L., & Zitti, M. (2009). "Territorial disparities, natural resource distribution, and land degradation: A case study in southern Europe." *Geojournal, 74*(2), 115-130.

Salvati, L., Perini, L., Sabbi, A., & Bajocco, S. (2012). Climate aridity and land use changes: A regional-scale analysis. Geographical Research, 50(2), 193–203.

Sánchez, E., Colmenarejo, M. F., Vicente, J., Rubio, A., García, M. G., Travieso, L., & Borja, R. (2007). Use of the water quality index and dissolved oxygen deficit as simple indicators of watersheds pollution. *Ecological indicators*, *7*(2), 315-328.

Schaller, J., Brackhage, C., & Dudel, E. G. (2011). *Interactions of iron and silicon in the uptake of heavy metals by wetland plants*. Journal of Hazardous Materials, 186(2–3), 1410–1417.

Schindler, D. W. (2006). The paradox of the phosphorous enrichment of lake ecosystems. Science, 314(5805), 1071-1072.

Seddon, N. (2022). Harnessing the potential of nature-based solutions for mitigating and adapting to climate change. *Science*, *376*(6600), 1410-1416.

Seddon, N., Chausson, A., Berry, P., Girardin, C. A., Smith, A., & Turner, B. (2020). Understanding the value and limits of nature-based solutions to climate change and other global challenges. *Philosophical Transactions of the Royal Society B*, *375*(1794), 20190120.

Seitzinger, S.P., & Kroeze, C. (2008). Global Patterns of Dissolved Oxygen in Aquatic Systems in Global Biogeochemical Cycles, 22(3), GB3005.

Senzia, M. A., Mashauri, D. A., & Mayo, A. W. (2003). Suitability of constructed wetlands and waste stabilisation ponds in wastewater treatment: nitrogen transformation and removal. *Physics and Chemistry of the Earth, Parts A/B/C*, *28*(20-27), 1117-1124.

Serra-Llobet, A., Jähnig, S. C., Geist, J., Kondolf, G. M., Damm, C., Scholz, M., ... & Schmitt, R. (2022). Restoring rivers and floodplains for habitat and flood risk reduction: experiences in multi-benefit floodplain management from California and Germany. *Frontiers in Environmental Science*, *9*, 778568.

Shacklette, H. T., & Boerngen, J. G. (1984). *Element concentrations in soils and other surficial materials of the conterminous United States* (Vol. 1270). Washington, DC: US Government Printing Office.

Sharashy, O. (2022). Application of Shannon and Simpson Diversity Index to Study Plant biodiversity on Coastal Rocky Ridges Habitats with Reference to

Census Data in the Ras El-Hekma and Omayed Area on the Western Coastal Region of Egypt. *Journal of Pure & Applied Sciences*, *21*(1), 41-45.

Shen, W., Li, S., Mi, M., Zhuang, Y., & Zhang, L. (2021). What makes ditches and ponds more efficient in nitrogen control?. *Agriculture, Ecosystems & Environment*, *314*, 107409.

Sherman, J., Tzortziou, M., Turner, K. J., Greenfield, D. I., & Menendez, A. (2023). Deciphering the water quality impacts of COVID-19 human mobility shifts in estuaries surrounding New York City. *Science of The Total Environment*, *896*, 164953.

Sina, I., & Zulkarnaen, I. (2019). Margalef Index, Simpson Index and Shannon-Weaiver Index calculation for diversity and abudance of beetle in tropical forest. *STATMAT: JURNAL STATISTIKA DAN MATEMATIKA*, *1*(2).

Skidmore, M., Andarge, T., & Foltz, J. (2023). The impact of extreme precipitation on nutrient runoff. *Journal of the Agricultural and Applied Economics Association*, *2*(4), 769-785.

Smith, V. H. (2003). Eutrophication of freshwater and coastal ecosystems: A global problem. Environmental Science and Pollution Research, 10(2), 126-139.

Song, X., Dong, J., Wang, H., Xie, H., Yu, Y., Geng, L., ... & Du, Y. (2023). Factors influencing the distribution of organic carbon in four different coastal sedimentary environments. *Journal of Soils and Sediments*, *23*(3), 1539-1551.

Sparks, D.L. (2003). *Environmental Soil Chemistry*. Academic Press.

Statology. (2025). *How to Calculate and Interpret Margalef's Richness Index*. Retrieved from https://www.statology.org/how-to-calculate-interpret-margalef-richness-index/

Steinfeld, C. M. M., & Kingsford, R. T. (2013). Disconnecting the floodplain: earthworks and their ecological effect on a dryland floodplain in the Murray–Darling Basin, Australia. *River Research and Applications*, *29*(2), 206-218.

Stevenson, F. J. (1994). *Humus chemistry: genesis, composition, reactions*. John Wiley & Sons.

Stoltefaut, T., Haubrock, P. J., Welti, E. A., Baker, N. J., & Haase, P. (2024). A long-term case study indicates improvements in floodplain biodiversity after river restoration. *Ecological Engineering*, *198*, 107143.

Stumm, W., & Morgan, J. J. (2013). *Aquatic chemistry: chemical equilibria and rates in natural waters*. John Wiley & Sons.

Stutter, M.I., Chardon, W.J. and Kronvang, B. (2012), Riparian Buffer Strips as a Multifunctional Management Tool in Agricultural Landscapes: Introduction. J. Environ. Qual., 41: 297-303.

Sukitprapanon, T. S., Jantamenchai, M., Tulaphitak, D., & Vityakon, P. (2020). Nutrient composition of diverse organic residues and their long-term effects on available nutrients in a tropical sandy soil. *Heliyon*, *6*(11).

Susini G., (1980). Bonifica e paesaggio cispadano: l'evo antico. Estratto da I settant'anni del Consorzio della Bonifica Renana 1909-1979. Forni Editore. 9-23.

Tamme, R., Hiiesalu, I., Laanisto, L., Szava-Kovats, R., & Pärtel, M. (2010). Environmental heterogeneity, species diversity and co-existence at different spatial scales. *Journal of Vegetation Science*, *21*(4), 796-801.

Tan, K.H. (2010). *Principles of Soil Chemistry* (4th ed.). CRC Press.

Tang, Z., Cao, C., Tang, K., Qi, H., Sun, Y., & Yang, J. (2020). Distribution of carbon and nitrogen as indictors of environmental significance in coastal sediments of Weizhou Island, Beibu Gulf. *Water*, *12*(11), 3285.

Teatini, P., Ferronato, M., Gambolati, G., Bertoni, W., & Gonella, M. (2005). A century of land subsidence in Ravenna, Italy. *Environmental Geology*, *47*, 831-846.

That, L. T., & Hoang, H. Y. (2024). Utilizing a settling pond-based constructed wetland for the treatment of shrimp aquaculture wastewater–From laboratory to field scale: A case study in Ben Tre Province, Vietnam. *Ecological Engineering*, *199*, 107172.

Tilman, D. (1999). Global environmental impacts of agricultural expansion: the need for sustainable and efficient practices. *Proceedings of the national Academy of Sciences*, *96*(11), 5995-6000.

Tipping, E., Hurley, M. A., Smith, E. J., Gibson, G. J., & Benham, D. G. (2002). *Aluminium solubility in soils and waters at acid deposition levels in the UK*. Environmental Pollution, 119(1), 31–48.

Tockner, K., & Stanford, J. A. (2002). Riverine flood plains: Present state and future trends. Environmental Conservation, 29(3), 308–330.

Tölgyesi, C., Torma, A., Bátori, Z., Šeat, J., Popović, M., Gallé, R., ... & Török, P. (2022). Turning old foes into new allies—Harnessing drainage canals for biodiversity conservation in a desiccated European lowland region. *Journal of Applied Ecology*, *59*(1), 89-102.

Trentini, G., Monaci, M., Goltara, A., Comiti, F., Gallmetzer, W., & Mazzorana, B. (2012). Riqualificazione fluviale e gestione del territorio.

Tschikof, M., Gericke, A., Venohr, M., Weigelhofer, G., Bondar-Kunze, E., Kaden, U. S., & Hein, T. (2022). The potential of large floodplains to remove nitrate in river basins–The Danube case. *Science of the Total Environment*, *843*, 156879.

UBA (2010). The Isar-Plan: Integrated restoration of the Isar River in Munich. *German Federal Environment Agency Report*.

Uddin, M. G., Nash, S., & Olbert, A. I. (2021). A review of water quality index models and their use for assessing surface water quality. *Ecological Indicators*, *122*, 107218.

Università di Udine. (s.d.). Progetto Finale: Qualità delle acque. Recuperato da http://calliope.dem.uniud.it/CLASS/ING-AMB/ProgettoFinale-Qual2E.pdf

US Geological Survey. (n.d.). *Conium maculatum*. Nonindigenous Aquatic Species. U.S. Department of the Interior. Retrieved May 20, 2025, from https://nas.er.usgs.gov/queries/greatLakes/FactSheet.aspx?Species_ID=2669

Viaroli, P., Bartoli, M., Giordani, G., Magni, P., & Welsh, D. T. (2004). Biogeochemical indicators as tools for assessing sediment quality/vulnerability in transitional aquatic ecosystems. *Aquatic Conservation: Marine and Freshwater Ecosystems*, *14*(S1), S19-S29.

Vilà, M., Espinar, J. L., Hejda, M., Hulme, P. E., Jarošík, V., Maron, J. L., ... & Pyšek, P. (2011). Ecological impacts of invasive alien plants: a meta-analysis of

their effects on species, communities and ecosystems. *Ecology letters*, *14*(7), 702-708.

Violante, A., Cozzolino, V., Perelomov, L., Caporale, A.G., & Pigna, M. (2010). Mobility and bioavailability of heavy metals and metalloids in soil environments. *Journal of Soil Science and Plant Nutrition*, 10(3), 268–292.

Vitousek, P. M., Mooney, H. A., Lubchenco, J., & Melillo, J. M. (1997). Human domination of Earth's ecosystems. Science, 277(5325), 494-499.

Vittori Antisari L., Trivisano C., Gessa C., Gherardi M., Simoni A., Vianello G., Zamboni N. (2010). Quality of municipal wastewater compared to surface waters of the river and artificial canal network in different areas of the Eastern Po Valley (Italy). Water Quality Expo Health 2: 1–13.

Vittori Antisari, L., Speranza, M., Ferronato, C., De Feudis, M., Vianello, G., & Falsone, G. (2020). Assessment of water quality and soil salinity in the agricultural coastal plain (Ravenna, North Italy). *Minerals*, *10*(4), 369.

Vymazal, J. (2007). *Removal of nutrients in various types of constructed wetlands*. Science of the Total Environment, 380(1–3), 48–65

Wagai, R., Kajiura, M., & Asano, M. (2020). Iron and aluminum association with microbially processed organic matter via meso-density aggregate formation across soils: organo-metallic glue hypothesis. *SOIL Discussions*, *2020*, 1-42.

Walling, D. E., & Collins, A. L. (2008). The catchment sediment budget as a management tool. *environmental science & policy*, *11*(2), 136-143.

Wang, F., Zhang, J., Qin, X., & Zhang, H. (2025). The law of flowing water grouting travel and sedimentary plugging under the influence of many factors. *Scientific Reports*, *15*(1), 11079.

Wang, P., Yu, H., Xiao, H., Wan, J., Ma, Q., Tao, G., ... & Ma, L. (2023). Effects of habitat factors on the plant diversity on naturally-restored wind farm slopes. *PeerJ*, *11*, e14912.

Wang, Z. J., Yue, F. J., Wang, Y. C., Qin, C. Q., Ding, H., Xue, L. L., & Li, S. L. (2022). The effect of heavy rainfall events on nitrogen patterns in agricultural surface and underground streams and the implications for karst water quality protection. *Agricultural Water Management*, *266*, 107600.

Water balance analysis for the Tonle Sap Lake–floodplain system. Hydrol. Process., 28 (4) (2014), pp. 1722-1733

Wendland, F., Blum, A., Coetsiers, M., Gorova, R., Griffioen, J., Grima, J., ... & Walraevens, K. (2008). European aquifer typology: a practical framework for an overview of major groundwater composition at European scale. *Environmental Geology*, *55*, 77-85.

Wetzel, R. G. (2001). Limnology: Lake and River Ecosystems (3rdedn.) Academi c Press. *San Diego*.

Whalen, J. K., Bottomley, P. J., & Myrold, D. D. (2000). Carbon and nitrogen mineralization from light-and heavy-fraction additions to soil. *Soil Biology and Biochemistry*, *32*(10), 1345-1352.

Wijnhoven, S., Walvoort, D. J. J., & Schilder, J. (2023). Condition of Benthic Habitat Communities: Margalef diversity in Region II. *OSPAR, 2023: The 2023 Quality Status Report for the North-East Atlantic*.

Williams, R. J., & Boorman, D. B. (2012). Modelling in-stream temperature and dissolved oxygen at sub-daily time steps: An application to the River Kennet, UK. *Science of the Total Environment*, *423*, 104-110.

Willis, B. E., & Bishop, W. M. (2016). Understanding fate and effects of copper pesticides in aquatic systems. *Journal of Geoscience and Environment Protection*, *4*(5), 37-42.

Wissmar, R. C., & Beschta, R. L. (1998). Restoration and management of riparian ecosystems: a catchment perspective. *Freshwater Biology*, *40*(3), 571-585.

Withers, P. J. A., & Haygarth, P. M. (2007). Agriculture, phosphorus and eutrophication: a European perspective. *Soil Use and Management*, *23*, 1-4.

Wohl, E., Lininger, K. B. & Baron, J. Land before water: The relative temporal sequence of human alteration of freshwater ecosystems in the conterminous United States. Anthropocene 18, 27–46 (2017)

Wolch, J. R., Byrne, J., & Newell, J. P. (2014). *Urban green space, public health, and environmental justice: The challenge of making cities "just green enough"*. Landscape and Urban Planning, 125, 234-244.

Yao, X., Zhao, Z., Wang, J., Ding, Q., Ren, M., Kimirei, I. A., & Zhang, L. (2022). Sediment organic matter properties facilitate understanding nitrogen transformation potentials in East African lakes. *Science of the Total Environment*, *841*, 156607.

Yazdi, M. N., Scott, D., Sample, D. J., & Wang, X. (2021). Efficacy of a retention pond in treating stormwater nutrients and sediment. *Journal of cleaner production*, *290*, 125787.

Yunus, A. P., Masago, Y., & Hijioka, Y. (2020). COVID-19 and surface water quality: Improved lake water quality during the lockdown. *Science of the Total Environment*, *731*, 139012.

Zak, D., Gelbrecht, J., & Steinberg, C. E. W. (2004). Phosphorus retention at the redox interface of peatlands adjacent to surface waters in northeast Germany. *Biogeochemistry*, 70(3), 357–368.

Zawiska, I., Jasiewicz, J., Rzodkiewicz, M., & Woszczyk, M. (2023). Relative impact of environmental variables on the lake trophic state highlights the complexity of eutrophication controls. *Journal of Environmental Management*, *345*, 118679.

Zhang, C., Wang, Y., Zhu, X. (2022). Influence of river restoration on heavy metal dynamics in urban sediments. *Science of the Total Environment*, 834, 155296.

Zhang, F., Yan, J., Fang, J., Yan, Y., Zhang, S., & Benoit, G. (2023). Sediment phosphorus immobilization with the addition of calcium/aluminum and lanthanum/calcium/aluminum composite materials under wide ranges of pH and redox conditions. *Science of the Total Environment*, *863*, 160997.

Zhang, S., Xia, X., Xin, Y., Li, X., Wang, J., Yu, L., ... & Yang, Z. (2023). Electrical conductivity as a reliable indicator for assessing land use effects on stream N2O concentration. *Journal of Hydrology*, *626*, 130253.

Zhang, Y., Li, Z., Xu, H., Ge, W., Qian, H., Li, J., ... & Jiao, Y. (2024). Impact of floods on the environment: A review of indicators, influencing factors, and evaluation methods. *Science of The Total Environment*, 175683.

Zhu, G., et al. (2021). "Effects of vegetation restoration on nitrogen and phosphorus removal from agricultural runoff." *Science of the Total Environment*, 765,

Zhu, G., Shangguan, Z., Hu, X., & Deng, L. (2021). Effects of land use changes on soil organic carbon, nitrogen and their losses in a typical watershed of the Loess Plateau, China. *Ecological Indicators*, *133*, 108443.

Zhu, L., Zhang, H., Li, Y., Cheng, G., Zhu, Y., Song, C., ... & Du, G. (2023). Long-term variation characteristics of nutrients in the water and sediments of a surface flow constructed wetland with micro-polluted water sources. *Ecological Engineering*, *187*, 106848.

Zhu, T., & Dittrich, M. (2016). Carbonate precipitation through microbial activities in natural environment, and their potential in biotechnology: a review. *Frontiers in bioengineering and biotechnology*, *4*, 4.

Appendix

Study sites

Hydraulic sector between right bank of the Idice river and left bank of the Sillaro river, Municipality of Medicina.

Site S1

Total area: 3,000 m²

Coordinates: 44°32'20"N 11°43'17"E

Elevation: 4-7 m asl

Location: left bank of the Garda Basso canal (Municipality of Medicina) (Figure A1).

Figure A1 - S1 after intervention.

Canal

The Garda Basso canal is an incised, multipurpose watercourse used both for storm-water drainage and for irrigation. It originates near the locality of Villa Fontana within the Municipality of Medicina and flows for 14.2 km before reaching the locality of Casotto del Palone, where it converges with two other multipurpose incised canals - the Menata and Sesto Basso. The confluence of these canals forms the Collettore Menata precisely at the boundary between two Natura 2000 sites: IT4050022 - SAC-SPA “Biotopes and Environmental Restorations of Medicina and Molinella” and IT4060001 - SCI-SPA “Valli di Argenta”. Within this protected area, which is part of the Po Delta Regional Park, the Collettore Menata continues until it reaches the Valle Santa water detention basin at Campotto.

Irrigation district

Site S1 lies within the irrigation district that bears the same name as the canal, “Garda Basso”. The district covers 1,067 ha and annually about 470 ha are irrigated. According to data provided by the Renana Remediation Consortium for the 2023–2024 irrigation seasons, average irrigated surfaces for the main crops are: maize 247 ha, sugar beet 84 ha, alfalfa 49 ha, sorghum 33 ha, and soybean 22 ha.

This canal reach is supplied mainly from the “Garda” intake on the Canale Emiliano Romagnolo (CER), which discharges into the Garda Superiore canal near the town of Medicina; downstream this canal becomes the Garda Basso.

At S1 the canal exhibits a summer irrigation depth of c. 0.5 m and a bank-to-bank width of 5 m.

Based on irrigation records from 2020-2024, an area of about 52 ha located within 1 km upstream of the site is irrigated each year by a single farm, predominantly cultivating maize (40 ha) and sugar beet (12 ha).

Site location and morphology

Site S1 is situated 4.7 km upstream from the canal outfall, close to the eastern boundary of the Natura 2000 site IT4050022 - SAC-SPA - “Biotopes and Environmental Restorations of Medicina and Molinella”, and adjacent to the

wetlands of “Tenuta Vallona”. It is also 1 km from the “Oasi del Quadrone”, an historic wetland complex representative of Po Plain habitats (Figure A2).

Access is along a 1.7 km track following the left bank of the Garda Basso canal from the Via Bassa bridge southwards, running along the embankment of the Garda Alto canal.

The intervention stretches 140 m along the left bank beginning at the point where the Garda Basso passes beneath the Garda Alto.

Morphologically the site consists of two zones: a long, gently sloping bank rising from the canal to the crown of the levee, and a service track bordered by a linear strip of mixed native trees and shrubs.

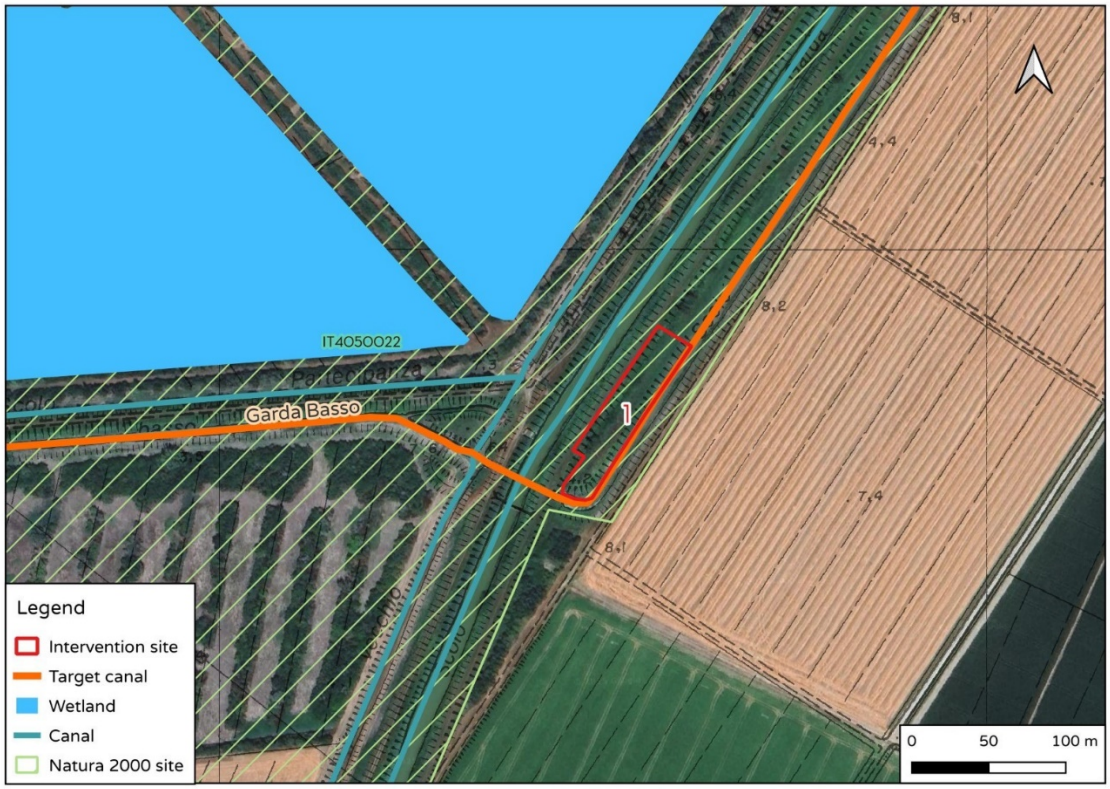

Figure A2 - Cartographic framing of S1.

Soil features before intervention

Soil at site S1 was classified as an Udic Haplustert (Soil Survey Staff, 2014) and a Haplic Vertisol (hypereutric) according to the World Reference Base (IUSS, 2015).

This soil type presents limiting factors that include a high content of expandable clays (> 50%) and poor internal drainage capacity, which may affect both plant development and soil workability.

In Table A1 are reported the main features of pedogenetic horizons identified within three soil profiles dug at site S1.

Table A1 - Depth interval, pH, electrical conductivity (EC), contents of total carbonates (CaCO3 tot), sand, silt and clay of three soil profiles (1A, 1B, 1C) dug in site S1 before the intervention.

Profile	Horizon	Depth	pH	E.C.	$CaCO_3$ tot.	Texture		
			H_2O			sand	silt	clay
		(cm)		dS cm^{-1}	g kg^{-1}	g kg^{-1}		
1A	Oi	1-0	nd	nd	nd	nd	nd	nd
	A	0-10	7,6	0,31	85	93	457	450
	BC	10-50	7,8	0,28	132	79	376	545
	C1	50-80	7,9	0,28	133	72	372	556
	C2	80-100+	8,0	0,27	141	65	434	501
1B	Oi	1-0	nd	nd	nd	nd	nd	nd
	AO	0-5,5	7,2	0,44	83	145	476	379
	A	5,5-26,5	7,7	0,35	134	7	435	558
	BC	26,5-48	7,9	0,30	134	12	439	549
	C1	48-75	7,9	0,29	150	11	432	557
	C2	75-100+	8,0	0,30	136	10	422	568
1C	A1	0-13	7,7	0,36	8	18	415	567
	A2	13-28	7,8	0,33	127	35	381	584
	BC	28-53	7,9	0,31	133	51	386	563
	2C1	53-83	8,0	0,32	134	147	325	528
	3C2	83-100+	8,1	0,25	142	75	589	486

Type of intervention

At this site, the intervention focused on the hydraulic easement strip along the bank and scarp up to the service road, including a berm at the foot of the right embankment of the Garda Alto Canal. Prior to intervention the area was unmanaged, bearing spontaneous woody shrubs and herbaceous vegetation.

The most substantial action involved reshaping the left bank to a gentle, uniform gradient, thereby promoting the establishment of hygrophilous and helophytic

species - both spontaneous and nursery-grown - and reducing suitability for burrowing by the invasive alien species coypu - *Myocastor coypus.*

In addition to earthworks, native tree and shrub species characteristic of the EU habitat “92A0 - “Riparian galleries forest of *Populus alba* and *Salix alba*” were planted. A total of 84 woody plants were introduced to supplement existing cover, creating an afforested area of 1,000 m². Of these, 43 are trees and 41 shrubs. To enhance structural diversity, a mixed-age stand was established, comprising 25 forest saplings (50–70 cm) and 59 larger, more mature specimens (Table A2).

Subsequently, 147 pots of autochthonous aquatic plants produced in the project nursery were installed along the bank, representing 11 helophytic herb species (Table A3) (Figure A3).

Table A2 - List of plants per tree and shrub species planted at S1.

Trees and shrubs planted at site 1		
Species	**Saplings (0.50-0.90 m)**	**Young plants (1-3 m)**
Trees	**13**	**30**
Fraxinus angustifolia		1
Fraxinus excelsior	1	1
Populus alba	4	7
Populus nigra	3	4
Salix alba	5	17
Shrubs	**12**	**29**
Cornus sanguinea	1	3
Corylus avellana	1	1
Euonymus europaeus	1	2
Prunus padus	1	2
Prunus spinosa		2
Rhamnus frangula	1	3
Rosa canina	1	1
Sambucus nigra	5	11
Viburnum lantana		1
Viburnum opulus	1	3
Total	**25**	**59**

Table A3 - List of pots per herbaceous plant species planted at S1.

Herbaceous plants planted at site 1	
Species	**N. of pots**
Alisma plantago-aquatica	34
Althaea officinalis	5
Carex pendula	8
Cyperus longus	8
Juncus articulatus	6
Juncus sp.	12
Limniris pseudacorus	4
Lycopus europaeus	8
Lythrum salicaria	22
Sparganium erectum	1
Typha latifolia	9
Typha sp.	30
Total	**147**

Figure A3 - Vegetation along S1 bank.

Implementation schedule and costs

All modelling and planting works were carried out by the Renana Remediation Consortium and completed in February 2022.

Total expenditure, calculated in the Executive Project using the 2020 Emilia-Romagna Regional Price List, amounted to € 6,211.00 (Table A4).

Table A4 - Calculation of the cost of intervention at S1, based on the Emilia-Romagna Region price list (2020 edition) and the actual costs incurred for the purchase of trees and shrubs.

Intervention costs at site 1		
Cost item	**Quantity**	**Cost**
Mechanical mowing of heterogeneous spontaneous vegetation consisting mainly of reeds and bushes, carried out by mechanical means on canal floodplains and embankment surfaces, flat and sloping, including the cost of collecting and transporting the resulting material to waste.	1820 m^2 x 0.16 €/m^2	€ 291.20
Excavator, shovel, or bulldozer, including operator, fuel, and lubricant, for setting up hydraulic appurtenances	6 hours x 69.10 €/h	€ 414.60
Excavation for the reshaping of canal bed section, performed by mechanical means, in the presence of water, including all charges and displacement and frontal placement of the resulting material	413 m^3 x 2 €/m^3	€ 826.00
Formation of embankment with excavated soil for thin bank body reroutes and elevations, including excavation and all other charges	413 m^3 x 5.6 €/m^3	€ 2,312.80
Planting of tree/arbustive plants	45 hours x 13.20 €/h	€ 594.00
Planting herbaceous plants	12 hours x 13.20 €/h	€ 158.40
Purchase and supply of trees and shrubs	30 trees, 29 shrubs	€ 1,614.00
Free supply of trees and shrubs saplings	13 trees and 12 shrubs	
Herbaceous plants from the nursery	147 plants	
Total		**€ 6,211.00**

Site S2

Total area: 1,300 m²

Coordinates: 44°34'11"N 11°45'32"E

Elevation: 5 m a.s.l.

Location: Confluence of the Sesto Basso and Sant'Antonio canals (Municipality of Medicina) (Figure A4).

Figure A4 – S2 after intervention.

Canal

The Sesto Basso canal is an incised, multipurpose watercourse – conveying both storm-water runoff and irrigation flows – with a total length of 16.3 km. It originates near the locality of La Motta in the Municipality of Budrio, close to the boundary of the SAC-SPA IT4050022. For almost 10 km it runs within that protected area, skirting the Idice river, the "Valle Orsona" wetland, the "Tenuta Boscosa", and the Quaderna Stream. Outside protected areas, the canal passes beneath the

Garda Alto Canal near Casotto del Palone, where it joins the Menata and Garda Basso canal. Their confluence forms the Collettore Menata at the border between Natura 2000 sites IT4050022 “Biotopes and environmental restorations of Medicina and Molinella” and IT4060001 - SCI-SPA “Valli di Argenta”, within the Po Delta Regional Park. From there it continues to the Valle Santa water detention basin at Campotto (FE).

Irrigation district

Site S2 lies in the “Sesto Basso – valle travata Cencio” irrigation district, which comprises the final reach of the canal downstream of the village of Sant’Antonio (Municipality of Medicina). The district covers 211 ha and irrigates on average 118 ha each year. Data from the Renana Remediation Consortium (2023–2024) indicate the following average irrigated areas: maize 65 ha, sugar beet 31 ha, and alfalfa 17 ha. The reach is supplied primarily from the “Corla” intake on the Canale Emiliano Romagnolo (CER), discharging into the Corla canal that becomes the Sesto Basso.

Along its course, upstream municipal wastewater treatment plants at Sant’Antonio (Medicina) and Selva Malvezzi (Molinella) discharge into the canal. At Site 2 the canal displays a summer irrigation depth of about 0.9 m and a bank-to-bank width of 9.6 m.

Irrigation data for 2020-2024 show that within 1 km upstream of the site an average of 47 ha are irrigated annually by four farms, mainly under maize (26 ha), sugar beet (11.5 ha) and alfalfa (7 ha).

Site location and morphology

The site is located at the end of the Sesto Basso canal, close to the upstream boundary of the Natura 2000 site IT4060001 - SAC-SPA “Valli di Argenta” (Figure A5). It occupies the flat tongue of land at the confluence where the Sant’Antonio canal enters the Sesto Basso, spanning both the right and left banks of the two canals. The area lies just outside the boundary of IT4050022. Access is along 700 m of the right bank of the Sesto Basso from the Via M. Cappelletti bridge,

heading south-east towards the Garda Alto embankment. Until 2021 the land was cultivated as arable by an adjacent farm.

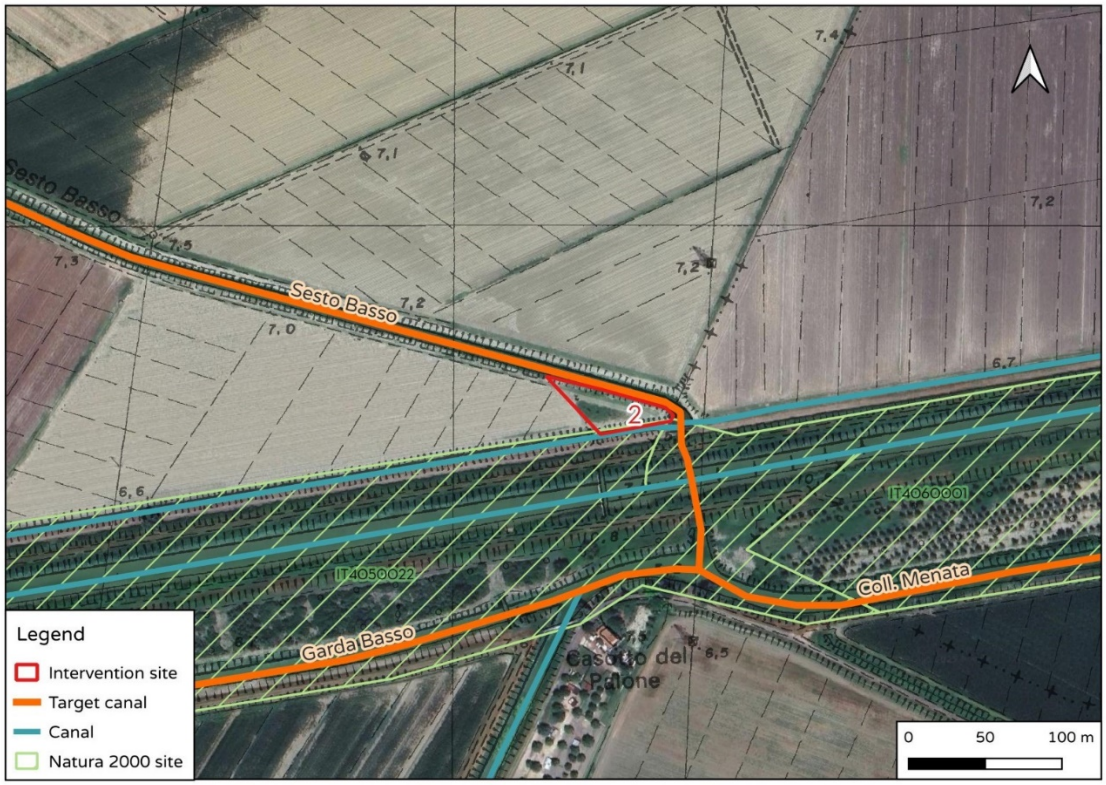

Figure A5 - Cartographic framing of S2.

Soil features before intervention

Soil at site S2 was classified as an Ustic Endoaquert (Soil Survey Staff, 2014) and a Haplic Vertisol (gleyic) according to the World Reference Base (IUSS, 2015).

This soil type presents limiting factors that surface water retention (> 50%), excess of expandable clays, and internal drainage impeded.

In Table A5 are reported the main features of pedogenetic horizons identified within three soil profiles dug at site S2.

Table A5 - Depth interval, pH, electrical conductivity (EC), contents of total carbonates (CaCO3 tot), sand, silt and clay of three soil profiles (2A, 2B, 2C) dug in site S2 before the intervention.

Profile	Horizon	Depth	pH H_2O	E.C.	$CaCO_3$ tot.	Texture		
						sand	silt	clay
		(cm)		dS cm^{-1}	g kg^{-1}	g kg^{-1}		
2A	Ap	0-20	8,0	0,29	119	40	366	595
	BC	20-60	8,0	0,32	123	16	338	647
	C1	60-80	8,2	0,32	123	29	309	661
	C2g	80-100+	8,2	0,35	149	21	369	610
2B	Ap1	0-6	7,8	0,44	122	11	390	599
	Ap2	6-20	8,0	0,34	123	41	361	598
	BCg	20-50	8,1	0,41	120	12	336	652
	C1g	50-80	8,1	0,46	122	30	304	666
	C2g	80-100+	8,2	0,42	127	19	370	611
2C	Ap1	0-6	7,8	0,44	121	34	378	588
	Ap2g	6-20	7,9	0,35	122	39	370	591
	BCg	20-50	8,0	0,34	119	19	339	642
	C1g	50-80	0,8	0,72	123	28	315	657
	C2g	80-100+	7,8	0,73	129	22	369	609

Type of intervention

Given the simple geomorphology and limited surface area (1,300 m²), earthworks concentrated on reducing bank slope to enlarge the riparian strip and shift the maintenance track further upslope (Figure A6). The gentle new gradient favors the development of hygrophilous and helophytic vegetation – spontaneous and nursery-grown – and discourages burrowing invasive alien species coypu - *Myocastor coypus.*

Spoil material was used to create a slight mound at the centre of the plot for tree planting.

A nucleus of woody vegetation typical of habitat 91F0 - “Mixed riparian forests” was established: 40 native woody plants over 400 m² (20 trees and 20 shrubs). Structural diversity was ensured by planting both 20 saplings (50–70 cm) and 20 larger specimens (Table A6).

Along the remodelled bank, a total of 93 pots of native aquatic-plant species (18 helophytic herbs) were installed (Table A7).

Table A6 - List of plants per tree and shrub species planted at S2.

Trees and shrubs planted at site 2		
Species	**Saplings (0.50-0.90 m)**	**Young plants (1-3 m)**
Trees	**10**	**10**
Alnus glutionsa	1	1
Fraxinus angustifolia	1	1
Fraxinus excelsior	1	1
Quercus robur	2	1
Populus alba	1	17
Populus nigra	1	1
Salix alba	1	2
Ulmus minor	2	3
Shrubs	**10**	**10**
Cornus sanguinea	2	2
Corylus avellana	1	1
Euonymus europaeus	1	2
Prunus padus	1	2
Rhamnus frangula	1	1
Rosa canina	1	1
Sambucus nigra	2	2
Viburnum lantana	5	1
Viburnum opulus	2	2
Viburnum opulus	1	3
Total	**20**	**20**

Table A7 - List of pots per herbaceous plant species planted at S2.

Herbaceous plants planted at site 2	
Species	**N. of pots**
Althaea officinalis	8
Butomus umbellatus	3
Carex riparia	8
Cyperus longus	1
Euphorbia palustris	1
Juncus maritimus	4
Limniris pseudacorus	8
Lycopus europaeus	8
Lysimachia vulgaris	8
Lythrum salicaria	1
Phragmites australis	1
Ranunculus sceleratus	1
Schoenoplectus lacustris	5
Schoenoplectus tabernaemontani	4
Scirpus maritimus	5
Sparganium erectum	3
Typha angustifolia	1
Typha latifolia	23
Total	**93**

Figure A6 - Bank modification intervention at S2.

Implementation schedule and costs

All modelling and planting works were carried out by the Renana Remediation Consortium and completed in February 2022.

Total expenditure, calculated in the Executive Project using the 2020 Emilia-Romagna Regional Price List, amounted to € 3,122.00 (Table A8).

Table A8 - Calculation of the cost of intervention at S2, based on the Emilia-Romagna Region price list (2020 edition) and the actual costs incurred for the purchase of trees and shrubs.

Intervention costs at site 2		
Cost item	**Quantity**	**Cost**
Mechanical mowing of heterogeneous spontaneous vegetation consisting mainly of reeds and bushes, carried out by mechanical means on canal floodplains and embankment surfaces, flat and sloping, including the cost of collecting and transporting the resulting material to waste.	1,750 m^2 x 0.16 €/m^2	€ 280.00
Excavator, shovel, or bulldozer, including operator, fuel, and lubricant, for setting up hydraulic appurtenances	12 hours x 69.10 €/h	€ 829.00
Excavation for the reshaping of canal bed section, performed by mechanical means, in the presence of water, including all charges and displacement and frontal placement of the resulting material	434 m^3 x 3.30 €/m^3	€ 1,432.20
Planting of tree/arbustive plants	26 hours x 13.20 €/h	€ 343.20
Planting herbaceous plants	18 hours x 13.20 €/h	€ 237.60
Purchase and supply of trees and shrubs	10 trees, 10 shrubs	€ 561.00
Free supply of trees and shrubs saplings	10 trees and 10 shrubs	
Herbaceous plants from the nursery	72 plants	
Total		**€ 3,683.00**

Hydraulic sector between right bank of the Reno river and left bank of the Idice river, Municipality of Molinella.

Site S4

Total area: 3,000 m²

Coordinates: 44°37'16"N 11°45'29"E

Elevation: 5-7 m asl

Location: Embankment between the left bank of the Lorgana canal and the right embankment of the Botte canal (Municipality of Molinella) (Figure A7).

Figure A7 – S4 after intervention.

Canal

The Lorgana canal is the terminal collector of the lowland drainage network between the Reno and the Idice rivers. It originates downstream of Malalbergo at the confluence of the Lorgana Inferiore canal and the Tombe canal. With its

incised bed it conveys storm-water runoff, receives flows from minor drains and, along most of its 28.6 km course, supplies irrigation water. At the Saiarino pumping station (Municipality of Argenta), discharge and water level are regulated to meet drainage or irrigation needs. Because of multiple tributary inputs, the canal is never completely dry; its minimum winter depth is about 0.9 m.

Along its entire course the Lorgana crosses four Natura 2000 sites. It first runs inside, then along the boundary of I IT4050024 - SCI-SPA “Biotopes and environmental restorations of Bentivoglio, San Pietro in Casale, Malalbergo and Baricella”; then briefly enters IT4060017 - SPA “Po di Primaro e Bacini di Traghetto”. The final reach flows for 2.3 km within IT4050022 “Biotopes and environmental restorations of Medicina and Molinella” and, for a further 2.2 km downstream to Saiarino, inside IT4060001 - SCI-SPA “Valli di Argenta”, which also lies in the Po Delta Regional Park.

Irrigation district

S4 lies in the terminal segment of the irrigation district “Canale Lorgana da Fiumicello di Dugliolo”, covering 523 ha, of which on average 250 ha are irrigated yearly. According to data provided by the Renana Remediation Consortium for the 2023–2024 irrigation seasons, average irrigated surfaces for the main crops are: maize 166 ha, soybean 35 ha, mixed orchards 23 ha and sugar beet 12 ha.

Irrigation water is mainly supplied from the Fiumicello di Dugliolo intake on the Canale Emiliano Romagnolo (CER); after 18 km it joins the Allacciante IV Circondario canal, which enters the Botte canal near San Pietro Capofiume. A pumping station lifts water into a network that ultimately discharges to the Lorgana.

Upstream of the S4, the canal also receives effluents from the wastewater treatment plants of Altedo, Malalbergo and San Pietro Capofiume, as well as water from the Navile Canal (via the Diversivo Navile–Savena Abbandonato).

At S4 the Lorgana has a summer irrigation depth of ≈ 1.3 m and a bed width of 36 m.

Based on irrigation records from 2020-2024, an area of about 130 ha located within 1 km upstream of the site is irrigated each year by a single farm, predominantly cultivating maize (70 ha), soybean (38 ha) and potato (13 ha).

Site location and morphology

S4 is situated within the Municipality of Molinella (Bologna) (Figure A8), 400 m upstream of the point where the Lorgana canal enters the Natura 2000 site IT4050022 “Biotopes and environmental restorations of Medicina and Molinella”. It is reached by proceeding 300 m westwards along the left bank of the Lorgana canal from the parking area near the Via Zanolini bridge.

From the S5 km upstream lies the protected area IT4060017 - SPA “Po di Primaro e Bacini di Traghetto”, whereas 2.7 km downstream begins IT4060001 - SCI-SPA “Valli di Argenta.” Close to the site, on the opposite bank of the adjacent Botte canal, stands the Cornacchia water detention basin, which comprises various wetlands and woodlands owned by the Renana Remediation Consortium.

The intervention area corresponds to a 120 m long, 25 m wide embankment between the left bank of the Lorgana canal and the right embankment of the Botte canal. The two canals run parallel for most of their courses resulting in a continuous belt chiefly composed of shrubs, mature trees and patches of reedbed.

Figure A8 - Cartographic framing of S4.

Soil features before intervention

Soil at site S4 was classified as an Udertic Haplustept (Soil Survey Staff, 2014) and a Vertic Eutric Cambisol (clayic) according to the World Reference Base (IUSS, 2015).

This soil has imperfect internal drainage as its main limiting factor.

In Table A9 are reported the main features of pedogenetic horizons identified within three soil profiles dug at site S4.

Table A9 - Depth interval, pH, electrical conductivity (EC), contents of total carbonates (CaCO3 tot), sand, silt and clay of three soil profiles (4A, 4B, 4C) dug in site S4 before the intervention.

Profile	Horizon	Depth	pH H_2O	E.C.	$CaCO_3$ tot.	Texture		
						sand	silt	clay
		(cm)		dS cm^{-1}	g kg^{-1}	g kg^{-1}		
4A	Oi	2-0	nd	nd	nd	nd	nd	nd
	A1	0-7	7,8	0,35	133	93	511	396
	A2	7-34	7,9	0,29	135	42	500	458
	AB	34-65	8,0	0,29	154	37	488	475
	Bw	65-83	7,9	0,29	156	33	491	476
	C	83-100+	8,0	0,27	157	21	531	448
4B	A	0-18	7,7	0,37	135	80	508	412
	AB	18-50	8,0	0,31	152	38	497	465
	Bw	50-80	8,0	0,30	156	35	479	486
	BC	80-100+	8,0	0,27	158	15	549	436
4C	A	0-20	7,8	0,32	134	87	509	404
	AB	20-35	7,9	0,29	150	49	499	452
	Bw	35-75	8,0	0,27	155	36	484	480
	BC	75-100+	8,1	0,27	157	18	540	442

Type of Intervention

The site is elongated, ribbon-like morphology required only minimal earthworks to establish the stepping stone habitat. The canal bank was lightly re-profiled, imparting a gentler slope that encourages the expansion of hygrophilous and helophytic vegetation - both spontaneous and nursery-raised - while reducing suitability for burrowing by invasive alien species coypu - *Myocastor coypus*.

The core intervention consisted of excavating a shallow, hydraulically connected pond covering 220 m² with a maximum depth of 1.3 m (Figure A9). This basin maintains the same hydraulic head as the Lorgana canal; should canal levels fall, a clapet (flap) valve preserves an optimal water level in the depression until normal head is restored.

Along the canal margin, the pond's edges were planted with herbaceous species characteristic of local watercourses, sourced from the nursery.

Spoil from the excavation was redistributed to give the peripheral area a uniform slope, linking the site's lowest point - the pathway along the canal bank - to its

highest - the walkway at the foot of the Botte canal embankment. In total 116 potted specimens of native aquatic plants, representing 16 helophytic herbaceous species, were installed (Table A11).

Woody vegetation characteristic of EU habitat 91F0 - “Mixed riparian forests” was planted around the pond. A total of 56 native woody plants now occupy 1,000 m², integrating with the pre-existing stand: 30 tree species and 26 shrub species. To enhance structural diversity, individuals of varying size were used - 11 saplings (50–70 cm) and 45 more mature specimens - thereby establishing an uneven-aged plantation composed of the principal woody species typical of habitat 91F0 (Table A10).

Table A10 - List of plants per tree and shrub species planted at S4.

Trees and shrubs planted at site 4		
Species	**Saplings (0.50-0.90 m)**	**Young plants (1-3 m)**
Trees	**7**	**23**
Alnus glutionsa	1	1
Fraxinus angustifolia	1	2
Fraxinus excelsior	1	3
Quercus robur	2	3
Populus alba		1
Populus nigra		1
Salix alba	1	5
Ulmus minor	1	7
Shrubs	**4**	**22**
Cornus sanguinea	1	4
Corylus avellana		1
Euonymus europaeus		1
Prunus padus		1
Prunus spinosa		1
Rhamnus frangula	1	2
Rosa canina		1
Sambucus nigra	1	5
Viburnum lantana		1
Viburnum opulus	1	5
Total	**11**	**45**

Table A11 - List of pots per herbaceous plant species planted at S4.

Herbaceous plants planted at site 4	
Species	**N. of pots**
Alisma plantago-aquatica	*2*
Althaea officinalis	*14*
Butomus umbellatus	*3*
Carex riparia	*9*
Cyperus longus	*1*
Euphatorium cannabinum	*1*
Juncus maritimus	*3*
Limniris pseudacorus	*7*
Lycopus europaeus	*15*
Lysimachia vulgaris	*8*
Lythrum salicaria	*1*
Phragmites australis	*3*
Schoenoplectus tabernaemontani	*9*
Sparganium erectum	*3*
Typha angustifolia	*1*
Typha latifolia	*36*
Total	**116**

Figure A9 – Ponde created at S4.

Implementation schedule and costs

Excavation was contracted to an earthmoving firm; profiling and planting were carried out by Renana Remediation Consortium and finished in March 2022.

Total expenditure, calculated in the Executive Project using the 2020 Emilia-Romagna Regional Price List, amounted to € 12,558.56 (Table A12).

Table A12 - Calculation of the cost of intervention at S4, based on the Emilia-Romagna Region price list (2020 edition) and the actual costs incurred for the purchase of trees and shrubs.

Intervention costs at site 4		
Cost item	**Quantity**	**Cost**
Mechanical mowing of heterogeneous spontaneous vegetation consisting mainly of reeds and bushes, carried out by mechanical means on canal floodplains and embankment surfaces, flat and sloping, including the cost of collecting and transporting the resulting material to waste.	2,880 m^2 x 0.16 €/m^2	€ 460.80
Overburden excavation for creation of wetland and banks	942.2 m^3 x 3.70 €/m^3	€ 3,486.14
Compulsory section excavation up to a maximum depth of 4 m from the ground level for laying pipeline even in the presence of water, performed by machine, including backfilling of artifacts, placement of excess material in the area adjacent to the construction site	26.40 m^3 x 7.70 €/m^3	€ 203.28
Rigid pvc pipes diameter of 250 mm, thickness 7.3 mm, supplied and laid, in accordance with UNI EN 1401, including and compensated in the price every charge for the laying excluding the formation of the laying bed and backfill in suitable material	11 m x 32.87 €/m	€ 361.57
PVC end-of-line clapet backflow preventer valve, 250 mm diameter, supplied and installed with coupling on pipe complete with all accessories	1 x 299 € each	€ 299.00
Excavator, shovel, or bulldozer, including operator, fuel, and lubricant, for setting up hydraulic appurtenances	6 hours x 69.10 €/h	€ 414.60
Excavation for the reshaping of canal bed section, performed by mechanical means, in the presence of water, including all charges and displacement and frontal placement of the resulting material	203 m^3 x 5.60 €/m^3 + 268.24 m^3 x 3.30 €/m^3	€ 2,021.99
Embankment formation for embankment construction and landslide recovery, using spoil from excavation in the riverbed	739 m^3 x 1.60 €/m^3	€ 1,182.40
Quarried limestone supplied and placed for formation of bank defenses	13.65 t x 3.50 €/t	€ 443.63
Planting of tree/arbustive plants	30 hours x 13.20 €/h	€ 396.00
Planting herbaceous plants	12 hours x 13.20 €/h	€ 158.40
Purchase and supply of trees and shrubs	23 trees, 22 shrubs	€ 1,287.00
Free supply of trees and shrubs saplings	7 trees and 4 shrubs	
Herbaceous plants from the nursery	116 plants	
Total		**€ 12,558.56**

Site S5

Total area: 7,000 m²

Coordinates: 44°37'56"N 11°37'49"E

Elevation: 5-7 m asl

Location: Left embankment and riparian strip of the Allacciante IV Circondario canal (Municipality of Molinella) (Figure A10).

Figure A10 – S5 after intervention.

Canal

The Allacciante IV Circondario canal is a multi-purpose watercourse which, not only supplies irrigation water during the summer but also acts as an “allacciante” - that is, a receiving canal for small and medium-sized drains that collect runoff from the hydraulic sector lying between the Navile canal and the Idice river.

The canal originates near the A13 Bologna–Padua motorway in the municipality of Bentivoglio (Bologna), where it receives the flows of the Fossa Quadra

Superiore canal. For the next 3 km it runs on the hydraulic right of the Diversivo Navile - Savena Abbandonato canal, serving as a guard ditch for this embanked regional watercourse. Over the first 7 km its bed is incised-lacking levees and lying below ground level. Approximately 1.5 km downstream of the town center of Minerbio the canal becomes embanked, with levee height increasing toward the outfall, though the bed remains beneath the surrounding land surface. Despite these embankments, needed to contain stormwater discharges, the canal continues to receive a steady inflow from the dense network of minor drains that traverse the area.

After a total course of 20 km the canal reaches the Botte canal at San Pietro Capofiume (Bologna), conveying the waters of the central Bologna plain into the main upper-water collector of the drainage district.

Along its entire length the Allacciante IV Circondario canal intersects the Natura 2000 site IT4050023 - SCI-SPA “Biotopes and environmental restorations of Budrio and Minerbio”, forming its northern boundary for 2.7 km. Just 500 m downstream of the confluence, the Botte canal itself enters the Natura 2000 site IT4060017 - SPA “Po di Primaro e Bacini di Traghetto”.

Along the Allacciante IV Circondario canal three intervention sites have been identified - S5, S6 and S7 - located, respectively, 2.2 km, 4.4 km and 7.2 km upstream of the canal’s terminus.

Irrigation district

S5 lies within the downstream reach of the irrigation district named “Allacciante IV Circondario da Fiumicello di Dugliolo.” The district extends over 954 ha, of which an average of 293 ha per year is irrigated. Renana Remediation Consortium data for the 2023–2024 seasons indicate mean irrigated areas for the principal crops as follows: 59 ha sugar beet, 47 ha maize, 35 ha green beans, 30 ha pea, 25 ha soybean, 18 ha mixed orchard, 18 ha tomato, and 17 ha alfalfa.

Irrigation water is supplied mainly by the Fiumicello di Dugliolo intake on the Canale Emiliano Romagnolo (CER) which discharges into the canal of the same name. After a course of 18 km the Fiumicello di Dugliolo canal flows into the Allacciante IV Circondario.

Along its course - and that of its tributaries - the Allacciante IV Circondario canal at the level of S5 receives effluents from the municipal wastewater treatment plants serving the towns of Minerbio, Dugliolo and Mezzolara. At S5 the canal exhibits a summer irrigation depth of approximately 3.5 m and a bed width of 30.7 m.

Irrigation records for 2020–2024 were analysed for lands within 1 km upstream of S5. On average 31 ha per year are irrigated by four farms, principally cultivating maize (14 ha), sugar beet (8 ha) and green beans (4 ha).

Figure A11 - Cartographic framing of S5.

Site location and morphology

S5 lies 150 m downstream of the Via Idice Abbandonato bridge in the Municipality of Molinella (Bologna) (Figure A11). It occupies a position almost equidistant between two Natura 2000 sites, within a predominantly agricultural landscape that lacks natural or semi-natural areas: it is 2.5 km from Natura 2000 site IT4050023 - SCI-SPA “Biotopes and environmental restorations of Budrio and

Minerbio” and 3 km from Natura 2000 site IT4060017 - SPA “Po di Primaro e Bacini di Traghetto”.

The site can be reached by proceeding 1,000 m along the unpaved Via Vescovo on the right bank of the canal to the farm bridge that provides access.

The intervention area corresponds to the left embankment of the canal downstream of the Via Idice Abbandonato bridge, extending for 300 m. In addition, it includes the adjoining plot situated between the canal and the small Bonello di San Pietro drain, of equal linear extent and an average width of 20 m. Apart from the canal embankment, the land owned by the Renana Remediation Consortium was usede as arable fields by the neighbouring farmer until mid-2022.

Soil features before intervention

Soil at site S4 was classified as a Udifluventic Haplustept (Soil Survey Staff, 2014) and a Fluvic Cambisol (loamy) according to the World Reference Base (IUSS, 2015).

In Table A13 are reported the main features of pedogenetic horizons identified within three soil profiles dug at site S1.

Table A13 - Depth interval, pH, electrical conductivity (EC), contents of total carbonates (CaCO3 tot), sand, silt and clay of three soil profiles (5A, 5B, 5C) dug in site S5 before the intervention.

Profile	Horizon	Depth	pH H_2O	E.C.	$CaCO_3$ tot.	Texture		
						sand	silt	clay
		(cm)		dS cm^{-1}	g kg^{-1}	g kg^{-1}		
5A	Ap	0-23	8,0	0,29	172	366	419	216
	AB	23-52	8,0	0,27	172	361	424	215
	B	52-77	8,0	0,22	182	359	416	225
	C	77-100+	8,1	0,22	177	350	440	210
5B	Ap1	0-11	7,9	0,23	173	363	420	217
	Ap2	11-55	7,9	0,22	175	359	421	219
	Bw	55-80	7,9	0,20	178	369	410	220
	BC	80-100+	8,0	0,18	175	346	443	211
5C	Ap1	0-12	7,8	0,27	174	364	418	218
	Ap2	12-46	7,9	0,24	172	361	423	216
	Bw	46-78	8,0	0,22	172	364	413	223
	BC	78-100+	8,0	0,23	174	348	441	211

Type of intervention

The site's linear form permitted only a single major modification: the relocation of the left embankment to create the stepping stone habitat. Specifically, the crown of the embankment was set back 12 m toward the cultivated fields, thereby widening the canal and gentling the bank slope to foster the development of hygrophilous and helophytic plants - both spontaneous and nursery-raised - and to make the zone less suitable for burrowing by invasive alien species coypu - *Myocastor coypus*.

The embankment relocation was a work of considerable importance, as this structure ensures the hydraulic safety of a large sector of the surrounding territory.

Upon completion of the earthworks, 162 woody plants were installed within 1,000 m² of contiguous land adjoining the embankment, arranged in two nuclei at the beginning and end of the linear tract. All belong to native species characteristic of habitat 92A0 - "Riparian galleries forest of *Populus alba* and *Salix alba*". Of these, 81 are tree species and 81 shrub species. To increase structural diversity, individuals of the same species were planted in different size classes, namely 82 forest saplings (50–70 cm) and 80 more mature specimens, thus establishing an

uneven-aged stand composed of the principal woody species of habitat 92A0 (Table A14).

Subsequently, 789 pots of native aquatic plants—representing 21 helophytic herbaceous species produced in the Action C.1 nursery—were inserted along the bank (Table A15) (Figure A12).

Table A14 - List of plants per tree and shrub species planted at S5.

Trees and shrubs planted at site 5		
Species	**Saplings (0.50-0.90 m)**	**Young plants (1-3 m)**
Trees	**41**	**40**
Fraxinus angustifolia	2	1
Fraxinus excelsior	2	1
Populus alba	12	9
Populus nigra	8	6
Salix alba	17	23
Shrubs	**41**	**40**
Cornus sanguinea	4	4
Corylus avellana	2	2
Euonymus europaeus	2	2
Prunus padus	2	2
Prunus spinosa	2	2
Rhamnus frangula	4	4
Rosa canina	2	2
Sambucus nigra	17	16
Viburnum lantana	2	2
Viburnum opulus	4	4
Total	**82**	**80**

Table A15 - List of pots per herbaceous plant species planted at S5.

Herbaceous plants planted at site 5	
Species	**N. of pots**
Alisma plantago-aquatica	19
Butomus umbellatus	16
Carex pendula	9
Carex riparia	2
Cyperus longus	23
Eleocharis sp.	14
Juncus articulatus	25
Juncus sp.	70
Limniris pseudacorus	39
Lycopus europaeus	26
Lythrum salicaria	23
Mentha aquatica	10
Oenanthe fistulosa	4
Phragmites australis	21
Samolus valerandi	1
Schoenoplectus lacustris	43
Scirpoides holoschoenus	7
Sparganium erectum	12
Typha angustifolia	89
Typha latifolia	38
Typha sp.	16
Total	**507**

Figure A12 - Planting wetland plants at S5.

Implementation schedule and costs

The earthmoving and construction of the new embankment were entrusted to a firm specialising in earthworks, whereas the profiling and planting operations were carried out entirely by the Renana Remediation Consortium and completed in March 2023.

The total cost foreseen in the Executive Project for the creation of S5, calculated according to the Emilia-Romagna regional price list (2020), amounts to € 27,793.68 (Table A16).

Table A16 - Calculation of the cost of intervention at S5, based on the Emilia-Romagna Region price list (2020 edition) and the actual costs incurred for the purchase of trees and shrubs.

Intervention costs at site 5		
Cost item	**Quantity**	**Cost**
Mechanical mowing of heterogeneous spontaneous vegetation consisting mainly of reeds and bushes, carried out by mechanical means on canal floodplains and embankment surfaces, flat and sloping, including the cost of collecting and transporting the resulting material to waste.	2,800 m^2 x 0.16 €/m^2	€ 448.00
Overburden excavation for creation of wetland and banks	546 m^3 x 3.70 €/m^3	€ 2,020.20
Excavator, shovel, or bulldozer, including operator, fuel, and lubricant, for setting up hydraulic appurtenances	30 hours x 69.10 €/h	€ 2,072.40
Excavation for the reshaping of canal bed section, performed by mechanical means, in the presence of water, including all charges and displacement and frontal placement of the resulting material	2,996 m^3 x 2 €/m^3	€ 5,992.00
Chestnut wood poles, 18-25 cm in diameter, fitted with spikes and up to 5 m long, driven into the ground, supplied and erected	560 m x 5.80 €/m	€ 3,248.00
Supply and installation of two-leaf steel driveway gate, span equal to 4.00 m, height 2.20 m, complete with deadbolt closure with padlock holder. Including excavation, formwork, electrowelded mesh, rolled concrete steel	3,360 m^3 x 2.70 €/m^3	€ 9,072.00
Worksite safety activities and facilities		€ 1,830.68
Planting of tree/arbustive plants	35 hours x 13.20 €/h	€ 462.00
Planting herbaceous plants	37 hours x 13.20 €/h	€ 488.40
Purchase and supply of trees and shrubs	40 trees, 40 shrubs	€ 2,160.00
Free supply of trees and shrubs saplings	41 trees and 41 shrubs	
Herbaceous plants from the nursery	789 plants	
Total		**€ 27,793.68**

Site S6

Total area: 3.500 m²

Coordinates: 44°37'50"N 11°36'29"E

Elevation: 7-10 m asl

Location: Right bank and riparian strip of the Allacciante IV Circondario canal (Municipality of Molinella) (Figure A13).

Figure A13 – S6 after intervention.

Canal and Irrigation district

Like S5, S6 is located along the Allacciante IV Circondario canal. Because of this position, S6 belongs to the same irrigation district as S5. At the level of Site 6 the canal has a summer irrigation depth of approximately 3 m and a bed width of 16 m.

Irrigation records for 2020 – 2024 were examined for lands within 1 km upstream of S6. On average 56 ha yr^{-1} are irrigated by seven farms, chiefly cultivating

mixed orchard (23 ha), alfalfa (13 ha), maize (6 ha), soybean (5 ha), potato (5 ha) and sugar-beet seed (3 ha).

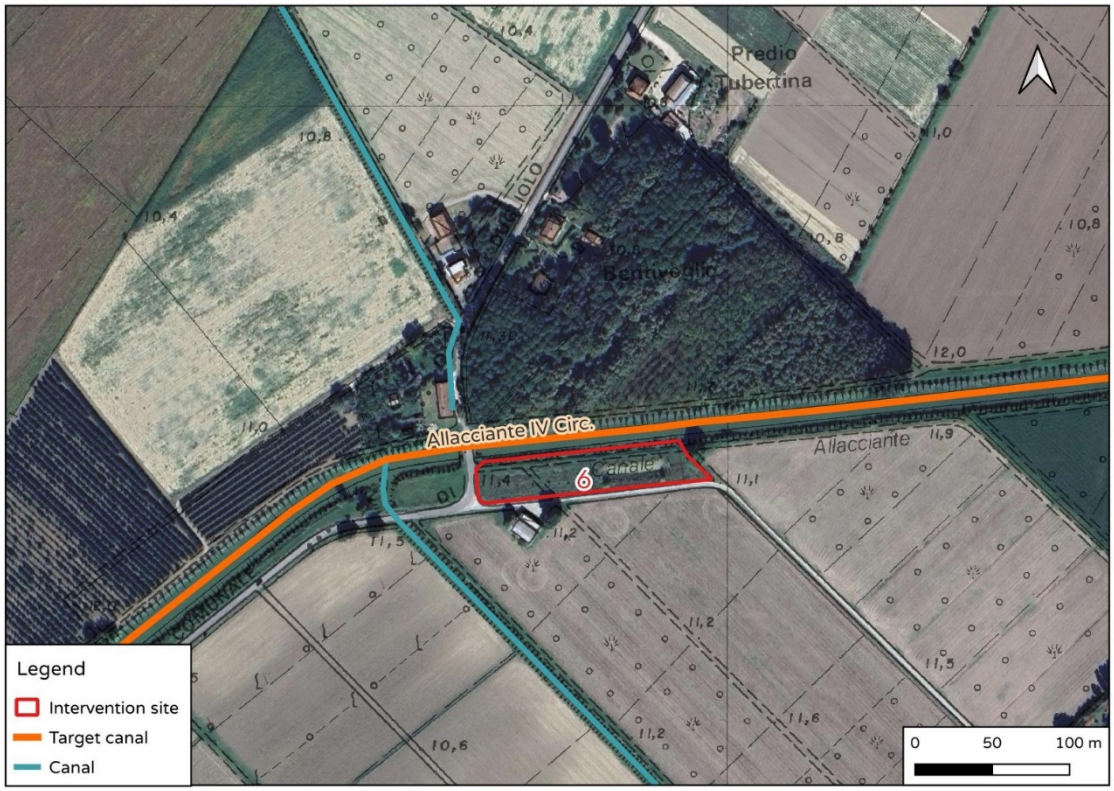

Figure A14 - Cartographic framing of S6.

Site location and morphology

S6 corresponds to the right bank of the Allacciante IV Circondario canal immediately downstream of the Via Dugliolo bridge in the Municipality of Molinella (Bologna) (Figure A14). It occupies an intermediate position between the other intervention sites on the canal, lying 1.7 km from S5 and 2.8 km from S7. Situated in an entirely agricultural landscape, it is 1.3 km from Natura 2000 site IT4050023 - SCI-SPA “Biotopes and environmental restorations of Budrio and Minerbio”.

The intervention area extends for 130 m along the canal’s right bank. It also includes the adjoining plot bounded by the canal, Via Dugliolo and the unpaved Via Baraccano. This parcel, owned by the Renana Remediation Consortium, covers 3,500 m² and was cultivated by the neighbouring farmer until mid-2022.

On the opposite bank a privately own ed area has been afforested with native tree species.

The short reach targeted for intervention is unembanked, owing to the relatively high elevation of the surrounding terrain.

Soil features before intervention

Soil at site S6 was classified as a Oxyaquic Ustifluvent (Soil Survey Staff, 2014) and a Eutric Fluvisol (siltic, oxyaquic) according to the World Reference Base (IUSS, 2015).

This soil type has an organic carbon content of <1% along the entire profile as the main limiting factor.

In Table A17 are reported the main features of pedogenetic horizons identified within three soil profiles dug at site S6.

Table A17 - Depth interval, pH, electrical conductivity (EC), contents of total carbonates (CaCO3 tot), sand, silt and clay of three soil profiles (6A, 6B, 6C) dug in site S6 before the intervention.

Profile	Horizon		pH	E.C.	$CaCO_3$ tot.	Texture		
		Depth	H_2O			sand	silt	clay
		(cm)		dS cm^{-1}	g kg^{-1}	g kg^{-1}		
6A	Ap	0-20	7,9	0,22	163	238	538	224
	C1	20-50	8,0	0,19	169	246	536	218
	C2	50-90	8,0	0,20	171	291	499	210
	C3	90-100	8,1	0,21	175	372	469	159
6B	Ap	0-20	7,9	0,21	164	235	534	231
	C1	20-50	8,1	0,22	171	242	534	224
	C2	50-80	8,1	0,27	171	297	500	203
	C3	80-100	8,0	0,29	175	377	465	158
6C	Ap	0-25	8,1	0,21	158	241	541	218
	C1	25-50	8,0	0,22	169	250	538	212
	C2	50-90	7,9	0,24	167	284	498	218
	C2	90-100	7,9	0,23	171	367	473	160

Type of intervention

The site's morphology allowed several modifications, making it a particularly representative example of the project's aims of bank re-profiling and aquatic-

habitat diversification along an artificial canal. The right bank was reshaped to achieve a gentler slope, thereby fostering the expansion of hygrophilous and helophytic vegetation - both spontaneous and nursery-raised - and reducing suitability for burrowing by invasive alien species coypu - *Myocastor coypus*.

Within the former arable land a hydraulically connected pond of 270 m² was excavated (Figure A15). This basin, with a maximum depth of 1 m, maintains the same hydraulic head as the canal; should canal levels fall, a clapet (flap) valve retains an optimal volume of water in the depression for a limited period until irrigation levels are restored.

Soil from the bank re-profiling and pond excavation was spread uniformly over the remaining site area.

Regarding the woody component, a nucleus of forest species of the habitat 91F0 - “Mixed riparian forests” was established at the centre of the plot and around the basin. In total 164 native woody plants now occupy 1,700 m²: 82 trees and 82 shrubs. To diversify structure, individuals of the same species were planted in two size classes - 75 forest saplings (50–70 cm) and 89 more mature specimens - creating an uneven-aged stand of the principal habitat 91F0 species (Table A18).

Along the canal and pond margins, herbaceous species typical of local watercourse banks were installed, sourced from the Action C.1 nursery. Altogether 241 pots representing 19 native helophytic species were planted (Table A19).

Table A18 - List of plants per tree and shrub species planted at S6.

Trees and shrubs planted at site 6		
Species	**Saplings (0.50-0.90 m)**	**Young plants (1-3 m)**
Trees	**39**	**43**
Acer campestre	1	1
Alnus glutionsa	1	2
Carpinus betulus	1	1
Fraxinus angustifolia	6	4
Fraxinus excelsior	6	5
Fraxinus ornus	1	1
Quercus robur	8	4
Populus alba	3	3
Populus nigra	3	3
Salix alba	4	9
Ulmus minor	5	10
Shrubs	**36**	**46**
Cornus sanguinea	6	8
Corylus avellana	2	3
Euonymus europaeus	2	3
Prunus padus	2	3
Prunus spinosa	2	3
Rhamnus frangula	6	4
Rosa canina	2	3
Sambucus nigra	6	8
Viburnum lantana	2	3
Viburnum opulus	6	8
Total	**75**	**89**

Table A19 - List of pots per herbaceous plant species planted at S6.

Herbaceous plants planted at site 6	
Species	**N. of pots**
Alisma plantago-aquatica	10
Butomus umbellatus	7
Carex pendula	7
Cyperus longus	12
Eleocharis sp.	7
Juncus articulatus	4
Juncus maritimus	10
Juncus sp.	24
Limniris pseudacorus	18
Lythrum salicaria	12
Mentha aquatica	5
Oenanthe fistulosa	2
Phragmites australis	16
Schoenoplectus lacustris	15
Scirpoides holoschoenus	5
Scirpus maritimus	17
Sparganium erectum	7
Typha angustifolia	44
Typha sp.	19
Total	**241**

Figure A15 – Pond created at S6.

Implementation schedule and costs

Excavation of the pond and redistribution of spoil were entrusted to an earthmoving firm, while profiling and planting were carried out entirely by the Renana Remediation Consortium and completed in March 2023.

The total cost foreseen in the Executive Project for S6, based on the 2020 Emilia-Romagna regional price list, is € 31,081.18 (Table A20).

Table A20 - Calculation of the cost of intervention at S6, based on the Emilia-Romagna Region price list (2020 edition) and the actual costs incurred for the purchase of trees and shrubs.

Intervention costs at site 6		
Cost item	**Quantity**	**Cost**
Mechanical mowing of heterogeneous spontaneous vegetation consisting mainly of reeds and bushes, carried out by mechanical means on canal floodplains and embankment surfaces, flat and sloping, including the cost of collecting and transporting the resulting material to waste.	3,000 m^2 x 0.16 €/m^2	€ 480.00
Overburden excavation for creation of wetland and banks	1,035.92 m^3 x 3.70 €/m^3	€ 3,832.90
Compulsory section excavation up to a maximum depth of 4 m from the ground level for laying pipeline even in the presence of water, performed by machine, including backfilling of artifacts, placement of excess material in the area adjacent to the construction site	102 m^3 x 7.70 €/m^3	€ 785.40
Rigid pvc pipes diameter of 250 mm, thickness 7.3 mm, supplied and laid, in accordance with UNI EN 1401, including and compensated in the price every charge for the laying excluding the formation of the laying bed and backfill in suitable material	13.60 m x 32.87 €/m	€ 447.03
PVC end-of-line clapet backflow preventer valve, 250 mm diameter, supplied and installed with coupling on pipe complete with all accessories	1 x 299 € each	€ 299.00
Excavator, shovel, or bulldozer, including operator, fuel, and lubricant, for setting up hydraulic appurtenances	48 hours x 69.10 €/h	€ 3,316.80
Excavation for the reshaping of canal bed section, performed by mechanical means, in the presence of water, including all charges and displacement and frontal placement of the resulting material	805.06 m^3 x 5.60 €/m^3 + 422.52 m^3 x 3.30 €/m^3	€ 5,902.66
Transport of material from earthmoving work carried out by trucks, including spreading and leveling of material for transport up to 10 km	3,900 m^3/km x 0.72 €/m^3/km	€ 2,808.00
Embankment formation for embankment construction and landslide recovery, using spoil from excavation in the riverbed	739 m^3 x 1.60 €/m^3	€ 1,182.40
Quarried limestone supplied and placed for formation of bank defenses	18.54 t x 32.50 €/t	€ 602.55
Supply and installation directly in the ground of fencing consisting of galvanized iron wire mesh, wire 2.2 mm, mesh 50x50 mm, in accordance with UNI 8018/79, height 2.00 m, installed on galvanized T-shaped iron posts, height 3.00 m. Including anchoring elements	130 m x 33 €/m	€ 4,290.00
Supply and installation of two-leaf steel driveway gate, span equal to 4.00 m, height 2.20 m, complete with deadbolt closure with padlock holder. Including excavation, formwork, electrowelded mesh, rolled concrete steel	1 x 2,610.00 €	€ 2,610.00
Formation of embankment with excavated soil for thin bank body reroutes and elevations, including excavation and all other charges	95 m^3 x 5.60 €/m^3	€ 532.00
Worksite safety activities and facilities		€ 915.34
Planting of tree/arbustive plants	38 hours x 13.20 €/h	€ 501.60
Planting herbaceous plants	12 hours x 13.20 €/h	€ 158.40
Purchase and supply of trees and shrubs	43 trees, 46 shrubs	€ 2,417.10
Free supply of trees and shrubs saplings	39 trees and 36 shrubs	
Herbaceous plants from the nursery	241 plants	
Total		**€ 31,081.18**

Hydraulic sector between right bank of the Reno river and left bank of the Idice river, Municipality of Budrio.

Site S7

Total area: 900 m²

Coordinates: 44°37'16"N 11°45'29"E

Elevation: 7-8 m asl

Location: Point of discharge of the Gallina Superiore canal into the Allacciante IV Circondario canal (Municipality of Budrio) (Figure A16).

Figure A16 – S7 after intervention.

Canal and Irrigation District

Like S5, S7 is located along the Allacciante IV Circondario canal. The Gallina Superiore canal is a multi-purpose canal whose primary role is storm-water collection. It originates at the foot of the left floodbank of the Idice river,

south-east of the village of Mezzolara in the Municipality of Budrio, where it receives the water of the Pianella Alto canal. After a total course of 7 km the Gallina Superiore canal discharges into the Allacciante IV Circondario canal at the level of S7. The first 4.7 km of the canal have an incised bed lying below ground level, whereas the subsequent 1.7 km are embanked to protect the surrounding farmland. 4 km from the head of the canal lies S8, situated at its confluence with the Cornamonda Nuova canal - an incised canal whose main function is also storm-water collection.

Because S7 lies along the Allacciante IV Circondario canal, it falls within the same irrigation district as S5. At S7 the canal has a summer irrigation depth of approximately 2.5 m and a bank-to-bank bed width of 19 m.

Irrigation data for 2020 – 2024 were analysed for land within 1 km upstream of S7. On average 6.5 ha per year are irrigated by seven farms, chiefly producing nursery stock (1.6 ha), biomass sorghum (1.5 ha) and sugar beet (1.5 ha).

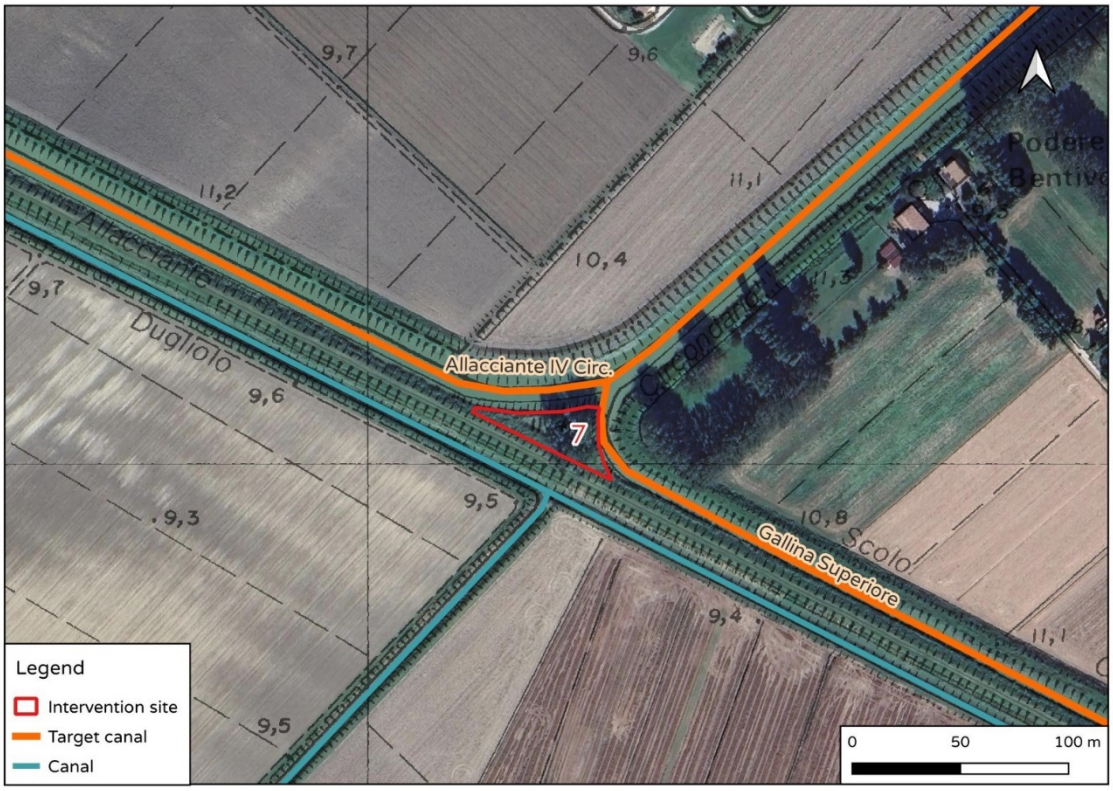

Figure A17 - Cartographic framing of S7.

Site location and morphology

S7 is situated at the point where the Gallina Superiore canal discharges into the Allacciante IV Circondario canal, 600 m upstream of the Via Dugliolo bridge at the outskirts of the hamlet of the same name, in the Municipality of Budrio (Bologna) (Figure A17). It lies halfway between S6 and S8: 2.8 km upstream of S6 along the Allacciante IV Circondario canal and 2.5 km downstream of S8 along the Gallina Superiore canal.

At a distance of 1 km west of the intervention area is Natura 2000 site IT4050023 - SCI-SPA “Biotopes and environmental restorations of Budrio and Minerbio”.

The intervention area corresponds to the sub-levee strip located at the confluence where the Gallina Superiore canal enters the Allacciante IV Circondario canal, affecting the left bank of the former and the right bank of the latter. This small parcel, owned by the Renana Remediation Consortium, has a total surface of 900 m², most of which is covered by dense spontaneous woody vegetation.

The area lies below the crest of the surrounding embankments; being enclosed within the levees, it is subject to prolonged inundation during periods of heavy rainfall, thereby fostering ecological dynamics typical of lowland floodplain forests. The luxuriant stand of mature *Populus alba* and *Salix alba* attests to the optimal spontaneous development of habitat 92A0 - “Riparian galleries forest of *Populus alba* and *Salix alba*”.

For these unique characteristics the site is regarded as an existing example of the desired outcome foreseen for the other intervention sites.

Soil features before intervention

Soil at site S7 was classified as a Haplustept (Soil Survey Staff, 2014) and a Gleyic Cambisol (siltic) according to the World Reference Base (IUSS, 2015).

The main limiting factors of this type of soil are slow internal drainage and in the first 50 cm the concentration of total zinc varies from 273 to 469 mg/kg and that of tin from 3.73 to 6.31 mg/kg.

In Table A21 are reported the main features of pedogenetic horizons identified within three soil profiles dug at site S7.

Table A21- Depth interval, pH, electrical conductivity (EC), contents of total carbonates (CaCO3 tot), sand, silt and clay of three soil profiles (7A, 7B, 7C) dug in site S7 before the intervention.

Profile	Horizon		pH	E.C.	$CaCO_3$ tot.	Texture		
		Depth	H_2O			sand	silt	clay
		(cm)		dS cm^{-1}	g kg^{-1}	g kg^{-1}		
7A	A	0-25	7,8	0,54	122	318	453	229
	AB	25-44	8,0	0,42	138	269	461	270
	Bw	44-83	8,1	0,23	218	239	376	385
	Bc	83-100+	8,2	0,20	191	161	362	477
7B	A	0-20	7,5	0,49	118	359	426	215
	AB	20-40	7,7	0,49	114	268	462	270
	Bcg	40-60	7,9	0,42	149	234	377	389
	Cg	60-100*	7,9	0,40	155	150	371	479
7C	A	0-15	7,6	0,39	115	322	454	224
	AB	15-35	7,8	0,31	135	271	460	269
	Bw	35-46	8,0	0,23	168	244	375	381
	BC1	46-85	8,2	0,17	204	200	346	454
	BC2	85-100	8,1	0,23	184	162	365	473

Type of interventions

As the site already possessed a cover of spontaneous native woody plants, the only action undertaken was the excavation of a hydraulically connected pond of 80 m² with a maximum depth of 1 m (Figure A18). This basin maintains the same hydraulic head as the Allacciante IV Circondario canal; when the canal level falls, a clapet (flap) valve preserves an optimal water level within the pond for a certain period, until normal head is restored in the canal.

The soil derived from excavating the pond was spread uniformly over the site's ground surface.

Vegetation insertion was confined to the pond margin, where herbaceous species typical of aquatic habitats - raised in nursery - were planted. In total 107 pots belonging to 15 different helophytic herbaceous species were installed (Table A22).

Table A22 - List of pots per herbaceous plant species planted at S7.

Herbaceous plants planted at site 7	
Species	**N. of pots**
Alisma plantago-aquatica	6
Butomus umbellatus	3
Carex pendula	3
Cyperus longus	6
Eleocharis sp.	5
Juncus effusus	4
Juncus sp.	18
Limniris pseudacorus	9
Lysimachia vulgaris	3
Lythrum salicaria	7
Phragmites australis	8
Schoenoplectus lacustris	6
Scirpoides holoschoenus	3
Sparganium erectum	4
Typha angustifolia	22
Total	**107**

Figure A18 – Pond created at S7.

Implementation schedule and costs

Excavation of the pond and redistribution of spoil were entrusted to an earth-moving company, whereas all planting operations were carried out entirely by the Renana Remediation Consortium and completed in March 2023.

The total cost foreseen in the Executive Project for the creation of S7, calculated according to the 2020 Emilia-Romagna regional price list, amounts to € 5,281.90 (Table A23).

Table A23 - Calculation of the cost of intervention at S7, based on the Emilia-Romagna Region price list (2020 edition) and the actual costs incurred for the purchase of trees and shrubs.

Intervention costs at site 7		
Cost item	**Quantity**	**Cost**
Mechanical mowing of heterogeneous spontaneous vegetation consisting mainly of reeds and bushes, carried out by mechanical means on canal floodplains and embankment surfaces, flat and sloping, including the cost of collecting and transporting the resulting material to waste.	1,000 m^2 x 0.16 €/m^2	€ 160.00
Overburden excavation for creation of wetland and banks	360 m^3 x 3.70 €/m^3	€ 1,332.00
Compulsory section excavation up to a maximum depth of 4 m from the ground level for laying pipeline even in the presence of water, performed by machine, including backfilling of artifacts, placement of excess material in the area adjacent to the construction site	11.25 m^3 x 7.70 €/m^3	€ 86.63
Rigid pvc pipes diameter of 250 mm, thickness 7.3 mm, supplied and laid, in accordance with UNI EN 1401, including and compensated in the price every charge for the laying excluding the formation of the laying bed and backfill in suitable material	7.5 m x 32.87 €/m	€ 246.53
PVC end-of-line clapet backflow preventer valve, 250 mm diameter, supplied and installed with coupling on pipe complete with all accessories	1 x 299 € each	€ 299.00
Excavation for the reshaping of canal bed section, performed by mechanical means, in the presence of water, including all charges and displacement and frontal placement of the resulting material	360 m^3 x 5.60 €/m^3 + 40 m^3 x 3.30 €/m^3	€ 2,148.00
Quarried limestone supplied and placed for formation of bank defenses	14.55 t x 32.50 €/t	€ 472.88
Worksite safety activities and facilities		€ 457.67
Planting herbaceous plants	6 hours x 13.20 €/h	€ 79.20
Herbaceous plants from the nursery	107 plants	
Total		**€ 5,281.91**

Site S8

Total area: 380 m²

Coordinates: 44°36'20"N 11°35'13"E

Elevation: 9-11 m asl

Location: Point of discharge of the Cornamonda Nuova canal into the Gallina Superiore canal (Municipality of Budrio) (Figure A19).

Figure A19 – S8 after intervention.

Canals

Like S7, S8 is located along the Gallina Superiore canal.

The Cornamonda Nuova canal is an incised canal whose primary function is to collect storm-water run-off from land situated on the hydraulic left of the Idice river floodbank and downstream of the Canale Emiliano Romagnolo (CER), in the Mezzolara hamlet of the Municipality of Budrio (Bologna). Over its 6.4 km course

the canal flows 270 m from the eastern boundary of Natura 2000 site IT4050023 - SCI-SPA “Biotopes and environmental restorations of Budrio and Minerbio”.

Irrigation district

Because S8 coincides with the point where the Cornamonda Nuova canal enters the Gallina Superiore canal, it lies on the boundary between two irrigation districts that share a common origin. The “Canaletta di Mezzolara” district is the larger of the two and supplies the second, named “Scolo Gallina Superiore valle Canaletta di Mezzolara.”

The former district covers 1,187 ha and on average irrigates 200 ha per year. Based on Renana Remediation Consortium irrigation-service data for 2023 and 2024, mean irrigated areas for the main crops in this district are: maize 55 ha, sorghum 34 ha, sugar beet 30 ha, potato 25 ha, soybean 16 ha, onion 3 ha, and alfalfa 8 ha.

This district draws water directly from the namesake intake on the Canale Emiliano Romagnolo (CER), located near the left bank of the Idice river, from which a buried pipeline conveys the water to the outskirts of Mezzolara (Budrio). North of the built-up area the Canaletta di Mezzolara bifurcates, supplying water to both the Cornamonda Nuova canal and the Gallina Superiore canal.

The reach of the Gallina Superiore canal downstream of the Canaletta outfall constitutes a specific 170-ha irrigation district, within which an average of 31 ha per year is irrigated. For 2023-2024 the mean irrigated areas for the main crops are: maize 24 ha, onion 3 ha, sorghum 3 ha, and nursery stock 2 ha.

At S8, the two canal display a summer irrigation depth of 1.25 m and bank-to-bank widths of 5 m (Cornamonda Nuova) and 9 m (Gallina Superiore).

Irrigation records for 2020 – 2024 were analysed for land within 1 km upstream of S8. On average 32 ha per year are irrigated by eight farms, mainly producing potato (11 ha), onion (7 ha), maize (6 ha), sorghum for biomass (5.6 ha), grain sorghum (3.5 ha) and soybean (3 ha).

Figure A20 - Cartographic framing of S8.

Site location and morphology

S8 is situated at the confluence where the Cornamonda Nuova canal enters the Gallina Superiore canal, south-east of the hamlet of Dugliolo in the Municipality of Budrio (Bologna) (Figure A20). It lies 2.5 km from S7 and 2 km in a straight line from the boundary of Natura 2000 site IT4050023 - SCI-SPA “Biotopes and environmental restorations of Budrio and Minerbio”. The surrounding landscape is dominated by arable fields.

The intervention area corresponds to the wedge of level agricultural land at the junction of the two canals, which had been farmed until 2022 by the adjoining holding.

Soil features before intervention

Soil at site S7 was classified as an Udifluventic Haplustept (Soil Survey Staff, 2014) and a Fluvic Cambisol (siltic) according to the World Reference Base (IUSS, 2015).

This soil type has an organic carbon content of <1% along the entire profile as the main limiting factor.

In Table A24 are reported the main features of pedogenetic horizons identified within three soil profiles dug at site S8.

Table A24 - Depth interval, pH, electrical conductivity (EC), contents of total carbonates (CaCO3 tot), sand, silt and clay of three soil profiles (8A, 8B, 8C) dug in site S8 before the intervention.

Profile	Horizon	Depth	pH	E.C.	$CaCO_3$ tot.	Texture		
			H_2O			sand	silt	clay
		(cm)		dS cm^{-1}	g kg^{-1}	g kg^{-1}		
8A	Ap1	0-12	7,9	0,22	171	327	446	227
	Ap2	12-40	7,9	0,21	176	306	447	247
	Bw	40-80	7,9	0,22	194	298	453	249
	2BC	80-100+	8,0	0,19	216	480	393	127
8B	Ap1	0-11	8,1	0,21	175	333	440	227
	Ap2	11-40	8,2	0,20	178	314	446	240
	Bw	40-63	8,1	0,20	171	295	466	240
	2BC	63-100+	8,1	0,19	223	474	396	130
8C	Ap1	0-20	8,0	0,17	174	321	452	227
	Ap2	20-50	8,1	0,17	175	298	448	254
	Bw	50-70	7,9	0,21	184	301	459	240
	2BC	70-100+	8,1	0,14	218	487	389	124

Type of intervention

Given the site's simple morphology, only limited bank re-profiling was required to create the steppingstone habitat. The slopes of both canal banks were eased to provide a broader surface for the development of hygrophilous and helophytic vegetation - both spontaneous and nursery-raised - and to render the banks less suitable for burrowing by invasive alien species coypu - *Myocastor coypus* (Figure A21).

Soil from this re-profiling was spread evenly across the site.

For the woodland component, a nucleus of species typical of habitat 91F0 - "Mixed riparian forests" was planted at the center of the plot and along the pond edges. In total 20 native woody plants were installed over 60 m²: 10 trees and 10 shrubs. To diversify structure, individuals of the same species were set out in two

size classes - 10 forest saplings (50-70 cm) and 10 more mature specimens - thus establishing an uneven-aged stand of the principal habitat 91F0 species (Table A25).

Along the banks of both canals, herbaceous species typical of local watercourse margins were planted, sourced from the nursery. Altogether 128 pots representing 15 different helophytic herbaceous species were introduced (Table A26).

Table A25 - List of plants per tree and shrub species planted at S8.

Trees and shrubs planted at site 8		
Species	**Saplings (0.50-0.90 m)**	**Young plants (1-3 m)**
Trees	**5**	**5**
Fraxinus angustifolia	1	1
Fraxinus excelsior	1	1
Quercus robur	1	1
Salix alba	1	1
Ulmus minor	1	1
Shrubs	**5**	**5**
Cornus sanguinea	1	2
Prunus padus	1	
Rhamnus frangula	1	1
Sambucus nigra	1	1
Viburnum opulus	1	1
Total	**10**	**10**

Table A26 - List of pots per herbaceous plant species planted at S8.

Herbaceous plants planted at site 8	
Species	**N. of pots**
Alisma plantago-aquatica	6
Butomus umbellatus	3
Carex pendula	12
Cyperus longus	6
Eleocharis sp.	5
Juncus inflexus	12
Juncus sp.	23
Limniris pseudacorus	9
Lycopus europaeus	3
Lythrum salicaria	6
Phragmites australis	8
Schoenoplectus lacustris	6
Scirpoides holoschoenus	3
Sparganium erectum	4
Typha angustifolia	22
Total	**128**

Figure A21 - Planting wetland plants at S8.

Implementation schedule and costs

All profiling and planting works were carried out entirely by the Renana Remediation Consortium and were completed in March 2023.

The total cost foreseen in the Executive Project for the construction of S8, calculated according to the 2020 Emilia-Romagna regional price list, amounts to € 2,740.55 (Table A27).

Table A27 - Calculation of the cost of intervention at S8, based on the Emilia-Romagna Region price list (2020 edition) and the actual costs incurred for the purchase of trees and shrubs.

Intervention costs at site 8		
Cost item	**Quantity**	**Cost**
Mechanical mowing of heterogeneous spontaneous vegetation consisting mainly of reeds and bushes, carried out by mechanical means on canal floodplains and embankment surfaces, flat and sloping, including the cost of collecting and transporting the resulting material to waste.	900 m^2 x 0.16 €/m^2	€ 144.00
Excavator, shovel, or bulldozer, including operator, fuel, and lubricant, for setting up hydraulic appurtenances	20 hours x 69.10 €/h	€ 1,382.00
Excavation for the reshaping of canal bed section, performed by mechanical means, in the presence of water, including all charges and displacement and frontal placement of the resulting material	227.50 m^3 x 3.30 €/m^3	€ 750.75
Planting of tree/arbustive plants	6 hours x 13.20 €/h	€ 79.20
Planting herbaceous plants	8 hours x 13.20 €/h	€ 105.60
Purchase and supply of trees and shrubs	5 trees, 5 shrubs	€ 279.00
Free supply of trees and shrubs saplings	5 trees and 5 shrubs	
Herbaceous plants from the nursery	128 plants	
Total		**€ 2,740.55**

Hydraulic sector between right bank of the Reno river and left bank of the Idice river, Municipality of Baricella.

Site S9

Total area: 9,800 m²

Coordinates: 44°40'48"N 11°36'48"E

Elevation: 9 m asl

Location: Bank situated between the left bank of the Botte canal and the right embankment of the Savena Abbandonato, a natural watercourse (Municipality of Baricella) (Figure A22).

Figure A22 – S9 after intervention.

Canal

The Botte canal is the terminal collector of the upper drainage network within the territory bounded by the Reno and the Idice rivers. It originates downstream of

the built-up area of Malalbergo (Province of Bologna), where it receives the waters of the Riolo canal - the principal canal draining the land between the Reno river and the Navile Canal. The Botte canal extends for 31.5 km and, along its entire course, the canal is flanked by high embankments designed to convey storm-water runoff from the upper plain across terrain of progressively lower elevation.

The canal runs almost entirely parallel to the course and right-bank levees of the Reno river, crossing the town of San Pietro Capofiume (Bologna), skirting the municipality of Molinella, and finally discharging into the Reno river at the Valli di Argenta (Ferrara). Owing to its role as collector of multiple tributaries, the Botte canal is never completely dry; its lowest stage occurs in winter, when the hydraulic depth is approximately 1.4 m.

Throughout its length, the Botte canal traverses four distinct Natura 2000 sites. The initial reach flows for 9.5 km within site IT4050024 - SCI-SPA “Biotopes and environmental restorations of Bentivoglio, San Pietro in Casale, Malalbergo and Baricella”. It then enters, for a distance of 3.5 km, site IT4060017 - SPA “Po di Primaro e Bacini di Traghetto.” The terminal part of the canal lies entirely within areas protected at European level: for 4 km it runs inside site IT4050022 – SCI-SPA “Biotopes and environmental restorations of Medicina and Molinella” (from Ponte Zanolini at Molinella to the boundary between the Metropolitan City of Bologna and the Province of Ferrara), and the subsequent 5 km downstream (from the provincial boundary to the Saiarino pumping station) form part of site IT4060001 - SCI-SPA “Valli di Argenta.” This latter section is also included within the perimeter of the Po Delta Regional Park.

Irrigation district

S9 lies within the upper reach of the Botte canal irrigation district, which covers 1,190 ha and irrigates, on average, 380 ha per year. Renana Remediation Consortium records for the 2023- 2024 seasons indicate mean irrigated areas for the principal land uses as follows: 159 ha maize, 98 ha wetlands managed for hunting, 72 ha sugar beet, 21 ha alfalfa, and 12 ha soybean.

This reach of the canal is supplied mainly by the Crevenzosa intake on the Canale Emiliano Romagnolo (CER), which discharges into the Crevenzosa canal and subsequently into the Canale Riolo; at the built-up area of Malalbergo (Bologna) the Canale Riolo becomes the Botte canal.

At S9 the Botte canal exhibits a summer irrigation depth of 1.5 m and a bank-to-bank bed width of 10.5 m.

Irrigation data for 2020 – 2024 were analysed for land within 1 km upstream of S9. On average 33 ha per year are irrigated by the Renana Remediation Consortium's own farm holding for the maintenance of wetlands in the nearby Gandazzolo water retention basin.

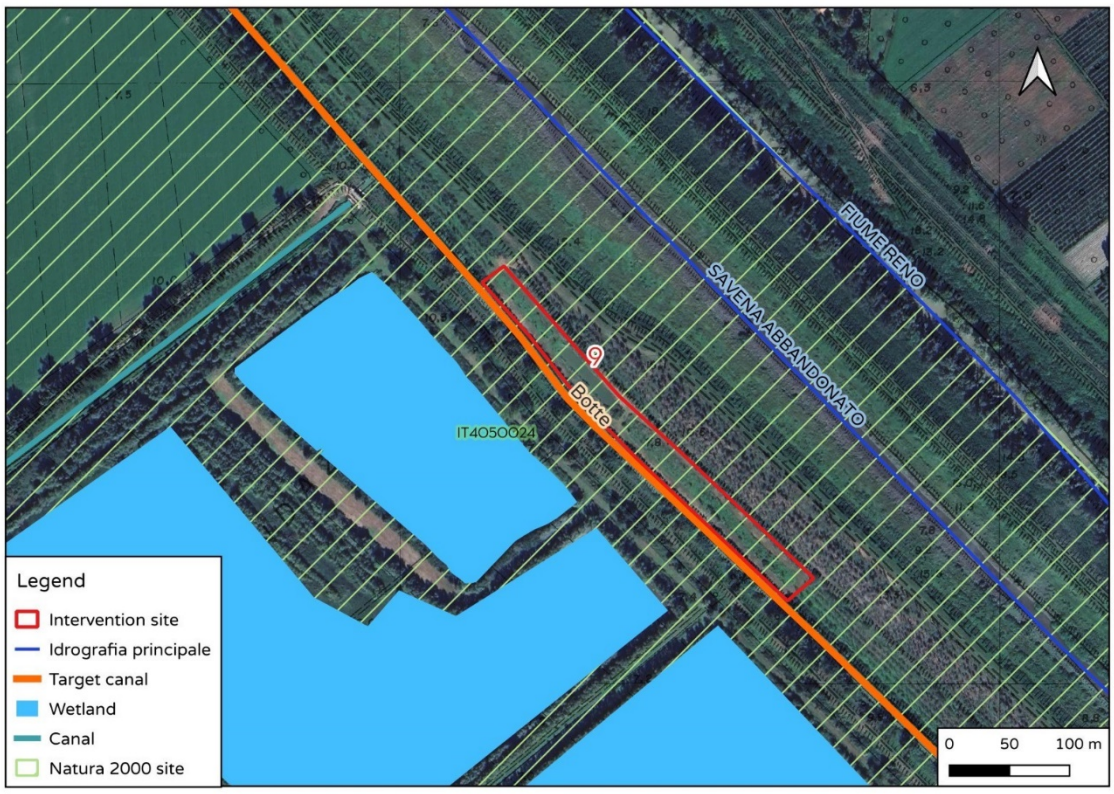

Figure A23 - Cartographic framing of S9.

Site location and morphology

The S9 is the largest intervention area and is situated on the left bank of the Botte canal, inside and toward the northern boundary of Natura 2000 site IT4050024 - SCI-SPA "Biotopes and environmental restorations of Bentivoglio, San Pietro in

Casale, Malalbergo and Baricella", within the Municipality of Baricella (Bologna) (Figure A23). On the opposite bank lies the Gandazzolo Vecchia water retention basin, which comprises various wetlands owned by the Renana Remediation Consortium.

The intervention area consists of a level bank segment 370 m long and 25 m wide between the left bank of the Botte canal and the right embankment of the Savena Abbandonato, a natural watercourse. The parcel covers 9,800 m² and, until 2021, was managed as a pulp-wood poplar plantation by the farm owned by Renana Remediation Consortium. The site lies below the crests of the surrounding levees; because it is enclosed within the embankments, the emergent area may experience prolonged inundation during heavy-rainfall periods, favouring ecological processes typical of lowland floodplain forests.

Soil features before intervention

Soil at site S9 was classified as an Oxyaquic Ustifluvent (Soil Survey Staff, 2014) and a Eutric Fluvisol (oxyaquic) according to the World Reference Base (IUSS, 2015).

The main limiting factor for this type of soil is the presence in the first 50 cm of a total zinc concentration ranging from 170 to 185 mg/kg and that of tin from 3.88 to 5.01 mg/kg.

In Table A28 are reported the main features of pedogenetic horizons identified within three soil profiles dug at site S9.

Table A28 - Depth interval, pH, electrical conductivity (EC), contents of total carbonates (CaCO3 tot), sand, silt and clay of three soil profiles (9A, 9B, 9C) dug in site S9 before the intervention.

Profile	Horizon		pH	E.C.	$CaCO_3$ tot.	Texture		
		Depth	H_2O			sand	silt	clay
		(cm)		dS cm^{-1}	g kg^{-1}	g kg^{-1}		
9A	Ap1	0-25	7,6	0,42	131	107	544	349
	Ap2	25-50	7,7	0,33	143	118	497	385
	C1	50-90	7,8	0,40	133	127	478	395
	2C2	90-110+	7,8	0,52	144	357	347	296
9B	Ap1	0-25	7,5	0,42	127	115	515	370
	Ap2	25-45	7,6	0,36	131	129	492	379
	C1	45-60	7,9	0,54	139	131	475	394
	2C2	60-100	8,0	0,75	167	379	333	288
9C	Ap1	0-15	7,7	0,36	139	111	525	364
	Ap2	15-27	7,7	0,44	129	124	494	382
	C1	27-50	7,9	0,61	133	127	478	395
	2C2	50-70	8,0	0,68	167	321	358	321
	2C3	90-100	8,0	0,54	153	368	340	292

Type of intervention

The site's large size permitted substantial works to create the stepping stone habitat. The left canal bank was re-profiled to a gentler slope, allowing greater development of hygrophilous and helophytic vegetation - both spontaneous and produced in nursery - and reducing suitability for burrowing by invasive alien species coypu - *Myocastor coypus.*

Within the former poplar stand, a hydraulically connected pond (650 m², depth ≈ 1.5 m) was excavated (Figure A24). The basin maintains the same hydraulic head as the Botte canal; when canal levels drop, a clapet valve preserves an optimal water volume in the basin until irrigation head is restored.

Soil from bank re-profiling and pond excavation was spread across the remaining site surface.

For the woodland component, a nucleus of species typical of habitat 91F0 - "Mixed riparian forests" was planted in the center of the plot and along the basin margins. In total 328 native woody plants were planted over 3,800 m²: 160 trees and 168 shrubs. To diversify structure, individuals of the same species were

planted in two size classes - 168 forest saplings (50–70 cm) and 160 more mature specimens - establishing an uneven-aged stand of the principal habitat 91F0 species (Table A29).

Along the canal and pond margins, 825 pots of native aquatic plants, representing 29 helophytic herbaceous species raised nursery, were planted (Table A30).

Table A29 - List of plants per tree and shrub species planted at S9.

Trees and shrubs planted at site 9		
Species	**Saplings (0.50-0.90 m)**	**Young plants (1-3 m)**
Trees	**81**	**79**
Alnus glutionsa	3	4
Fraxinus angustifolia	13	8
Fraxinus excelsior	12	10
Quercus robur	21	11
Populus alba	4	4
Populus nigra	4	4
Salix alba	7	16
Ulmus minor	17	22
Shrubs	**87**	**81**
Cornus sanguinea	8	17
Corylus avellana	8	4
Euonymus europaeus	8	4
Prunus padus	8	4
Prunus spinosa	10	4
Rhamnus frangula	8	8
Rosa canina	9	4
Sambucus nigra	9	16
Viburnum lantana	10	4
Viburnum opulus	9	16
Total	**168**	**160**

Table A30 - List of pots per herbaceous plant species planted at S9.

Herbaceous plants planted at site 9	
Species	**N. of pots**
Alisma plantago-aquatica	110
Althaea officinalis	15
Butomus umbellatus	15
Carex pendula	20
Carex riparia	11
Cyperus longus	38
Eleocharis sp.	7
Euphatorium cannabinum	1
Juncus acutus	21
Juncus articulatus	18
Juncus maritimus	4
Juncus sp.	78
Limniris pseudacorus	37
Lycopus europaeus	57
Lysimachia vulgaris	9
Lythrum salicaria	74
Mentha aquatica	5
Oenanthe fistulosa	3
Phragmites australis	23
Polygonum hydropiper	1
Ranunculus sceleratus	2
Schoenoplectus lacustris	37
Schoenoplectus tabernaemontani	6
Scirpoides holoschoenus	5
Scirpus maritimus	3
Sparganium erectum	15
Typha angustifolia	1
Typha latifolia	45
Typha sp.	164
Total	**825**

Figure A24 - Pond created at S9.

Implementation schedule and costs

Excavation and spoil spreading were entrusted to an earthmoving firm; profiling and planting were carried out entirely by the Renana Remediation Consortium and completed in March 2022.

The total cost foreseen in the Executive Project for the creation of S9, based on the 2020 Emilia-Romagna regional price list, amounts to € 20,861.12 (Table A31).

Table A31 - Calculation of the cost of intervention at S9, based on the Emilia-Romagna Region price list (2020 edition) and the actual costs incurred for the purchase of trees and shrubs.

Intervention costs at site 9		
Cost item	**Quantity**	**Cost**
Mechanical mowing of heterogeneous spontaneous vegetation consisting mainly of reeds and bushes, carried out by mechanical means on canal floodplains and embankment surfaces, flat and sloping, including the cost of collecting and transporting the resulting material to waste.	3,150 m^2 x 0.16 €/m^2	€ 504.00
Overburden excavation for creation of wetland and banks	805 m^3 x 3.70 €/m^3	€ 2,978.50
Compulsory section excavation up to a maximum depth of 4 m from the ground level for laying pipeline even in the presence of water, performed by machine, including backfilling of artifacts, placement of excess material in the area adjacent to the construction site	15.75 m^3 x 7.70 €/m^3	€ 121.28
Rigid pvc pipes diameter of 250 mm, thickness 7.3 mm, supplied and laid, in accordance with UNI EN 1401, including and compensated in the price every charge for the laying excluding the formation of the laying bed and backfill in suitable material	10.5 m x 32.87 €/m	€ 345.14
PVC end-of-line clapet backflow preventer valve, 250 mm diameter, supplied and installed with coupling on pipe complete with all accessories	1 x 299 € each	€ 299.00
Excavator, shovel, or bulldozer, including operator, fuel, and lubricant, for setting up hydraulic appurtenances	20 hours x 69.10 €/h	€ 1,382.00
Excavation for the reshaping of canal bed section, performed by mechanical means, in the presence of water, including all charges and displacement and frontal placement of the resulting material	805.06 m^3 x 5.60 €/m^3 + 60 m^3 x 3.30 €/m^3	€ 4,706.34
Embankment formation for embankment construction and landslide recovery, using spoil from excavation in the riverbed	739 m^3 x 1.60 €/m^3	€ 1,182.40
Quarried limestone supplied and placed for formation of bank defenses	12.45 t x 32.50 €/t	€ 404.63
Worksite safety activities and facilities		€ 2,765.63
Planting of tree/arbustive plants	60 hours x 13.20 €/h	€ 792.00
Planting herbaceous plants	71 hours x 13.20 €/h	€ 937.20
Purchase and supply of trees and shrubs	79 trees, 81 shrubs	€ 4,443.00
Free supply of trees and shrubs saplings	81 trees and 87 shrubs	
Herbaceous plants from the nursery	825 plants	
Total		**€ 20,861.12**